TUM

Technische Universität München

Fakultät für Chemie – Lehrstuhl für Biochemie

Nutrition of intracellular bacteria: Investigation of the metabolic networks in *Legionella pneumophila* and *Coxiella burnetii* using GC/MS based isotopologue profiling

Ina Franziska Häuslein

Vollständiger Abdruck der von der Fakultät für Chemie der Technischen Universität München zur Erlangung des akademischen Grades eines

Doktors der Naturwissenschaften

genehmigten Dissertation.

Vorsitzender: Prof. Dr. Tobias A. M. Gulder

Prüfer der Dissertation: 1. apl. Prof. Dr. Wolfgang Eisenreich

2. Prof. Dr. Hubert Hilbi

(Universität Zürich / Schweiz)

Die Dissertation wurde am 19.06.2017 bei der Technischen Universität eingereicht und durch die Fakultät für Chemie am 20.07.2017 angenommen.

Für meinen Papa

"Sometimes science is more art than science, Morty.

Lot of people don't get that."

Rick Sanchez C-137 (smartest person in the universe)

LIST OF PUBLICATIONS

Häuslein, I.[#], Manske, C.[#], Goebel, W., Eisenreich W.[†], and Hilbi, H[†]. (**2015**). Pathway analysis using ^{13}C-glycerol and other carbon tracers reveals a bipartite metabolism of *Legionella pneumophila. Molecular microbiology* 100**,** 229-246.

Personal contribution: Ina Häuslein developed the experimental setup of the *in vitro* and *in vivo* labelling experiments together with Christian Manske, established a new isotopologue profiling method for analyzing polar metabolites extracted from *Legionella pneumophila*, performed the isotopologue analysis of the data, prepared the figures, drafted the manuscript and revised the final version.

# Authors contributed equally to this work, † Corresponding authors

Häuslein, I., Cantet, F., Reschke, S., Chen, F., Bonazzi, M., and Eisenreich, W. (**2017**). Multiple substrate usage of *Coxiella burnetii* to feed a bipartite metabolic network. *Frontiers in Cellular and Infection Microbiology* 7.

Personal contribution: Ina Häuslein developed the experimental setup of the labelling experiments, performed the isotopologue analysis of the data, prepared the figures, drafted the manuscript and revised the final version.

Further publications:

Häuslein, I., Sahr, T., Escoll, P., Klausner, N., Eisenreich, W., and Buchrieser, C., (**2017**). *Legionella pneumophila* CsrA regulates a metabolic switch from amino acid to glycerolipid metabolism. **Submitted**

Chen, F., Rydzewski, K., Kutzner, E., **Häuslein, I.,** Schunder, E., Wang, X., Meighen-Berger, K., Grunow, R., Eisenreich, W., and Heuner, K. (**2017**). Differential substrate usage and metabolic fluxes in *Francisella tularensis* subspecies *holarctica* and *Francisella novicida. Frontiers in Cellular and Infection Microbiology* 7.

_____

Prof. Dr. Wolfgang Eisenreich (Supervisor)

SUMMARY

Legionnaires´ disease is a life-threatening illness caused by the facultative intracellular bacterium *Legionella pneumophila*. This pathogen preferably uses amino acids, especially serine as prime carbon and energy source, but recent transcriptome and proteome data as well as genome analysis and labeling experiments suggest a greater metabolic capacity. Accordingly, expression of the glycerol kinase (*glpK*) and the glycerol 3-phosphate dehydrogenase (*glpD*) was found to be upregulated during infection of macrophages, indicating that glycerol represents an additional substrate in the nutrition of *L. pneumophila*. In the present thesis, the metabolic potentials of *L. pneumophila* and its close relative *Coxiella burnetii* were investigated. The goal of this study was to determine a general metabolic concept for these bacteria as an aspect of their survival strategy in their environmental niches. This is of special interest, as a broad knowledge about the metabolism of intracellular bacteria can be helpful to identify potential targets for the developments of new antibiotics.

We found that glycerol does not enhance extracellular growth of *L. pneumophila*, but promotes intracellular replication in *Acanthamoeba castellanii* and macrophages dependent on *glpD*. Furthermore, a *L. pneumophila glpD* deletion mutant was outcompeted by the wild-type strain during coinfection in amoeba, illustrating the importance of further substrates besides amino acids during intracellular replication. For a detailed investigation of the glycerol metabolism in *L. pneumophila*, a novel minimal defined medium (MDM) was designed, which includes essential amino acids, proline and phenylalanine. Isotopologue profiling experiments were performed in MDM using [U-^{13}C$_3$]glycerol, [U-^{13}C$_6$]glucose or [U-^{13}C$_3$]serine as tracers in a time dependent manner. Glycerol and glucose were predominantly utilized by *L. pneumophila* at later growth phases for gluconeogenetic reactions and in the pentose phosphate pathway (PPP), since ^{13}C-label was predominantly shuffled into histidine (His) and mannose (Man). On the other hand, serine was used at earlier time points predominantly in the tricarboxylic acid cycle (TCA cycle) for energy generation. Similar results were obtained using the same ^{13}C-tracers in *in vivo* labeling experiments with *L. pneumophila* wild-type and Δ*glpD* mutant bacteria in *A. castellanii*. Collectively, these data reflect a bipartite metabolism in which amino acids and especially serine are predominantly used for energy generation in early developmental stages, whereas glycerol and carbohydrates like glucose are mainly employed

---

in anabolic processes at later growth phases. Furthermore, the role of the central carbon storage regulator A (CsrA) in the adjustment of core metabolic fluxes within the bipartite metabolism of this pathogen was investigated. CsrA is crucial for the developmental switch from the replicative to the transmissive stage in the life cycle of *L. pneumophila*. Comparative labeling and oxygen consumption experiments were performed with the *L. pneumophila* wild-type and its CsrA knock down mutant to determine its role in the growth phase dependent metabolism. Isotopologue profiling experiments using [U-^{13}C$_3$]serine, [U-^{13}C$_6$]glucose or [U-^{13}C$_3$]glycerol demonstrated that CsrA induces serine incorporation and metabolism *via* the TCA cycle and glucose degradation *via* the Entner-Doudoroff pathway (ED pathway) during replication. Simultaneously, CsrA represses glycerol incorporation and catabolism *via* gluconeogenetic reactions and the PPP during the exponential growth phase. Using [1,2,3,4-^{13}C$_4$]palmitic acid as tracer, we demonstrated that this fatty acid can efficiently serve as a substrate for *L. pneumophila* nutrition. Thereby, the fatty acid is predominantly used for the biosynthesis of the storage compound polyhydroxybutyrate (PHB) *via* ^{13}C$_2$-acetyl-CoA. Notably, comparative labeling experiments using [1,2,3,4-^{13}C$_4$]palmitic acid with the wild-type and the CsrA knock down mutant revealed higher ^{13}C-incorporation rates in the *csrA* mutant especially at earlier growth phases, indicating that CsrA is repressing fatty acid degradation and/or PHB biosynthesis, predominantly during exponential growth. Collectively, this study demonstrated the crucial role of CsrA in the life stage specific coordination of substrate usage and carbon flux regulation in *L. pneumophila*.

As a bipartite metabolism might be a general strategy of intracellular bacteria, isotopologue profiling experiments with [U-^{13}C$_3$]serine, [U-^{13}C$_6$]glucose or [U-^{13}C$_3$]glycerol were also performed with *C. burnetii* RSA 439 NMII in a recently developed axenic medium. From today's perspective, the metabolic potential of *C. burnetii* seems to be highly diverse. Nevertheless, metabolism of this pathogen is still only poorly investigated and predominantly inferred from genome analysis. This thesis now shows that similar to *L. pneumophila*, *C. burnetii* metabolizes all three above ^{13}C-tracers in a bipartite type metabolic network. However, carbon fluxes and metabolic potential also differed in some aspects compared to *L. pneumophila*.

Taken together, this thesis expanded the understanding of *L. pneumophila* metabolism and proved that the bacteria use glycerol and fatty acids as substrates. The concept of a bipartite metabolism was established and the crucial role of CsrA in the regulation of growth phase dependent carbon fluxes was determined. Comparative analysis of the metabolic capacity in *C. burnetii* and *L. pneumophila* revealed a similar topology of a bipartite metabolic network, which could be the result of an effective adaption strategy of intracellular bacteria to replication and survival under intracellular conditions.

_____

ZUSAMMENFASSUNG

Die lebensbedrohliche Legionärskrankheit wird durch das fakultativ intrazelluläre Bakterium *L. pneumophila* verursacht. Dieses Pathogen bevorzugt Aminosäuren, im Speziellen Serin als Kohlenstoff- und Energiequelle. Jüngste Transkriptom- und Proteomdaten sowie Genomanalysen und Markierungsexperimente weisen jedoch auf ein weitaus größeres metabolisches Potential hin. Dementsprechend war die Expression der für den Abbau von Glycerol wichtigen Enzyme Glycerolkinase (*glpK*) und Glycerol-3-phosphat-Dehydrogenase (*glpD*) während der Infektion von Makrophagen hochreguliert, was darauf schließen lässt, dass Glycerol ein Substrat für die intrazelluläre Ernährung von *L. pneumophila* darstellt. In der vorliegenden Arbeit wurde das metabolische Potential von *L. pneumophila* sowie seines nahen Verwandten *Coxiella burnetii* mit dem Ziel untersucht, ein generelles Konzept im Metabolismus dieser Bakterien zu identifizieren, welches die jeweilige Überlebensstrategie in ihren Replikationsnischen reflektieren könnte. Dies ist von besonderem Interesse, da ein fundiertes Wissen über die metabolische Struktur von intrazellulär replizierenden Bakterien hilfreich bei der Identifizierung potentieller Angriffspunkte für die Entwicklung neuer Antibiotika ist.

Wir konnten zeigen, dass Glycerol die intrazelluläre Replikation von *L. pneumophila* in Abhängigkeit von *glpD* in *A. castellanii* sowie in Makrophagen fördert, obwohl kein positiver Effekt auf das extrazelluläre Wachstum zu erkennen war. Des Weiteren unterlag eine *L. pneumophila* ΔglpD Mutante dem Wildtyp während der Co-Infektion in Amöben, was den Stellenwert weiterer Substrate neben Aminosäuren in der intrazellulären Ernährung von Legionellen hervorhebt. Zur eingehenden Untersuchung des Metabolismus von Glycerol in *L. pneumophila* wurde ein neues Minimalmedium (MDM) entwickelt, welches essentielle Aminosäuren sowie Prolin und Phenylalanine beinhaltet. Dieses Medium wurde für zeitabhängige Markierungsexperimente in Anwesenheit von [U-^{13}C$_3$]Glycerol, [U-^{13}C$_6$]Glukose oder [U-^{13}C$_3$]Serin verwendet. *L. pneumophila* verstoffwechselte dabei Glukose und v.a. Glycerol bevorzugt während späteren Wachstumsphasen in Reaktionen der Glukoneogenese und des Pentosephosphatwegs (PPP), da die meiste ^{13}C-Markierung in diesen Versuchen in His und Man detektiert werden konnte. Im Gegensatz dazu wurde Serin effektiv während frühen Wachstumsphasen verwendet und dabei bevorzugt im Citratzyklus zur

Energiegewinnung verstoffwechselt. Diese Ergebnisse konnten durch Infektionsexperimente unter Verwendung derselben ^{13}C-Vorläufer mit dem *L. pneumophila* Wildtyp sowie der Δ*glpD* Mutante in *A. castellanii in vivo* bestätigt werden. Zusammengefasst konnte dadurch für *L. pneumophila* das Konzept eines zweigeteilten Metabolismus etabliert werden. Dabei werden in der replikativen Wachstumsphase bevorzugt Aminosäuren, wie z.B. Serin, zur Energiegewinnung im Citratzyklus verwendet, wohingegen Glycerol und Kohlenwasserstoffe wie Glukose speziell in späteren Wachstumsphasen in anabolen Reaktionen metabolisiert werden. Des Weiteren wurde die Rolle des „central carbon storage regulators A" (CsrA) in der Koordination von Hauptkohlenstoffflüssen im zweigeteilten Metabolismus dieses Pathogens untersucht. CsrA ist der zentrale Modulator im Übergang von der replikativen zur transmissiven Wachstumsphase im Lebenszyklus von *L. pneumophila*. Zur Auflösung seiner Rolle im wachstumsphasenabhängigen Metabolismus wurden vergleichende Markierungsexperimente sowie Untersuchungen zum Sauerstoffverbrauch mit dem *L. pneumophila* Wildtyp sowie einer CsrA Knockdown-Mutante durchgeführt. In den Markierungsexperimenten mit [U-^{13}C$_3$]Serin, [U-^{13}C$_6$]Glukose oder [U-^{13}C$_3$]Glycerol konnte gezeigt werden, dass CsrA die Aufnahme von Serin und die Verstoffwechselung im Citratzyklus sowie den Metabolismus von Glukose über den Entner-Doudoroff Biosyntheseweg während der Replikation induziert. Gleichzeitig wird durch CsrA die Aufnahme und die Verstoffwechselung von Glycerol in der Glukoneogenese sowie über den PPP während der replikativen Wachstumsphase gehemmt. Zudem konnte durch Markierungsexperimente mit [1,2,3,4-^{13}C$_4$]Palmitinsäure gezeigt werden, dass Fettsäuren als Substrate in der Ernährung von *L. pneumophila* eine Rolle spielen. Die bei dem Abbau der Fettsäure entstehenden ^{13}C$_2$-acetyl-CoA Einheiten werden dabei fast ausschließlich für die Bildung des Speicherstoffs Polyhydroxybutyrat (PHB) verwendet. Vergleichende Markierungsexperimente in Anwesenheit von [1,2,3,4-^{13}C$_4$]Palmitinsäure mit dem *L. pneumophila* Wildtyp sowie der CsrA Knockdown-Mutante führten zu erhöhten ^{13}C-Anreicherungen in PHB im Experiment mit der *csrA* Mutante, speziell während der replikativen Wachstumsphase. Dies lässt auf eine inhibierende Rolle von CsrA im Fettsäurestoffwechsel und/oder in der Biosynthese von PHB während der exponentiellen Phase schließen. Zusammengefasst verdeutlicht diese Studie die essentielle Rolle von CsrA in der

_____

Koordination der wachstumsphasenabhängigen Substratnutzung und in der Regulation von Kohlenstoffflüssen im Lebenszyklus von *L. pneumophila*.

Zur Validierung des Modells des zweigeteilten Metabolismus als generelle Strategie für intrazellulär replizierende Bakterien wurden zudem Markierungsexperimente in Anwesenheit von [U-$^{13}C_3$]Serin, [U-$^{13}C_6$]Glucose oder [U-$^{13}C_3$]Glycerol mit *C. burnetii* RSA 439 NMII in einem vor kurzem entwickelten axenischen Wachstumsmedium durchgeführt. Aus heutiger Sicht zeigt *C. burnetii* ein hohes metabolisches Potential. Trotzdem ist das Wissen über das Stoffwechselnetzwerk dieses Pathogens bis dato begrenzt, da es fast ausschließlich auf genombasierten Analysen beruht. Mit Hilfe der in dieser Arbeit durchgeführten Versuche konnte die Verstoffwechselung der drei obigen ^{13}C-Vorläufer in einem zweigeteilten Metabolismus in *C. burnetii* gezeigt werden. Im Vergleich zu dem in *L. pneumophila* identifizierten metabolischen Konzepts waren jedoch auch Unterschiede in den Hauptkohlenstoffflüssen sowie in der metabolischen Kapazität zu erkennen.

Zusammengefasst leistet diese Arbeit einen essentiellen Beitrag zum Verständnis des Stoffwechselnetzwerks und der Kohlenstoffflüsse in *L. pneumophila*. Zudem konnte gezeigt werden, dass dieses Bakterium Glycerol sowie Fettsäuren als Nahrungsquelle nutzt. Das metabolische Konzept eines zweigeteilten Metabolismus wurde etabliert und zudem die zentrale Rolle des posttranskriptionellen Regulators CsrA in der wachstumsphasenabhängigen Koordination der Hauptkohlenstoffflüsse demonstriert. Eine vergleichende Studie der Stoffwechselstrategie in *C. burnetii* zeigte eine dem in *L. pneumophila* präsenten zweigeteilten Metabolismus ähnliche Topologie. Diese metabolische Strategie könnte daher das Ergebnis einer effizienten Anpassungsstrategie dieser Bakterien sein, welche eine erfolgreiche Vermehrung sowie das Überleben in intrazellulären Nischen ermöglicht.

TABLE OF CONTENT

14

_____

1 __INTRODUCTION__

1.1 Evolution, lifestyle, and nutrition of intracellular pathogens

1.1.1 Evolution and lifestyle of obligate and facultative intracellular pathogens

In general, the term "intracellular" in combination with bacteria refers to pathogens which are able to reside and/or replicate inside a cell. However, since a high portion of these numerous pathogens also spend time in the extracellular milieu before or after the residence inside a host, the term "intracellular" mostly refers to a defined period in the life cycle of these pathogens (Casadevall, 2008).

In addition, intracellular pathogens are organized in two groups: obligate and facultative. Thereby, the term "obligate intracellular" summarizes pathogens which are not able to live outside their host cells. This includes all kinds of viruses as well as bacterial pathogens like *Chlamydia* spp. or *C. burnetii* (Hackstadt and Williams, 1981b; Amann *et al.*, 1997; Casadevall, 2008)*.* On the other hand, facultative intracellular pathogens like fungi or bacteria such as *L. pneumophila* or *Francisella tularensis* are capable of replicating outside their hosts for example on biofilms (Casadevall, 2008; Hindre *et al.*, 2008; Durham-Colleran *et al.*, 2010). Additionally, obligates can be separated from the facultative pathogens *via* their action of infection, since they are required to be transferred directly from one host cell to another host while facultative bacteria can be acquired also from the environment (Casadevall, 2008).

It is difficult to define the origin of an intracellular lifestyle for bacteria since no fossil is reported that could give a hint to the time point at which the capacity of replication or survival inside a host cell was acquired. Furthermore, there are various intracellular microbes which hardly differ from each other in their survival strategy and additionally feature very characteristic host-microbe interactions, which makes it challenging to carve out general strategies and solutions of the intracellular lifestyle (Casadevall, 2008). However, if we consider the endosymbiotic theory as origin of some organelles in eukaryotic cell it can be concluded that the intracellular survival is an ancient process which appeared prior to the appearance of eukaryotic cells (Margulis, 1971; 1973; Casadevall, 2008).

Nevertheless, some basic requirements had to be present in the ancient cells to manage the establishment of this intracellular life. This concerns the difference in size of the invading cell

and the host cell or the availability of mechanisms that allowed the uptake of a cell or at least of some small particles. Also the possibility to survive autophagy mechanisms inside a host cell had to be present (Casadevall, 2008). This important membrane transport pathway is known to be crucial for the elimination of intracellular pathogens in eukaryotic cells and it is seen as an evolutionarily conserved defense strategy to avoid infection (Choy and Roy, 2013).

Replication of facultative or obligate intracellular bacteria usually takes place in the cytosol of their respective host cells or in a special compartment, a pathogen containing vacuole, which is established by the bacteria inside their hosts. The latter survival and replication strategy can be found e.g. with *L. pneumophila* or *C. burnetii* (Howe and Heinzen, 2006; Isberg *et al.*, 2009). However, some bacteria are also capable of escaping e.g. the phagosome or further compartments derived from the invasion procedure and replicate in the cytosol of their host cells, as is observed for *Listeria monocytogenes* or *Shigella* (Isberg *et al.*, 2009). This fact leads to a further classification of facultative and obligate intracellular bacteria.

Depending on the intracellular living mode of the bacteria, vesicular or within the cytosol, the intracellular environment offers different challenges. Firstly, phagosomal compartments exhibit extreme conditions since they include various degradation and antimicrobial proteins but also a reduced pH value and high amounts of free-radicals (Karupiah *et al.*, 1999; Casadevall, 2008). The same is true in vacuolar compartments derived from internalization which is mediated by the bacteria due to fusion with endosomes and/or lysosomes (O'Riordan and Portnoy, 2002; Casadevall, 2008). Furthermore, the acquisition of sustainable amounts of nutrients is more complex in a vesicular compartment, since bacteria are separated by a membrane from the nutrient rich cytosol. Therefore, bacteria which are surviving in a vacuolar compartment must be capable of specific defense mechanism like prevention of fusion with e.g. lysosomes or other vesicles of endocytosis and additionally be able to establish the acquisition of sustainable amounts of nutrients from the cytosol e.g. *via* degradation of proteins in the cytosolic compartment and subsequent transport into the respective vesicular replication niche (O'Riordan and Portnoy, 2002; Casadevall, 2008). In general, the cytosol is seen as a nutrient rich milieu with less antimicrobial defense mechanisms leading to the question if this environment is permissive for growth of any bacteria (O'Riordan and Portnoy, 2002; Casadevall, 2008). However, experiments with a bunch of different extracellular and

intracellular bacteria, which were directly injected into the cytosolic compartment of mammalian cells showed that only microorganism usually replicating in the cytosol are capable to survive in this environment whereas bacteria which are usually replicating in a vacuolar compartment are not. This indicates that the survival strategy of escaping the phagosomal compartment and replication in the cytosol, which is only featured by very few bacterial pathogens, relies on specifically evolved mechanisms (Goetz *et al.*, 2001).

In general, resistance or replication inside a cell can result in three different kinds of interaction modes between the host and the invading pathogen. Firstly, the host could benefit from this process like it is observed for endosymbiotic bacteria. Secondly, the two antagonists could live together in a symbiotic way. Nevertheless, most of the time this interplay results in the death of the intracellular pathogen or in the damage of the host cell, thus the latter scenario defines the action of an intracellular pathogen (Casadevall, 2008). Thereby, the death of the invading bacteria is predominantly related to mechanisms of the immune defense system of the host whereas the death of the host cell is related to degrading mechanisms, which are established by the intracellular microbe, or to apoptosis (Casadevall and Pirofski, 1999).

1.1.2   Nutritional adaption of intracellular pathogens

Concepts of intracellular nutrition are manifold within the group of intracellular pathogens. This is due to very different types of microbes, which are adapted to various intracellular niches in different host cells, thereby using diverse nutrients from their hosts (metal ions, carbon, nitrogen or energy) at very different rates (Abu Kwaik and Bumann, 2015). However, every intracellular pathogen has to acquire enormous levels of energy (ATP) whether directly from their hosts or from catabolic processes *via* metabolites which are directly incorporated from the host cell, to provide sufficient amounts of energy for their replication processes (Orth *et al.*, 2011). Simultaneously, the high efflux of the respective metabolites from the host to the microbe needs to be balanced by the host itself, otherwise nutrients would be exhausted very quickly (Orth *et al.*, 2011; Kentner *et al.*, 2014). This leads to unique metabolic adaptions of both antagonists in a complex metabolic network. Furthermore, the high efflux of the respective preferred nutrient also has to be established across the pathogen-containing vacuole in case of vacuolar replicating intracellular pathogens (Abu Kwaik and Bumann, 2015). Most of the time, amino acids represent the main energy sources of the latter group e.g. in case of *L.*

pneumophila (Pine *et al.*, 1979; Ristroph *et al.*, 1981; Tesh and Miller, 1981; Tesh *et al.*, 1983) or *Anaplasma phagocytophilum* (Niu *et al.*, 2012). Glucose in case of *Brucella* (Essenberg *et al.*, 2002) or glycerol and fatty acids in case of *Salmonella enterica* (Steeb *et al.*, 2013) can also serve as preferred carbon and energy supply for this group of intracellular microbes.

The nutritional evolution of these pathogens, meaning the specific metabolic adaption to the intracellular lifestyle and the respective nutrient supply, is thereby probably related to the different prototrophies and auxotrophies of their respective host cells, especially concerning amino acids (Price *et al.*, 2014; Abu Kwaik, 2015). The intracellular pathogen *L. pneumophila* predominantly uses amino acids, especially Ser and Cys, as preferred carbon and energy source, when replicating inside amoeba or human macrophages (George *et al.*, 1980; Ristroph *et al.*, 1981; Tesh and Miller, 1981; Eylert *et al.*, 2010). Therefore, this microbe triggers host cell degradation of proteins to elevate amino acid concentrations in the cytosol (Price *et al.*, 2014). Subsequently, amino acids are carried into the replication vacuole *via* numerous transporters and amino acid permeases (Cazalet *et al.*, 2004; Chien *et al.*, 2004). Genome analysis and labeling experiments with *L. pneumophila* revealed, that this pathogen is auxotroph for Cys as well as for Arg, Ile, Leu, Met, Thr and Val (Cazalet *et al.*, 2004; Chien *et al.*, 2004; Eylert *et al.*, 2010). Interestingly, their preferred host for replication in aquatic environments *Acanthamoeba* is also auxotroph for Arg, Ile, Leu, Met and Val (Ingalls and Brent, 1983; Price *et al.*, 2014). Furthermore, *Dictyostelium discoideum*, which is another host of *L. pneumophila*, shows auxotrophy for 11 amino acids, including the same amino acids which were classified as auxotroph for *L. pneumophila,* except for Cys (Payne and Loomis, 2006; Price *et al.*, 2014). However, this amino acid is the most absent one in this amoebic host and *in vitro* growth experiments in a minimal defined medium devoid of Cys revealed reduced growth rates of *D. discoideum* (Franke and Kessin, 1977). Interestingly, *L. pneumophila* prefers Cys as carbon and energy source (George *et al.*, 1980; Ristroph *et al.*, 1981; Tesh and Miller, 1981). Similar microbial adaption of auxotrophy to their hosts have also been found in further intracellular pathogens like e.g. *Francisella tularensis* (Alkhuder *et al.*, 2009), especially concerning Cys. Therefore, the synchronization of auxotrophies for certain amino acids between the intracellular microbe and their amoebic or mammalian host seems to be a general adaption process which is likely beneficial for the pathogens for their intracellular survival (Abu Kwaik and Bumann, 2013; Price *et al.*, 2014).

_____

Furthermore, intracellular pathogens feature different systems to enhance nutrient levels in their host cell. The general strategies which are used by most of the known intracellular pathogens to establish sufficient nutrient supply are predominantly based on targeting host protein degradation systems like e.g. proteasomes, autophagy or lysosomes. This finally leads to higher concentrations of low molecular weight nutrients, which are then incorporated and metabolized by the pathogen. The combination of these processes with further microbial strategies, which target alternative nutrient sources like e.g. glutathione, was recently termed as "nutritional virulence" (Abu Kwaik and Bumann, 2013). However, the respective carbon and energy sources need to be transported into the pathogen itself or additionally thought the vacuolar membrane in case of intracellular microbes that are replicating in a specific membrane bound compartment. Therefore, the microbe must establish numerous carbon transport systems to get access to sufficient amounts of nutrients.

1.1.3   Nutrient transport systems of bacteria

In general, beside the uptake of sufficient amounts of nutrients from the respective environment of the bacteria, transport systems are also important for the interaction between cells, iron acquisition or excretion of substrates (Mitchell, 1967). However, this chapter will concentrate on the most abundant transporter systems that play a certain role in bacterial nutrient acquisition. One important system of sugar transport in bacterial pathogens is the phosphoenolpyruvate: carbohydrate phosphotransferase system (PTS), which was discovered in 1964 in *Escherichia coli* (Kundig *et al.*, 1964). Extracellular sugars are thereby transported into the cell by simultaneously transferring one phosphoryl group derived from phosphoenolpyruvate (PEP) upon glucose or further carbohydrates like fructose, Man or galactose (Gal) (Kotrba *et al.*, 2001; Deutscher *et al.*, 2014). Phosphotransfer of the phosphoryl group from PEP onto hexose thereby occurs *via* a cascade reaction of three enzymes, which are termed enzyme I (EI), heat-stable or histidinephosphorylatable protein (HPr) and enzyme II (EII) (Kundig *et al.*, 1964; Deutscher *et al.*, 2006; Saier Jr, 2015). The EII comprises an enzyme complex, which is carbohydrate specific for one or more hexoses, whereas the cytoplasmic enzymes HPr and EI are universal participants of the PTS (Robillard and Broos, 1999; Saier, 2000a; Kotrba *et al.*, 2001). In general, the EII complex includes membrane associated domains as well as domains that are soluble in the cytosol. However, this complex is needed for the effective transport of the respective sugars through the membrane and

simultaneous phosphorylation, whereas the PEP/HPr/EI seems to be a general phosphoryl transfer system (Deutscher *et al.*, 2006). Since the EII complexes are carbohydrate specific, bacteria have a set of different EIIs. For example, *E. coli* features fifteen different complexes of EII, but studies of further bacteria revealed numerous homologues like e.g. in *Bacillus subtilis,* where genome and further biological studies revealed similar numbers like in *E. coli* for this transport complex (Reizer *et al.*, 1999; Deutscher *et al.*, 2002; Deutscher *et al.*, 2006). However, homologs are present in a bunch of bacterial pathogens (Barabote and Saier, 2005). The PTS is additionally crucial to the regulation of catabolic repression mechanisms and the regulation of carbohydrate metabolism in microbes (Stülke and Hillen, 1999; Deutscher *et al.*, 2006). Furthermore, it has been recently demonstrated, that the PTS is responsible for gene transcription as well as for the regulation of virulence factors in numerous bacteria e.g. in *Borrelia burgdorferi* or *Vibrio cholerae* (Wang *et al.*, 2015; Khajanchi *et al.*, 2016). In addition, an alternative PTS system called Nitrogen PTS system, which is not responsible for substrate transport but features a regulatory task, has been found in several bacteria (Powell *et al.*, 1995; Reizer *et al.*, 1996).

Pore-forming membrane bound proteins (porins) represent a second big family of bacterial constructs, which facilitate the uptake of nutrients *via* the outer membrane (Koebnik *et al.*, 2000). Such hydrophilic channels were first reported in *E. coli* and termed OmpC and OmpF (Nikaido, 1996). Since then, numerous porins have been identified in Gram positive and Gram negative bacteria as well as in eukaryotic cells. These protein channels are responsible either for the uptake of a specific substrate or represent a non-specific gateway (Achouak *et al.*, 2001). Thereby, the amount of porins in the outer membrane of the bacteria is related to their environment e.g. to salt-concentrations or availability of certain nutrients, adjusting the permeability of the cell wall (Achouak *et al.*, 2001). The direct link between the permeability of the outer membrane and persistence of intracellular pathogens inside their host was demonstrated e.g. for *Mycobacterium smegmatis* (Sharbati-Tehrani *et al.*, 2005). Furthermore, they are crucial for the regulation of intracellular transition metal concentrations, since they ensure that sufficient amounts are available but simultaneously avoid harmful effects (Hood and Skaar, 2012).

A further big group of membrane transporters represent the major facilitator superfamily (MFS). These transporters are ubiquitary, thereby translocating single molecules or acting as symporter or antiporter (Marger and Saier, 1993; Piao *et al.*, 2006). These types of transporters do not bind ATP, but translocation occurs *via* direct binding and subsequently conformational changes of this protein, thereby addressing a high number of different substrates (Pao *et al.*, 1998; Law *et al.*, 2008).

Same as the MFS, the ATP-binding cassette (ABC) transporters are also present in all living organisms (Higgins, 1992; Dean and Allikmets, 1995). These two groups of membrane transport systems are the most abundant ones present in microorganism, comprising almost fifty percent (Paulsen *et al.*, 1998). However, in contrast to the MFS, ABC transporter systems do actively import or export small molecules or macromolecules, using the energy of ATP hydrolysis (Fath and Kolter, 1993). Nevertheless, both transporter systems show high diversity concerning their targeted substrates, including almost every biological important compound (Pao *et al.*, 1998).

In contrast, there are also numerous membrane transporters, which show a high substrate specialization e.g. nucleoside transporters. In general, two groups of these transporters have been described: concentrative nucleoside transporters and equilibrative nucleoside transporters (Molina-Arcas *et al.*, 2009). Thereby, members of the latter group act as diffusion facilitators in both directions, whereas the unidirectional acting concentrative nucleoside transporters are energy consuming, utilizing the potential energy of a transmembrane sodium gradient (Baldwin *et al.*, 2004; Gray *et al.*, 2004; Molina-Arcas *et al.*, 2009). However, nucleoside transporters are found in eukaryotes and prokaryotes, enabling the usage of nucleosides as carbon and nitrogen source (Acimovic and Coe, 2002). Remarkably, intracellular bacteria seem to use these kinds of carriers predominantly for "energy parasitism", importing adenosine triphosphate (ATP) from the cytosol by simultaneously exporting adenosine diphosphate (ADP), thereby acting in the opposite direction than the well-known mitochondrial ADP/ATP carrier (Winkler and Neuhaus, 1999; Linka *et al.*, 2003). Interestingly, high sequence similarities between these transport proteins and ATP/ADP carriers from chloroplast have been identified (Winkler and Neuhaus, 1999).

However, besides the transporter system discussed so far, many further transport proteins have been classified in bacterial pathogens, like e.g. decarboxylation-driven, oxidoreduction-driven or methyltransferase-driven active transporters (Saier, 2000b).

1.1.4 Genome reduction as a concept of metabolic adaption and virulence

The common idea of the evolutional process is, that it somehow results in more complex organisms, starting from simple protocells which have finally developed into humans. Therefore, the development of genomes in the direction of higher complexity is expected (Wolf and Koonin, 2013). However, some time ago it was found, that the opposite event takes place in numerous microorganisms, especially in intracellular bacteria, although they show a high diversity in their adaption and survival strategies inside their respective host cells (Moran, 2002; Wolf and Koonin, 2013). However, genome-sequencing experiments in very different groups of bacteria like e.g. *Alphaproteobacteria, Gammaproteobacteria, Mollicutes* or *Spirochaetes* revealed, that all of them show genome reduction, indicating that this is a widespread ability of bacteria (McCutcheon and Moran, 2012). Simplification is therefore probably a general concept in the evolution from a free-living bacterium to an intracellular living pathogen (obligate or facultative), that leads to the deficiency of large parts of their genome (Gil *et al.*, 2004; Fraser-Liggett, 2005; Casadevall, 2008). Up to 95% of bacterial genes can thereby be depleted, whereas a core set of genes related to basic cellular functions (host cell invasion or core metabolic functions) remain (Moran, 2002; McCutcheon and Moran, 2012; Wolf and Koonin, 2013).

However, bacterial symbionts predominantly show massive reduction in their genomes (McCutcheon and Moran, 2012). For example *Mycoplasma* features one of the smallest genomes evolved from a bacterial ancestor (Woese *et al.*, 1980). Interestingly, the smallest bacterial genome overlaps extensively with viral genomes as well as with that of organelles. Therefore, the assignment of symbiotic intracellular pathogens and organelles is starting to blur (McCutcheon, 2010). However, mitochondria as well as chloroplasts are probably the result of extensive genome reduction processes, which directly demonstrates the significance of this process in evolution (Wolf and Koonin, 2013).

The deleted genes or gene sets are often related to central biosynthetic pathways which are responsible e.g. for the biosynthesis of sugars or amino acids, since the respective end product

can be probably taken up easily from the hosts which are offering a rich nutrient source (Casadevall, 2008). The obligate intracellular growing *Rickettsia* show e.g. loss of genes involved in amino acid biosynthesis, purine biosynthesis or the formation of sugars (Renesto *et al.*, 2005). Furthermore, genes related to DNA repair mechanisms are often depleted, though a specific set of repair genes always is retained in the genome in the respective pathogens (Moran *et al.*, 2008).

In general, the intracellular bacteria might benefit from this process of genome reduction, since it increases the fitness of the bacteria inside the host due to improvements in the bacterial-host interactions (pathoadaption) (Casadevall, 2008). This is for example seen in *Shigella* spp., which has lost the lysine decarboxylase enzyme, which converts lysine to cadaverine. This reaction product normally inhibits certain violence factors of bacteria. Due to this gene loss, the inhibitory effect is depleted, which leads to an improved virulence and therefore probably enhanced fitness of *Shigella* in the interaction with its host (Maurelli *et al.*, 1998). Interestingly, the presence of this gene is characteristic for non-pathogenic bacteria and it is present in most of the *E. coli* strains (Edwards and Ewing, 1972). Furthermore, a high number of intracellularly living microbes have lost their mobility due to the loss of flagellation. This might be beneficial, since the flagellin protein might be recognized by the immune system. However, the loss of this protein could also be a result of changes in the bacterial metabolism (Pallen and Wren, 2007; Casadevall, 2008).

Nevertheless, gene acquisition by the intracellular pathogens from the eukaryotic host is also possible, as it was discovered e.g. for *L. pneumophila.* Amoeba represent the preferred host of this microbe. However, it could be shown that *L. pneumophila* feature numerous eukaryotic-like genes, which are probably derived from their amoeba host though horizontal gene transfer (Cazalet *et al.*, 2004).

1.2 Legionella pneumophila

1.2.1 History and clinical relevance

L. pneumophila is a Gram negative, flagellated, facultative intracellular bacterium, which owned its name from its first epidemic outbreak in 1979 in Philadelphia. Thereby, 180 people got infected during a convention of the American Legion and developed pneumonia symptoms. In consequence, 29 people died due to the infection with this pathogen, which was identified

3 years later (Brenner *et al.*, 1979). The disease was therefore termed Legionnaires´ disease while the causative agent was named *Legionella pneumophila* (Fraser *et al.*, 1977; McDade *et al.*, 1977). However, the first isolation occurred earlier in 1943 from guinea pigs as a bacteria, which showed high similarity to Rickettsia (Tatlock, 1944). Furthermore, a second documented isolation from a sick guinea pig occurred only four years later in 1947 (McDade *et al.*, 1979). Interestingly, this guinea pig got infected by human blood derived from a patient, who showed symptoms of pneumonia (McDade *et al.*, 1979). In addition, Drozanski was able to isolate a further strain in 1954 from a soil sample, which was a first demonstration that this bacteria has the ability for amoeba infection (Drozanski, 1956). All these strains where identified as *L. pneumophila* several years later in 1996 (Hookey *et al.*, 1996).

In general, *L. pneumophila* is widespread in natural aquatic systems, normally replicating in numerous free-living protozoan hosts (Rowbotham, 1980; Steinert *et al.*, 2002; Steinert and Heuner, 2005; Valster *et al.*, 2010). Until now, 14 different amoeba species like e.g. *A. castellanii* or *Hartmannella vermiformis*, two ciliated protozoa species and furthermore one slime mold species have been identified as potential hosts for this intracellular pathogen (Rowbotham, 1980; Fields, 1996). *L. pneumophila* is often found in human made artificial aquatic systems like air conditioners, water towers or whirlpools (Fields, 1996; Nguyen *et al.*, 2006). Therefore, these bacteria are able to replicate at temperatures between 25°C and 42°C, but prefer a replication temperature of 35°C, which is higher than the normal ambient temperature (Katz and Hammel, 1987). This explains the increased presence of this microbe in artificial water systems, which often offer higher water temperatures, what subsequently leads to higher transmission rates upon humans (Fields *et al.*, 2002). Due to the inhalation of contaminated aerosols derived from these artificial bacterial reservoirs, *L. pneumophila* is also able to infect human alveolar macrophages, thereby causing the severe pneumonia Legionnaires´ disease (Fraser *et al.*, 1977; Fields, 1996; Nguyen *et al.*, 2006). Since a direct transfer from one person to another was not reported for a long time, human alveolar macrophages have been seen as the dead end of *L. pneumophila* replication (Ensminger *et al.*, 2012). Nevertheless, in 2016 a first person-to-person transition was reported (Correia *et al.*, 2016).

The infection with *L. pneumophila* does not necessarily lead to any disease symptoms (Boshuizen *et al.*, 2001). However, immunodeficient patients can develop severe pneumonia,

_____

or a weaker flu like infection (Fraser *et al.*, 1977; Glick *et al.*, 1978). Currently, more than 50 members of the *Legionella* species have been identified and almost half of them can cause human illness. However, most of the clinical cases are related to infections with *L. pneumophila* or *L. longbeachae* (Newton *et al.*, 2010; Hilbi *et al.*, 2011).

1.2.2 Infection of host cells and developmental life cycle

As mentioned before, *L. pneumophila* is an intracellular pathogen, which replicates in various protozoan hosts, but is also able to survive extracellularly in biofilms (Rowbotham, 1980; Fields, 1996; Declerck, 2010). In both cases, this microbe alters between at least two morphological forms, that differ in e.g. shape or motility (Molofsky and Swanson, 2004). This biphasic life cycle of *L. pneumophila* comprises a non-virulent replicative phase, in which the bacteria appear as rod shaped, non-motile and metabolically active microbes. In the second growth phase, the transmissive stage, *L. pneumophila* appears as a shorter thicker rod, which is motile, stress resistant and infectious (Rowbotham, 1986; Byrne and Swanson, 1998; Molofsky and Swanson, 2004; Brüggemann *et al.*, 2006). The developmental switch is thereby triggered by the respective environment and nutrient conditions. This means that, after host cell invasion, the nutrient rich surrounding triggers the expression of replicative traits, leading to proliferating and metabolically active bacteria. In contrast, if nutrients are getting limited, the expression of transmissive traits is induced, leading to shortened and motile microbes, which are now able to leave their host cell and infect new ones, subsequently developing into the replicative form (Byrne and Swanson, 1998; Molofsky and Swanson, 2004; Brüggemann *et al.*, 2006; Faucher *et al.*, 2011). This biphasic life cycle can be remodeled in broth culture, were *L. pneumophila* switches between an exponential phase form (EPF) and a stationary phase form (SPF). Thereby, the EPF resembles the replicative phase form (RPF) inside a host cell and the SPF resembles the virulent and motile transmissive form, also called the mature infections form (MIF), which is developed *in vivo* (Molofsky and Swanson, 2004; Robertson *et al.*, 2014). The two morphological forms which developed during replication *in vitro* (EPS) or *in vivo* (RPF) do not differ from each other, whereas the *in vitro* infectious form (SPF) is not as resistant to e.g. antibiotics, does not show as many inclusions of the bacterial storage compound PHB and is furthermore not as infectious as the *in vivo* developed MIF (Faulkner and Garduno, 2002; Garduno *et al.*, 2002). Therefore, the SPF is presumably more similar to the transmissive forms which are produced in biofilms in the natural replication cycle of this

pathogen (Robertson *et al.*, 2014). However, further developmental forms like e.g. a non-cultivatable spore like form or a filamentous form, have been reported, which indicates that the life cycle of *L. pneumophila* rather resembles a developmental network (Al-Bana *et al.*, 2014; Robertson *et al.*, 2014).

The infection of protozoan hosts as well as of macrophages by *L. pneumophila* occurs *via* phagocytosis (Horwitz, 1984). This process and furthermore the establishment of a special replication compartment inside the host cell, the so-called *Legionella*-containing vacuole (LCV), is dependent on a functional Icm/Dot (intracellular multiplication/defective organelle trafficking) type IV secretion system (T4SS), which enables the translocation of more than 300 effectors (Ensminger and Isberg, 2009; Zhu *et al.*, 2011; Isaac and Isberg, 2014; Burstein *et al.*, 2016). The indispensability of this secretory machinery in this microbe was demonstrated *via* deletion mutants, which were unable to replicate inside a host cell and in contrast were soon degraded by the host cell lysosomal system (Roy and Isberg, 1997; Zink *et al.*, 2002).

The numerous translocated effectors target various cellular processes of the host cell, thereby also inducing the recruitment of endoplasmic reticulum-derived compartments, which are used to establish the replication niche (LCV) of *L. pneumophila* (Shin and Roy, 2008). Furthermore, the effector proteins directly target signaling molecules in the host, like small GTPases or phosphoinositide lipids as well as ubiquitination of apoptosis related factors (Hubber and Roy, 2010; Rolando and Buchrieser, 2012; Haneburger and Hilbi, 2013; Rothmeier *et al.*, 2013; Hoffmann *et al.*, 2014a). Also secretory mechanisms of the host cell as well as retrograde trafficking mechanisms are manipulated by this predator (Hubber and Roy, 2010; Rolando and Buchrieser, 2012; Horenkamp *et al.*, 2014; Weber *et al.*, 2014). However, most of the functions of this high number of effector proteins are still unknown, although some show functional redundancy, which is probably related to the adaption to various host systems (O'Connor *et al.*, 2011; Isaac and Isberg, 2014). However, *L. pneumophila* features further secretory systems besides the well-studied Icm/Dot T4SS. It was shown that also a type V, a Lss type I and a Lss type II secretory system is present in this intracellular pathogen. It was furthermore demonstrated that the latter one is also essential for intracellular replication of this microbe in amoeba and macrophages (Hales and Shuman, 1999; Liles *et al.*, 1999).

_____

1.2.3   CsrA as a key player in the developmental regulatory network

During the developmental switch from the transmissive to the replicative phase or the other way around, *L. pneumophila* undergoes a transcriptional switch, which leads to morphological and metabolic changes, which are characteristic for the respective growth phase (Brüggemann *et al.*, 2006; Faucher *et al.*, 2011). Thereby, the availability of certain nutrients like amino acids, iron or nucleosides represent a key regulatory trigger, inducing changes in the developmental life cycle (Byrne and Swanson, 1998; Wieland *et al.*, 2005; Cianciotto, 2007; Faucher *et al.*, 2011; Fonseca *et al.*, 2014). However, various regulatory proteins have been identified in *L. pneumophila*, interacting within a complex regulatory network, which is under the control of the life stage specific appearance of this intracellular pathogen. One of the key players for the developmental switch is CsrA, which acts on a post-transcriptional level. During replication, this protein induces the expression of replicative traits by simultaneously repressing transmissive traits, like motility or virulence (Molofsky and Swanson, 2003; Vakulskas *et al.*, 2015). Nevertheless, further regulatory factors take part in the developmental system of *L. pneumophila,* which are, amongst others also responsible for the regulation of CsrA. This network will schematically be described in the following passage.

Under nutrient starvation, the production of the second messenger guanosine-3´,5´-bispyrophosphate (ppGpp) is induced, which leads to further downstream regulatory processes (Hammer and Swanson, 1999; Dalebroux *et al.*, 2010). Thereby, this alarmone is synthesized *via* two enzymes. The first one is RelA, which is induced due to low amino acid concentrations leading to higher amounts of uncharged tRNAs, which are recognized by this ribosome-associated enzyme due to accumulation at the ribosome (Dalebroux *et al.*, 2009; Dalebroux *et al.*, 2010). The second ppGpp synthesizing protein is SpoT, which is induced when the concentration of short chain fatty acids increases, thereby directly linking reduced fatty acid biosynthesis with the induction of virulence traits (Edwards *et al.*, 2009). In consequence of high levels of the alarmone ppGpp, activity and stability of the central regulator RpoS is induced. This alternative sigma factor represents a further key regulator, besides CsrA, for the developmental switch of *L. pneumophila* (Bachman and Swanson, 2001; Zusman *et al.*, 2002; Molofsky and Swanson, 2003). Besides others, RpoS is responsible for gene regulation, activation of the quorum sensing system or the induction of the two-component system LetA/LetS (Hammer and Swanson, 1999; Bachman and Swanson, 2001; Tiaden *et al.*, 2007;

Hovel-Miner *et al.*, 2009; Dalebroux *et al.*, 2010). It has been shown earlier, that the latter one, the two-component system LetA/LetS, is crucial for the induction of transmissive traits (Hammer *et al.*, 2002). Furthermore, experiments with a LetA deletion mutant demonstrated that besides the significance of this system in intracellular replication in *A. castellanii* numerous *icm/dot* virulence genes showed altered expression in a LetA dependent manner (Gal-Mor and Segal, 2003). However, the most important effect of the induction of LetA/LetS *via* RpoS is, that in consequence the transcription of the three small non-coding RNAs RsmX, RsmY and RsmZ is induced, which leads to the downregulation of CsrA (Rasis and Segal, 2009; Sahr *et al.*, 2009; Sahr *et al.*, 2012). As mentioned above, CsrA acts as a post-transcriptional regulator, thereby activating genes important for replication while simultaneously repressing transmissive trait proteins. In presence of high amounts of the three non-coding RNAs, the concentration of CsrA is reduced due to the binding of this central regulator by RsmX, RsmY and RsmZ. In consequence, this leads to the induction of the developmental switch towards the transmissive phenotype while simultaneously replicative traits are repressed (Rasis and Segal, 2009; Sahr *et al.*, 2009; Sahr *et al.*, 2012). Beside these non-coding RNAs, further systems are responsible for the adjustments of CsrA levels in *L. pneumophila*. One is the two-component system PmrA/PmrB, which itself is regulated by RpoS (Hovel-Miner *et al.*, 2009). PmrA/PmrB depletion mutants showed reduced levels of CsrA and replication defects, confirming its role in this regulatory network (Al-Khodor *et al.*, 2009). Another participant in this network, that determines the developmental switch of *L. pneumophila* by the adjustment of CsrA concentrations, is the integration host factor (IHF) (Morash *et al.*, 2009). Its expression is again controlled by RpoS and it enhances, together with the LetA/LetS two-component system, the production of the small non-coding and CsrA binding RNAs (Zhao *et al.*, 2007).

1.2.4   Metabolic potential of *L. pneumophila*

Early metabolic studies revealed, that amino acids represent the main carbon and energy source for the facultative intracellular pathogen *L. pneumophila,* whereas especially serine but also threonine were supposed to be the major metabolic substrates (Pine *et al.*, 1979; George *et al.*, 1980; Tesh and Miller, 1981). This was in agreement with later investigations, which demonstrated high activities for the serine dehydratase enzyme (*lpp0854*) as well as for the pyruvate carboxylase enzyme (*lpp0531*), again highlighting the importance of this amino acid

_____

as nutrient for this microbe (Keen and Hoffman, 1984). Thereby, serine is presumably taken up *via* the serine transporter Lpp2269 (Cazalet *et al.*, 2004; Eylert *et al.*, 2010). Recent labelling experiments with ^{13}C-serine revealed, that this amino acid is indeed incorporated and metabolized in high rates, subsequently feeding energy generating metabolic pathways, but also serving as precursor for *de novo* biosynthesis of amino acids and PHB (Eylert *et al.*, 2010; Gillmaier *et al.*, 2016).

Nevertheless, experiments in defined media as well as labeling experiments revealed, that this pathogen is also auxotroph for several amino acids including arginine, cysteine, isoleucine, leucine, methionine, valine, serine and threonine (Pine *et al.*, 1979; George *et al.*, 1980; Tesh and Miller, 1981; Eylert *et al.*, 2010). This is in agreement with later conducted genome analysis experiments with several strains of *L. pneumophila* as well as with *L. longbeachae* (Cazalet *et al.*, 2004; Chien *et al.*, 2004; Steinert *et al.*, 2007; Cazalet *et al.*, 2010; D'Auria *et al.*, 2010). However, the dependency on amino acids as nutrients is also reflected in the genome of this pathogen, where a bunch of amino acid and protein transporters like e.g. ATP dependent transporters, permeases or proteases have been identified (Cazalet *et al.*, 2004; Chien *et al.*, 2004).

The whole metabolic potential of *L. pneumophila* for the usage of further substrates, like carbohydrates or fatty acids besides amino acids, remained unclear for a long time, although enzymes of all core metabolic pathway e.g. the glycolytic pathway, the TCA cycle, the non-oxidative part of the PPP, with the exception of a transaldolase, or the ED pathway are present in the genome of this pathogen (Cazalet *et al.*, 2004; Chien *et al.*, 2004; Cazalet *et al.*, 2010). In addition, early studies with ^{14}C labeled glucose and further substrates like glycerol or acetate indicated the usage of these precursors by *L. pneumophila*, although glucose did not support bacterial growth *in vitro* (Pine *et al.*, 1979; Warren and Miller, 1979; Weiss *et al.*, 1980; Tesh *et al.*, 1983). Furthermore, the preferred degradation pathway of glucose was unclear. However, it was suggested that *L. pneumophila* uses more efficiently the PPP and the ED pathway for glucose degradation than glycolytic reactions (Weiss *et al.*, 1980; Tesh *et al.*, 1983). Using isotopologue profiling experiments it could finally be demonstrated that this microbe is indeed able to efficiently incorporate and metabolize glucose predominantly *via* the ED pathway (Eylert *et al.*, 2010). Mutants concerning enzymes of this biosynthetic pathway were unable to efficiently metabolize this hexose and furthermore showed significant

replication defects inside *Acantamoeba castellanii*, also highlighting the importance of this metabolic pathway (Harada *et al.*, 2010). Besides glucose, *L. pneumophila* is also able to use exogenous polysaccharides as carbon source. Experiments with the eukaryotic-like glucoamylase (GamA) revealed, that this enzyme enables the effective degradation and therefore metabolisation of glycogen and starch probably during intracellular replication in *A. castellanii,* although this enzyme is not essential for *in vitro* or *in vivo* replication (Herrmann *et al.*, 2011). In addition, this bacterium is equipped with a chitinase as well as with an endoglucanase, which enables the degradation of cellulose and underlines the importance of polysaccharides in the *L. pneumophila* nutrition (DebRoy *et al.*, 2006; Pearce and Cianciotto, 2009).

Early *in vitro* studies indicated, that *L. pneumophila* uses glycerol as carbon source (Tesh *et al.*, 1983). These findings were emphasized by following transcriptome experiments, which showed that genes responsible for glycerol metabolism e.g. *glpK* or *glpD* were highly upregulated during intracellular replication in macrophages (Faucher *et al.*, 2011). Furthermore, a mutant concerning *glpD* in *L. oakridgensis* was not able to replicate in *A. castellanii* (Brzuszkiewicz *et al.*, 2013). However, the metabolic potential of *L. pneumophila* for glycerol metabolism remained unknown. Nevertheless, it was demonstrated for further intracellular pathogens that glycerol nutrition plays a central role in the metabolic concept of e.g. *Listeria monocytogenes* (Grubmüller *et al.*, 2014) or *Salmonella enterica* (Steeb *et al.*, 2013).

Currently, the metabolic potential of fatty acids as nutrients is not well studied for *L. pneumophila*. However, genes involved in the biosynthesis as well as in the degradation of fatty acids have been found to be present due to genome analysis (Cazalet *et al.*, 2004; Chien *et al.*, 2004). In addition, this pathogen features numerous phospholipases which are largely known to be involved in *L. pneumophila* virulence and are predominantly expressed in the mid exponential or transmissive growth phase (Flieger *et al.*, 2000; Flieger *et al.*, 2004; Schunder *et al.*, 2010). Thereby, the cell-associated hemolytic phospholipase A (PlaB), which preferably hydrolyzes long-chain fatty acids with more than twelve carbon atoms, represents the main hydrolytic activity of this intracellular pathogen. In general, the hydrolytic potential of *L. pneumophila* could be crucial in *L. pneumophila* pathogenicity (Bender *et al.*, 2009). Furthermore, short chain fatty acids seem to trigger the switch between the two growth phases,

the replicative and the transmissive phase, again indicating that fatty acid metabolism and virulence are linked in this pathogen (Edwards *et al.*, 2009). Further studies now suggest a metabolic role of fatty acids in the core metabolism of *L. pneumophila*, especially concerning the biosynthesis of the bacterial carbon and energy storage compound PHB (Edwards *et al.*, 2009; Hayashi *et al.*, 2010; Gillmaier *et al.*, 2016).

1.3 Coxiella burnetii

1.3.1 History and clinical relevance

The intracellular pathogen *C. burnetii* was first described in 1937 as the causative agent of a newly recognized fever which appeared in numerous abattoir workers in Queensland, Australia (Derrick, 1937). In the same year the causative organism was defined as a new type of the Rickettsia species (Burnet and Freeman, 1937) and subsequently the first isolation from ticks occurred in 1938 in the USA (Davis *et al.*, 1938). However, due to genomic and phylogenetic studies this pathogen is no longer categorized in the α-proteobacteria Rickettsia group but was identified as a γ-proteobacteria with *L. pneumophila* as its closest relative (Roux *et al.*, 1997; Seshadri *et al.*, 2003; Beare *et al.*, 2009). Nevertheless, recent studies revealed that these two intracellular pathogens developed in a rather distant evolutionary process (Pearson *et al.*, 2013; Duron *et al.*, 2015). Thereby, an endosymbiont of ticks was recently identified as the ancestor of *C. burnetii* (Duron *et al.*, 2015).

It is now known that this obligate intracellular Gram negative bacterium is distributed worldwide and capable of infecting various hosts including diverse vertebrate and invertebrate species as well as a multitude of mammalian tissues (Babudieri, 1959; Weber *et al.*, 2013; Larson *et al.*, 2016). In humans, this pathogen causes a worldwide-distributed zoonosis called Q-fever, which is characterized by typical flu-like symptoms, but could also lead to pneumonia in its acute form or to hepatitis and endocarditis if the infection becomes chronical (Maurin and Raoult, 1999; Arricau-Bouvery and Rodolakis, 2005; van Schaik *et al.*, 2013; Larson *et al.*, 2016). Human outbreaks of Q-fever are predominantly related to infected goats, sheep or dairy cattle which spread *C. burnetii* into the environment *via* contaminated fluids like milk, urine, amniotic fluids or feces (Raoult *et al.*, 2000; Angelakis and Raoult, 2010). Therefore, humans mainly get infected *via* the direct contact to infected animals due to the inhalation of contaminated aerosols. Besides that no direct contact to a farm animal can also lead to an infection due to the fact that this very robust bacteria can be spread by the wind and is thereby

able to cover long distances (Raoult *et al.*, 2000). Oral infection (*via* contaminated food) as well as direct human to human transfer has also been reported but appear rarely (Marrie and Raoult, 1997; Raoult *et al.*, 2000). Animals predominantly carry chronical infections of *C. burnetii* but predominantly do not show any symptoms (Maurin and Raoult, 1999). Distribution between animals generally occurs *via* tick bites (Philip *et al.*, 1966). The fact, that only one bacterium is sufficient to cause an infection and its ability to form very robust bacterial spores, makes this pathogen a type-B bioweapon (Fournier *et al.*, 1998; Madariaga *et al.*, 2003; Cogliati *et al.*, 2016).

1.3.2   Infection and developmental life cycle

As mentioned above, the intracellular pathogen *C. burnetii* can form specific small-cell variants (SCVs), which are capable to survive long time-periods in the environment due to high robustness to various harsh environmental conditions e.g. heat or dryness (Coleman *et al.*, 2004; Coleman *et al.*, 2007). After host cell invasion the transition into the large-cell variants, which are metabolically active, is induced (Coleman *et al.*, 2004).

Alveolar macrophages represent the prime target of *C. burnetii* in the natural host cell invasion, but these bacteria are also capable of subsequently invading further cells and tissues (Khavkin and Tabibzadeh, 1988; Stein *et al.*, 2005; Calverley *et al.*, 2012; Graham *et al.*, 2013; Graham *et al.*, 2016). For example, adipocytes serve as a reservoir for the persistence of this pathogen whereas trophoblasts are favored targets of *C. burnetii* in female hosts (Sánchez *et al.*, 2006; Bechah *et al.*, 2014). The internalization of host cells occurs passively due to invasion studies with macrophages and fibroblasts, which revealed that internalization of both, living or dead *C. burnetii*, was comparably effective (Baca *et al.*, 1992; Tujulin *et al.*, 1998). This is in agreement with experiments with protease treated *C. burnetii*, which were subsequently unable to invade host cells, indicating that proteins on the surface of this bacteria act as invasins (Baca *et al.*, 1992). Using a microscopy-based high-throughput screening, the surface protein OmpA could recently be identified as an invasin of this intracellular pathogen (Martinez *et al.*, 2014). After the invasion process, this pathogen establishes a replicative niche in the respective host cell, which is termed *Coxiella*-containing vacuole (CCV) and which occupies most of the cytosolic space at later developmental stages (Howe *et al.*, 2003; Larson *et al.*, 2016). This phagolysosome-like replication compartment is unique compared to the replication niches of other intracellular bacteria due to the acidic conditions which are present in the CCV (Howe *et*

al., 2010; Schulze-Luehrmann *et al.*, 2016). The CCV also differs to the replication compartment of the close relative *L. pneumophila*, the LCV, which is predominantly derived from the endoplasmic reticulum and comprises a neutral environment (Hubber and Roy, 2010). However, *C. burnetii* depends on acidic conditions since they trigger the developmental switch from the SCV to the LCV and therefore induce metabolic activity of the pathogen as well as the induction of protein expression of various effectors, which are involved in numerous infection processes as well as inhibition of apoptosis (Howe *et al.*, 2003; Coleman *et al.*, 2004; Voth *et al.*, 2007; Larson *et al.*, 2016).

Intracellular survival, acquisition of sufficient amounts of nutrients and in particular the establishment of the specific intracellular replication compartment CCV is dependent on a type IVB secretion system (T4BSS), which is a homologue of the secretion system used by *L. pneumophila* (Seshadri *et al.*, 2003; Beare *et al.*, 2011; Carey *et al.*, 2011). Both systems translocate high numbers of effector proteins into the host cell. Up to now, more than 300 effector proteins are known for *L. pneumophila* (Burstein *et al.*, 2016; Hofer, 2016) whereas the secretion system of *C. burnetii* is responsible for the translocation of a smaller number of 60 effector proteins, most of which the function is still not known of (Chen *et al.*, 2010; Carey *et al.*, 2011; Newton *et al.*, 2013; Weber *et al.*, 2013).

Intracellular nutrient acquisition as well as vacuolar expansion during maturation of the CCV, which takes place over several days, is furthermore dependent on extensive fusion with autophagosomes (Winchell *et al.*, 2014). Furthermore, this pathogen interacts with endocytic and secretory pathways (Larson *et al.*, 2016). However, during the maturation process the host cell morphology is only minimally effected since this pathogen is adapted to maintain host cell viability (Coleman *et al.*, 2004).

1.3.3 Role of CsrA in the regulatory network of *C. burnetii*

Currently, only four regulatory two-component systems have been identified for *C. burnetii*, which illustrate a small number compared to other Gram-negative intracellular bacteria (Seshadri *et al.*, 2003; Beare *et al.*, 2009). However, the two-component system GacA/GacS, which is a homolog of the two-component system LetA/LetS of *L. pneumophila*, is present (Seshadri *et al.*, 2003; Chien *et al.*, 2004; Beare *et al.*, 2009). The LetA/LetS system is crucial in the CsrA-regulatory cascade in *L. pneumophila*, which was already discussed in section 1.2.3. In short, CsrA induces replicative traits by simultaneously repressing transmissive traits

on a post-transcriptional level during the replicative phase in *L. pneumophila* (Molofsky and Swanson, 2003). Nutrient limited conditions lead to the production of the alarmone ppGpp under the control of SpoT and RelA. Subsequently, activity and stability of the alternative sigma factor RopS is induced, which leads besides others to the induction of the two-component system LetA/LetS (Molofsky and Swanson, 2003; 2004). The LetA/LetS system is then responsible for the production of small non-coding RNAs, which bind and therefore inactivate CsrA, leading to the activation of transmissive traits (Rasis and Segal, 2009; Sahr *et al.*, 2009; Sahr *et al.*, 2012). Since one or two genes for all of these regulators are conserved in *C. burnetii* isolates (*spoT*: CBU0303; *relA*: CBU1375; *rpoS*: CBU1609; *csrA*: CBU0024 and CBU1050), a similar role to that in *L. pneumophila* appears likely. Therefore, also the function of GacA/GacS in *C. burnetii* is probably similar to that of the LetA/LetS system in *L. pneumophila* (Seshadri *et al.*, 2003; Mercante *et al.*, 2006; Beare *et al.*, 2009). Furthermore, the two-component system QseB/QseC of *C. burnetii* seems to be similar to the PmrA/PmrB system of *L. pneumophila*, which is also part of the CsrA-regulatory cascade in *L. pneumophila* (Seshadri *et al.*, 2003; Al-Khodor *et al.*, 2009; Beare *et al.*, 2009; Hovel-Miner *et al.*, 2009). In addition, it is also important in the regulation of the Dot/Icm type IV secretion in both pathogens (Zusman *et al.*, 2007; Beare *et al.*, 2009). On the other hand, the two-component system CpsA/CpxR, which is present in *L. pneumophila* and also involved in the Dot/Icm T4SS regulation, could not be found in the genome of *C. burnetii* until now (Feldman *et al.*, 2005; Beare *et al.*, 2009). Nevertheless, the developmental switch between the different morphological forms (SCV and LCV) in the biphasic life cycle is likely regulated by the interplay within the CsrA-regulatory network, similar to that reported for *L. pneumophila* (Coleman *et al.*, 2004).

1.3.4   Metabolic potential of *C. burnetii*

Since the possibility to grow this intracellular pathogen in an axenic medium has only been developed recently, the metabolic potential of *C. burnetii* is only poorly understood (Omsland *et al.*, 2009; Omsland *et al.*, 2011; Omsland *et al.*, 2013). However, the composition of the newly developed Acidified Citrate Cysteine Medium 2 (ACCM-2) as well as genome based analysis give a first idea about the preferred nutrients and the metabolic concept of this pathogen (Seshadri *et al.*, 2003; Omsland *et al.*, 2009; Omsland *et al.*, 2011). Compared to other intracellular bacteria, the process of genome reduction is at an early stage, since a high

percentage (more than 89.1%) of the genome is still coding for proteins (Andersson and Kurland, 1998; Seshadri *et al.*, 2003). Enzymes of the glycolytic cascade, gluconeogenesis, the PPP and the TCA cycle as well as some enzymes of the ED pathway are present in the genome of *C. burnetii* (Seshadri *et al.*, 2003). However, in contrast to its close relative *L. pneumophila*, which preferably uses the ED pathway for glucose degradation, *C. burnetii* seems to prefer glycolytic reactions, although a classical hexokinase has not been identified based on genome analysis of this pathogen (McDonald and Mallavia, 1971; Hackstadt and Williams, 1981a; Hackstadt and Williams, 1981b). Anyway, the activity of a hexokinase as well as the conversion of glucose 6-phosphate (Glu-6-P) to 6-phosphogluconate (6-PG) and ribulose 5-phosphate have been demonstrated, although the respective enzymes have not been identified based on genome analysis (Consigli and Paretsky, 1962; Paretsky *et al.*, 1962; McDonald and Mallavia, 1970). Furthermore, also the shikimate/chorismate pathway is present in *C. burnetii*, although enzymes for the final steps in the biosynthesis of aromatic amino acids have not been identified (Seshadri *et al.*, 2003; Walter *et al.*, 2014). Nevertheless, enzymes for the production of further amino acids and fatty acids and the biosynthesis of vitamins and nucleic acids are present, whereas enzymes of the glyoxylate pathway are not (Seshadri *et al.*, 2003). Additionally, *C. burnetii* features a transporter for long chain fatty acids (CBU1242) as well as two sugar transporters (CBU0265 and CBU0347) and numerous amino acid and peptide transporters (Seshadri *et al.*, 2003; Kuley *et al.*, 2015). In combination with the composition of the recently developed axenic medium ACCM-2, which comprises high amounts of amino acids and peptides, this suggests that amino acids are among the major substrates of this pathogen (Seshadri *et al.*, 2003; Sandoz *et al.*, 2016). However, also further substrates seem to be used by *C. burnetii*, since glucose is present in ACCM-2 and since enzymes responsible for the degradation of glycerol are present in its genome (Seshadri *et al.*, 2003; Omsland *et al.*, 2009; Omsland *et al.*, 2011).

1.4 Aims of the thesis

The two closely related bacteria *L. pneumophila* and *C. burnetii* represent two examples of intracellular replicating pathogens featuring a biphasic life cycle (Coleman *et al.*, 2004; Molofsky and Swanson, 2004; Beare *et al.*, 2009). During their life cycle, both bacteria are exposed to numerous extra- and intracellular niches, thereby undergoing different morphological changes, which are controlled by a complex CsrA-dependent regulatory

network (Coleman *et al.*, 2004; Molofsky and Swanson, 2004). This regulatory network is triggered by the nutritional composition of the environment which changes permanently during the life cycle (Byrne and Swanson, 1998; Wieland *et al.*, 2005; Cianciotto, 2007; Faucher *et al.*, 2011; Fonseca *et al.*, 2014). Since there is not much known about nutrition and the metabolic potential of *L. pneumophila* and *C. burnetii*, the aim of this thesis was the metabolically characterization and the investigation of a general metabolic concept in a growth phase dependent manner. Thereby, also the role of CsrA in the regulation of substrate usage and of metabolic fluxes in *L. pneumophila* was studied.

To investigate the relevance of glycerol in the nutrition of *L. pneumophila*, a $\Delta glpD$ mutant was used in extra- and intracellular growth assays comparative to the wild-type. Furthermore, an new minimal defined medium (MDM) was developed and used to perform growth phase dependent isotopologue profiling experiments with [U-^{13}C$_3$]glycerol, [U-^{13}C$_3$]serine and [U-^{13}C$_6$]glucose as tracers. Based on these experiments, detailed information about the glycerol catabolism in comparison with further substrates could be obtained. Furthermore, *in vivo* infection experiments were performed with all three ^{13}C-tracers in *A. castellanii*.

The importance of CsrA in the regulation of the metabolic network and main carbon fluxes in a growth phase dependent manner was determined using comparative labeling and oxygen consumption experiments with the *L. pneumophila* wild-type and a CsrA knock down mutant. Isotopologue profiling experiments were performed with [U-^{13}C$_3$]serine, [U-^{13}C$_6$]glucose and [U-^{13}C$_3$]glycerol as tracers in a time dependent manner. In addition, the importance of fatty acids as further substrates of *L. pneumophila* and the role of CsrA in the regulation of fatty acid degradation and carbon flux was investigated performing labeling experiments with [1,2,3,4-^{13}C$_4$]palmitic acid with the *L. pneumophila* wild-type and the CsrA knock out mutant. In total, the crucial role of CsrA in the life stage specific coordination of substrate usage and carbon flux in *L. pneumophila* could be demonstrated.

In order to compare the metabolic concept of *L. pneumophila* to further intracellular pathogens, nutrient usage and metabolic fluxes in its close relative *C. burnetii* were analyzed. Therefore, *in vitro* labeling experiments were performed in a recently developed axenic medium, using [U-^{13}C$_6$]glucose, [U-^{13}C$_3$]serine and [U-^{13}C$_3$]glycerol as tracer. Similar metabolic concepts could be a result of effective adaption and survival strategies to their respective intracellular

replicative niches and help to understand the complex interactions between intracellular pathogens and their host, which could in consequence give essential information for the development of new antibiotics.

_____

2 <u>MATERIALS AND METHODS</u>

2.1 Materials

2.1.1 Laboratory Equipment

Table 2-1: Laboratory Equipment

Item		Manufacturer
Benchtop centrifuge	A-14	Jouan GmbH (Unterhaching, Germany)
Centrifuge	Biofuge primo R	Heraeus (Traunstein, Germany)
Drying oven	E28	Binder GmbH (Tuttlingen, Germany)
Freeze-dryer	Alpha 2-4 LD plus Vacuum pump: RC 5	Christ (Osterrode, Germany) Vacuurbrand GmbH & Co. KG (Staufen, Germany)
GC/MS	Gas Chromatograph GC-2010 Mass Spectrometer QP-2010 Auto Injector AOC-20i Auto Sampler AOC-20s GC Column: Equity^{TM}-5, FUSED SILICA Capillary Column, 30 m x 0.25 mm x 0.25 µm film thickness	Shimadzu (Neufahrn, Germany) Shimadzu (Neufahrn, Germany) Shimadzu (Neufahrn, Germany) Shimadzu (Neufahrn, Germany) SUPELCO (Bellefonte, USA)
Glass beads	0.25 – 0.55 mm	Roth (Karlsruhe, Germany)
Heating block	Techne DRI-Block® DB 2A	Thermo-DUX GmbH (Wertheim, Germany)
Magnetic stirrer	MR Hei-Standard	Heidolph (Schwabach, Germany)
Micro scales	VWR-503B, (0.001 g – 500 g)	VWR (Radnor, USA)
Ribolyser		Hybaid (Kalletal, Germany)
Rotary evaporator	Rotavapor-R Diaphragm vacuum pump Water bath	Büchli (Flawil, Switzerland) Vacuubrand GmbH & Co. KG (Wertheim, Germany) Heidolph (Schwabach, Germany)
Thermostat	IKATRON® ETS-D4 fuzzy	IKA-Werke GmbH & Co. KG (Staufen, Germany)
Ultrasonic bath	USC 300T	VWR (Radnor, USA)
Vortex mixer	Reax 2000	Heidolph Elektro GmbH & Co. KG (Kelheim, Germany)

2.1.2 Software used

Table 2-2: Software used

Software		Manufacturer
Adobe Illustrator	Adobe Illustrator CS4	Adobe Systems GmbH (Munich, Germany)
ChemOffice 2015	ChemDraw Professional 15.0 ChemFinder 15.0	CambridgeSoft (Massachusetts; USA)
CorelDRAW Graphics Suite X7 (64-bit)	CorelDRAW X7 (64-bit)	Corel GmbH (Munich, Germany)
EndNote	EndNote Version X8 (Windows)	Clarivate Analytics (New York, USA)
GCMS Solution	GCMS Analysis Editor GCMS Postrun Analysis GCMS Real Time Analysis	Shimadzu Corporation (Kyoto, Japan)
GraphPad Prism	Prism 4.03 (Windows)	GraphPad Software (La Jolla, USA)
Microsoft Office 2013	Excel 2013 Word 2013 PowerPoint 2013	Microsoft (Redmond, USA)

2.1.3 Chemicals

Labeled precursors ($[U-^{13}C_6]$glucose, $[U-^{13}C_3]$glycerol, $[U-^{13}C_3]$serine and $[1,2,3,4-^{13}C_4]$palmitic acid) were received from Isotec/Sigma-Aldrich (St. Louis, USA) or Cambridge Isotope Laboratories (Tewksbury, USA).

Further chemicals used in this work where received from AppliChem GmbH (Darmstadt, Germany), BD Biosciences (Franklin Lakes), Bio-Rad (Munich, Germany), Eppendorf (Hamburg, Germany), Merck (Darmstadt, Germany), Carl Roth GmbH & Co. KG (Karlsruhe, Deutschland), Sigma-Aldrich (St. Louis, USA), Thermo Fisher Scientific (Waltham, USA) and VWR (Radnor, USA).

All the solvents used were at least of HPLC grade.

2.2 Methods

2.2.1 Experiments with *L. pneumophila* JR32 Philadelphia-1 serogroup 1 and its Δ*glpD* mutant

Construction of a *L. pneumophila* JR32 Δ*glpD* mutant, development of the MDM, extracellular growth of *L. pneumophila*, infection assays with *A. castellanii* and Murine Raw 264.7

macrophages as well as *in vitro* and *in vivo* cultivation in presents of ^{13}C tracers ([U-^{13}C$_6$]glucose, [U-^{13}C$_3$]serine and [U-^{13}C$_3$]glycerol) were performed by Christian Manske at the Max von Pettenkofer Institut at the Ludwig-Maximilians Universität in Munich under the supervision of Prof. Dr. Hubert Hilbi. Sample preparations, GC/MS measurements, establishment of a new isotopologue profiling method for analyzing polar metabolites, isotopologue analysis and calculations (see sections 2.2.4.1-2.2.4.5) were performed by Ina Häuslein in the laboratory of Prof. Dr. Wolfgang Eisenreich (TUM). The experimental setups of all experiments were developed and evaluated by Christian Manske and Ina Häuslein under the supervision of Prof. Dr. Hubert Hilbi and Prof. Dr. Wolfgang Eisenreich. For further details see „Häuslein, I., Manske, C., Goebel, Eisenreich, W., and Hilbi, H. (2015). Pathway analysis using ^{13}C-glycerol and other carbon tracers reveals a bipartite metabolism of *Legionella pneumophila*. *Molecular Microbiology* 100, 229-246".

2.2.2 Experiments with *L. pneumophila* Paris and its *csrA* mutant

Construction of a *csrA* mutant of *L. pneumophila* Paris, bacterial cultivation, oxygen consumption experiments and labeling experiments with [U-^{13}C$_6$]glucose, [U-^{13}C$_3$]serine, [U-^{13}C$_3$]glycerol and [1,2,3,4-^{13}C$_4$]palmitic acid were performed by Tobias Sahr at the Institut Pasteur in Paris. Sample preparations, GC/MS measurements, isotopologue analysis and calculations (see sections 2.2.4.1-2.2.4.5) were performed by Ina Häuslein in the laboratory of Prof. Dr. Wolfgang Eisenreich (TUM). The experimental setups were developed and evaluated by Tobias Sahr and Ina Häuslein under the supervision of Prof. Dr. Carmen Buchrieser and apl. Prof. Dr. Wolfgang Eisenreich. Further details will be published in „**Häuslein, I.**, Sahr, T., Escoll, P., Klausner, N., Eisenreich, W., and Buchrieser, C., (**2017**). *Legionella pneumophila* CsrA regulates a metabolic switch from amino acid to glycerolipid metabolism".

2.2.2.1 *Bacteria, cells and growth conditions*

L. pneumophila strains were grown in N-(2-acetamido)-2-aminoethanesulfonic acid (ACES)-buffered yeast extract broth or an ACES-buffered charcoal-yeast extract (BCYE) agar under aerobic conditions at 37°C (**Table 2-3** and **2-4**).

In case of labeling experiments, *L. pneumophila* was grown at 37°C in a carbon enriched minimal defined media (CE MDM) (**Table 2-5**).

Table 2-3: Composition and operating instructions for the preparation of ACES-buffered yeast extract broth

ACES-buffered yeast extract broth (Horwitz and Maxfield, 1984)		
Component	**[g/L]**	Dissolve ACES and yeast extract in 900 mL ddH$_2$O. L-Cysteine and Fe(NO$_3$)$_3$ are dissolved in 10 mL ddH$_2$O respectively and added dropwise. Adjust pH to 6.9 using 10 M KOH and fill up to 1 L using ddH$_2$O. Add antibiotics at the indicated concentrations if needed. Medium is filter sterilized through a 0.2 µm filter and store it at 4°C in the dark.
ACES	10.00	
Yeast extract	10.00	
L-cysteine	0.40	
FeN$_3$O$_9$ x 9 H$_2$O	0.25	

Table 2-4: Composition and operating instructions for the preparation of BCYE agar

BCYE agar (Feeley *et al.*, 1979)		
Component	**[g/L]**	Dissolve ACES and yeast extract in 900 mL ddH$_2$O. Adjust pH to 6.9 using 10 M KOH and fill up to 1 L with ddH$_2$O. Weigh out agar and activated charcoal, add ACES/yeast extract solution and autoclave. L-Cysteine and Fe(NO$_3$)$_3$ are dissolved in 10 mL ddH$_2$O respectively, filter-sterilized and added dropwise to the cooled down solution. Add antibiotics at the indicated concentrations if needed. The mixture is distributed standard petri dishes and dried for 1 day at room temperature. Agar plates can be stored in the dark at 4°C.
ACES	10.00	
Yeast extract	10.00	
Activated charcoal	2.00	
Agar	15.00	
L-cysteine	0.40	
FeN$_3$O$_9$ x 9 H2O	0.25	

Table 2-5: Composition and operating instructions for the preparation of CE MDM

CE MDM		
Component	**[g/L]**	All components are weigh out and dissolved in 950 mL ddH$_2$O, except of Fe-pyrophosphate. Adjust pH to 6.9 with 10 M KOH, dissolve Fe-pyrophosphate and fill up to 1 L using ddH$_2$O afterwards. Filter sterilise and store in the dark at 4°C.
ACES	10.00	
L-arginine	0.35	
L-cysteine	0.40	
L-isoleucine	0.47	
L-leucine	0.64	
L-methionine	0.20	
L-threonine	0.33	
L-valine	0.48	
L-serine (6 mM)	0.65	

L-proline	0.115
L-phenylalanine	0.35
D-glucose (11 mM)	1.98
Glycerol (50 mM)	4.60g (3.7 mL)
NH$_4$Cl	0.315
NaCl	0.05
CaCl$_2$ x 2 H$_2$O	0.025
KH$_2$PO$_4$	1.18
MgSO$_4$ x 7 H$_2$O	0.07
Fe-pyrophosphate hydrate	0.25

2.2.2.2 Constructions of a csrA mutant strain

The construction of the *csrA* mutant strain of *L. pneumophila* Paris was performed by Tobias Sahr at the Institut Pasteur in Paris by inserting an apramycin-resistance cassette after the amino acid Tyr48 of the *lpp0845* gene encoding the major CsrA in *L. pneumophila* Paris (Lomma *et al.*, 2010; Sahr *et al.*, 2017).

2.2.2.3 Oxygen consumption experiments

Oxygen consumption experiments with the *L. pneumophila* Paris wild-type and the *csrA* mutant strain were performed by Tobias Sahr at the Institut Pasteur in Paris according to the following protocol: *L. pneumophila* were cultivated in BYE to exponential phase (OD$_{600}$ = 2 - 2.5) at 37°C and 170 rpm in a light-protected and humidity-controlled incubator shaker. After centrifugation, bacteria were resuspended to a final concentration of OD$_{600}$ = 0.1 using Phosphate-Buffered Saline (PBS) (**Table 2-6**). Following, 90 µL of the resuspended bacterial cells were transferred to wells of the Poly-D-lysine- (PDL) coated Microplate. To coat XF Cell Culture Microplate (Seahorse Bioscience), 15 µL of 1 mg/mL PDL in 100 mM Tris-HCl (**Table 2-7**) was added to each well. After drying overnight, the XF Cell Culture Microplate was washed two times with ddH$_2$O.

Table 2-6: Composition and operating instructions for the preparation of PBS

PBS (10 x stock solution)		
Component	**[g/L]**	
MgSO$_4$ x 7 H$_2$O	80.00	All components are dissolved in 950 mL ddH$_2$O. Adjust pH to 7.4 using 1 M NaOH or 1 M HCl and fill up to 1 L afterwards. Autoclave and store at room temperature.
CaCl$_2$	2.00	
Sodium citrate x 2 H$_2$O	14.20	
Na$_2$HPO$_4$ x 7 H$_2$O	2.40	

Table 2-7: Composition and operating instructions for the preparation of 100 mM Tris-HCl buffer

100 mM Tris-HCl		
Tris Base	12.11 g/L	Tris Base is dissolved in 900 mL ddH$_2$O. Adjust pH to 8.4 using 1 M HCl and fill up to 1 L afterwards. Autoclave and store at room temperature.

Attachment of bacterial cells occurred *via* 10 min centrifugation at 4,000 rpm using a benchtop swinging bucket centrifuge. The volume in each well was raised to 175 µL by adding PBS afterwards.

Bacterial respiration was measured in oxygen consumption rates (OCR) according to the manufacturer instructions. For quantification, a XFe96 Extracellular Flux Analyzer (Seahorse Bioscience) was used. To assure uniform cellular seeding, basal OCR were measured for approximately 30 min prior to the injections.

The final concentration of the different substances added was as follows: L-serine, L-alanine and L-glutamate: 0.1 g/L; D-glucose, glycerol, butanoate, α-ketoglutarate (α-KGL) and pyruvate: 0.2 g/L; palmitate, oleate and arachidonic acid: 0.1 mM.

2.2.2.4 *Labeling experiments with* L. pneumophila *Paris wild-type and* csrA *mutant*

For labeling experiments with [U-^{13}C$_3$]serine, [U-^{13}C$_6$]glucose, [U-^{13}C$_3$]glycerol and [1,2,3,4-^{13}C$_4$]palmitic acid as ^{13}C-precursor, *L. pneumophila* strains were grown in CE MDM. Thereby the amount of the respective unlabeled compound was displaced with 6 mM [U-^{13}C$_3$]serine, 11 mM [U-^{13}C$_6$]glucose and 50 mM [U-^{13}C$_3$]glycerol respectively. In case of labeling experiments with [1,2,3,4-^{13}C$_4$]palmitic acid, CE MDM was supplemented with additional 0.02% (0.8 mM) of this ^{13}C-precursor. The respective *L. pneumophila* strain was grown over night in 50 mL unlabeled CE MDM. The inoculum was suspended in 50 mL of CE MDM

_____

comprising the respective ^{13}C-tracer and diluted to an OD_{600} of 0.1. For every labeling experiment, bacteria were harvested at E ($OD_{600} = 0.35$) and PE ($OD_{600} = 0.80$) growth phase by centrifugation at 5000 g for 5 min at 4°C. Cells were autoclaved for 30 min at 120°C, freeze-dried and stored at −80°C until further analysis.

2.2.3 Experiments with *C. burnetii* RSA 439 NMII

Bacterial cultivation and labeling experiments with [U-[13]C_6]glucose, [U-[13]C_3]serine and [U-[13]C_3]glycerol were performed by Franck Cantet at the Infectious Disease Research Institute in Montpellier. GC/MS measurements, isotopologue analysis and calculations (see sections 2.2.4.1-2.2.4.5) were performed by Ina Häuslein under the supervision of Prof. Dr. Wolfgang Eisenreich (TUM). The experimental setups of all experiments were developed and evaluated by Franck Cantet and Ina Häuslein under the supervision of Dr. Matteo Bonazzi and apl. Prof. Dr. Wolfgang Eisenreich. For further details see **"Häuslein, I.,** Cantet, F., Reschke, S., Chen, F., Bonazzi, M., and Eisenreich, W. (**2017**). Multiple substrate usage of *Coxiella burnetii* to feed a bipartite metabolic network. *Frontiers in Cellular and Infection Microbiology* 7.*"*

2.2.4 Sample preparation and derivatization for GC/MS based isotopologue profiling

2.2.4.1 *Sample preparation of protein derived amino acids, DAP and PHB*

For isotopologue profiling of protein derived amino acid, DAP and PHB, 1 mg of the freeze dried bacterial cell pellet was resolved in 0.5 mL of 6 N HCl. Following, the sample was incubated for 24 h at 105°C, as described earlier (Eylert *et al.*, 2010). Removal of the HCl occurred under a stream of nitrogen at 70°C. The remaining residue was resolved in 200 µL acetic acid. Purification of the sampled was done *via* a cation exchange column of Dowex 50Wx8 (H+ form, 200-400 mesh, 5 x 10 mm). For this purpose, the column was washed previously with 1 mL of MeOH and 1 mL ddH$_2$O. After addition of the sample the column was evolved with 2 mL of ddH2O (eluate 1) and 1 mL of 4 M ammonium hydroxide (eluate 2). Both samples were dried at 70°C under a steam of nitrogen. The remaining residue of eluate 1 was used for PHB analysis, whereas the residue of eluate 2 was used for the analysis of protein derived amino acids and DAP.

For derivatization of 3-hydroxybutyrate (3-HBA), derived from hydrolysis of PHB during treatment with HCl, 100 µL of *N*-methyl-*N*-(trimethylsilyl)-trifluoroacetamide were added to the dried samples of eluate 1. Samples were incubated overnight at 60°C in a shaking incubator

at 110 rpm. The resulting trimethylsilyl (TMS) derivative of 3-HBA was used in following GC/MS analysis and calculations for isotopologue profiling.

For analysis of protein derived amino acids and DAP, 50 µL dry acetonitrile and 50 µL *N*-(tert-butyldimethylsilyl)-*N*-methyl-trifluoroacetamide were added to the dry residue of eluate 2. Samples were incubated for 30 min at 70°C. The resulting tert-butyl-dimethylsilyl (TBDMS) derivatives were used in following GC/MS analysis and calculations for isotopologue profiling.

The amino acids tryptophan, arginine, methionine and cysteine could not be analyzed due to degradation by acid hydrolysis. Furthermore, conversion of glutamine and asparagine to glutamate and aspartate occurred due to acid hydrolyzation. Therefore, results for aspartate and glutamate correspond to asparagine/aspartate and glutamine/glutamate, respectively.

2.2.4.2 Sample preparation of methanol-soluble polar metabolites including fatty acids

For isotopologue profiling of methanol-soluble polar metabolites, approximately 5 mg of the freeze-dried bacteria were mixed with 0.8 g of glass beads (0.25-0.05 mm) and 1 mL of pre-cooled 100% methanol. Mechanical cell lysis occurred for 3 x 20 s at 6.5 m/s using a ribolyser (Hybaid). Samples were immediately cooled down on ice for 5 min. After centrifugation at $2.300 \times g$ for 10 min the supernatant was dried under a stream of nitrogen. 50 µL of dry acetonitrile and 50 µL *N*-(tert-butyldimethyl-silyl)-*N*-methyl-trifluoroacetamide containing 1% tert-butyl-dimethyl-silylchlorid were added to the remaining residue and incubated at 70°C for 30 min. The resulting TBDMS derivates of methanol-soluble polar metabolites and fatty acids were used in following GC/MS analysis and calculations for isotopologue profiling.

2.2.4.3 Sample preparation of Man and Gal

For isotopologue profiling of Man and Gal, 5 mg of the freeze-dried bacteria sample were methanolized by adding 0.5 mL of methanolic HCl (3 M). The samples were kept at 80°C over night. Following, the supernatant was dried at 25°C under a stream of nitrogen. 1 mL acetone containing 20 µL concentrated H_2SO_4 was added to the remaining residue and kept at 25°C for 1 h. After the addition of 2 mL of saturated NaCl and 2 mL of saturated Na_2CO_3, extraction occurred 2 x with 3 mL ethyl acetate. Organic phases were combined and dried under a stream of nitrogen. The dry residue was incubated overnight at 60°C with 200 µL of a 1:1 mixture of dry ethyl acetate and acetic anhydride. Reagents were removed under a stream of nitrogen and

_____

the remaining residue was resolved in 100 µL anhydrous ethyl acetate. Resulting diisopropylidene/acetate derivatives were used for GC/MS analysis and calculations for isotopologue profiling.

2.2.4.4 Sample preparation of cell wall-derived glucosamine (GlcN) and muramic acid (Mur)

For isotopologue profiling of GlcN and Mur, approximately 15 mg of the freeze-dried bacterial sample was used in cell wall hydrolyzation with 0.5 mL of 6 M HCl overnight at 105°C. Afterwards, solid components were removed by filtration. Subsequently, the filtrate was dried under a stream of nitrogen. 100 µL of hexamethyldisilazane (HMDS) was added to the remaining residues and kept at 120°C for 3 h. Resulting TMS-derivatives were used for GC/MS analysis and calculations for isotopologue profiling.

2.2.4.5 Gas chromatography/mass spectrometry

Samples were prepared as mentioned in sections 2.2.4.1-2.2.4.4 and subsequently used in GC/MS-analysis using a QP2010 Plus gas chromatograph/mass spectrometer equipped with a 30 m long and 0.25 mm wide fused silica capillary column comprising a 0.25 μm film thickness. For m/z detection, a quadrupole detector working with electron impact ionization at 70 eV was used. Detailed information is listed in **Table 2-1**. For sample analysis, an aliquot (0.1 to 6 μL) of the respective derivatized samples (sections 2.2.4.1-2.2.4.4) were injected (1:5 split mode) at an interface temperature of 260°C and a helium inlet pressure of 70 kPa. For isotopologue profiling, GC/MS measurements were run in Selected Ion Monitoring mode (SIM mode), with a sampling rate of 0.5 s. GCMS-Solution software (**Table 2-2**) was used for data collection and analysis. Samples were measured three times respectively to generate technical replicates. Overall ^{13}C-excess values (^{13}C-excess) and isotopologue distribution in the respective metabolites where calculated as described previously (Eylert *et al.*, 2008). This includes (i) the detection of unlabeled derivatized metabolites *via* GC/MS analysis, (ii) the evaluation of the absolute ^{13}C enrichments and distributions in the respective labeled metabolites of the experiment and (iii) correction of the absolute ^{13}C-incorporation by subtracting the heavy isotopologue contributions due to the natural abundances to calculate ^{13}C-excess and isotopologue distribution.

To analyze protein-derived amino acid and the cell wall component DAP (section 2.2.4.1), the column was held at 150°C for 3 min after sample injection. Following, the column was developed with a temperature gradient of 7°C min^{-1} to a final temperature of 280°C which was held for further 3 min. TBDMS-derivatives of alanine (6.7 min), glycine (7.0 min), valine (8.5 min), leucine (9.1 min), isoleucine (9.5 min), proline (10.1 min), serine (13.2 min), phenylalanine (14.5 min), aspartate (15.4 min), glutamate (16.8 min), lysine (18.1 min), histidine (20.4 min), tyrosine (21.0 min), and the cell wall component DAP (23.4 min) were detected and isotopologue calculations were performed with m/z [M-57]$^{+}$ or m/z [M-85]$^{+}$.

For the analysis of 3-hydroxybutyric acid derived from PHB (section 2.2.4.1), the column was held at 70°C for 3 min after sample injection. Afterwards, the column was developed with a first temperature gradient of 10°C/min to a final temperature of 150°C followed by a second temperature gradient of 50°C min^{-1} to a final temperature of 280°C, which was held for further 3 min. The respective TMS-derivative of 3-hydroxybutyric acid, was detected at a retention time of 9.1 min. Isotopologue calculations were performed with m/z [M-15]$^{+}$ fragments.

For analysis of methanol-soluble metabolites including fatty acids (section 2.2.4.2), the silica column first was kept at 100°C for 2 min after the injection of the sample. Following, the column was developed with a first temperature gradient of 3°C min^{-1} to a final temperature of 234°C. Afterwards, column development occurred with a second temperature gradient of 1°C min^{-1} to a final temperature of 237°C, followed by a third gradient of 3°C min^{-1} until the final temperature of 260°C was reached. TBDMS-derivatives of lactate (17.8 min), succinic acid (27.5 min), fumaric acid (28.7 min), malic acid (39.1 min), palmitic acid (44.0 min), stearic acid (49.4 min) and citric acid (53.3 min) were detected. Isotopologue calculations were performed with m/z [M-57]$^{+}$ respectively.

For the analysis of diisopropylidene/acetate derivatives of Man and Gal (section 2.2.4.3), the silica column was hold at 150°C for 3 min after the injection of the sample. This was then followed by a first temperature gradient of 10°C min^{-1} until a final temperature of 220°C. Afterwards, the column was developed with a second temperature gradient of 50°C min^{-1} until the final temperature of 280°C was reached, which was then held for further 3 min. Isotopologue calculations were performed with m/z 287 [M-15]$^{+}$, since these fragments still contain all six C-atoms of the hexoses.

For analysis of the cell wall sugars GlcN and Mur as TMS-derivatives (section 2.2.4.4), the silica column was held at 70°C for 5 min after sample injection. This was followed by a temperature gradient of 5°C min^{-1} to a final temperature of 310°C. The final temperature was held for 1 min. Isotopologue calculations of the respective TMS-derivatives were performed with m/z [M-452]$^+$ and m/z [M-434]$^+$. Retention times and mass fragments that were used for calculations of overall ^{13}C-exces values and isotopologue composition are shown in **Table 2-8**.

Table 2-8: Retention times and mass fragments used for isotopologue calculations

Metabolite	RT [a] [min]	[M-15]$^+$	[M-57]$^+$	[M-85]$^+$	[M-176]$^+$
Ala	6.7		m/z 260		
Gly	7.0		m/z 246		
Val	8.5		m/z 288		
Leu	9.1			m/z 274	
Ile	9.5			m/z 274	
Pro	10.1		m/z 286		
Ser	13.2		m/z 390		
Phe	14.5		m/z 336		
Asp	15.4		m/z 418		
Glu	16.8		m/z 432		
Lys	18.1		m/z 431		
His	20.4		m/z 440		
Tyr	21.0		m/z 466		
DAP	23.4		m/z 589		
PHB	9.1	m/z 233			
Lactate	17.8		m/z 261		
3-Hydroxybutyric acid	21.6		m/z 275		
Succinic acid	27.5		m/z 289		
Fumaric acid	28.7		m/z 287		
Malic acid	39.1		m/z 419		
Palmitic acid	44.0		m/z 313		
Stearic acid	49.4		m/z 341		
Citric acid	53.3		m/z 591		
Man	8.7	m/z 287			
GlcN	32.6	m/z 452			
Mur	36.7				m/z 434

3 __RESULTS__

3.1 **Pathway analysis using ^{13}C-glycerol and other carbon tracers reveals a bipartite metabolism of *Legionella pneumophila***

Häuslein, I.[#], Manske, C.[#], Goebel, W., Eisenreich W.[†], and Hilbi, H[†]. (**2015**). *Molecular microbiology* 100**, 229-246.

In this section, *L. pneumophila JR32* was used for all experiments. *L. pneumophila* is an intracellular pathogen which can replicate in numerous protozoan hosts in its natural environment, thereby showing a biphasic life cycle which comprises a transmissive and a replicative phase (Molofsky and Swanson, 2004; Steinert and Heuner, 2005; Hoffmann *et al.*, 2014b). This bacterium can accidentally infect human alveolar macrophages, causing a life-threatening pneumonia called Legionnaires´ disease (Molofsky and Swanson, 2004). Although it is known that amino acids, especially serine, represent the main carbon and energy source of *L. pneumophila* (Pine *et al.*, 1979; Ristroph *et al.*, 1981; Tesh and Miller, 1981; Tesh *et al.*, 1983), carbon metabolism of this pathogen is only poorly investigated. However, recent proteome and transcriptome data indicated that *L. pneumophila* can use glycerol as further substrate (Faucher *et al.*, 2011). This agrees with genome based analysis and recent labeling experiments, confirming a greater metabolic potential of *L. pneumophila* (Cazalet *et al.*, 2004; Chien *et al.*, 2004; Steinert *et al.*, 2007; Cazalet *et al.*, 2010). In this work, it was shown that, although glycerol does not support extracellular growth of *L. pneumophila*, this substrate promotes replication inside *A. castellanii* or macrophages dependent on *glpD*. The importance of glycerol as an intracellular substrate was also demonstrated in competition assays with the *L. pneumophila* wild-type and a mutant strain lacking *glpD,* since the mutant was outcompeted upon coinfection. For a detailed analysis of the glycerol metabolism in comparison to carbon metabolism of further substrates in *L. pneumophila, in vitro* labeling experiments were performed with [U-^{13}C$_3$]glycerol and further ^{13}C-precursors ([U-^{13}C$_6$]glucose and [U-^{13}C$_3$]serine) in the newly developed MDM comprising essential amino acids, proline and phenylalanine. The results of the labeling experiments revealed a bipartite metabolism in which serine is predominantly used in the TCA cycle for energy generation during replication whereas further carbon sources like glucose and glycerol are shuffled into gluconeogenetic reactions at later growth phases. This bipartite metabolism is also present during intracellular replication, since similar results were obtained during *in vivo* labeling experiment with *L. pneumophila* wild-type and the Δ*glpD* mutant in *A. castellanii* using the same three ^{13}C-tracers.

Pathway analysis using ^{13}C-glycerol and other carbon tracers reveals a bipartite metabolism of *Legionella pneumophila*

**Ina Häuslein,[1][†] Christian Manske,[2][†]
Werner Goebel,[2] Wolfgang Eisenreich[1]* and
Hubert Hilbi[2,3]***
[1]*Lehrstuhl für Biochemie, Technische Universität
München, Munich, Germany*
[2]*Max von Pettenkofer Institut, Ludwig-Maximilians
Universität, Munich, Germany*
[3]*Institute of Medical Microbiology, University of
Zürich, Switzerland*

Summary

**Amino acids represent the prime carbon and energy
source for *Legionella pneumophila*, a facultative intra-
cellular pathogen, which can cause a life-threatening
pneumonia termed Legionnaires' disease. Genome,
transcriptome and proteome studies indicate that
L. pneumophila also utilizes carbon substrates other
than amino acids. We show here that glycerol pro-
motes intracellular replication of *L. pneumophila* in
amoeba or macrophages (but not extracellular growth)
dependent on glycerol-3-phosphate dehydrogenase,
GlpD. An *L. pneumophila* mutant strain lacking *glpD*
was outcompeted by wild-type bacteria upon co-
infection of amoeba, indicating an important role of
glycerol during infection. Isotopologue profiling stud-
ies using ^{13}C-labelled substrates were performed in a
novel minimal defined medium, MDM, comprising
essential amino acids, proline and phenylalanine. In
MDM, *L. pneumophila* utilized ^{13}C-labelled glycerol or
glucose predominantly for gluconeogenesis and the
pentose phosphate pathway, while the amino acid ser-
ine was used for energy generation via the citrate
cycle. Similar results were obtained for *L. pneumo-
phila* growing intracellularly in amoeba fed with [13]C-
labelled glycerol, glucose or serine. Collectively, these**

results reveal a bipartite metabolism of *L. pneumo-
phila*, where glycerol and carbohydrates like glucose
are mainly fed into anabolic processes, while serine
serves as major energy supply.

Introduction

Legionella pneumophila is a facultative intracellular
pathogen that can replicate in a wide range of protozoan
host cells, including *Acanthamoeba* and *Hartmanella*
spp. (Steinert and Heuner, 2005; Hoffmann *et al.*,
2014b). *L. pneumophila* can also infect humans, as the
bacteria are able to replicate within alveolar macro-
phages, causing a severe pneumonia called Legion-
naires' disease. The pathogen adopts a biphasic life
style, which comprises a replicative and a transmissive
(virulent) stage and is regulated by the growth phase
(Molofsky and Swanson, 2004). While exponentially
growing bacteria repress transmissive features such as
virulence, motility and stress resistance, bacteria in
post-exponential phase induce these traits (Byrne and
Swanson, 1998; Brüggemann *et al.*, 2006; Faucher
et al., 2011).

The mechanism underlying intracellular survival of the
bacteria in different phagocytic host cells seem to be
evolutionarily conserved (Hoffmann *et al.*, 2014b) and
includes the formation of a replication-permissive com-
partment termed the *Legionella*-containing vacuole
(LCV). The LCV acquires components of early and late
endosomes, mitochondria, the endoplasmic reticulum as
well as ribosomes, yet it avoids fusion with lysosomes
and concomitant degradation (Isberg *et al.*, 2009; Hub-
ber and Roy, 2010; Hilbi and Haas, 2012; Sherwood
and Roy, 2013; Hoffmann *et al.*, 2014a). To establish its
replicative intracellular niche, *L. pneumophila* uses the
Icm/Dot type IV secretion system (T4SS), which translo-
cates a plethora of 'effector' proteins into the host cell.
These effectors target central eukaryotic pathways like
endocytic, secretory or retrograde vesicle trafficking and
modulate host factors such as small GTPases,

phosphoinositide lipids or phytate (Finsel *et al.*, 2013; Haneburger and Hilbi, 2013; Rothmeier *et al.*, 2013; Weber *et al.*, 2014; Finsel and Hilbi, 2015).

While the mechanisms of intracellular survival of *L. pneumophila* are rather well studied, the carbon metabolism of intracellular and extracellular bacteria is still poorly understood. Early *in vitro* studies of *L. pneumophila* metabolism showed a preference for amino acids as main source of carbon and energy, and auxotrophy for several amino acids including arginine, cysteine, isoleucine, leucine, methionine, serine and threonine was reported (Pine *et al.*, 1979; Ristroph *et al.*, 1981; Tesh and Miller, 1981; Tesh *et al.*, 1983). The *L. pneumophila* genome encodes various amino acid transporters and proteases, which is further highlighting the importance of amino acids for the bacterial metabolism (Cazalet *et al.*, 2004; Chien *et al.*, 2004). The identification of the phagosomal transporter family (Pht) revealed a role of amino acid metabolism during intracellular growth, as *L. pneumophila* mutants lacking the threonine transporter PhtA, the valine transporter PhtJ or the thymidine transporters PhtC and PhtD no longer grow inside macrophages (Sauer *et al.*, 2005; Chen *et al.*, 2008; Fonseca *et al.*, 2014). Also, Icm/Dot-translocated effectors seem to promote the usage of amino acids during intracellular growth. The *L. pneumophila* ubiquitin ligase AnkB highjacks host cell amino acid metabolism by exploiting the proteasome to create a pool of free amino acids within the host cell (Price *et al.*, 2009; Lomma *et al.*, 2010; Price *et al.*, 2011). Using host cell transporters, these amino acids can then be shuttled into the LCV. The eukaryotic neutral amino acid transporter SLC1A5, for example, is upregulated in infected cells and essential for intracellular growth of *L. pneumophila* (Wieland *et al.*, 2005).

In addition to amino acids, *L. pneumophila* is also able to metabolize carbohydrates. This is reflected in the genomes of sequenced *Legionella* species, which encode complete Embden-Meyerhof-Parnas (EMP) and Entner-Doudoroff (ED) pathways, but only the non-oxidative part of the pentose phosphate pathway (PPP) (Chien *et al.*, 2004; D'Auria *et al.*, 2010; Cazalet *et al.*, 2010). The incomplete PPP lacking 6-phosphogluconate dehydrogenase suffices to catalyze the interconversion of sugars needed for cell wall biosynthesis, but does not yield $NADPH/H^+$. *L. pneumophila* mutants lacking different genes of the ED pathway are defective for intracellular growth in amoeba and mammalian cells, and wild-type bacteria indeed catabolize glucose via the ED pathway, as shown by transcriptome and proteome studies as well as by isotopologue profiling (Eylert *et al.*, 2010; Harada *et al.*, 2010; Schunder *et al.*, 2014; Hoffmann *et al.*, 2014b).

Isotopologue profiling is a powerful tool for metabolic studies and can give detailed insights into metabolic pathways and fluxes. The method is based upon ^{13}C-incorporation derived from labelled precursors that are metabolized by bacteria or eukaryotic cells. To this end, the overall ^{13}C-enrichment and the isotopologue composition in key metabolic products are determined, preferably using gas chromatography/mass spectrometry (GC/MS). This technique has been used for a range of bacteria, including *Listeria monocytogenes* (Gillmaier *et al.*, 2012), *Streptococcus pneumonia* (Härtel *et al.*, 2012), *Staphylococcus aureus* (Kriegeskorte *et al.*, 2014), *Campylobacter jejuni* (Vorwerk *et al.*, 2014) or *Xanthomonas campestris* (Schatschneider *et al.*, 2014).

Glycerol is an important carbon source for different intracellular pathogens, such as *L. monocytogenes* (Grubmüller *et al.*, 2014) or *Salmonella enterica* (Steeb *et al.*, 2013). Upon intracellular growth of *L. pneumophila* in macrophages, the expression of glycerol kinase (*lpg1414*, *glpK*) and glycerol-3-phosphate dehydrogenase (*glpD*) is highly upregulated (Faucher *et al.*, 2011), and early studies using a defined medium indicated that glycerol might also be metabolized by *L. pneumophila* (Tesh *et al.*, 1983). In this study, we analysed glycerol metabolism of extra- and intracellularly growing *L. pneumophila* using different growth assays, isotopologue profiling and a newly developed *Legionella* minimal growth medium. The use of [U-$^{13}C_3$]glycerol as a tracer indicated that the compound indeed serves as a nutrient for *L. pneumophila* and is predominantly metabolized via gluconeogenesis and the PPP. Furthermore, ^{13}C-incorporation into key metabolites of *L. pneumophila* growing either with [U-$^{13}C_3$]glycerol, [U-$^{13}C_6$]glucose or [U-$^{13}C_3$]serine revealed a bipartite metabolism, where glycerol and carbohydrates such as glucose are predominantly channelled into glycolysis, gluconeogenesis and the PPP respectively, and hence are used mainly for anabolic reactions, while especially serine is used effectively in the TCA cycle to deliver reducing equivalents for energy production in the electron transport chain.

Results

Designing a new chemically defined Legionella *growth medium*

In initial attempts, we used chemically defined medium (CDM) (Eylert *et al.*, 2010) modified from 'Ristroph medium' (Ristroph *et al.*, 1981) to assess with different microbiological assays and by isotopologue profiling the effect of glycerol on extracellular growth of *L. pneumophila* strains (Supporting Information Table S1). However, under the conditions used no significant ^{13}C-enrichment was detectable in any metabolite (data not shown). To

3. RESULTS

develop a new *Legionella* growth medium, we minimized the carbon sources in CDM as far as possible but did not alter salt composition and iron concentration. A medium that contained only essential amino acids (arginine, cysteine, isoleucine, leucine, methionine, serine, threonine, valine) was not suitable, as *L. pneumophila* did not replicate in this medium anymore (data not shown).

Next, we depleted single non-essential amino acids from CDM. Depletion of histidine, lysine, proline, tryptophan and aspartate did not alter *L. pneumophila* growth compared to normal CDM (Supporting Information Fig. S1A). CDM lacking serine did not support growth of *L. pneumophila*, highlighting the importance of serine for *Legionella* growth. Leaving out pairs of amino acids such as aspartate and histidine or aspartate and tryptophan yielded a medium that supported robust growth of *L. pneumophila* similar to CDM. Depletion of aspartate and lysine or aspartate and proline resulted in reduced growth compared to CDM. We then used a medium, lacking all amino acids that had no significant influence on *L. pneumophila* growth, namely histidine, aspartate, tryptophan, lysine and glutamate. The medium still contained proline, as depletion of this amino acid significantly reduced growth. In this medium, *L. pneumophila* did not reach optical densities as high as in CDM (Supporting Information Fig. S1B), but the bacteria did reach stationary growth phase as judged by the production of the brown pigment, motility and shape of the bacteria (data not shown). Finally, the omission of the aromatic amino acid tyrosine from CDM had no effect on growth, but leaving out phenylalanine or both, phenylalanine and tyrosine, significantly reduced growth (Supporting Information Fig. S1C). Tyrosine can be directly synthesised from phenylalanine in the reaction catalyzed by phenylalanine hydroxylase (*phhA*), explaining why depletion of tyrosine had no growth effect and why phenylalanine is more required in the medium than tyrosine. In summary, the optimized new medium termed minimal defined medium (MDM) was composed of CDM lacking aspartate, glutamate, histidine, lysine, tryptophan and tyrosine (Supporting Information Table S2).

Glycerol promotes intracellular growth of *L. pneumophila*

To analyse the role of glycerol in the metabolism of *L. pneumophila*, we constructed the deletion mutant Δ*glpD*, lacking the glycerol-3-phosphate dehydrogenase GlpD (strain CM01, Supporting Information Table S1). The growth of *L. pneumophila* Δ*glpD* was indistinguishable from wild-type bacteria in AYE broth (data not shown) and slightly reduced in CDM (Fig. 1A) or MDM (Fig 1B). The addition of glycerol had no effect on extracellular growth of *L. pneumophila* in AYE (data not

shown), CDM (Fig. 1A) or MDM (Fig. 1B). Moreover, the addition of 10 mM or 20 mM glycerol-3-phosphate did not affect the growth of *L. pneumophila* in MDM, but 50 mM of the compound decreased the growth of wild-type or Δ*glpD* mutant bacteria (Fig. 1C and Supporting Information Fig. S2). Thus, under the conditions tested, neither glycerol nor glycerol-3-phosphate promotes the extracellular growth of *L. pneumophila* in different media.

The effect of glycerol on intracellular growth of *L. pneumophila* was determined by fluorescence-based assays and colony-forming units (cfu). As expression of *glpD* was upregulated upon growth in macrophages (Faucher *et al.*, 2011), we used RAW 264.7 macrophages to analyse intracellular growth. The addition of 50 mM glycerol 4 h post infection increased the cell numbers of wild-type *L. pneumophila* in stationary growth phase (Fig. 1D and E). The Δ*glpD* mutant strain grew intracellularly like wild-type *L. pneumophila*, but glycerol did not promote growth. The mutant phenotype was complemented by providing *glpD* on a plasmid (Fig. 1E). Furthermore, glycerol promoted the growth of *L. pneumophila* not only in macrophages, but also in *A. castellanii* (Fig. 1F). Interestingly, upon co-infection of *A. castellanii* with *L. pneumophila* wild-type and Δ*glpD*, the mutant was outcompeted within 3–6 days, indicating that lack of *glpD* reduced intracellular growth and/or persistence in presence of the amoeba (Fig. 1G, Supporting Information Fig. S3). The competition defect was complemented by providing *glpD* on a plasmid (Fig. 1H). Taken together, glycerol does not have an effect on extracellular growth of *L. pneumophila* in complex or defined minimal media, but promotes intracellular growth in macrophages and amoeba.

Glycerol metabolism of *L. pneumophila* growing in MDM

To further study glycerol metabolism of *L. pneumophila* we used isotopologue profiling, which is a sensitive method to monitor also minor carbon flows. Initial experiments with *L. pneumophila* grown in CDM and fed with [U-^{13}C$_3$]glycerol did not yield significant ^{13}C-enrichments in any metabolite (data not shown). However, isotopologue measurements of *L. pneumophila* growing in the newly developed MDM revealed that glycerol was indeed metabolized (Fig. 2A). Under the experimental conditions used, ^{13}C-label derived from [U-^{13}C$_3$]glycerol was primarily found in histidine (3.01%), a marker of the PPP (through its precursor phosphoribosyl pyrophosphate, PRPP), and in mannose (5.75%), a valid reporter metabolite for gluconeogenesis. To a small amount, ^{13}C-enrichment was also detectable in lactate (0.97%) and in diaminopimelic acid (DAP) (0.74%) as well as in malate (0.70%), 3-
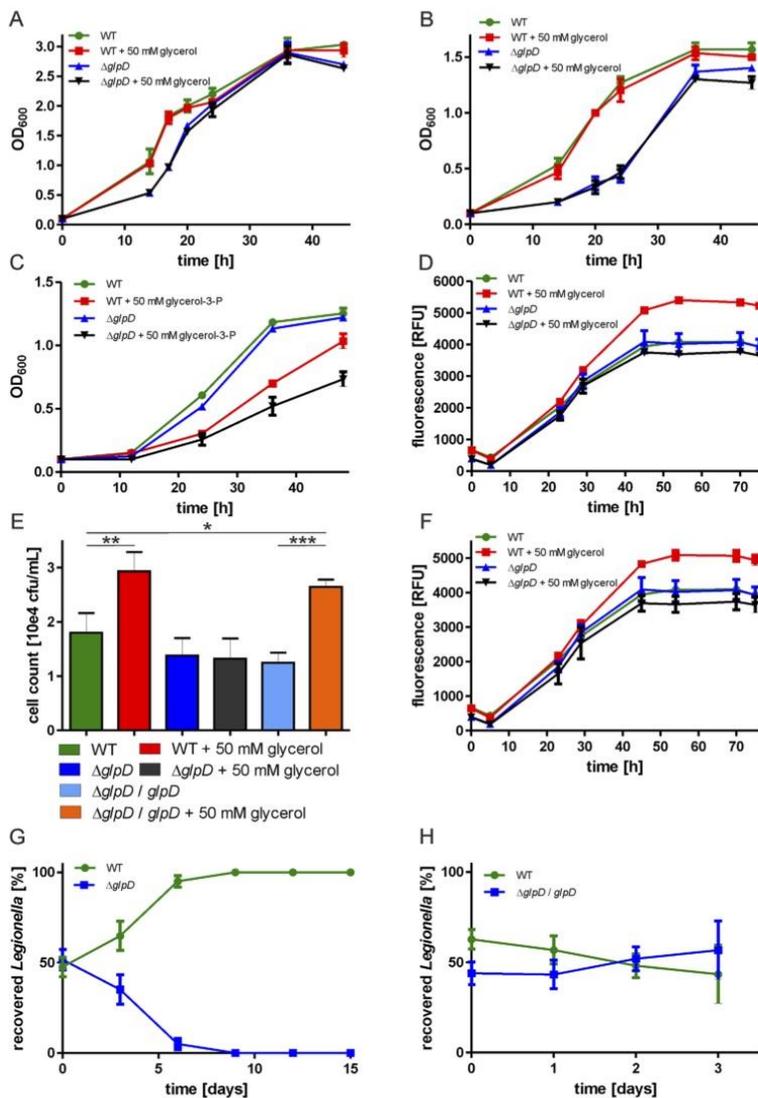
Fig. 1. Glycerol promotes intracellular growth of *L. pneumophila*. Extracellular growth of *L. pneumophila* wild-type or mutant Δ*glpD* in (A) CDM or (B) MDM with and without 50 mM glycerol or (C) in MDM with and without 50 mM glycerol-3-phosphate. Optical density at 600 nm was determined at the time points indicated. (D) Murine RAW 264.7 macrophages were infected (MOI 20) with *L. pneumophila* wild-type or Δ*glpD* harboring pNT-28 (constitutive GFP). Glycerol was added 4 h post infection, and replication was determined by fluorescence. (E) Macrophages were infected (MOI 0.1) with *L. pneumophila* wild-type, Δ*glpD* or Δ*glpD* harboring pCR33 (vector) or pCM021 (*glpD*). Glycerol was added 4 h post infection, and cfu were determined 2 days post infection (1 way ANOVA test with Dunett's multiple comparison test: * < 0.05, **<0.01, *** < 0.0001). (F) *A. castellanii* amoeba were infected (MOI 20) with *L. pneumophila* wild-type or Δ*glpD* harboring pNT-28 (constitutive GFP). Glycerol was added 4 h post infection, and replication was determined by fluorescence. (G) Competition defect of Δ*glpD*. *A. castellanii* were infected with *L. pneumophila* wild-type and Δ*glpD* at a 1:1 ratio (MOI 0.01 each). After 3 days, cells were lysed and bacteria were used to infect new amoeba. cfu were quantified by plating aliquots on CYE agar plates. (H) Complementation of Δ*glpD* competition defect. *A. castellanii* amoeba were infected with *L. pneumophila* wild-type and Δ*glpD* harboring pCM021 at a 1:1 ratio (MOI 0.1 each). After 1, 2 and 3 days, the infected cells were lysed, and cfu were quantified by plating aliquots on CYE agar plates. Mean and SD of triplicates are shown. Data are representative of three independent experiments.

55
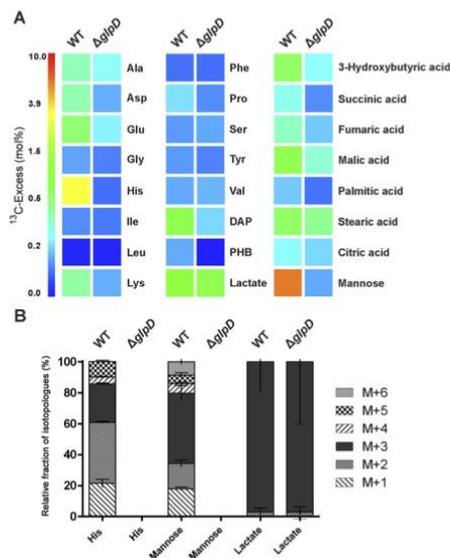
Fig. 2. Glycerol metabolism of *L. pneumophila* grown in MDM.
A. *L. pneumophila* wild-type or Δ*glpD* were grown in MDM with 50 mM [U-$^{13}C_3$]glycerol as precursor, and cells were harvested after 48 h. ^{13}C-Excess (in mol% as colour map) of protein-derived amino acids, diaminopimelic acid (DAP), polyhydroxybutyrate (PHB), methanol soluble metabolites and mannose was quantified by isotopologue profiling.
B. The isotopologue pattern of histidine, mannose and lactate from *L. pneumophila* wild-type or Δ*glpD* was determined. The columns indicate the relative fraction (in %) of the ^{13}C-isotopologues (M+1 to M+6). Data shown are mean and SD from three independent experiments. For numerical values, see Supporting Information.

M+3 or M+6 labelled. Subsequently, C_5-sugars are built in transketolase reactions in the PPP, yielding M+3 and M+2 labels of C_5-sugars, such as PRPP. This pentose is a precursor unit in histidine biosynthesis, in agreement with the observed labelling pattern of histidine (Fig. 2B). Transketolase reactions also lead to M+3 or M+1 label in erythrose-4-phosphate, M+1 supposedly at position C-1. The single label in mannose, which was detected in minor amounts, is then the result of a transketolase reaction that transfers the M+1 label at position C-1 onto xylulose-5-phosphate (Fig. 2B).

No ^{13}C-label was detected in essential amino acids (isoleucine, leucine, serine, valine) and in most of the amino acids derived from the TCA cycle (alanine, aspartate, lysine, proline) or TCA cycle intermediates (succinate, fumarate, citrate) (Fig. 2A). Collectively, these results implied that glycerol is metabolized by the TCA cycle only to a minor extent and instead is used predominantly for gluconeogenesis and the PPP. Notably, lactate was the only metabolite that showed some ^{13}C-enrichment in the Δ*glpD* mutant strain (0.71%, Fig. 2A). The labelling pattern for lactate was identical in wild-type *L. pneumophila* and the Δ*glpD* mutant and showed only completely labelled isotopologues (M+3, Fig. 2B). ^{13}C-Excess and isotopologue profiles of endpoint experiments are shown in Supporting Information Table S3.

Time-dependent usage of glycerol by L. pneumophila

For an in-depth analysis of the determinants of glycerol metabolism by *L. pneumophila*, we assessed glycerol utilization in a time-dependent manner in comparison to other carbon sources used by the bacteria. To this end, we chose serine and glucose, as it is known that both compounds are metabolized by *L. pneumophila in vitro* (Eylert *et al.*, 2010). To compare the metabolism of these substrates in parallel, we added 11 mM glucose and 50 mM glycerol to MDM, which already contained 6 mM serine as an essential amino acid. This adjusted medium was termed 'carbon-enriched minimal defined medium' (CE MDM). In the following time series experiments, one of these substrates was added as ^{13}C-labelled compound. After 12 h, 24 h, 36 h or 48 h of growth, the bacteria were harvested. ^{13}C-Enrichment and isotopologue pattern of protein-derived amino acids, mannose and DAP (both compounds presumably produced by cell wall hydrolysis), 3-hydroxybutyrate (named polyhydroxybutyrate (PHB) in the following, as presumably derived from PHB hydrolysis) and other polar metabolites, as well as fatty acids were analysed as described above. The time points were chosen to represent early exponential (12 h), exponential (24 h), late exponential (36 h) and stationary (48 h) growth phase of

hydroxybutyric acid (0.61%), stearic acid (0.60%) and glutamate (0.55%). With the exception of lactate (0.71%), incorporation of ^{13}C-label was not detected in these metabolites using the mutant strain Δ*glpD* (Fig. 2A). These results provided a strong indication that glycerol was metabolized by *L. pneumophila* wild-type dependent on the glycerol-3-phosphate dehydrogenase GlpD.

The isotopologue profile of mannose mainly displayed M+3 (i.e. specimens that carry 3 ^{13}C-atoms) and to minor extent M+6 (i.e. specimens that carry 6 ^{13}C-atoms), suggesting that glycerol was metabolized via gluconeogenesis to yield hexoses (Fig. 2B). Histidine as a marker amino acid for the PPP, showed mainly M+2 and M+3 labelling. This pattern supports the notion that the gluconeogenetic pathway is active. Here, fully labelled glyceraldehyde-3-phosphate or dihydroxyacetone-phosphate derived from [U-$^{13}C_3$]glycerol is used for the synthesis of fructose-1,6-bisphosphate and fructose-6-phosphate, the direct precursor of mannose-6-phosphate. Due to one or two ^{13}C-precursors used for the assembly, these hexoses are

Fig. 3. ^{13}C-Excess in key metabolites of *L. pneumophila* grown with [U-^{13}C$_3$]glycerol, [U-^{13}C$_6$]glucose or [U-^{13}C$_3$]serine as precursors. *L. pneumophila* wild-type was grown in CE MDM with either (A) 50 mM [U-^{13}C$_3$]glycerol, (B) 11 mM [U-^{13}C$_6$]glucose or (C) 6 mM [U-^{13}C$_3$]serine as precursors in the medium. Samples were taken after 12 h, 24 h, 36 h and 48 h. ^{13}C-Incorporation (A–C) into protein-derived amino acids, diaminopimelic acid (DAP) and polyhydroxybutyrate (PHB) for all time points and (D) into methanol-soluble metabolites and mannose after 48 h was quantified. Colour map correlates to mean value and SD of three independent experiments. For numerical values, see Supporting Information.

L. pneumophila growing in MDM (Fig. 1B). ^{13}C-Excess and isotopologue profiles of all time-series experiments are documented in Supporting Information Table S4.

The time-series experiment with *L. pneumophila* grown in CE MDM with [U-^{13}C$_3$]glycerol as precursor yielded significant enrichments especially in histidine (3.00% after 48 h) and mannose (4.51% after 48 h) (Fig. 3A and D). Although this medium contained glucose as possible carbon source besides glycerol, the ^{13}C-enrichment in histidine was similar compared to the experiment in MDM after 48 h (Fig. 2A). The ^{13}C-abundance in mannose was decreased by only approximately 20%, suggesting that glucose had only a minor influence on the metabolism of glycerol. Additionally, ^{13}C-enrichments were also found to a minor extent in alanine (0.61%), aspartate (0.49%), glutamate (0.77%), DAP (0.80%), PHB (0.52%), lactate (1.44%) and malate (0.55%) after 48 h of growth. Notably, significant enrichment in any metabolite was only detectable after 36 h incubation, indicating that glycerol was only used in later stages of exponential growth and in the stationary growth phase (48 h), where the highest ^{13}C-abundances were measured. Furthermore, the isotopologue pattern in histidine, mannose and lactate were almost identical compared to their isotopologue pattern during growth in MDM (Supporting Information Fig. S4A),

indicating that also in CE MDM glycerol was predominantly used for gluconeogenesis and the PPP and only to a minor extent in the TCA cycle.

Similar to the time-series experiments with [U-^{13}C$_3$]glycerol, [U-^{13}C$_6$]glucose added as a supplement to the medium yielded the highest ^{13}C-enrichments in histidine and mannose (20.72% and 31.88% after 48 h). Additionally, several other metabolites were also significantly labelled when grown with ^{13}C-glucose, including alanine, aspartate, glutamate, lysine, proline, DAP, PHB, succinate, fumarate, palmitate and stearate (ranging from 4.26% to 1.38% overall excess after 48 h) (Fig. 3B and D). The isotopologue profile of histidine did not differ from labelling experiments with [U-^{13}C$_3$]glycerol and mainly showed M+2 and M+3. The label of mannose was primarily M+3 and M+6 (Supporting Information Fig. S4B). This data confirmed that glucose was predominantly metabolized via the ED pathway (Eylert *et al.*, 2010; Harada *et al.*, 2010), gluconeogenesis and the PPP, and was also used to a minor extent via the TCA cycle to yield precursors for amino acids and fatty acids. Different to glycerol, glucose was moderately used as a carbon source already at earlier stages of *L. pneumophila* growth (significant enrichment after 12 h). Intermediates of the TCA cycle (succinate,

3. RESULTS

fumarate, malate) and amino acids derived from the TCA cycle (aspartate, glutamate) were mainly M+1 and M+2 labelled (Supporting Information Fig. S4B). The M+2 label is derived from fully labelled acetyl-CoA, while M+1 label could reflect the decarboxylation reaction of the α-ketoglutarate-dehydrogenase or multiple rounds of TCA cycle, where unlabelled acetyl-CoA is transferred onto labelled oxaloacetate. Besides histidine, alanine was the highest labelled amino acid (4.26%) with mainly M+3, which indicates that this compound was directly derived from fully labelled pyruvate presumably derived from reactions of the ED pathway as the major route of glucose metabolism in *L. pneumophila* (Eylert *et al.*, 2010; Harada *et al.*, 2010). Interestingly, lactate showed no significant ¹³C-enrichment, thus differing from labelling experiments with glycerol.

To rule out that the metabolism of glycerol and glucose was mutually influenced by the presence of the other carbon substrate, we also performed time series experiments in MDM where either glycerol or glucose was added as ¹³C-labelled precursor in absence of the other substrate. The change in setup resulted in no significant change in ¹³C-incorporation and labelling pattern (data not shown), compared to time series experiments in CE MDM, where the metabolism of one labelled carbon source was analyzed in presence of the other, unlabelled substrate. These findings indicate that serine, glycerol and glucose are co-metabolized independently by *L. pneumophila*.

When incubated with [U-¹³C₃]serine as precursor, ¹³C-enrichment was detected in the same metabolites as in the time series experiment with labelled glucose. Additionally, also glycine was highly ¹³C-enriched (28.58% after 24 h) (Fig. 3C and D). The isotopologue pattern of glycine showed that it was directly synthesised from serine, as it was almost completely M+2 labelled (Supporting Information Fig. S4C). In difference to the above labelling experiments the overall ¹³C-enrichment reached its peak already after 24 h and dropped steadily afterwards. The ¹³C-excess from significantly labelled amino acids, DAP and PHB after 24 h ranged between 91.61% in serine to 28.58% in glycine (serine > alanine > histidine > DAP > lysine > PHB > aspartate > glutamate > glycine). This shows that serine was very efficiently taken up from the medium and metabolized (Fig. 3C). After 48 h of growth, also intermediates of the TCA cycle, fatty acids and mannose were highly labelled, ranging between 3.53% and 40.40% overall enrichment (Fig. 3D). The high enrichment in alanine (74.60% after 24 h) and in amino acids derived from the TCA cycle could reflect that serine was mainly fed into the TCA cycle. This notion is in agreement with the high abundance of ¹³C-label in succinate, fumarate and malate, as well as in fatty acids, which also indicates a high carbon flow into the TCA cycle. The isotopologue profile of pal-

mitate and stearate mainly showed M+2, M+4, M+6, M+8, M+10 and M+12 labelling (Supporting Information Fig. S4C). This fractional profile shows high carbon flux from serine to acetyl-CoA, which is then incorporated as C2-building blocks into fatty acids. The profile was different in experiments with ¹³C-glucose, where mostly M+2 labelling was detected in the isotopologue pattern of fatty acids, suggesting a lower flow of acetyl-CoA into fatty acid biosynthesis. Labelled acetyl-CoA derived from ¹³C-labelled serine was also used for the synthesis of PHB and its precursor 3-hydroxybutyrate. The isotopologue pattern of both metabolites was identical (mostly M+2) and contained also a fraction of M+4 derived from the condensation of two fully labelled acetyl-CoA. Again, the profile was different from experiments with ¹³C-glucose, where the M+4 fraction was not detectable (Supporting Information Figs. S4B and S4C).

Aspartate is synthesized from oxaloacetate which is either derived from the TCA cycle or directly by carboxylation of pyruvate via pyruvate carboxylase. This is also reflected in the isotopologue pattern of aspartate, where we found fractions of M+1, M+2 and M+4 as a result of one or more rounds of TCA cycle and also a fraction of M+3 derived directly from fully labelled pyruvate. Since DAP is synthesized from aspartate and pyruvate, the pattern of DAP also showed a large fraction of M+3, again derived from fully labelled pyruvate. The other fractions resulted from differentially labelled pyruvate and aspartate. Also, a small fraction of M+7 was found, derived from fully labelled aspartate and fully labelled pyruvate. Lysine is made by a decarboxylation of DAP, and therefore, all fractions except M+7 were also found in the isotopologue pattern of lysine (Supporting Information Fig. S4C).

The isotopologue pattern of glutamate as a derivative of α-ketoglutarate was different from the pattern of glutamate in the time series experiments with ¹³C-glucose, since in addition to M+1 and M+2, also M+3, M+4 and M+5 label was found. This could be explained by the high flux of serine into acetyl-CoA and then into the TCA cycle. Proline is made directly from glutamate, and therefore, the isotopologue pattern of proline was almost identical to that of glutamate. Proline (but not glutamate) was also a component of the growth medium, and ¹³C-enrichment in proline was detected only after 36 h (4.70%). This finding is in agreement with the notion that proline from the medium was consumed at that time and had to be synthesized *de novo* by *L. pneumophila* (Fig. 3C and Supporting Information Fig. S4C).

Finally, upon incubation with [U-¹³C₃]serine as precursor also histidine and mannose were found to be highly ¹³C-enriched (55.88% and 40.40% after 48 h), although also unlabelled glucose and glycerol were present in the medium. Mannose showed the same isotopologue

58
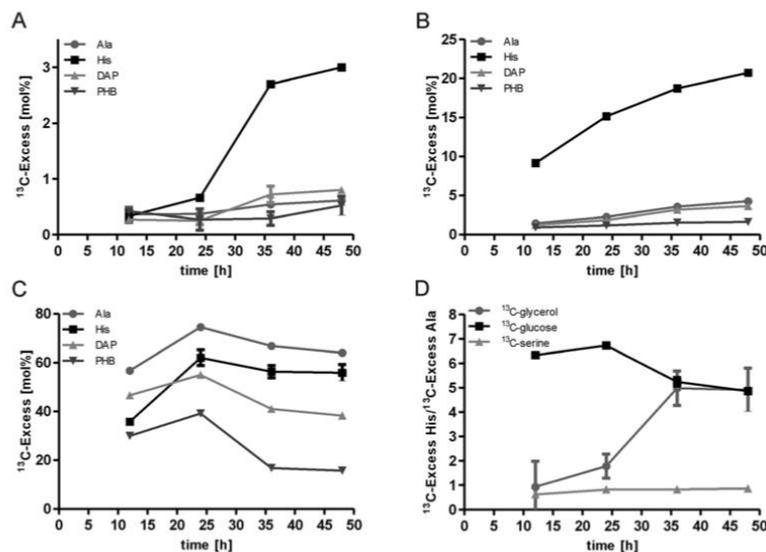
Fig. 4. Analysis of carbon flux from different substrates into metabolic markers. Incorporation of ^{13}C-label over time into alanine, histidine, DAP and PHB of *L. pneumophila* fed with (A) 50 mM [U-^{13}C$_3$]glycerol, (B) 11 mM [U-^{13}C$_6$]glucose or (C) 6 mM [U-^{13}C$_3$]serine as precursor. (D) Ratio of ^{13}C-excess in histidine to ^{13}C-excess in alanine with ^{13}C-glycerol, ^{13}C-glucose or ^{13}C-serine as substrate shows carbon fluxes into the TCA cycle or into gluconeogenesis/PPP.

pattern as in the labelling experiments with ^{13}C-glucose being mostly M+3 and M+6 labelled. Histidine on the other hand also had a larger M+6 fraction derived from fully labelled ribose via the PPP and a ^{13}C-labelled atom from ATP that is finally transferred onto the PRPP unit in the course of this biosynthetic pathway (Fig. 3C and D; Supporting Information Fig. S4C).

Carbon flux of substrates into different metabolic markers

For an overview of the time-dependent metabolism of glycerol, glucose and serine by *L. pneumophila* in CE MDM, we chose four metabolites that are characteristic for different metabolic pathways and not present in the medium, so that they had to be synthesized *de novo* by the bacteria. Thus, the overall ^{13}C-excess of alanine (from pyruvate), histidine (through the PPP), DAP (through the TCA cycle and from pyruvate) and PHB (from acetyl-CoA) was followed over time in the period of 12–48 h (Fig. 4).

When grown with ^{13}C-glycerol as precursor, only histidine showed high ^{13}C-abundances and only after 36 h and 48 h growth (Fig. 4A). In time series with ^{13}C-glucose, histidine also showed by far the highest ^{13}C-enrichment of the four metabolites. However, significant enrichment in histidine was found already after 12 h of growth. Also, the overall enrichment in all metabolites was higher compared with ^{13}C-glycerol as precursor, and it increased continuously over the entire time course (Fig. 4B). When fed with

^{13}C-serine, the overall enrichment peaked after 24 h and dropped afterwards for all metabolites. In general, the overall enrichment was much higher in this case compared with glycerol or glucose as precursor, and alanine was the highest labelled metabolite (Fig. 4C). Taken together, these findings illustrate how different carbon sources are used in specific ways by *L. pneumophila*. Serine serves as an effective carbon source that is metabolized during all growth phases, while glycerol does not seem to be used during the exponential but only in the stationary growth phase. The same holds true for glucose, although this compound is already partly shuffled into the PPP during earlier growth phases, providing the precursors for histidine.

To illustrate the different carbon flow from glycerol, glucose and serine, we calculated the ratio of ^{13}C-excess in histidine and alanine and plotted it against time (Fig. 4D). These amino acids were chosen as markers for different metabolic pathways: alanine as marker for carbon flux directed towards the TCA cycle and histidine for the PPP. Thus, the ratio between these amino acids shows how a carbon source is preferentially used. A high ratio value indicates a strong carbon flux into the PPP, while a small value indicates preferential flow into the TCA cycle. With ^{13}C-serine as a precursor, the ratio always stayed below 1, indicating that the main carbon flow was directed into the TCA cycle. In contrast, when fed with ^{13}C-glycerol or ^{13}C-glucose, the ratio was high, reaching a value of 5 after 36 h, demonstrating that the carbon flow was mainly directed to the PPP.

Glycerol was only used after 36 h of growth, and incorporation into alanine and histidine was not significant at earlier time points, resulting in a low ratio of histidine to alanine. However, this is a mere result of the low overall ^{13}C-excesses in histidine and alanine and does not indicate that the carbon flow was directed towards the TCA cycle (Fig. 4D). In summary, these results clearly show that serine is used as a major carbon source by *L. pneumophila* and carbon flow from serine is mainly directed towards the TCA cycle, while glucose and especially glycerol are not used as effectively as serine and carbon flow from these compounds is preferentially directed towards gluconeogenesis and the PPP.

Intracellular production of mannose by L. pneumophila growing in A. castellanii

To analyse the role and fate of different substrates during intracellular growth of *L. pneumophila*, we performed *in vivo* growth assays with *A. castellanii*. To this end, we infected *A. castellanii* with either *L. pneumophila* wild-type or the mutant strain Δ*glpD*. The infected amoeba were washed and incubated in Ac buffer, which does not contain any nutrients. Immediately after infection, more than 90% of the bacteria localized intracellularly (Supporting Information Fig. S5; data not shown). Five hours post infection, ^{13}C-glycerol, ^{13}C-glucose or ^{13}C-serine was added to the infected amoeba and it was assessed whether the compounds affect the growth of *L. pneumophila* residing in the LCV and how they are metabolized. The infection was stopped before the bacteria could lyse the LCV or the host cell to prevent contact of the bacteria with labelled substrate in the extracellular milieu. This was tested by microscopy, before the samples were further processed.

At 15 h post infection, the infected amoeba were lysed and eukaryotic cell debris and bacteria were separated using an established protocol (Schunder *et al.*, 2014). This procedure yielded 3 fractions, containing eukaryotic components (F1), *L. pneumophila* bacteria (F2) or soluble proteins/factors (F3). ^{13}C-Excess and isotopologue profiles of amino acids, DAP, PHB and mannose from all fractions were measured. As ^{13}C-excess and isotopologue profiles in the fractions F1 and F3 were always identical (data not shown), we focussed only on F1 and F2. Furthermore, to rule out possible bacterial cross contamination in F1, samples were always visually inspected by microscopy, and aliquots were plated on CYE agar. As an internal control, we also monitored the amount of DAP in F1 and F2, as DAP is a cell wall component specific for bacteria. The amount of DAP in fraction F1 did never exceed 10%, so we concluded that bacterial contamination in F1 was always below 10%. Lastly, we also used uninfected amoeba fed either with ^{13}C-glycerol, ^{13}C-glucose or ^{13}C-serine to assess the influence of *L. pneumophila* infection on the metabolism of the amoeba. ^{13}C-Excess and isotopologue profiles of all *in vivo* experiments are documented in Supporting Information Table S5.

Uninfected *A. castellanii* incorporated ^{13}C-glycerol very efficiently into the amino acids alanine, aspartate, glutamate, glycine and serine, indicating that glycerol is a good carbon substrate for *A. castellanii*. Upon infection with *L. pneumophila* wild-type or Δ*glpD*, the incorporation of label into amino acids was completely abolished (Supporting Information Fig. S6A, F1). Also, in the fraction F2 containing *L. pneumophila* wild-type or Δ*glpD*, no significant incorporation of ^{13}C-label into any of the measured amino acids was detectable.

The bacterial fraction F2 of ^{13}C-glycerol-fed amoeba infected with wild-type *L. pneumophila* yielded significant label in mannose (Fig. 5A). Substantially less mannose was labelled in fraction F1 of wild-type-infected or in F1 and F2 of Δ*glpD*-infected *A. castellanii*. The isotopologue profile of mannose in fraction F2 of amoeba infected with wild-type *L. pneumophila* revealed that the sugar was mostly M+3 labelled (Fig. 5D). This result is in line with our *in vitro* experiments, suggesting that also *in vivo* glycerol was used in gluconeogenesis for the production of hexoses. Moreover, the fact that no label was found in the Δ*glpD* mutant indicates that incorporation of ^{13}C-label into mannose in wild-type bacteria was a result of the direct uptake of glycerol into the LCV and the synthesis of mannose from glycerol by *L. pneumophila* via the glycerol-3-phosphate dehydrogenase GlpD (Fig. 5A).

[13]C-Glucose was also efficiently metabolized by uninfected *A. castellanii*, as already observed in previous studies (Schunder *et al.*, 2014). Again, an infection with wild-type *L. pneumophila* resulted in a significant drop in ^{13}C-incorporation in fraction F1. In contrast, the bacterial fraction F2 yielded significant ^{13}C-label in alanine, glutamate, DAP and PHB (Supporting Information Fig. S6B). Notably, fraction F1 of wild-type-infected amoeba showed only minor ^{13}C-enrichment in mannose, while this carbohydrate was highly enriched in the bacterial fraction F2 (4.47%) (Fig. 5B). The isotopologue pattern of mannose in F2 was characterized by M+3 and M+6 labels (Fig. 5D), and therefore, almost identical to *L. pneumophila* grown in MDM. These results indicate that also glucose was taken up directly from the host (M+6) and metabolized by the bacteria. The M+3 label reflects glycolytic cycling via glycolysis and/or the ED pathway, followed by gluconeogenesis and/or the PPP using a [13]C_3-triose phosphate unit and an unlabelled substrate in the assembly process.

Finally, ^{13}C-serine was not as efficiently metabolized by uninfected amoeba as glucose and glycerol, since
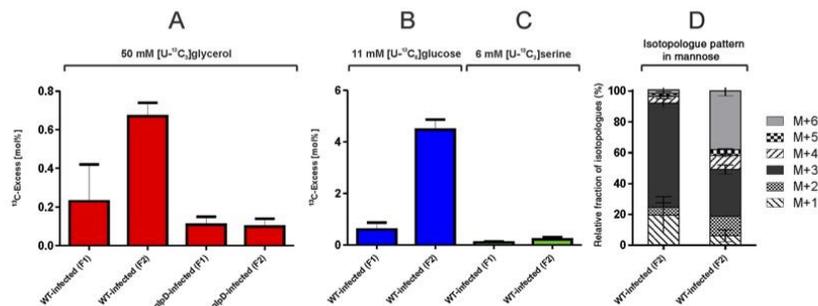
Fig. 5. Analysis of mannose from *L. pneumophila* grown in *A. castellanii*. *A. castellanii* amoeba were infected with either *L. pneumophila* wild-type or Δ*glpD* (MOI 50) and washed 1 h post infection to remove extracellular bacteria. 5 h post infection (A) 50 mM [U-^{13}C$_3$]glycerol, (B) 11 mM [U-^{13}C$_6$]glucose or (C) 6 mM [U-^{13}C$_3$]serine were added. 15 h post infection, the cells were lysed and eukaryotic cell debris and bacteria were separated, resulting in fractions F1, containing eukaryotic cell debris and fraction F2, containing *L. pneumophila*. (D) The isotopologue pattern of mannose from fraction F2 of wild-type-infected amoeba fed with [U-^{13}C$_3$]glycerol (left bar) or [U-^{13}C$_6$]glucose (right bar) was determined. Mean and SD of two independent experiments are shown. For numerical values, see Supporting Information.

^{13}C-incorporation was observed only in serine and its direct derivative glycine. Significantly more ^{13}C-incorporation was detected in fraction F1 of *A. castellanii* infected with wild-type *L. pneumophila*. However, the highest values of label from [U-^{13}C$_3$]serine were observed in F2, especially in alanine, serine, DAP and PHB (Supporting Information Fig. S6C), in agreement with earlier observations (Schunder *et al.*, 2014). Interestingly, absolutely no incorporation occurred into mannose neither in F1 nor in F2, indicating that serine was not used for synthesis of this hexose by *L. pneumophila* or *A. castellanii* respectively (Fig. 5C). Notably, in all *in vivo* experiments, no label occurred in histidine, suggesting that this amino acid was efficiently taken up from the host cell and not synthesised *de novo* by *L. pneumophila* growing intracellularly.

Taken together, the data show that glycerol and glucose were taken up by *A. castellanii*, transported to the LCV predominantly without being metabolized and then directly utilized by *L. pneumophila*. Using this experimental setup, we proved that *L. pneumophila* also uses glycerol intracellularly as a substrate and exclusively in anabolic reactions, as shown in MDM minimal growth medium. The absence of label in mannose, when fed with ^{13}C-serine, suggests that similar to growth *in vitro* (Fig. 4), *L. pneumophila* growing *in vivo* preferentially directs the flow of carbon from different substrates to distinct metabolic branches.

Discussion

Using genetic and biochemical approaches we show in this study that *L. pneumophila* catabolizes glycerol under extracellular and intracellular conditions. To our knowl-edge this is the first study to show the direct usage of glycerol (or glucose) by intracellularly growing *L. pneumophila*. The Δ*glpD* mutant showed a replication and competition defect compared with wild-type *L. pneumophila*, suggesting that glycerol might be used as an intracellular carbon source by the bacteria. In agreement with this notion, the *gpsA* gene encoding glycerol-3-phosphate dehydrogenase in *Legionella oak-ridgensis*, was recently identified as a virulence factor using *Acanthamoeba lenticulata* as a host (Brzuszkiewicz *et al.*, 2013).

Isotopologue profiling of *L. pneumophila* grown in MDM with [U-^{13}C$_3$]glycerol revealed carbon flux from glycerol through gluconeogenesis (for the production of mannose) and through the PPP (for the *de novo* synthesis of histidine). *L. pneumophila* metabolizes glucose preferentially via the ED pathway, and thus, the EMP pathway is not the preferred route for carbohydrate catabolism (Eylert *et al.*, 2010; Harada *et al.*, 2010). Our study now proves that the gluconeogenic pathway is active in *L. pneumophila*. A critical step in this pathway is the conversion of fructose-1,6-diphosphate to fructose-6-phosphate catalyzed by fructose-1,6-bisphos-phatase. A corresponding homologue is not found in *Legionella* spp. genomes, and only phosphofructokinase (*lpg1913* alias *pfkA*) is annotated (Chien *et al.*, 2004; Cazalet *et al.*, 2010). Yet, fructose-1,6-bisphosphatase activity in *L. pneumophila* cell extracts is 10-fold higher than phosphofructokinase activity, indicating that this step in the EMP pathway favors the gluconeogenic rather than the glycolytic direction (Keen and Hoffman, 1984). Interestingly, the putative *L. pneumophila* phos-phofructokinase is homologous to eukaryotic and bacte-rial PfkA enzymes that do not use ATP but
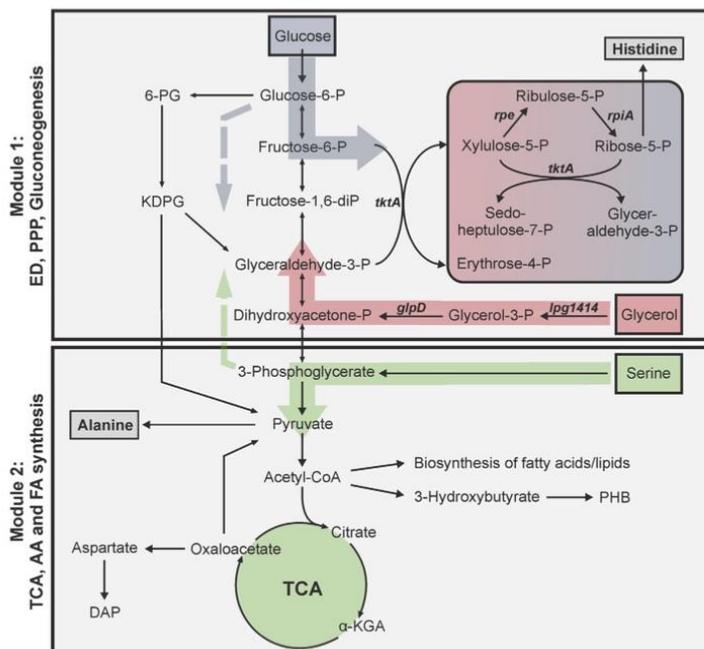
Fig. 6. The bipartite metabolism of *L. pneumophila*. The metabolism of *L. pneumophila* is divided into two modules, containing the ED pathway, gluconeogenesis and the PPP (red-blue rectangle) in module 1 and the TCA cycle (green cycle) as well as amino acid and fatty acid synthesis in module 2. Thick coloured arrows represent main routes of carbon flow from glucose (blue), glycerol (red) and serine (green). Metabolic flow of glucose and glycerol is mainly restricted to the upper part of metabolism (module 1), while serine is mainly used in the lower, energy-generating part of metabolism (module 2). Whereas glycerol is exclusively used for gluconeogenesis and the PPP in module 1, glucose and serine are channeled through module 2 (dotted blue arrow) as well as module 1 (dotted green arrow) respectively. *Abbreviations*: 6-PG, 6-phosphogluconate; KDPG, 2-keto-3-desoxy-phosphogluconate; PPP, pentose phosphate pathway; PHB, poly-hydroxybutyrate; TCA, tricarboxylic acid cycle; α-KGA, α-ketoglutaric acid; DAP, diaminopimelic acid. *Genes*: *tktA*, transketolase; *rpe*, ribulose-5-phosphate-epimerase; *rpiA*, ribulose-5-phosphate-isomerase; *lpg1414*, glycerol kinase; *glpD*, glycerol-3-phosphate dehydrogenase.

pyro-phosphate as cofactor and are reversible (Arimoto *et al.*, 2002; Costa dos Santos *et al.*, 2003). Thus, *L. pneumophila* PfkA might also catalyze both the forward (glycolytic) and the reverse (gluconeogenic) reaction.

Our data show for the first time activity of at least parts of the PPP in *L. pneumophila*. The genome of *L. pneumophila* encodes complete EMP and ED pathways, but only an incomplete PPP lacking the oxidative branch (6-phosphogluconate-dehydrogenase) and trans-aldolase (Cazalet *et al.*, 2004; Chien *et al.*, 2004). Accordingly, the key metabolite for entry into the PPP is likely fructose-6-phosphate rather than glucose-6-phosphate. The non-oxidative branch of the PPP is essential for the conversion of carbohydrates. The C5-sugars required for the synthesis of histidine, purines and pyrimidines can be made directly from fructose-6-phosphate (together with glyceraldehyde-3-phosphate) in the transketolase reaction. Ribose-5-phosphate is then produced through reactions catalyzed by ribulose-5-phopsphate isomerase and epimerase. While the non-oxidative PPP branch is sufficient for the interconversion of sugars, it cannot provide NADPH/H⁺. *L. pneumophila* can compensate the lack of the oxidative PPP branch

by utilizing the ED pathway, which also generates NADPH/H⁺.

Unexpectedly, when the *L. pneumophila* Δ*glpD* mutant strain was grown *in vitro* in the presence of ¹³C-glycerol, lactate (but no other metabolites) showed some ¹³C-enrichment. Lactate could be produced by a detoxifica-tion reaction of methylglyoxal, which is a byproduct of glycerol metabolism. Methylglyoxal can be generated non-enzymatically from glyceraldehyde-3-phosphate or dihydroxyacetone-phosphate in wild-type bacteria. As this route is blocked in the mutant lacking *glpD*, the bac-teria might use glycerol dehydrogenase to make dihy-droxyacetone, which is converted non-enzymatically to methylglyoxal. Since this intermediate is toxic, it is con-verted to lactate via the glyoxalase system (Supporting Information Fig. S7) (Riddle and Lorenz, 1973; Cooper, 1984; Subedi *et al.*, 2008).

L. pneumophila utilized glycerol only in the stationary growth phase, while serine and (to a lower extent) glu-cose were metabolized already in early growth phases. The amount of ¹³C-incorporation from these substrates indicates that serine is indeed the preferred carbon source for *L. pneumophila* as shown also in previous

studies (Eylert *et al.*, 2010). ^{13}C-Incorporation from ^{13}C-labelled glucose was high (20.72% in histidine after 48 h), while ^{13}C-incorporation from ^{13}C-glycerol was rather low (3.00% in histidine after 48 h). These findings suggest that glycerol plays only a minor role for *L. pneumophila* in the hierarchy of carbon substrates, at least under extracellular conditions. The ratio of ^{13}C-excess, calculated from histidine as marker of the PPP and alanine as marker of the energy-generating lower part of glycolysis and the TCA cycle, showed that glycerol and glucose were predominantly used for gluconeogenesis and the PPP respectively, while serine was fed mainly into the lower part of the glycolytic pathway and the TCA cycle.

Based on these results, we propose a bipartite model for the metabolism of *L. pneumophila* (Fig. 6). According to this model, the carbon metabolism of *L. pneumophila* can be divided into two modules: module 1, comprising the ED pathway, gluconeogenesis and the PPP, provides essentially NADPH/H$^+$ and the precursors for the anabolic, energy-consuming pathways, leading to cell wall components, nucleotides, histidine and aromatic amino acids and module 2, comprising the lower part of the glycolytic pathway and the TCA cycle, which provides ATP, NADH/H$^+$, FADH$_2$ and the precursors for the biosynthesis of aliphatic amino acids and fatty acids/lipids. Module 1 is thus the energy-consuming part, essential for cell wall biosynthesis and hence cell division and proliferation, while module 2 is the major energy-generating part of the metabolism, which supplies ATP by substrate phosphorylation and by oxidative phosphorylation via NADH/H$^+$-dependent aerobic respiration. In *L. pneumophila*, the metabolic flow of glycerol and glucose is predominantly directed towards gluconeogenesis and PPP thus serving module 1, while serine is mainly used for energy-generating reactions and thus serves module 2 (Fig. 6).

Noteworthy, our *in vivo* data also support a bipartite metabolism of intracellularly growing *L. pneumophila*. Addition of ^{13}C-glycerol to infected *A. castellanii* resulted in the exclusive incorporation of ^{13}C-label into mannose in the bacterial fraction. This was dependent on GlpD and did not occur in the host cell. Moreover, ^{13}C-glucose was also metabolized mainly to mannose by intracellular *L. pneumophila*. Interestingly, no ^{13}C-incorporation from ^{13}C-serine into mannose was detectable *in vivo*, neither in the host nor in intracellular *L. pneumophila*, while substantial incorporation was observed into amino acids, DAP and PHB.

A modular metabolism is also employed by other intracellular bacterial pathogens, and thus, seems to represent a general concept. However, depending on the microorganism, the same substrate might be metabolized by different modules. Other than *L. pneumophila*, *L. monocytogenes* can grow on glycerol as sole carbon source *in vitro* (Schneebeli and Egli, 2013). Intracellularly,

L. monocytogenes uses amino acids, glucose-6-phosphate and glycerol imported from the host cell (Grubmüller *et al.*, 2014). Yet, amino acids are not catabolized by *L. monocytogenes* but directly used for protein synthesis, while glycerol is efficiently used for energy generation, and glucose-6-phosphate predominantly serves anabolic purposes (Grubmüller *et al.*, 2014). Intracellularly growing *Mycobacterium tuberculosis* also employs a modular metabolism, such that acetate is used for energy generation, while an unknown C$_3$ substrate is used for anabolic purposes and in the PPP (de Carvalho *et al.*, 2010). Furthermore, carbon flux from dextrose only occurs in the PPP, and the sugar is not used for energy generation. Under these conditions, *M. tuberculosis* also imports amino acids from the host, but uses these compounds only for protein synthesis (Beste *et al.*, 2013).

As *L. pneumophila* seems to metabolize glycerol in later growth phases, a prominent source of intracellular glycerol might be the disintegration of host cell membranes upon LCV lysis through secreted phospholipases (Lang and Flieger, 2011). The finding that glycerol and glucose are directly metabolized by intracellular *L. pneumophila* suggests that the LCV is also accessible for substrates from the extracellular milieu of infected cells. Yet, the mode of uptake of these compounds into LCVs is unclear. Glycerol could enter the host cell via diffusion or transport. Aquaglyceroporines are common transporters in eukaryotes that facilitate uptake of water and glycerol and were also shown to be involved in innate immunity (Zhu *et al.*, 2011). Intracellularly growing *L. pneumophila* exploits host cell transporters (Wieland *et al.*, 2005), and the proteome of purified LCVs revealed a large number of eukaryotic transporters (Hoffmann *et al.*, 2014a), including glucose transporters (Slc2a1, Slc2a6) and a glycerol transporter (Slc37a1). Thus, these transporters likely associate with the LCV membrane and facilitate the uptake of substrates into the pathogen compartment.

Phosphorylated carbon substrates might play an important role for the nutrition of *L. pneumophila*. In the genome of *L. pneumophila* only a glycerol-3-phosphate transporter (GlpT) is annotated, suggesting that the bacteria transport glycerol-3-phosphate rather than glycerol, even though the growth of *L. pneumophila* in MDM was not enhanced by glycerol-3-phosphate (Fig. 1C). The proteome of purified LCVs indicates that the eukaryotic glycerol kinase (Gk) might be associated with the LCV membrane (Hoffmann *et al.*, 2014a). This enzyme could phosphorylate cytoplasmic glycerol to glycerol-3-phosphate, which could be taken up into the LCV and subsequently transported into the bacteria. Isotopologue profiling experiments revealed that *L. pneumophila* growing extracellularly in presence of ^{13}C-glucose and unlabelled glucose-6-phosphate incorporated much less

[13]C-label compared to ^{13}C-glucose alone (data not shown). Thus, intracellular *L. pneumophila* might also prefer glucose-6-phosphate as a growth substrate rather than glucose. To transport glucose-6-phosphate, the intracellular bacterium *Chlamydia pneumoniae* uses the transporter UhpC (*alias* HPTcp) (Schwoppe *et al.*, 2002), which also seems to be encoded in the *L. pneumophila* genome. Finally, *L. monocytogenes* also relies on glucose-6-phosphate rather than glucose for intracellular growth (Chico-Calero *et al.*, 2002; Grubmüller *et al.*, 2014).

L. pneumophila's metabolic strategy that relies on amino acids as substrates for energy production and uses carbohydrates mainly for anabolic purposes might put less nutritional stress on the host cell and therefore ensure successful infection and prolonged intracellular replication. Intracellular levels of glucose are a regulator of apoptosis in eukaryotes (Zhao *et al.*, 2008). As long as intracellular glucose levels are normal, antiapoptotic proteins of the Bcl-2 family prevent cell death through apoptosis. The loss of glucose leads to decreased levels of Bcl-2 regulators (Alves *et al.*, 2006; Zhao *et al.*, 2007), which in consequence causes the activation of pro-apoptotic proteins (Chi *et al.*, 2000). Further studies are required to elucidate the intricate links between metabolism and virulence of *L. pneumophila*.

Experimental procedures

Bacteria, cells and growth conditions

L. pneumophila strains (Supporting Information Table S1) were cultured under aerobic conditions at 37°C in AYE broth or grown on CYE agar plates supplemented with chloramphenicol (Cm; 5 μg mL^{-1}) or kanamycin (Km; 50 μg mL^{-1} in broth or 10 μg mL^{-1} in agar plates), if necessary. Alternatively, *L. pneumophila* was cultivated at 37°C in chemically defined medium (CDM) (Eylert *et al.*, 2010) modified from 'Ristroph medium' (Ristroph *et al.*, 1981), minimal defined medium (MDM) (Supporting Information Table S2) or, in case of time series experiments, in MDM containing 50 mM glycerol and 11 mM glucose (carbon-enriched minimal defined medium; CE MDM) (Supporting Information Table S2). The media were prepared by dissolving all components except Fe-pyrophosphate in 950 ml ddH$_2$0. The pH was adjusted to 6.3 (CDM) or 6.5 (MDM and CE MDM) using KOH, Fe-pyrophosphate was dissolved and filled up to 1 L.

Escherichia coli TOP10 was used for cloning and grown in LB medium at 37°C containing 30 μg mL^{-1} Cm or 50 μg mL^{-1} Km, if necessary. *A. castellanii* (ATCC 30234, lab collection) was grown in PYG medium at 23°C. Murine RAW 264.7 macrophages (ATCC: TIB-71^{Tm}, lab collection) were cultivated in RPMI 1640 medium containing 10% heat inactivated fetal bovine serum (FBS) and 2 mM glutamine at 37°C and 5% CO$_2$.

Construction of chromosomal deletion mutant strain

Chromosomal deletion of *glpD* in *L. pneumophila* wild-type JR32 was performed as described previously (Wiater *et al.*, 1994; Tiaden *et al.*, 2007), yielding strain CM01. The allelic exchange vector pCM018 (Supporting Information Table S1) was constructed in a four-way ligation using 0.8 kb of the 5′ and 0.8 kb of the 3′ flanking region of *glpD* and a Km resistance cassette from vector pUC4K. The flanking regions were amplified using the primer pairs *glpD*-LB-XbaI-fo, *glpD*-LB-SalI-re and *glpD*-RB-SalI-fo, *glpD*-RB-XbaI-re (Supporting Information Table S1) respectively, and digested using the restriction enzymes SalI and XbaI. The plasmid pUC4K was digested using SalI resulting in a 1.4 kB fragment containing the Km resistance cassette. The flanking regions and Km resistance cassette were then cloned into vector pLAW344 in a four-way ligation and transformed into *E.coli* TOP10. Clones were analysed by restriction digestion and sequenced using the primers Kan2-fo and Kan2-re. *L. pneumophila* JR32 was transformed with pCM018 by electroporation. Km^R colonies were selected after 5 days growth at 30°C, grown overnight in AYE broth containing 50 μg mL^{-1} Km and then spotted on CYE/Km, CYE/Km/2% sucrose and CYE/Cm plates, and grown at 30°C to select for Cm^S/Km^R/Suc^R colonies. Double-cross-over mutants were confirmed by PCR and sequenced. The *Legionella* homepage of the Pasteur Institute (http://genolist.pasteur.fr/Legiolist/) and the NCBI database (http://www.ncbi.nlm.nih.gov/) were used for sequence comparison.

The vector pCM021 (Supporting Information Table S1) for complementation of mutant strain CM01 was constructed using primer pair *glpD*-BamHI-fo-Kompl and *glpD*-SalI-re-Kompl. PCR products were digested using BamHI and SalI, cloned into vector pCR33 and transformed into *E. coli* TOP10. Cells were plated on LB/Cm plates, plasmids were re-isolated from single colonies, analysed by restriction digestion and sequenced.

Extracellular growth of L. pneumophila

To investigate the influence of glycerol on extracellular growing bacteria, *L. pneumophila* wild-type or Δ*glpD* were resuspended from CYE agar plates and grown in CDM overnight at 37°C (starting OD$_{600}$ of 0.1) to an OD$_{600}$ of maximum 1.0. Cultures were then diluted to OD$_{600}$ = 0.1 in CDM or MDM with and without 50 mM glycerol or 50 mM glycerol-3-phosphate and further incubated for 48 h at 37°C. The optical density was assessed at several time points.

Intracellular replication of L. pneumophila

To analyse intracellular replication of *L. pneumophila*, we used previously published protocols (Harrison *et al.*, 2013). In brief, *A. castellanii* were grown in PYG medium, seeded in 96 well plates at 4 × 10^5 cells per well and incubated overnight at 23°C to allow replication (doubling) of the amoeba. *L. pneumophila* strains harboring plasmid pNT-28 (constitutive GFP production) were resuspended from AYE

plates in AYE/Cm (5 μg mL^{-1}) and grown overnight at 37°C from a starting OD_{600} of 0.1 to an OD_{600} of 3. Bacteria were diluted in LoFlo medium (ForMedium), and amoeba were infected with *L. pneumophila* (MOI 20). Infections were synchronised by centrifugation at 500 × *g* for 10 min. 50 mM glycerol was added 4 h post infection to certain wells and infected amoeba were incubated at 30°C. GFP fluorescence was measured in a plate spectrophotometer (Optima FluoStar, BMG Labtech) at specific intervals. Murine RAW 264.7 macrophages were grown in RPMI medium containing 10% FBS and 2 mM glutamine at 37°C/ 5% CO_2. Infections were performed as described above for assays with *A. castellanii*, but the bacteria were diluted in RPMI 1640 medium prior to infection, and the plates were incubated at 37°C/5% CO_2. As the cell culture media used do not support growth of *L. pneumophila*, GFP fluorescence only reflects intracellular bacteria replication.

Intracellular growth of *L. pneumophila* was also assessed by determining cfu. To this end, *A. castellanii* or RAW 264.7 macrophages were suspended in Ac buffer [4 mM $MgSO_4$ × 7 H_2O, 0.4 mM $CaCl_2$, 3.4 mM sodium citrate dihydrate, 0.05 mM $Fe(NH_4)_2(SO_4)_2$ × 6 H_2O, 0.05 mM Na_2HPO_4 × 7 H_2O, 2.5 mM KH_2PO_4, 0.05 mM NH_4Cl, pH 6.5] or RPMI 1640 medium respectively. 5 × 10^4 cells per well were seeded into 96-well plates and incubated at 23°C (amoeba) or 37°C/5% CO_2 (macrophages) for 1 h. The cells were then infected with *L. pneumophila* (MOI 0.1), and the infection was synchronized by centrifugation at 500 × *g* for 10 min. The cells were further incubated for 1 h and washed with Ac buffer or RPMI 1640 medium. 50 mM glycerol was added 4 h post infection to certain wells. For complementation assays, the Δ*glpD* mutant strain harboring plasmid pCM021 was grown overnight with 1 mM IPTG to induce expression of *glpD*. Infection was performed as described above. After 48 h (macrophages) or 72 h (amoeba), the *L. pneumophila*-infected cells were lysed with 0.8% saponin, and appropriate dilutions were plated on CYE agar plates to determine cfu.

Intracellular growth of L. pneumophila *in competition assays*

For the competition assay, we used a previously published protocol (Kessler *et al.*, 2013). Briefly, *A. castellanii* (5 × 10^4 per well, 96-well plate) amoeba were infected at a 1:1 ratio with *L. pneumophila* wild-type and mutant strain Δ*glpD* (MOI 0.01 each) in Ac buffer. After centrifugation (500 × *g*, 10 min) and 1 h of infection, the amoeba were washed and fresh Ac buffer was added. The infection continued for 3 days at 37°C. After 3 days, the supernatant and lysed amoeba (0.8% saponin) were combined, diluted 1:1000 and used to infect fresh amoeba (5 × 10^4 per well, 96-well plate; 50 μL homogenate per 200 μL amoeba culture). Aliquots of the homogenates were plated in parallel on CYE agar plates with and without Km (10 μg mL^{-1}) to determine cfu and to distinguish between wild-type and Km-resistant mutants. Cells were then further incubated at 37°C for another 3 days, and lysis and reinfection was repeated. For complementation assays, the Δ*glpD* mutant harboring plasmid pCM021 was grown overnight with 1 mM IPTG to

induce expression of *glpD*. *A. castellanii* were infected at a 1:1 ratio with wild-type *L. pneumophila* and Δ*glpD* harboring pCM021 (MOI 0.1 each) as described above. After 1, 2 and 3 days samples were taken as described above and aliquots were plated in parallel on CYE agar plates with and without Km (10 μg mL^{-1}).

Labelling of extracellular growing L. pneumophila

For isotopologue profiling, *L. pneumophila* wild-type or Δ*glpD* mutant bacteria were grown overnight in CDM (starting $OD_{600} = 0.1$). The next day, bacteria were diluted to an OD_{600} of 0.1 in 100 mL MDM containing 50 mM [U-$^{13}C_3$]glycerol and incubated in a shaking incubator at 180 rpm and 37°C for 48 h. The cells were harvested by centrifugation at 3500 × *g* for 15 min at 4°C and washed three times with cold Ac buffer (2 × 50 mL, 1 × 1 mL). An aliquot was plated on CYE agar plates. The resulting bacterial cell pellet was autoclaved at 120°C for 20 min, freeze-dried and then stored at −20°C until analysis.

For time course experiments, an overnight culture of *L. pneumophila* wild-type grown in CDM was diluted in CE MDM to a starting OD_{600} of 0.1. The CE MDM contained either 50 mM [U-$^{13}C_3$]glycerol, 11 mM [U-$^{13}C_6$]glucose or 6 mM [U-$^{13}C_3$]serine as a labelled substrate. Bacteria were cultivated in a shaking incubator at 180 rpm and 37°C. 30 mL samples were taken after 12 h, 24 h, 36 h and 48 h, OD_{600} was determined, and an aliquot was plated on CYE agar plates. Cells were harvested as described above.

Labelling of L. pneumophila *growing in* A. castellanii

To label intracellularly growing *L. pneumophila* with ^{13}C-substrates, we used previously published protocols (Heuner and Eisenreich, 2013). In brief, *A. castellanii* was cultivated in 8 T75 cell culture flasks per bacterial strain (10 mL PYG/75 cm^2 flask). After the cells reached confluency (∼2 × 10^7 cells per flask), the amoeba were infected with *L. pneumophila* wild-type or Δ*glpD* (MOI 50), by adding bacteria grown in AYE to an OD_{600} of 3 at appropriate dilutions. The flasks were then centrifuged to synchronize infection (500 × *g*, 10 min) and incubated for 1 h at 37°C. To remove extracellular bacteria, cells were washed once with 10 mL pre-warmed Ac buffer, overlaid with 10 mL pre-warmed Ac buffer and further incubated at 37°C. 5 h post infection, either 50 mM [U-$^{13}C_3$]glycerol, 11 mM [U-$^{13}C_6$]glucose or 6 mM [U-$^{13}C_3$]serine was added to the flasks, and the cells were further incubated for 10 h. To determine the portion of extracellular *L. pneumophila*, the infected amoeba were washed as described above, spun onto microscopy slides, fixed with PFA, and extracellular bacteria were stained with a rabbit polyclonal FITC-conjugated anti-*L. pneumophila* antibody (Thermo Scientific; 1:50 in 5% FBS/Ac buffer, 1 h room temperature).

Fifteen hours post infection the amoeba were detached using a cell scraper, transferred into 50 mL reaction tubes, frozen at −80°C for 1 h and again thawed to room temperature. The suspension was then centrifuged at 200 × *g* for 10 min at 4°C, and the supernatant was transferred to new 50 mL reaction tubes. The pellet, representing eukaryotic cell debris (F1) was washed twice with 50 mL and once with 1 mL cold Ac buffer. The supernatant harvested after

3. RESULTS

the first centrifugation step contained *L. pneumophila* bacteria (F2). This fraction was centrifuged at 3500 × *g* for 15 min at 4°C, and the resulting pellet was washed twice with 50 mL and once with 1 mL cold Ac buffer. The supernatant of F2 was filtered through a 0.22 μm pore filter to remove bacteria, and then 100% trichloroacetic acid was added to a final concentration of 10%. The supernatant was incubated on ice for 1 h and centrifuged at 4600 × *g* for 30 min at 4°C. The resulting pellet (F3) contained cytosolic proteins of *A. castellanii*. The pellets of F1, F2 and F3 were autoclaved at 120°C for 20 min, freeze-dried and stored at −20°C until analysis. To monitor cell lysis and the purity of F1 and F2, samples were analyzed by microscopy, and aliquots were plated on CYE agar plates.

Sample preparation of protein-derived amino acids, DAP and PHB

For isotopologue profiling of amino acids, diaminopimelic acid (DAP) and polyhydroxybutyrate (PHB), bacterial cells (approximately 10^9) or 1 mg of the freeze-dried host protein fraction were hydrolyzed in 0.5 mL of 6 M HCl for 24 h at 105°C, as described earlier (Eylert *et al.*, 2010). The HCl was removed under a stream of nitrogen, and the remainder was dissolved in 200 μL acetic acid. The sample was purified on a cation exchange column of Dowex 50Wx8 (H^+ form, 200–400 mesh, 5 × 10 mm), which was washed previously with 1 mL methanol and 1 mL ultrapure water. The column was eluted with 2 mL distilled water (eluate 1) and 1 mL 4 M ammonium hydroxide (eluate 2). An aliquot of the respective eluates was dried under a stream of nitrogen at 70°C.

The dried remainder of eluate 2 was dissolved in 50 μL dry acetonitrile and 50 μL *N*-(tert-butyldimethylsilyl)-*N*-methyl-trifluoroacetamide containing 1% tert-butyldimethylsilyl chloride (Sigma) and kept at 70°C for 30 min. The resulting mixture of tert-butyldimethylsilyl derivates (TBDMS) of amino acids and DAP was used for further GC/MS analysis. Due to acid degradation, the amino acids tryptophan and cysteine could not be detected with this method. Furthermore, the hydrolysis condition led to the conversion of glutamine and asparagine to glutamate and aspartate. PHB was hydrolyzed to its monomeric component 3-hydroxybutyric acid. For derivatization of 3-hydroxybutyric acid, the dried aliquot of eluate 1 was dissolved in 100 μL *N*-methyl-*N*-(trimethylsilyl)-trifluoroacetamide (Sigma) and incubated in a shaking incubator at 110 rpm (30 min, 40°C). The resulting trimethylsilyl derivative (TMS) of 3-hydroxybutyric acid derived from PHB was used for GC/MS analysis without further treatment.

Sample preparation of methanol soluble metabolites including fatty acids

For isotopologue profiling of methanol soluble metabolites, 5 mg of the freeze-dried bacterial cells were mixed with 0.8 g of glass beads (0.25–0.05 mm) and 1 mL cooled 100% methanol. The mechanical cell lysis was performed for 3 × 20 s at 6.5 m/s using a ribolyser (Hybaid). After centrifugation at 2300 × *g* for 10 min, the supernatant was dried under a stream of nitrogen. The remainder was dis-

solved in 50 μL dry acetonitrile and 50 μL *N*-(tert-butyldimethylsilyl)-*N*-methyl-trifluoroacetamide containing 1% tert-butyldimethylsilyl chloride (Sigma) and kept at 70°C for 30 min. The resulting mixture of tert-butyldimethylsilyl derivates (TBDMS) of polar metabolites and fatty acids was used for GC/MS analysis without further treatment.

Sample preparation of mannose

For isotopologue profiling of mannose, 5 mg of the freeze-dried bacterial cells were dissolved in 0.5 mL 3 M methanolic HCl and kept at 80°C overnight. After cooling to room temperature, the supernatant was dried under a stream of nitrogen. For derivatization, the residue was dissolved in 1 mL acetone containing 20 μL concentrated H_2SO_4 and kept at room temperature for 1 h. After addition of 2 mL saturated NaCl solution and 2 mL saturated Na_2CO_3 solution the mixture was extracted twice with 3 mL ethyl acetate. The organic phases were combined and dried under a stream of nitrogen. The residue was dissolved in a mixture of 100 μL ethyl acetate and 100 μL acetic anhydride and kept at 60°C overnight. The derivatization reagent was removed under a stream of nitrogen, and the sample was dissolved in 100 μL anhydrous ethyl acetate. The resulting mixture of diisopropylidene/acetate derivatives was used for further GC/MS analysis. As this procedure leads to the dephosphorylation of sugar-phosphates, the mannose detected could also originate from mannose-6-phosphate and mannose-1-phosphate.

Gas chromatography/mass spectrometry and isotopologue analysis

GC/MS-analysis was performed with a QP2010 Plus gas chromatograph/mass spectrometer (Shimadzu) equipped with a fused silica capillary column (Equity TM-5; 30 m × 0.25 mm, 0.25 μm film thickness; SUPELCO) and a quadrupol detector working with electron impact ionization at 70 eV. A volume of 0.1–6 μL of the sample was injected in 1:5 split mode at an interface temperature of 260°C and a helium inlet pressure of 70 kPa. With a sampling rate of 0.5 s, selected ion monitoring was used. Data was collected using LabSolution software (Shimadzu). All samples were measured three times (technical replicates). ^{13}C-Excess values and isotopologue compositions were calculated as described before (Eylert *et al.*, 2008) including: (i) determination of the spectrum of unlabelled derivatized metabolites, (ii) determination of mass isotopologue distributions of labelled metabolites and (iii) correction of ^{13}C-incorporation concerning the heavy isotopologue contributions due to the natural abundances in the derivatized metabolites.

For analysis of amino acids, the column was kept at 150°C for 3 min and then developed with a temperature gradient of 7°C min^{-1} to a final temperature of 280°C that was held for 3 min. The amino acids alanine (6.7 min), glycine (7.0 min), valine (8.5 min), leucine (9.1 min), isoleucine (9.5 min), proline (10.1 min), serine (13.2 min), phenylalanine (14.5 min), aspartate (15.4 min), glutamate (16.8 min), lysine (18.1 min), histidine (20.4 min) and tyrosine (21.0

min) were detected, and isotopologue calculations were performed with m/z [M-57]$^+$ or m/z [M-85]$^+$.

For analysis of DAP, the column was developed at 280°C for 3 min and then with a temperature gradient of 10°C min^{-1} to a final temperature of 300°C that was held for 3 min. The TBDMS-derivative of DAP was detected at a retention time of 6.2 min, and isotopologue calculations were performed with m/z [M-57]$^+$. For the detection of 3-hydroxybutyric acid derived from PHB, the column was heated at 70°C for 3 min and then developed with a first temperature gradient of 10°C min^{-1} to a final temperature of 150°C. This was followed by a second temperature gradient of 50°C min^{-1} to a final temperature of 280°C, which was held for 3 min. The TMS-derivative of 3-hydroxybutyric acid, was detected at a retention time of 9.1 min, and isotopologue calculations were performed with m/z [M-15]$^+$.

For the analysis of methanol soluble metabolites, the column was heated at 100°C for 2 min and then developed with a first temperature gradient of 3°C min^{-1} to a final temperature of 234°C, a second temperature gradient of 1°C min^{-1} to a final temperature of 237°C, and a third temperature gradient of 3°C min^{-1} to a final temperature of 260°C. TBDMS-derivatives of lactate (17.8 min), 3-hydroxybutyric acid (21.6 min), succinic acid (27.5 min), fumaric acid (28.7 min), malic acid (39.1 min), palmitic acid (44.0 min), stearic acid (49.4 min) and citric acid (53.25 min) were detected, and isotopologue calculations were performed with m/z [M-57]$^+$.

For diisopropylidene/acetate derivatives of sugars, the column was heated at 150°C for 3 min and then developed with a first temperature gradient of 10°C min^{-1} to a final temperature of 220°C, and with a second temperature gradient of 50°C min^{-1} to a final temperature of 280°C, which was held for 3 min. Isotopologue calculations were performed with m/z 287 [M-15]$^+$, a fragment which still contains all C-atoms of mannose. Retention times and mass fragments of derivatized metabolites that were used for all isotopologue calculations are documented in Supporting Information Table S3A.

Acknowledgements

References

Alves, N.L., Derks, I.A., Berk, E., Spijker, R., van Lier, R.A., and Eldering, E. (2006) The Noxa/Mcl-1 axis regulates susceptibility to apoptosis under glucose limitation in dividing T cells. *Immunity* **24**: 703–716.

Arimoto, T., Ansai, T., Yu, W., Turner, A.J., and Takehara, T. (2002) Kinetic analysis of PPi-dependent phosphofructo-kinase from *Porphyromonas gingivalis*. *FEMS Microbiol Lett* **207**: 35–38.

Beste, D.J., Noh, K., Niedenfuhr, S., Mendum, T.A., Hawkins, N.D., Ward, J.L., et al. (2013) ^{13}C-flux spectral analysis of host-pathogen metabolism reveals a mixed diet for intracellular *Mycobacterium tuberculosis*. *Chem Biol* **20**: 1012–1021.

Brüggemann, H., Hagman, A., Jules, M., Sismeiro, O., Dillies, M.A., Gouyette, C., et al. (2006) Virulence strategies for infecting phagocytes deduced from the *in vivo* transcriptional program of *Legionella pneumophila*. *Cell Microbiol* **8**: 1228–1240.

Brzuszkiewicz, E., Schulz, T., Rydzewski, K., Daniel, R., Gillmaier, N., Dittmann, C., et al. (2013) *Legionella oakridgensis* ATCC 33761 genome sequence and phenotypic characterization reveals its replication capacity in amoebae. *Int J Med Microbiol* **303**: 514–528.

Byrne, B., and Swanson, M.S. (1998) Expression of *Legionella pneumophila* virulence traits in response to growth conditions. *Infect Immun* **66**: 3029–3034.

Cazalet, C., Gomez-Valero, L., Rusniok, C., Lomma, M., Dervins-Ravault, D., Newton, H.J., et al. (2010) Analysis of the *Legionella longbeachae* genome and transcriptome uncovers unique strategies to cause Legionnaires' disease. *PLoS Genetics* **6**: e1000851.

Cazalet, C., Rusniok, C., Brüggemann, H., Zidane, N., Magnier, A., Ma, L., et al. (2004) Evidence in the *Legionella pneumophila* genome for exploitation of host cell functions and high genome plasticity. *Nat Genet* **36**: 1165–1173.

Chen, D.E., Podell, S., Sauer, J.D., Swanson, M.S., and Saier, M.H., Jr. (2008) The phagosomal nutrient transporter (Pht) family. *Microbiology* **154**: 42–53.

Chi, M.M., Pingsterhaus, J., Carayannopoulos, M., and Moley, K.H. (2000) Decreased glucose transporter expression triggers BAX-dependent apoptosis in the murine blastocyst. *J Biol Chem* **275**: 40252–40257.

Chico-Calero, I., Suarez, M., Gonzalez-Zorn, B., Scortti, M., Slaghuis, J., Goebel, W., et al. (2002) Hpt, a bacterial homolog of the microsomal glucose-6-phosphate translocase, mediates rapid intracellular proliferation in *Listeria*. *Proc Natl Acad Sci USA* **99**: 431–436.

Chien, M., Morozova, I., Shi, S., Sheng, H., Chen, J., Gomez, S.M., et al. (2004) The genomic sequence of the accidental pathogen *Legionella pneumophila*. *Science* **305**: 1966–1968.

Cooper, R.A. (1984) Metabolism of methylglyoxal in microorganisms. *Ann Rev Microbiol* **38**: 49–68.

Costa dos Santos, A., Seixas da-Silva, W., de Meis, L., and Galina, A. (2003) Proton transport in maize tonoplasts supported by fructose-1,6-bisphosphate cleavage. Pyrophosphate-dependent phosphofructokinase as a pyrophosphate-regenerating system. *Plant Physiol* **133**: 885–892.

D'Auria, G., Jimenez-Hernandez, N., Peris-Bondia, F., Moya, A., and Latorre, A. (2010) *Legionella pneumophila* pangenome reveals strain-specific virulence factors. *BMC Genomics* **11**: 181.

de Carvalho, L.P., Fischer, S.M., Marrero, J., Nathan, C., Ehrt, S., and Rhee, K.Y. (2010) Metabolomics of *Mycobacterium tuberculosis* reveals compartmentalized co-catabolism of carbon substrates. *Chem Biol* **17**: 1122–1131.

Eylert, E., Herrmann, V., Jules, M., Gillmaier, N., Lautner, M., Buchrieser, C., *et al.* (2010) Isotopologue profiling of *Legionella pneumophila*: role of serine and glucose as carbon substrates. *J Biol Chem* **285**: 22232–22243.

Eylert, E., Schär, J., Mertins, S., Stoll, R., Bacher, A., Goebel, W., and Eisenreich, W. (2008) Carbon metabolism of *Listeria monocytogenes* growing inside macrophages. *Mol Microbiol* **69**: 1008–1017.

Faucher, S.P., Mueller, C.A., and Shuman, H.A. (2011) *Legionella pneumophila* transcriptome during intracellular multiplication in human macrophages. *Front Microbiol* **2**: 60.

Finsel, I., and Hilbi, H. (2015) Formation of a pathogen vacuole according to *Legionella pneumophila*: how to kill one bird with many stones. *Cell Microbiol* **17**: 935–950.

Finsel, I., Ragaz, C., Hoffmann, C., Harrison, C.F., Weber, S., van Rahden, V.A., *et al.* (2013) The *Legionella* effector RidL inhibits retrograde trafficking to promote intracellular replication. *Cell Host Microbe* **14**: 38–50.

Fonseca, M.V., Sauer, J.D., Crepin, S., Byrne, B. and Swanson, M.S. (2014) The *phtC-phtD* locus equips *Legionella pneumophila* for thymidine salvage and replication in macrophages. *Infect Immun* **82**: 720–730.

Gillmaier, N., Götz, A., Schulz, A., Eisenreich, W., and Goebel, W. (2012) Metabolic responses of primary and transformed cells to intracellular *Listeria monocytogenes*. *PLoS One* **7**: e52378.

Grubmüller, S., Schauer, K., Goebel, W., Fuchs, T.M., and Eisenreich, W. (2014) Analysis of carbon substrates used by *Listeria monocytogenes* during growth in J774A.1 macrophages suggests a bipartite intracellular metabolism. *Front Cell Infect Microbiol* **4**: 156.

Haneburger, I., and Hilbi, H. (2013) Phosphoinositide lipids and the *Legionella* pathogen vacuole. *Curr Top Microbiol Immunol* **376**: 155–173.

Harada, E., Iida, K., Shiota, S., Nakayama, H., and Yoshida, S. (2010) Glucose metabolism in *Legionella pneumophila*: dependence on the Entner-Doudoroff pathway and connection with intracellular bacterial growth. *J Bacteriol* **192**: 2892–2899.

Harrison, C.F., Kicka, S., Trofimov, V., Berschl, K., Ouertatani-Sakouhi, H., Ackermann, N., *et al.* (2013) Exploring anti-bacterial compounds against intracellular *Legionella*. *PLoS One* **8**: e74813.

Härtel, T., Eylert, E., Schulz, C., Petruschka, L., Gierok, P., Grubmüller, S., *et al.* (2012) Characterization of central carbon metabolism of *Streptococcus pneumoniae* by isotopologue profiling. *J Biol Chem* **287**: 4260–4274.

Heuner, K., and Eisenreich, W. (2013) The intracellular metabolism of *Legionella* by isotopologue profiling. *Methods Mol Biol* **954**: 163–181.

Hilbi, H., and Haas, A. (2012) Secretive bacterial pathogens and the secretory pathway. *Traffic* **13**: 1187–1197.

Hoffmann, C., Finsel, I., Otto, A., Pfaffinger, G., Rothmeier, E., Hecker, M., *et al.* (2014a) Functional analysis of novel Rab GTPases identified in the proteome of purified *Legionella*-containing vacuoles from macrophages. *Cell Microbiol* **16**: 1034–1052.

Hoffmann, C., Harrison, C.F., and Hilbi, H. (2014b) The natural alternative: protozoa as cellular models for *Legionella* infection. *Cell Microbiol* **16**: 15–26.

Hubber, A., and Roy, C.R. (2010) Modulation of host cell function by *Legionella pneumophila* type IV effectors. *Ann Rev Cell Dev Biol* **26**: 261–283.

Isberg, R.R., O'Connor, T.J., and Heidtman, M. (2009) The *Legionella pneumophila* replication vacuole: making a cosy niche inside host cells. *Nat Rev Microbiol* **7**: 13–24.

Keen, M.G., and Hoffman, P.S. (1984) Metabolic pathways and nitrogen metabolism in *Legionella pneumophila*. *Curr Microbiol* **11**: 81–88.

Kessler, A., Schell, U., Sahr, T., Tiaden, A., Harrison, C., Buchrieser, C., and Hilbi, H. (2013) The *Legionella pneumophila* orphan sensor kinase LqsT regulates competence and pathogen-host interactions as a component of the LAI-1 circuit. *Environ Microbiol* **15**: 646–662.

Kriegeskorte, A., Grubmüller, S., Huber, C., Kahl, B.C., von Eiff, C., Proctor, R.A., Peters, G., *et al.* (2014) *Staphylococcus aureus* small colony variants show common metabolic features in central metabolism irrespective of the underlying auxotrophism. *Front Cell Infect Microbiol* **4**: 141.

Lang, C., and Flieger, A. (2011) Characterisation of *Legionella pneumophila* phospholipases and their impact on host cells. *Eur J Cell Biol* **90**: 903–912.

Lomma, M., Dervins-Ravault, D., Rolando, M., Nora, T., Newton, H.J., Sansom, F.M., *et al.* (2010) The *Legionella pneumophila* F-box protein Lpp2082 (AnkB) modulates ubiquitination of the host protein parvin B and promotes intracellular replication. *Cell Microbiol* **12**: 1272–1291.

Molofsky, A.B., and Swanson, M.S. (2004) Differentiate to thrive: lessons from the *Legionella pneumophila* life cycle. *Mol Microbiol* **53**: 29–40.

Pine, L., George, J.R., Reeves, M.W., and Harrell, W.K. (1979) Development of a chemically defined liquid medium for growth of *Legionella pneumophila*. *J Clin Microbiol* **9**: 615–626.

Price, C.T., Al-Khodor, S., Al-Quadan, T., Santic, M., Habyarimana, F., Kalia, A., and Kwaik, Y.A. (2009) Molecular mimicry by an F-box effector of *Legionella pneumophila* hijacks a conserved polyubiquitination machinery within macrophages and protozoa. *PLoS Pathog* **5**: e1000704.

Price, C.T., Al-Quadan, T., Santic, M., Rosenshine, I. and Abu Kwaik, Y. (2011) Host proteasomal degradation generates amino acids essential for intracellular bacterial growth. *Science* **334**: 1553–1557.

Riddle, V.M., and Lorenz, F.W. (1973) Nonenzymic formation of toxic levels of methylglyoxal from glycerol and dihydroxyacetone in Ringer's phosphate suspensions of avian spermatozoa. *Biochem Biophys Res Commun* **50**: 27–34.

Ristroph, J.D., Hedlund, K.W., and Gowda, S. (1981) Chemically defined medium for *Legionella pneumophila* growth. *J Clin Microbiol* **13**: 115–119.

Rothmeier, E., Pfaffinger, G., Hoffmann, C., Harrison, C.F., Grabmayr, H., Repnik, U., Hannemann, M., *et al.* (2013) Activation of Ran GTPase by a *Legionella* effector promotes microtubule polymerization, pathogen vacuole motility and infection. *PLoS Pathog* **9**: e1003598.

Sauer, J.D., Bachman, M.A., and Swanson, M.S. (2005) The phagosomal transporter A couples threonine acquisition to differentiation and replication of *Legionella*

246 *I. Häuslein* et al. ■

pneumophila in macrophages. *Proc Natl Acad Sci USA* **102**: 9924–9929.

Schatschneider, S., Huber, C., Neuweger, H., Watt, T.F., Puhler, A., Eisenreich, W., *et al.* (2014) Metabolic flux pattern of glucose utilization by *Xanthomonas campestris* pv. *campestris*: prevalent role of the Entner-Doudoroff pathway and minor fluxes through the pentose phosphate pathway and glycolysis. *Mol Biosyst* **10**: 2663–2676.

Schneebeli, R., and Egli, T. (2013) A defined, glucose-limited mineral medium for the cultivation of *Listeria* spp. *Appl Environ Microbiol* **79**: 2503–2511.

Schunder, E., Gillmaier, N., Kutzner, E., Eisenreich, W., Herrmann, V., Lautner, M., and Heuner, K. (2014) Amino acid uptake and metabolism of *Legionella pneumophila* hosted by *Acanthamoeba castellanii. J Biol Chem* **289**: 21040–21054.

Schwoppe, C., Winkler, H.H., and Neuhaus, H.E. (2002) Properties of the glucose-6-phosphate transporter from *Chlamydia pneumoniae* (HPTcp) and the glucose-6-phosphate sensor from *Escherichia coli* (UhpC). *J Bacteriol* **184**: 2108–2115.

Sherwood, R.K., and Roy, C.R. (2013) A Rab-centric perspective of bacterial pathogen-occupied vacuoles. *Cell Host Microbe* **14**: 256–268.

Steeb, B., Claudi, B., Burton, N.A., Tienz, P., Schmidt, A., Farhan, H., *et al.* (2013) Parallel exploitation of diverse host nutrients enhances *Salmonella* virulence. *PLoS Pathog* **9**: e1003301.

Steinert, M., and Heuner, K. (2005) *Dictyostelium* as host model for pathogenesis. *Cell Microbiol* **7**: 307–314.

Subedi, K.P., Kim, I., Kim, J., Min, B., and Park, C. (2008) Role of GldA in dihydroxyacetone and methylglyoxal metabolism of *Escherichia coli* K12. *FEMS Microbiol Lett* **279**: 180–187.

Tesh, M.J., and Miller, R.D. (1981) Amino acid requirements for *Legionella pneumophila* growth. *J Clin Microbiol* **13**: 865–869.

Tesh, M.J., Morse, S.A., and Miller, R.D. (1983) Intermediary metabolism in *Legionella pneumophila*: utilization of amino acids and other compounds as energy sources. *J Bacteriol* **154**: 1104–1109.

Tiaden, A., Spirig, T., Weber, S.S., Brüggemann, H., Bosshard, R., Buchrieser, C., and Hilbi, H. (2007) The *Legionella pneumophila* response regulator LqsR promotes host cell interactions as an element of the virulence regulatory network controlled by RpoS and LetA. *Cell Microbiol* **9**: 2903–2920.

Vorwerk, H., Mohr, J., Huber, C., Wensel, O., Schmidt-Hohagen, K., Gripp, E., *et al.* (2014) Utilization of host-derived cysteine-containing peptides overcomes the restricted sulphur metabolism of *Campylobacter jejuni*. *Mol Microbiol* **93**: 1224–1245.

Weber, S., Stirnimann, C.U., Wieser, M., Frey, D., Meier, R., Engelhardt, S., *et al.* (2014) A type IV translocated *Legionella* cysteine phytase counteracts intracellular growth restriction by phytate. *J Biol Chem* **289**: 34175–34188.

Wiater, L.A., Sadosky, A.B., and Shuman, H.A. (1994) Mutagenesis of *Legionella pneumophila* using Tn*903*dII*lacZ*: identification of a growth-phase-regulated pigmentation gene. *Mol Microbiol* **11**: 641–653.

Wieland, H., Ullrich, S., F. Lang and Neumeister, B. (2005) Intracellular multiplication of *Legionella pneumophila* depends on host cell amino acid transporter SLC1A5. *Mol Microbiol* **55**: 1528–1537.

Zhao, Y., Altman, B.J., Coloff, J.L., Herman, C.E., Jacobs, S.R., Wieman, H.L., *et al.* (2007) Glycogen synthase kinase 3alpha and 3beta mediate a glucose-sensitive antiapoptotic signaling pathway to stabilize Mcl-1. *Mol Cell Biol* **27**: 4328–4339.

Zhao, Y., Wieman, H.L., Jacobs, S.R., and Rathmell, J.C. (2008) Mechanisms and methods in glucose metabolism and cell death. *Methods Enzymol* **442**: 439–457.

Zhu, N., Feng, X., He, C., Gao, H., Yang, L., Ma, Q., *et al.* (2011) Defective macrophage function in aquaporin-3 deficiency. *FASEB J* **25**: 4233–4239.

Supporting information

Additional supporting information may be found in the online version of this article at the publisher's web-site.

3.2 Regulation of core metabolic fluxes by CsrA in *L. pneumophila*

Häuslein, I., Sahr, T., Escoll, P., Klausner, N., Eisenreich, W., and Buchrieser, C., (**2017**). **Submitted**

3.2.1 Introduction

The central role of CsrA in the regulatory network, which determines the developmental switch from the replicative to the transmissive phase dependent on e.g. nutrient availability or population density, is well known for *L. pneumophila* (Byrne and Swanson, 1998; Molofsky and Swanson, 2003; Rasis and Segal, 2009; Manske and Hilbi, 2014). Thereby, this regulator acts on a post-transcriptional level, repressing virulence traits by simultaneously inducing replicative traits during exponential growth (Molofsky and Swanson, 2003; Rasis and Segal, 2009). It has been shown recently that the respective CsrA related regulatory mechanisms to alter RNA stability or the transcription effectivity are various (Sahr *et al.*, 2017).

As described in section 3.1, *L. pneumophila* features a bipartite metabolism in which amino acids like serine are used for energy generating processes in the TCA cycle, whereas carbohydrates like glucose and glycerol are shuffled into the upper part of metabolism serving anabolic reactions. This bipartite metabolism is furthermore growth phase dependent, since serine is preferred at early developmental stages by *L. pneumophila* as carbon and energy source, whereas glucose and especially glycerol are used at later growth phases (see section 3.1).

The role of CsrA in the regulation of core carbon fluxes derived from different substrates within this bipartite metabolism was now investigated by oxygen consumption experiments as well as by labeling experiments using four different ^{13}C-precusrors: [U-^{13}C$_3$]serine, [U-^{13}C$_6$]glucose, [U-^{13}C$_3$]glycerol and [1,2,3,4-^{13}C$_4$]palmitic acid. Experiments were performed with *L. pneumophila* Paris and its CsrA knock down mutant.

3.2.2 Oxygen consumption experiments

All experiments in this section were performed with *L. pneumophila* Paris and the respective *csrA* mutant. To evaluate changes in core metabolic fluxes in *L. pneumophila* dependent on CsrA, bacterial respiration of the wild-type compared to the *csrA* mutant were analyzed by measuring the oxygen consumption rates (OCR) as it was described in section 2.2.2.3. For this purpose, both bacterial strains were grown in presents of various carbon sources: L-serine, L-alanine and L-glutamate were used in a final concentration of 0.1 g/L. For experiments with

_____

D-glucose, glycerol, butanoate, α-ketoglutarate, and pyruvate a concentration of 0.2 g/L was used. Palmitic acid was used in a concentration of 0.025 g/L. Results of these experiments are shown in **Figure 3-1**. Furthermore, experiments with oleic acid and arachidonic acid were performed with a concentration of 0.1 g/L (**Figure 5-1**).
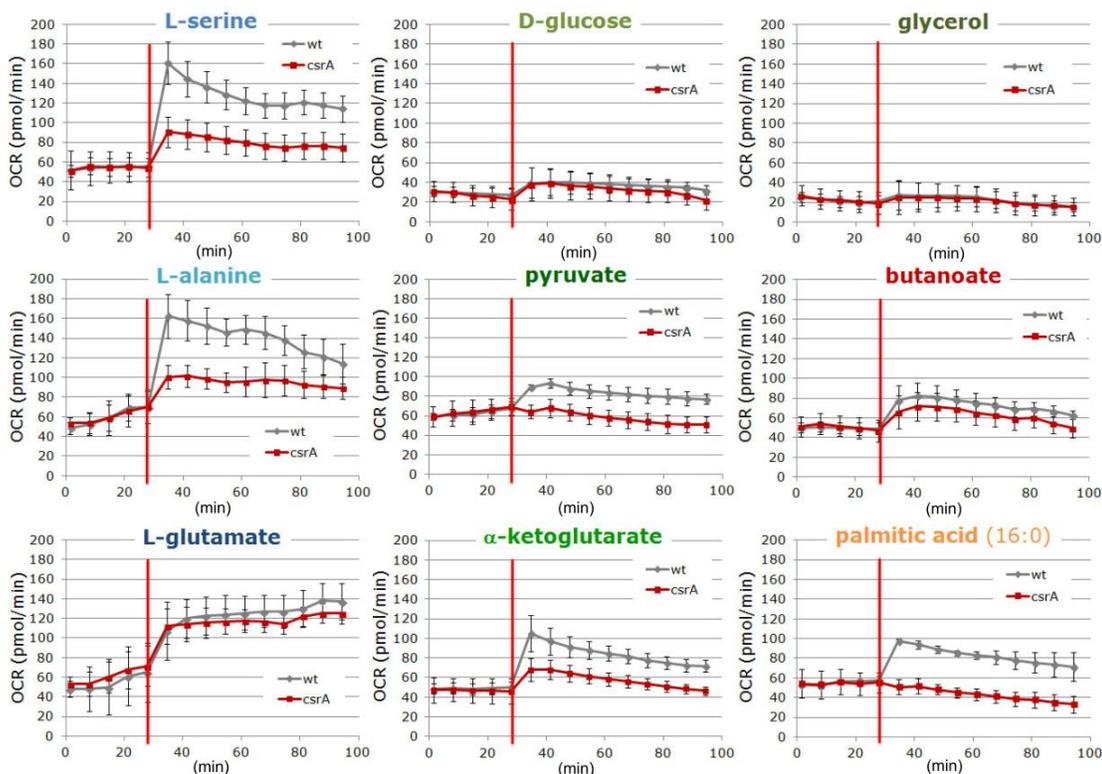

Figure 3-1: Oxygen consumption experiments. Bacterial respiration, expressed as OCR, was quantified using an XFe96 Extracellular Flux Analyzer according to the manufacturer instructions (Seahorse Bioscience). Basal OCR was measured prior to the injection to assure uniform cellular seeding (see section 2.2.2.3). Oxygen consumption experiments were performed with *L. pneumophila* wild-type and the *csrA* mutant in presence of serine (0.1 g/L), alanine (0.1 g/L), glutamate (0.1 g/L), glucose (0.2 g/L), pyruvate (0.2 g/L), α-ketoglutarate (0.2 g/L), glycerol (0.2 g/L) butanoate (0.2 g/L) and palmitic acid (0.025 g/L) (Adapted from Tobias Sahr, Institute Pasteur in Paris).

High respiration rates were obtained with *L. pneumophila* wild-type in presence of serine, alanine and glutamate, confirming that amino acids, especially serine are the preferred carbon source of this pathogen for energy generation (George *et al.*, 1980; Eylert *et al.*, 2010). The OCR in the comparative experiments with the *csrA* mutant was significantly downregulated in case of serine and alanine, indicating that CsrA induces their utilization in conjunction with respiration in the wild-type. However, respiration rates of the mutant strain in the experiment with glutamate was not reduced. In addition, oxygen consumption of *L. pneumophila* wild-

type slightly increased using pyruvate and α-KGA and only to a minor amount with glucose and glycerol, indicating that the latter ones are not used in high rates for bacterial respiration. Similar experiments with the *csrA* mutant revealed lower OCR with pyruvate and α-KGA but not with glucose and glycerol. Therefore, CsrA seems to have a positive effect on metabolism and/or uptake of pyruvate and α-KGA in conjunction with respiration (**Figure 3-1**).

Oxygen consumption experiments with palmitic acid resulted in increased OCR, indicating the usage of this substrate in respiration by *L. pneumophila* wild-type. This was also observed to a lesser extent using butanoate but not in experiments with unsaturated fatty acids (arachidonic acid and oleic acid, **Figure 5-1**). Furthermore, comparative experiments with the *csrA* mutant revealed a positive effect of CsrA on the metabolism and uptake of palmitic acid and butanoate (**Figure 3-1**).

In summary, OCR of *L. pneumophila* wild-type and its *csrA* mutant using different substrates show reduced respiration dependent on the CsrA knock down. Thereby, CsrA seems to induce utilization of serine, alanine, pyruvate and α-KGA in conjunction with respiration. On the other hand, the CsrA knock down has only minor effects on the utilization of glucose and glycerol. Furthermore, *L. pneumophila* seems to use palmitic acid and butanoate as substrate although metabolism and carbon fluxes from these compounds have not been reported so far for this pathogen. For a more detailed understanding of carbon fluxes and their regulation by CsrA, comparative labeling experiments with the *L. pneumophila* wild-type and its *csrA* mutant were performed, using ^{13}C-serine, ^{13}C-glucose, ^{13}C-glycerol and ^{13}C-palmitic acid as ^{13}C-tracers (see section 3.2.2).

3.2.3 Differential analysis of metabolism in *L. pneumophila* and its *csrA* mutant

For a detailed investigation of the role of CsrA in the regulation of central carbon fluxes derived from different substrates in the bipartite metabolic network of *L. pneumophila*, isotopologue profiling experiments were performed with the wild-type (*L. pneumophila* Paris) and the *csrA* mutant. Labeling experiments were performed in CE MDM using [U-^{13}C$_3$]serine, [U-^{13}C$_6$]glucose, [U-^{13}C$_3$]glycerol and [1,2,3,4-^{13}C$_4$]palmitic acid. Harvest of bacterial cell occurred at exponential growth phase (E phase) and post-exponential growth phase (PE phase) to evaluate the growth phase dependent effect of CsrA, since this regulator is crucial for the developmental switch from the replicative to the transmissive stage (Molofsky and Swanson,

2003; Vakulskas *et al.*, 2015). Overall ^{13}C-excess values and isotopologue compositions were determined in key metabolites as reported earlier (Eylert *et al.*, 2008) for each time point of cell harvest. ^{13}C-Excess values for all labeling experiments are summarized in **Figure 3-2**. Isotopologue patterns in the key metabolites Ala (derived from pyruvate), Glu (derived from the TCA cycle), His (derived from the PPP) and Man (derived from gluconeogenetic reaction) are summarized in **Figure 3-3**. Isotopologue distributions of further analyzed metabolites are shown in **Figure 5-2, 5-3**, and **5-4**. For numerical values see **Table 5-1, 5-2, 5 -3** and **5-4**.
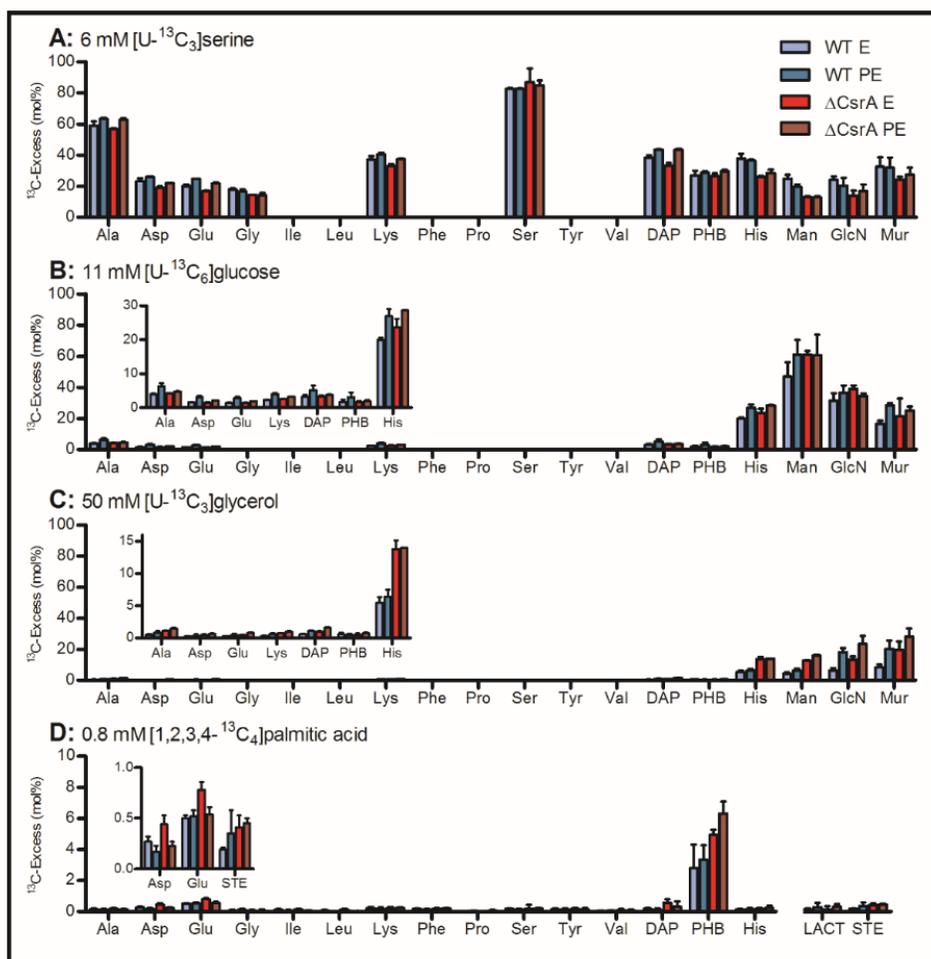
Figure 3-2: Overall excess values (mol%) in key metabolites from experiments with the *L. pneumophila* wild-type and its *csrA* mutant in CE MDM in presents of (**A**) 6 mM [U-^{13}C$_3$]serine, (**B**) 11 mM [U-^{13}C$_6$]glucose, (**C**) 50 mM [U-^{13}C$_3$]glycerol or (**D**) 0.8 mM [1,2,3,4-^{13}C$_4$]palmitic acid. Bacterial harvest occurred at the exponential (E) and post-exponential (PE) growth phase respectively. ^{13}C-Excess values (mol%) in protein-derived amino acids, diaminopimelic acid (DAP), polyhydroxybutyrate (PHB), mannose (Man), glucosamine (GlcN), muramic acid (Mur), lactate (LACT) and stearic acid (STE) where determined by isotopologue profiling. Data calculation is based on two independent biological experiments (x3 technical replicates). For numerical values, see **Table 5-1, 5-2, 5-3**, and **5-4**.
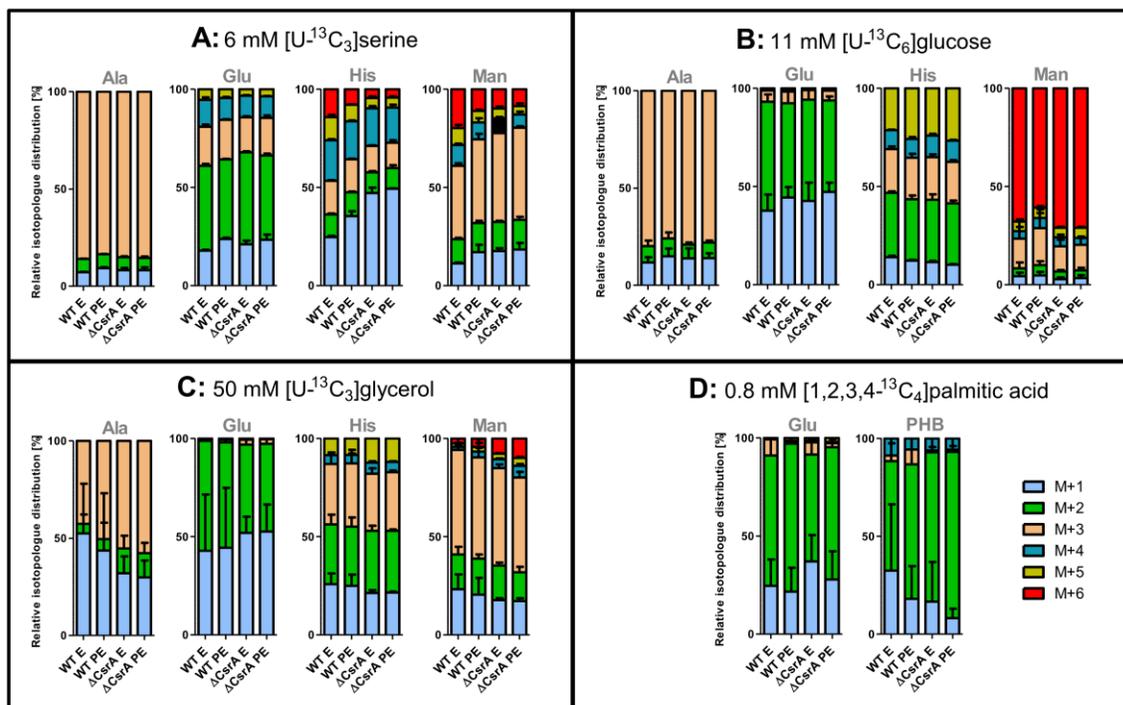
Figure 3-3: Relative isotopologue distributions (%) detected in key metabolites from experiments with the *L. pneumophila* wild-type and its *csrA* mutant. For labeling experiments, bacteria were grown in CE MDM using (**A**) 6 mM [U-^{13}C$_3$]serine, (**B**) 11 mM [U-^{13}C$_6$]glucose, (**C**) 50 mM [U-^{13}C$_3$]glycerol or (**D**) 0.8 mM [1,2,3,4-^{13}C$_4$]palmitic acid as ^{13}C-tracers. Bacteria harvested occurred at E phase and post-exponential PE phase growth phase. Shown are the relative fraction (in%) of isotopologues. Thereby, M+X represents the mass of the unlabeled metabolite plus X labeled ^{13}C-atoms. Data are means and standard deviations (SDs) of six values (3 technical replicates x 2 biological replicates). For numerical values, see **Table 5-1, 5-2, 5-3,** and **5-4.**

3.2.3.1 *Differential analysis of serine metabolism in* **L. pneumophila** *and its* **csrA** *mutant*

The fact that serine is the preferred amino acid serving as main carbon and energy source for *L. pneumophila* is underlined by early investigations, demonstrating high activities of the serine dehydratase enzyme (Lpp0854) as well as of the pyruvate carboxylase enzyme (Lpp0531) (Keen and Hoffman, 1984). Besides numerous amino acid transporters and proteases, which have been identified in the genome of this bacteria, the putative serine transporter protein Lpp2269 is probably responsible for serine incorporation in *L. pneumophila* (Cazalet *et al.*, 2004; Eylert *et al.*, 2010). The central role of this substrate for energy generation in this pathogen was furthermore confirmed by resent labeling experiments (Eylert *et al.*, 2010; Gillmaier *et al.*, 2016). However, additional carbon fluxes into PHB biosynthesis have also been identified (Gillmaier *et al.*, 2016).

_____

Differential analysis of *L. pneumophila* wild-type and its *csrA* mutant using isotopologue profiling experiments in a growth phase depended manner were now performed to evaluate the role of CsrA in serine metabolism. Therefore, both strains were grown in CE MDM supplemented with 6 mM [U-^{13}C$_3$]serine and harvested at E and PE phase. Overall ^{13}C-enrichments of protein derived amino acids, DAP, PHB, Man, GlcN and Mur are shown in **Figure 3-2A**. The respective isotopologue distribution is shown in **Figure 3-3A** and **5-2**.

The amino acids Ala, Asp, Glu, Gly, Lys, Ser and His, the cell wall component DAP as well as the carbon storage compound PHB showed high ^{13}C-Excess values in all experiments. Furthermore, ^{13}C-label was detectable in the cell wall sugars GlcN and Mur as well as in Man. These data confirm that the bipartite metabolism is present in *L. pneumophila* wild-type as well as in the mutant (see section 3.1), since highest ^{13}C-enrichments were found in Ala (besides Ser) and not in His or Man, since Ser is predominantly shuffled into the TCA cycle for energy generation. In both bacterial strains ^{13}C-lable increased from E to PE growth phase in Ala, Asp, Glu, Lys, DAP and PHB. Otherwise, Gly, His as well as detected sugars showed similar or slightly decreased enrichments in E and PE phase in both strains. The decrease of labeling in these metabolites indicate a reduced carbon flux from serine into gluconeogenetic reaction and/or into the PPP at later growth phases.

Comparative analysis of *L. pneumophila* wild-type and the *csrA* mutant revealed reduced ^{13}C-label in the detected metabolites during exponential growth. ^{13}C-enrichments in Asp, Glu, Gly, Lys and DAP were only slightly reduced whereas higher labeling was detectable in His as well as in Man, GlcN and Mur. Same effects were observable at later growth phases, but to a lesser extent. In total, these results reflect a downregulated uptake and metabolism of serine dependent on *csrA*. Since major differences have been observed in metabolites related to gluconeogenetic reactions and the PPP in E and in PE growth phase, CsrA seems to have a distinctive regulatory effect on the carbon flux from serine into these pathways. However, metabolites related to the TCA cycle did only show small differences compared to the wild-type, indicating a smaller regulatory effect of CsrA on carbon flux from serine towards the TCA cycle (**Figure 3-2A**).

These results were confirmed by the respective isotopologue distributions in marker metabolites reflecting distinct metabolic pathways (**Figure 3-3A**). Thereby, similar or slightly

different isotopologue patterns are observable in Ala and Glu in the wild-type compared to the *csrA* mutant, reflecting lower regulatory effects of CsrA on serine metabolism and carbon flux into the biosynthesis of these amino acids. This was not the case for His and Man, since experiments with the *csrA* mutant revealed clear differences in their isotopologue patterns, especially during the E phase. Especially the amount of M+6 but also of M+5 label was significantly reduced in the experiments with the mutant. These highly labeled isotopologues resulted from an intense carbon flux from serine into gluconeogenetic reaction and into the PPP, since a combination reaction of two fully labeled C_3-precursors is required for their formation. In detail, high amounts of fully labeled glyceraldehyde 3-phosphate (GAP) needs to be generated, which is subsequently used in gluconeogenetic reactions for the biosynthesis of Man and in the PPP for His formation. In addition, high amounts of M+6 label in His is a result of an intense carbon flux of serine into ATP biosynthesis, since one carbon atom of ATP is needed for His biosynthesis. Since experiments with the *L. pneumophila csrA* mutant strain revealed reduced amounts of M+5 and M+6 isotopologues in both, His and Man, carbon flux from serine into gluconeogenetic reactions and into the PPP was reduced in these experiments.

3.2.3.2   *Differential analysis of glucose metabolism in* **L. pneumophila** *and its* **csrA** *mutant*

Genome analysis of *L. pneumophila* reveals the metabolic potential of this pathogen to use glucose as substrate (glycolysis and ED pathway), since related enzymes have been identified (Chien *et al.*, 2004; D'Auria *et al.*, 2010). However, this substrate as well as polysaccharides did not support extracellular growth of this pathogen (Pine *et al.*, 1979; Warren and Miller, 1979). Nevertheless, the usage of glucose by *L. pneumophila* was proven recently using labeling experiments. (Eylert *et al.*, 2010; Gillmaier *et al.*, 2016). It was furthermore demonstrated, that degradation predominantly occurs *via* the ED pathway and only to a minor amount *via* glycolytic reactions (Eylert *et al.*, 2010; Harada *et al.*, 2010). In addition, the preferred usage of glucose in gluconeogenetic reaction and in the PPP as well as the low carbon flux from glucose into energy generating processes in the TCA cycle has been demonstrated (see section 3.1). Interestingly, *L. pneumophila* does not comprise a complete PPP since only genes for the transketolase (*lpp0154*) and no transaldolase has been identified. Furthermore, a direct link between the PPP and the ED pathway is missing, since the 6-phophogluconate dehydrogenase is missing in the genome of *L. pneumophila* (Chien *et al.*, 2004).

_____

To now evaluate the role of CsrA in the glucose metabolism, differential analysis of *L. pneumophila* wild-type and its *csrA* mutant was performed using labeling experiments in a growth phase dependent manner. Therefore both strains were grown in CE MDM supplemented with 11 mM [U-$^{13}C_6$]glucose and harvested at E and PE phase. Overall ^{13}C-enrichments of protein derived amino acids, DAP, PHB, Man, GlcN and Mur are shown in **Figure 3-2B**. The respective isotopologue distribution are shown in **Figure 3-3B** and **5-3**.

In contrast to labeling experiments with ^{13}C-serine, highest enrichments were detectable in His and the sugars Man, GlcN and Mur. Lower ^{13}C-lable occurred into Ala, Asp, Glu, Lys, DAP and PHB. These results again confirm the bipartite metabolism in *L. pneumophila* (see section 3.1). ^{13}C-Excess was higher at PE growth phase in almost every metabolite in the wild-type and in the *csrA* mutant. Only ^{13}C label in Man and GlcN remained constant or was slightly reduced in the *csrA* mutant from E to PE phase (**Figure 3-2B**).

Amino acids related to the TCA cycle such as Ala, Asp, Glu, Lys as well as DAP and PHB revealed similar ^{13}C-enrichments in the exponential growth phases in experiments with *L. pneumophila* wild-type and with its *csrA* mutant. This was different in metabolites related to gluconeogenetic reactions (Man and GlcN) as well as in His, which is a marker metabolite of the PPP, since partly higher labeling was detectable in these metabolites in experiments with the mutant during E phase. This indicates that carbon flux directed towards the TCA cycle was not affected in this early growth phase in the mutant, whereas metabolic flux into gluconeogenetic reactions and into the PPP was slightly increased. At later growth phases, metabolites related to the TCA cycle (Ala, Asp, Glu, Lys), DAP and PHB showed reduced ^{13}C incorporation in the experiments with the *csrA* mutant, whereas His, Man and GlcN incorporated slightly higher similar ^{13}C-enrichments. Only Mur showed slightly reduced overall enrichment values. In summary, the CsrA knock down seems to predominantly effect the carbon flux from glucose into the TCA cycle on both growth phases, whereas carbon flux into gluconeogenetic reactions and into the PPP seems to be induced dependent on the CsrA knock down (**Figure 3-2B**).

This is also reflected in the respective isotopologue distributions in the key metabolites Ala (derived from pyruvate), Glu (TCA related), His (derived from PPP) and Man (gluconeogenetic reactions), as shown in **Figure 3-3B**. Induced carbon flux from glucose into

the PPP and gluconeogenetic reactions is thereby reflected in increased amounts of M+5 isotopologues in His and M+6 isotopologues in Man during E and PE growth of the *L. pneumophila csrA* mutant. M+6 isotopologue in Man can thereby be directly formed from fully labeled glucose or *via* combination of two fully labeled C_3 precursors, which are built previously from degradation reactions of fully labeled glucose *via* glycolysis or the ED pathway. M+5 isotopologues in His can result from fully labeled fructose 6-phosphate (Fru-6-P), which is used in reactions of the PPP. Again, also the combination of two fully labeled C_3 precursors in gluconeogenetic reactions can result in M+5 labeling. In total, this indicates an induced carbon flux from glucose into the biosynthesis of sugars and into the PPP in the *csrA* mutant.

3.2.3.3 *Differential analysis of glycerol metabolism in* **L. pneumophila** *and its* **csrA** *mutant*

Recent transcriptome data showed that genes responsible for glycerol degradation (*lpp1369*: *glpK*, *lpp2257*: *glpD*) are upregulated in *L. pneumophila* during intracellular replication in macrophages (Faucher *et al.*, 2011). Also, early experiments using [U-^{14}C$_3$]glycerol indicated the usage of glycerol by *L. pneumophila* (Tesh *et al.*, 1983). Labeling experiments using [U-^{13}C$_3$]glycerol, which were performed in this work, now proofed that this intracellular pathogen indeed uses glycerol as a substrate predominantly at later growth phases. Thereby, carbon flux from glycerol is almost restricted to gluconeogenetic reactions and the PPP (see section 3.1).

To elucidate the regulatory role of CsrA in the glycerol metabolism, differential analysis of *L. pneumophila* wild-type and its *csrA* mutant was performed using labeling experiments in a growth phase depended manner. Therefore wild-type bacteria and the *csrA* mutant were grown in CE MDM supplemented with 50 mM [U-^{13}C$_3$]glycerol and harvested at E and PE phase. Overall ^{13}C-enrichments of protein derived amino acids, DAP, PHB, Man, GlcN and Mur are shown in **Figure 3-2C**. The respective isotopologue distributions are shown in **Figure 3-3C** and **5-4**.

Like in the experiments with fully labeled glucose, highest ^{13}C-enrichment values were again found in the sugars Man, GlcN and Mur, which are derived from gluconeogenetic reactions, as well as in His, which is derived from the PPP. This again confirms the bipartite metabolism, which is present in *L. pneumophila* (see section 3.1). Notably, ^{13}C-labeling increased in every metabolite in the experiments with both strains from E to PE phase except for His in the

experiment with the *csrA* mutant. There enrichment values remain constant from E to PE growth phase (**Figure 3-2C**).

Compared to the wild-type, ^{13}C-enrichments increased in every metabolite in the experiment with the mutant in E phase as well as in PE phase. However, CsrA knock down resulted in dramatically increased incorporation of ^{13}C-label into His. Thereby, overall ^{13}C-excess values increased from 45% in the wild-type to 13.79% in the *csrA* mutant in the E phase, whereas an increase from 6.40% in the wild-type to 13.99% in the csrA mutant was detectable in PE phase. Furthermore, the detected sugars (Man, GlcN and Mur), which are predominantly derived from the bacterial cell wall, also showed dramatically increased labeling related to the CsrA knock down mutation. In total, these results indicate that glycerol is already used in earlier growth phases in the *csrA* mutant, whereas it is predominantly used at later growth phases in the *L. pneumophila* wild-type. In addition, the uptake as well as the catabolism of glycerol is dramatically induced in the *csrA* mutant, emphasizing the crucial role of CsrA in the regulation of carbon fluxes derived from this substrate. In *L. pneumophila* wild-type, CsrA seems to repress the uptake and degradation of glycerol during E phase, which leads to a downregulated carbon flux in general. However, carbon flux into gluconeogenetic reactions and into the PPP seem to be particularly affected (**Figure 3-2C**).

This agrees with the respective isotopologue compositions in key metabolites (Ala, Glu, His and Man), which are illustrated in **Figure 3-3C**. Thereby, the upregulated incorporation and catabolism of glycerol in absence of CsrA is e.g. reflected in the increased amount of M+3 label in Ala, since this indicates direct formation of a fully labeled pyruvate intermediate, which is built from a fully labeled ^{13}C-glycerol molecule. Same is true for isotopologue distributions in TCA cycle related amino acids, which showed an increased amount of M+2 label, which is derived from M+2 labeled acetyl-CoA in the *csrA* mutant. Higher amounts of fully labeled acetyl-CoA in absents of CsrA is again built from a fully labeled pyruvate which is derived from fully labeled ^{13}C-glycerol, and subsequently shuffled into reactions of the TCA cycle. Major differences in the isotopologue composition have also been detected in His and Man, metabolites which are related to the PPP and to gluconeogenetic reactions, respectively. Thereby, higher amounts of M+6 isotopologues in Man as well as of M+5 isotopologues in His have been observed in E and PE growth phase in absence of CsrA. These highly labeled

metabolites can only be formed in combination reactions of two fully labeled C_3-precursors in gluconeogenetic reactions to generate M+6 in Man, as it was mentioned for the labeling experiments with ^{13}C-glucose. Same is true for M+5 labeling in His, which can be the result of fully labeled Fru-6-P entering the PPP. Furthermore, also combination reaction in the PPP including two fully labeled C_3-precursors can result in M+5 label in His.

These data clearly show that in absence of CsrA, glycerol uptake and metabolism is dramatically upregulated. Besides an increased carbon flux towards the TCA cycle, especially the carbon flux into gluconeogenetic reaction and into the PPP was dramatically affected. This indicates, that CsrA is responsible for the repression of glycerol metabolism in L. pneumophila wild-type, especially during the exponential growth phase.

3.2.3.4   *Differential analysis of palmitic acid and PHB metabolism in* **L. pneumophila** *and its* **csrA** *mutant*

The carbon and energy storage compound PHB was first discovered in the 1920s in *Bacillus megaterium* (Lemoigne, 1926). Until now, numerous bacteria were identified using this compound for energy storage (Anderson and Dawes, 1990; Anderson *et al.*, 1990; Steinbüchel and Schlegel, 1991; Poirier, 2002; Kadouri *et al.*, 2005). Also *L. pneumophila* uses PHB for energy storage and long-term survival (James *et al.*, 1999; Al-Bana *et al.*, 2014). Thereby, PHB is stored in cytoplasmic inclusions or granules, which predominantly appear at later growth phases of this pathogen (James *et al.*, 1999; Garduno *et al.*, 2002). The biosynthetic route which appears in most of the PHB building bacteria starts from two acetyl-CoA molecules, which are used to build (R)-3-hydroxybutanoyl-CoA, which is subsequently used to form PHB (Steinbüchel and Schlegel, 1991; Poirier, 2002; Gillmaier *et al.*, 2016). Investigations of the PHB metabolism in *L. pneumophila* during this work (see section 3.1) in combination with earlier studies using labeling experiments revealed, that the acetyl-CoA molecules, which are used for PHB formation, are predominantly derived from serine catabolism. However, also glucose served as a substrate for its biosynthesis (Gillmaier *et al.*, 2016). Interestingly, during early growth phases serine is preferably used for PHB formation, whereas carbon supply into PHB from glucose mainly occurs at later developmental stages (Gillmaier *et al.*, 2016). The respective regulatory mechanism, which is responsible for the adjustment of carbon supply and biosynthesis of this carbon and energy storage compound in a growth phase dependent manner, is still unknown.

An extensive characterization of the *csrA* mutant, which was also used in this work, revealed higher PHB concentrations during exponential and stationary growth phase (Sahr *et al.*, 2017). Furthermore, transcriptome and proteome analysis in combination with RNA-Co-immunoprecipitation experiments followed by deep sequencing of the wild-type and the *csrA* strain uncovered numerous direct targets of CsrA, which are involved in PHB biosynthesis (**Figure 5-7**) (Sahr *et al.*, 2017). This emphasizes the role of this regulator in the growth phase dependent formation of PHB. However, since the extensive differential analysis of the carbon fluxes in *L. pneumophila* wild-type and its *csrA* mutant using the three ^{13}C-precursors [U-^{13}C$_3$]serine, [U-^{13}C$_6$]glucose and [U-^{13}C$_3$]glycerol didn´t result in upregulated ^{13}C-enrichments in PHB (see section 3.2.3.1 - 3.2.3.3), the increased amount of this storage compound in the mutant is presumably synthesized from a further substrate.

Therefore, differential carbon flux analysis with *L. pneumophila* wild-type and its *csrA* mutant using [1,2,3,4-^{13}C$_4$]palmitic acid as ^{13}C-tracer was performed, since all genes needed for fatty acid degradation are present in this pathogen based on genome analysis (Chien *et al.*, 2004). Nevertheless, usage of fatty acids by *L. pneumophila* has not been investigated until now. However, the acetyl-CoA molecules, which are derived from fatty acid degradation could serve as precursors for PHB biosynthesis in this pathogen. For this purpose, both bacterial strains were grown in CE MDM supplemented with 0.8 mM [1,2,3,4-^{13}C$_4$]palmitic acid and harvested at E and PE phase. Overall ^{13}C-enrichment values and isotopologue compositions were determined for protein derived amino acids, DAP and PHB as well as for lactate and stearic acid (**Figure 3-2D** and **Figure 3-3D**).

^{13}C-label in the experiments using [1,2,3,4-^{13}C$_4$]palmitic acid as ^{13}C-tracer was exclusively transferred into the carbon storage compound PHB in the experiments with the *L. pneumophila* wild-type and the *csrA* mutant. On the one hand, this clearly shows for the first time the effective incorporation and degradation of a fatty acid by this pathogen. On the other hand, the acetyl-CoA molecules which are derived from fatty acid degradation are indeed directly used to form PHB in *L. pneumophila*. Besides that, small but significant ^{13}C-label was also detectable in Glu in the experiment with the wild-type. Since Glu is directly derived from an intermediate of the TCA cycle, this indicates that the acetyl-CoA monomers derived from degradation of [1,2,3,4-^{13}C$_4$]palmitic acid are also partly shuffled into the TCA cycle.

Interestingly, the *csrA* mutant showed slightly increased carbon flux from ^{13}C-palmitic acid into the TCA cycle during exponential growth, since ^{13}C-enrichment in Glu was increased compared to the wild-type (wild-type: 0.50%, csrA mutant: 0.78%). Furthermore, a minor carbon flux into the biosynthesis of stearic acid was also detectable in the *csrA* mutant. More importantly, overall enrichment values in the storage compound PHB increased in both growth phases in the *csrA* strain compared to the wild-type (E phase-wild-type: 2.79%, E phase- *csrA* mutant: 4.93%; PE phase-wild-type: 3.36%, PE phase-*csrA* mutant: 6.32%) (**Figure 3-2D** and **Table 5-4**).

In summary, these data indicate that fatty acids might be preferably serve as a carbon source for PHB biosynthesis in *L. pneumophila*. The comparative analysis with a CsrA knock down strain furthermore demonstrated that this regulator is involved in the regulatory network, which determines the growth phase dependent formation of the carbon and energy storage compound PHB.

3.2.4 Comparative analysis of carbon fluxes from ^{13}C-serine, ^{13}C-glucose and ^{13}C-glycerol in *L. pneumophila* wild-type and *csrA* mutant

All experiments in this section were performed with *L. pneumophila* Paris and the respective *csrA* mutant. For a more detailed elucidation of the changes in the carbon flux derived from the three different substrates [U-^{13}C$_3$]serine, [U-^{13}C$_6$]glucose and [U-^{13}C$_3$]glycerol dependent on the CsrA knock down, ratios were calculated from ^{13}C-excess values in specific marker metabolites. Following marker metabolites have been chosen to represent the carbon flux into specific biosynthetic pathway: His, Ala and Glu. His served as a marker for ^{13}C-carbon flux into the PPP, since it is synthesized from PRPP, an intermediate biosynthetic pathway. Since Ala is synthesized directly from pyruvate and Glu is derived from α-ketoglutaric acid, these marker metabolites represent ^{13}C-carbon flux directed towards the TCA cycle. Both ratios "^{13}C-excess (mol%) His/Ala" and "^{13}C-excess (mol%) His/Glu" were calculated for the experiments with the *L. pneumophila* wild-type and its *csrA* mutant for E and PE phase for labeling experiments with [U-^{13}C$_3$]serine, [U-^{13}C$_6$]glucose and [U-^{13}C$_3$]glycerol, respectively. High carbon fluxes directed towards energy generation in the TCA cycle is thereby indicated by small values of these ratios, whereas high values show an intense carbon flux towards gluconeogenetic reactions and the PPP (**Figure 3-4**).

_____

Calculations for carbon fluxes in the labeling experiment with ^{13}C-serine revealed small values for both ratios at E and PE growth phase in both, the wild-type and the *csrA* mutant. This is in accordance with previous described results (see section 3.1) and again illustrates the extensive carbon flux from this substrate toward energy generation in the TCA cycle. Nevertheless, small differences were detectable comparing the wild-type to the *csrA* mutant, since ratios are slightly reduced in the mutant, indicating that the carbon flux from serine towards the TCA cycle was partly upregulated compared to the wild-type. In combination with reduced overall enrichment values that had been observed in the experiments with the csrA mutant (see section 3.2.3.1) this illustrates a downregulated uptake and metabolism of serine in the mutant by a mountainously more restricted carbon flux towards the TCA cycle for energy generation. This indicates that CsrA induces serine metabolism and usage for energy generation in the wild-type. However, at later growth phases, where the amount of active CsrA is reduced in the bacterial cell due to binding to non-coding small mRNAs (Rasis and Segal, 2009; Sahr *et al.*, 2009; Sahr *et al.*, 2012), carbon flux from serine into gluconeogenetic reactions and the PPP is downregulated (**Figure 3-4**).

Ratios calculated for the experiments performed with [U-^{13}C$_6$]glucose as a tracer were high in both growth phases in the experiments with the *L. pneumophila* wild-type and with its CsrA knock down mutant. This agrees with previously discussed results (see section 3.1) and again shows the presence of a bipartite metabolism in this pathogen. In this bipartite metabolism glucose is predominantly shuffled into the PPP, ED pathway and gluconeogenetic reactions. Since values for both ratios, "^{13}C-excess (mol%) His/Ala" and "^{13}C-excess (mol%) His/Glu" increased in both growth phases in the experiment with the *csrA* mutant, carbon flux from glucose is more directed towards anabolic processes in this strain. Simultaneously, incorporation and metabolism of glucose is slightly reduced in the mutant strain (see section 3.2.3.2). This indicates that carbon flux from glucose differs in the *L. pneumophila* wild-type from E to PE phase. The presence of CsrA, glucose is also partly used for energy generation in the TCA cycle while absence of CsrA results in a more restricted usage in the upper part of metabolism (**Figure 3-4**).
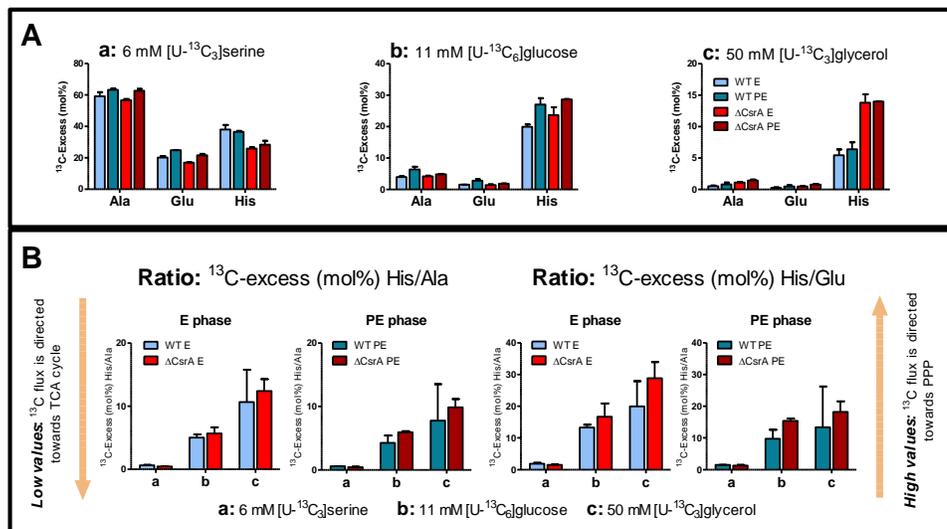
Figure 3-4: Comparative analysis of carbon fluxes in *L. pneumophila* wild-type and its *csrA* mutant. Bacterial cultivation occurred in CE MDM using (a) 6 mM [U-^{13}C$_3$]serine, (b) 11 mM [U-^{13}C$_6$]glucose or (c) 50 mM [U-^{13}C$_3$]glycerol as ^{13}C-tracer. Harvest of cell cultures occurred at E phase and PE growth phase. (**A**) Overall ^{13}C-excess values (%) in the key metabolites Ala (derived from pyruvate), Glu (TCA cycle) and His (PPP). Shown are data from two independent experiments. (**B**) Shown are ratios of ^{13}C-excess in His (PPP) to Ala (pyruvate) or Glu (TCA cycle) for E and PE phase, respectively. For numerical values, see **Table 5-9** and **5-10**.

Comparing the ratios of the labeling experiments with ^{13}C-serine, ^{13}C-glucose and ^{13}C-glycerol, highest values for both ratios were obtained in the experiment with [U-^{13}C$_3$]glycerol. This again demonstrates that carbon flux from this substrate is almost restricted to gluconeogenetic reactions and the PPP in the bipartite metabolism of *L. pneumophila* (see section 3.1). However, experiments with the *csrA* mutant showed increased values for both ratios in the E and PE growth phase. This clearly shows that carbon flux is even more directed to gluconeogenesis and PPP in absence of CsrA. Simultaneously, incorporation and metabolism of glycerol was upregulated extensively (see section 3.2.3.3) in the *csrA* strain. This clearly shows that this regulator is responsible for the repression of glycerol metabolism especially during exponential growth in the *L. pneumophila* wild-type (**Figure 3-4**).

3.3 Multiple substrate usage of *Coxiella burnetii* to feed a bipartite metabolic network

Häuslein, I., Cantet, F., Reschke, S., Chen, F., Bonazzi, M., and Eisenreich, W. (**2017**). *Frontiers in Cellular and Infection Microbiology* 7.

C. burnetii represents a human pathogen, which is categorized as a bio-weapon (Madariaga *et al.*, 2003). Based on genome analysis, this bacterium seems to have great metabolic potential (Seshadri *et al.*, 2003). However, its metabolism is still only poorly investigated. In this study, labeling experiments with [U-^{13}C$_3$]serine, [U-^{13}C$_6$]glucose and [U-^{13}C$_3$]glycerol were performed with the *C. burnetii* RSA 439 NMII strain in the recently developed axenic growth medium ACCM-2 to investigate the full metabolic potential of this pathogen. Using GC/MS based isotopologue profiling the effective usage of all three precursors by *C. burnetii* could be demonstrated. Therefore, overall ^{13}C-enrichment values and isotopologue compositions were analyzed in numerous key metabolites e.g. protein derived amino acids or specific cell wall components. Dependent on the respective tracer, ^{13}C-label was shuffled into different biosynthetic pathways. Glucose preferably served as a precursor for cell wall formation but it was also efficiently converted into pyruvate and subsequently shuffled into reactions of the TCA cycle. Furthermore, carbon flux from glucose occurred into erythrose 4-phosphate *via* the non-oxidative PPP, which was subsequently used in the shikimate/chorismate pathway for the formation of aromatic amino acids. In contrast, serine was predominantly converted into acetyl-CoA, which was shuffled into the TCA cycle and fatty acid biosynthesis, and did not serve efficiently as gluconeogenetic substrate. On the other hand, carbon flux from glycerol almost exclusively occurred towards gluconeogenetic reactions serving as a substrate for cell wall biosynthesis. In addition, glycerol could also partly be converted into PEP or pyruvate, again predominantly serving cell wall formation *via* the synthesis of diaminopimelic acid (DAP). Comparing the concept of the core metabolic fluxes in *C. burnetii* to the network which is present in *L. pneumophila*, a similar but not identical bipartite topology could be identified. This emphasizes the idea that this strategy might be in general a beneficial concept for intracellular replication and survival of these pathogens as a result of specific adaption processes on the respective nutrient supply and metabolism of the host. However, the lifestyle of these two pathogens is similar but not identical resulting in partly different bipartite metabolic concepts, which is presumably dependent on the respective replication niche.

Multiple Substrate Usage of *Coxiella burnetii* to Feed a Bipartite Metabolic Network

Ina Häuslein[1], Franck Cantet[2], Sarah Reschke[1], Fan Chen[1], Matteo Bonazzi[2]* and Wolfgang Eisenreich[1]*

[1] Department of Chemistry, Chair of Biochemistry, Technische Universität München, Garching, Germany, [2] IRIM-UMR 9004, Infectious Disease Research Institute of Montpellier, Université de Montpellier, Centre National de la Recherche Scientifique, Montpellier, France

The human pathogen *Coxiella burnetii* causes Q-fever and is classified as a category B bio-weapon. Exploiting the development of the axenic growth medium ACCM-2, we have now used ^{13}C-labeling experiments and isotopolog profiling to investigate the highly diverse metabolic network of *C. burnetii*. To this aim, *C. burnetii* RSA 439 NMII was cultured in ACCM-2 containing 5 mM of either [U-^{13}C$_3$]serine, [U-^{13}C$_6$]glucose, or [U-^{13}C$_3$]glycerol until the late-logarithmic phase. GC/MS-based isotopolog profiling of protein-derived amino acids, methanol-soluble polar metabolites, fatty acids, and cell wall components (e.g., diaminopimelate and sugars) from the labeled bacteria revealed differential incorporation rates and isotopolog profiles. These data served to decipher the diverse usages of the labeled substrates and the relative carbon fluxes into the core metabolism of the pathogen. Whereas, *de novo* biosynthesis from any of these substrates could not be found for histidine, isoleucine, leucine, lysine, phenylalanine, proline and valine, the other amino acids and metabolites under study acquired ^{13}C-label at specific rates depending on the nature of the tracer compound. Glucose was directly used for cell wall biosynthesis, but was also converted into pyruvate (and its downstream metabolites) through the glycolytic pathway or into erythrose 4-phosphate (e.g., for the biosynthesis of tyrosine) via the non-oxidative pentose phosphate pathway. Glycerol efficiently served as a gluconeogenetic substrate and could also be used via phosphoenolpyruvate and diaminopimelate as a major carbon source for cell wall biosynthesis. In contrast, exogenous serine was mainly utilized in downstream metabolic processes, e.g., via acetyl-CoA in a complete citrate cycle with fluxes in the oxidative direction and as a carbon feed for fatty acid biosynthesis. In summary, the data reflect multiple and differential substrate usages by *C. burnetii* in a bipartite-type metabolic network, resembling the overall topology of the related pathogen *Legionella pneumophila*. These strategies could benefit the metabolic capacities of the pathogens also as a trait to adapt for replication under intracellular conditions.

Keywords: *Coxiella*, isotopolog profiling, metabolism, nutrition, shikimate pathway, bipartite metabolism, *Legionella*

86

INTRODUCTION

The obligate intracellular Gram negative bacterium *Coxiella burnetii* is the causative agent of Q-fever, a worldwide-distributed zoonosis, except New Zealand (Maurin and Raoult, 1999; Arricau-Bouvery and Rodolakis, 2005). The disease can cause acute or chronic infections when the bacteria invade alveolar macrophages or other phagocytic and non-phagocytic cells in different tissues and organs, finally leading to endocarditis and hepatitis in its chronical form (Van Schaik et al., 2013). *C. burnetii* represents a category B bio-weapon due to its remarkable low infectious dose, since one bacterial cell in the lung is enough to cause the acute infection (Fournier et al., 1998; Madariaga et al., 2003). In addition, *C. burnetii* can form specific small cell variants (SCVs) that are stable for long time periods in the environment, also under harsh conditions (Coleman et al., 2004, 2007). After having invaded their target cells by passive phagocytosis, *C. burnetii* establishes an acidic phagolysosome-like replication compartment called *Coxiella*-containing vacuole (CCV) (Larson et al., 2016). Vacuolar acidification triggers the transition from SCV into the replicative large-cell variant (LCV) (Coleman et al., 2004). Establishment of the CCV as well as intracellular replication of *C. burnetii* inside of this specific compartment depends on a type IVB secretion system (T4SS), a homolog of the Icm/Dot secretion system in *Legionella pneumophila*, a closely relative of *Coxiella* (Seshadri et al., 2003; Beare et al., 2011; Carey et al., 2011). In both pathogens, these analog secretion systems translocate numerous effector proteins into their host cells to trigger the establishment of the replicative niche, to avoid degradation and to get access to sufficient amounts of nutrients (Zhu et al., 2011; Segal, 2013; Moffatt et al., 2015; Martinez et al., 2016). To date, more than 300 effector proteins are known for *L. pneumophila* and there seem to be even more along the *Legionella* species (Burstein et al., 2016; Hofer, 2016), whereas only about 60 proteins have been identified as effectors for *C. burnetii* (Chen et al., 2010; Carey et al., 2011; Newton et al., 2013). Still, the function of most of these effector proteins are not known, especially for *C. burnetii* (Chen et al., 2010; Weber et al., 2013).

However, these two pathogens also feature some major differences. Beside the fact that only few of the effector proteins are conserved, also the characteristics of the two replicative vacuoles differ. While *L. pneumophila* is replicating in a neutral environment within a compartment that is predominantly derived from the endoplasmatic reticulum, *C. burnetii* requires acidic conditions in its phagolysosome-like replication compartment (Hubber and Roy, 2010; Weber et al., 2013). Moreover, the invading pathogens target very different host cells for their multiplication. While *L. pneumophila* is specialized for replication inside protozoa and only accidentally infects human alveolar macrophages, *C. burnetii* is adapted for the infection of numerous mammalian species and tissues (Babudieri, 1959; Weber et al., 2013; Larson et al., 2016).

By now, it is well known that *L. pneumophila* preferably uses amino acids, especially serine as carbon and energy source (Tesh and Miller, 1981; Tesh et al., 1983). Recent studies showed that in addition to amino acids, *Legionella* uses further substrates like glucose and glycerol in a bipartite metabolic network (Eylert et al., 2010; Häuslein et al., 2015). Thereby, glucose is predominantly metabolized via the Entner-Doudoroff pathway (ED pathway) and not via glycolytic reactions (Schunder et al., 2014). However, glycerol predominantly serves gluconeogenetic reactions and is shuffled into the pentose phosphate pathway (PPP) (Häuslein et al., 2015).

In contrast to *L. pneumophila*, carbon metabolism of *C. burnetii* has been poorly investigated, since the possibility to grow this intracellular pathogen in an axenic medium has been developed only recently (Omsland et al., 2009, 2011).

On the basis of its genome, the pathogen shows high metabolic capacities, especially when compared to other intracellular replicating bacteria. This is probably due to a relatively low genome reduction process in *C. burnetii*, since more than 89.1% of its genome encode proteins (Andersson and Kurland, 1998; Seshadri et al., 2003). Different to *L. pneumophila*, which predominately utilizes the ED pathway for glucose degradation, *C. burnetii* seems to use glycolytic reactions for glucose catabolism, although a classical hexokinase is missing in the glycolytic cascade on the basis of the genome sequence (McDonald and Mallavia, 1971; Hackstadt and Williams, 1981a,b). Nevertheless, hexokinase activity has been demonstrated in cell-free extracts (Paretsky et al., 1962). Also, the conversion of glucose 6-phosphate to 6-phosphogluconate and ribulose 5-phosphate has been detected, although genes encoding these reactions have not yet been annotated (Consigli and Paretsky, 1962; McDonald and Mallavia, 1970). Enzymes important for fatty acid or amino acid biosynthesis, synthesis of vitamins and nucleic acids, and a complete TCA cycle are also present in *Coxiella* (Seshadri et al., 2003). Otherwise, enzymes for the glyoxylate pathway have not been identified until now, indicating that *Coxiella* does not use fatty acids for energy generation in contrast to *Mycobacterium tuberculosis* (Schnappinger et al., 2003; Seshadri et al., 2003), although a putative transporter for long chain fatty acids (CBU1242) was assigned in the genome of *C. burnetii* (Kuley et al., 2015). Notably, the shikimate/chorismate pathway is also evident from the genome sequence although some late steps leading to the aromatic amino acids appear to be missing (Seshadri et al., 2003; Walter et al., 2014) (**Figure 1**).

Based on the prediction of numerous amino acid and peptide transporters, amino acids seem to be among the major carbon and energy source of *C. burnetii* (Sandoz et al., 2016b). Moreover, the predicted presence of two sugar transporters (CBU0265 and CBU0347) indicates the uptake and subsequent metabolism of sugars (Seshadri et al., 2003). Additionally, although no glycerol transporter has been predicted, enzymes responsible for glycerol degradation (*glpK*: glycerol kinase, *glpD*: glycerol 3-phosphate dehydrogenase) are present in *C. burnetii*, indicating that glycerol could also serve as a nutrient (Seshadri et al., 2003) (**Figure 1**). Compared to *Chlamydia* or *Rickettsia*, intracellular *Coxiella* seems unable to import ATP from its host, since an ATP/ADP exchanger has not been identified (Zomorodipour and Andersson, 1999; Miller and Thompson, 2002).

Despite considerable efforts in investigating the usage of some substrates like glutamate, pyruvate, succinate and glucose by

3. RESULTS
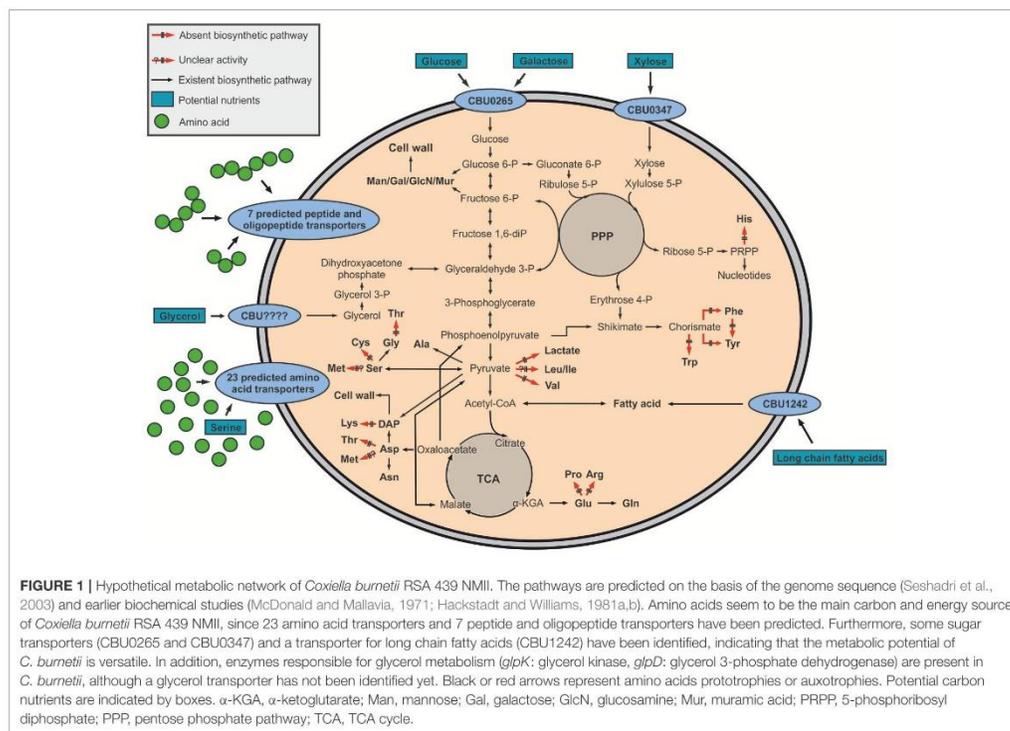
FIGURE 1 | Hypothetical metabolic network of *Coxiella burnetii* RSA 439 NMII. The pathways are predicted on the basis of the genome sequence (Seshadri et al., 2003) and earlier biochemical studies (McDonald and Mallavia, 1971; Hackstadt and Williams, 1981a,b). Amino acids seem to be the main carbon and energy source of *Coxiella burnetii* RSA 439 NMII, since 23 amino acid transporters and 7 peptide and oligopeptide transporters have been predicted. Furthermore, some sugar transporters (CBU0265 and CBU0347) and a transporter for long chain fatty acids (CBU1242) have been identified, indicating that the metabolic potential of *C. burnetii* is versatile. In addition, enzymes responsible for glycerol metabolism (*glpK*: glycerol kinase, *glpD*: glycerol 3-phosphate dehydrogenase) are present in *C. burnetii*, although a glycerol transporter has not been identified yet. Black or red arrows represent amino acids prototrophies or auxotrophies. Potential carbon nutrients are indicated by boxes. α-KGA, α-ketoglutarate; Man, mannose; Gal, galactose; GlcN, glucosamine; Mur, muramic acid; PRPP, 5-phosphoribosyl diphosphate; PPP, pentose phosphate pathway; TCA, TCA cycle.

C. burnetii (Hackstadt and Williams, 1981a, 1983), the nutritional diversity remains unknown. Nevertheless, the composition of the recently developed axenic medium is giving a welcome hint to the preferred metabolites of this pathogen, since it carries high amounts of peptides and amino acids. Furthermore, glucose is also present in ACCM-2 (Omsland et al., 2009, 2011), however not in ACCM-D (Sandoz et al., 2016a).

In recent years, isotopolog profiling has proven to be a powerful approach to describe substrate and pathway usages for a number of pathogens including *L. pneumophila* (Eylert et al., 2010; Schunder et al., 2014; Häuslein et al., 2015; Gillmaier et al., 2016; Kern et al., 2016). The method is based on ^{13}C-incorporation experiments using completely or selectively ^{13}C-labeled substrates such as glucose, serine or glycerol. Due to the isotopic labels, specific ^{13}C-enrichments and isotopolog compositions are generated in downstream metabolic products (e.g., amino acids, fatty acids and sugars) which can be determined by gas chromatography/mass spectrometry (GC/MS). By comparison of these patterns, the differential substrate usage and the metabolic pathways can be reconstructed. Here, we have used isotopolog profiling approaches to investigate the highly diverse metabolic network of *C. burnetii*. For this purpose, we grew *C. burnetii* RSA 439 NMII in the axenic medium ACCM-2 in the presence of either 5 mM [U-$^{13}C_6$]glucose, [U-$^{13}C_3$]serine or [U-$^{13}C_3$]glycerol. Isotopolog profiling revealed that the pathogen is capable to efficiently use all of these substrates in a bipartite-type metabolic network.

MATERIALS AND METHODS

Bacteria Strains and Growth Conditions

For each growth condition, Acidified Citrate Cysteine Medium 2 (ACCM-2, Table S1) was inoculated with *C. burnetii* RSA 439 NMII at 1×10^5 genome equivalents GE/mL. Bacteria were grown in a humidified atmosphere of 5% CO_2 and 2.5% O_2 at 37°C for the indicated times. GE/mL were calculated using the PicoGreen assay according to manufacturers' instructions. Briefly, 50 μL of bacterial culture were mixed to 5 μL of 10% Triton X-100 in a well of a 96-wells microplate with black bottom and sides and incubated 10 min at room temperature on a plate shaker. PicoGreen was then added to the mixture and the plates were incubated at room temperature and in the dark for 10 min. Sample fluorescence was measured using a fluorescence microplate reader using filters for standard fluorescein wavelengths (excitation ~480 nm, emission ~520 nm). DNA concentrations were obtained by

88

plotting the fluorescence readings on a standard curve obtained applying the same approach to a dilution of a plasmid of known concentration. Data were converted to GE/mL by dividing the DNA concentration by the mass of the *Coxiella* genome (2.2 fg).

Labeling and Growth Experiments of *Coxiella burnetii* RSA 439 NMII

[U-^{13}C$_3$]Serine, [U-^{13}C$_6$]glucose and [U-^{13}C$_3$]glycerol were purchased from Isotec/Sigma-Aldrich. 1 L ACCM-2 supplemented either with 5 M [U-^{13}C$_3$]serine, 5 mM [U-^{13}C$_6$]glucose or 5 mM [U-^{13}C$_3$]glycerol was inoculated with *C. burnetii* RSA 439 NMII as indicated above. Seven days post-inoculation, bacteria were harvested by centrifugation at 4.500 g for 45 min at 4°C. Bacterial pellet (ca. 10^{14} bacteria per condition) was autoclaved for 30 min at 120°C. Cells were freeze-dried and stored at −80°C until further analysis. To evaluate the impact of each compound on bacterial growth, ACCM-2 was supplemented with the corresponding unlabeled compounds at 5 mM and inoculated with *C. burnetii* RSA 439 NMII at 10^5 GE/mL. Bacterial growth was assessed at 0, 3, 5, and 7 days post-inoculation using the PicoGreen assay as previously described (Martinez et al., 2014).

Sample Preparation and Derivatization of Protein-Derived Amino Acids and Cell Wall-Derived Diaminopimelate (DAP)

For isotopolog profiling of protein-derived amino acids and cell wall-derived DAP, approximately 10^9 bacterial cells (about 1 mg of freeze-dried pellet) were hydrolyzed in 0.5 mL of 6 M HCl for 24 h at 105°C, as described earlier (Eylert et al., 2010). Samples were dried under a stream of nitrogen at 70°C. The residue was solved in 200 µL of acetic acid and purified on a cation exchange column of Dowex 50WX8 (H+-form, 200–400 mesh, 5 × 10 mM), which was previously washed with 1 mL MeOH and 1 mL ddH$_2$O. Elution occurred after washing with 2 mL of ddH$_2$O with 1 mL of 4 M ammonium hydroxide. 200 µL of the eluate were dried at 70°C under a stream of nitrogen and dissolved in 50 µL dry acetonitrile and 50 µL *N*-(tert-butyldimethyl-silyl)-*N*-methyl-trifluoroacetamide containing 1% tert-butyl-dimethyl-silylchlorid (Sigma). Derivatization occurred at 70°C for 30 min. The resulting tert-butyl-dimethylsilyl (TBDMS) derivates of protein-derived amino acids and cell wall-derived DAP were analyzed by GC/MS. Due to degradation during acid hydrolysis, tryptophan, methionine and cysteine could not be analyzed with this method. Furthermore, acid hydrolysis leads to conversion of glutamine and asparagine to glutamate and aspartate, respectively. Therefore, results given for aspartate and glutamate correspond to asparagine/aspartate and glutamine/glutamate, respectively. Due to inefficient derivatization, TBDMS-arginine could not be detected in sufficient amounts for isotopolog profiling.

Sample Preparation and Derivatization of Methanol-Soluble Polar Metabolites

For isotopolog profiling of methanol-soluble polar metabolites including fatty acids, approximately 5 mg of the freeze-dried

bacteria were mixed with 0.8 g of glass beads (0.25–0.05 mM). 1 mL of pre-cooled 100% methanol was added and mechanical cell lysis occurred for 3 × 20 s at 6.5 m/s using a ribolyser instrument (Hybaid). Samples were immediately cooled down on ice for 5 min followed by centrifugation at 2.300 × g for 10 min. The supernatant was dried under a stream of nitrogen. The residue was dissolved in 50 µL dry acetonitrile and 50 µL *N*-(tert-butyldimethyl-silyl)-*N*-methyl-trifluoroacetamide containing 1% tert-butyl-dimethyl-silylchlorid (Sigma) and kept at 70°C for 30 min. The resulting tert-butyl-dimethylsilyl (TBDMS) derivates of methanol-soluble polar metabolites and fatty acids were used in GC/MS analysis.

Sample Preparation and Derivatization of Mannose (Man) and Galactose (Gal)

For isotopolog profiling of Man and Gal, 5 mg of the freeze-dried bacteria were methanolized over night at 80°C with 0.5 mL methanolic HCl (3 M). Samples were cooled down and the supernatant was dried at 25°C under a stream of nitrogen. The first step of derivatization occurred at 25°C for 1 h in 1 mL acetone containing 20 µL concentrated H$_2$SO$_4$. After that, 2 mL of saturated NaCl and saturated Na$_2$CO$_3$ solution was added. The aqueous solution was extracted 2x with 3 mL ethyl acetate. The combined organic phases were dried under a stream of nitrogen. Dry residue was incubated overnight at 60°C with 200 µL of a 1:1 mixture of dry ethyl acetate and acetic anhydride in a second derivatization step. Derivatization reagents were removed under a stream of nitrogen and the remaining residue was resolved in 100 µL anhydrous ethyl acetate. Resulting diisopropylidene/acetate derivatives were used for GC/MS analysis.

Sample Preparation and Derivatization of Cell Wall-Derived Glucosamine (GlcN) and Muramic Acid (Mur)

For isotopolog profiling of GlcN and Mur, cell wall hydrolyzation was performed with approximately 15 mg of freeze-dried bacterial in 0.5 mL of 6 M HCl overnight at 105°C. Solid components were removed by filtration. The filtrate was dried under a stream of nitrogen and 100 µL of hexamethyldisilazane (HMDS) was added. Derivatization occurred for 3 h at 120°C. Resulting TMS-derivatives were used for GC/MS analysis.

Gas Chromatography/Mass Spectrometry

GC/MS-analysis was performed with a QP2010 Plus gas chromatograph/mass spectrometer (Shimadzu) equipped with a fused silica capillary column (Equity TM-5; 30 m × 0.25 mM, 0.25 µm film thickness; SUPELCO) and a quadrupole detector working with electron impact ionization at 70 eV. An aliquot (0.1 to 6 µL) of the derivatized samples were injected in 1:5 split mode at an interface temperature of 260°C and a helium inlet pressure of 70 kPa. Selected ion monitoring was used with a sampling rate of 0.5 s and LabSolution software (Shimadzu) was used for data collection and analysis. For technical replicates, samples were measured three times, respectively. Overall ^{13}C-excess values and isotopolog compositions where calculated as described earlier

(Eylert et al., 2008). This involved (i) determination of GC/MS spectra of unlabeled derivatized metabolites, (ii) determination of the absolute mass of isotopolog enrichments and distributions of labeled metabolites of the experiment and (iii) correction of the absolute ^{13}C-incorporation by subtracting the heavy isotopolog contributions due to the natural abundances in the derivatized metabolites.

For amino acid and DAP analysis, the following temperature program was used: After sample injection, the column was first kept at 150°C for 3 min and then developed with a temperature gradient of 7°C min^{-1} to a final temperature of 280°C. This temperature was held for further 3 min. TBDMS-derivatives of alanine (6.7 min), glycine (7.0 min), valine (8.5 min), leucine (9.1 min), isoleucine (9.5 min), proline (10.1 min), serine (13.2 min), phenylalanine (14.5 min), aspartate (15.4 min), glutamate (16.8 min), lysine (18.1 min), histidine (20.4 min), tyrosine (21.0 min), and the cell wall component DAP (23.4 min) were detected and isotopolog calculations were performed with m/z [M-57]$^{+}$ or m/z [M-85]$^{+}$.

For analysis of methanol-soluble metabolites including palmitate and stearate, the column was kept at 100°C for 2 min after sample injection. This was followed by a first temperature gradient, in which the column was heated to a final temperature of 234°C in rates of 3°C min^{-1}. Subsequently, a second temperature gradient of 1°C min^{-1} was used until a final temperature of 237°C, and a third temperature gradient of 3°C min^{-1} to a final temperature of 260°C. TBDMS-derivatives of lactate (17.8 min), succinate (27.5 min), fumarate (28.7 min), malate (39.1 min), palmitate (44.0 min) and stearate (49.4 min) were detected. Isotopolog calculations were performed with m/z [M-57]$^{+}$.

For diisopropylidene/acetate derivatives of the hexoses, Man and Gal, the column was kept at 150°C for 3 min after sample injection followed by a first temperature gradient of 10°C min^{-1} to a final temperature of 220°C, and a second temperature gradient of 50°C min^{-1} to a final temperature of 280°C. The final temperature was held for further 3 min. isotopolog calculations were performed with a fragment which still contains all six C-atoms of the hexoses (m/z 287 [M-15]$^{+}$).

For analysis of the TMS-derivatives of the cell wall components GlcN and Mur, the column was kept at 70°C for 5 min followed by a temperature gradient of 5°C min^{-1} to a final temperature of 310°C, which was then kept for an additional minute. isotopolog calculations were performed with m/z [M-452]$^{+}$ and m/z [M-434]$^{+}$. Retention times and mass fragments of derivatized metabolites that were used for all isotopolog calculations are summarized in Table S2.

RESULTS

Axenic Growth of *C. burnetii* Is Not Affected by Exogenous Serine, Glucose, and Glycerol

To investigate the effects of additional amounts of serine, glucose or glycerol on the axenic growth of *C. burnetii*, growth curves were calculated from ACCM-2 cultures supplemented with

5 mM of each substrate and compared to the growth curves of *C. burnetii* growing in standard ACCM-2. Cell densities were determined by calculating the genome equivalents/mL (GE/mL) at 3, 5, and 7 days post inoculation. No significant effect on the growth rates of *C. burnetii* could be observed under this experimental setup (Figure S1). To study the usage of serine, glucose and glycerol by this pathogen, we subsequently performed labeling experiments with [U-^{13}C$_3$]serine, [U-^{13}C$_6$]glucose and [U-^{13}C$_3$]glycerol.

Utilization of Serine by *C. burnetii* Growing in ACCM-2

To study serine metabolism in *C. burnetii*, we performed labeling experiments in ACCM-2 supplemented with 5 mM [U-^{13}C$_3$]serine. ^{13}C-Enrichments and isotopolog fractions of protein-derived amino acids, polar metabolites, fatty acids, DAP and amino sugars derived from cell wall biosynthesis were measured by GC/MS. No ^{13}C-incorporation occurred into His, Ile, Leu, Lys, Phe, Pro, Tyr, and Val that are obviously taken in unlabeled form from the respective amino acids and peptides present in the axenic medium. Only small fractions of ^{13}C-label (<5%) could be found in sugars (from cell wall hydrolysates). In sharp contrast, very high ^{13}C-enrichments were detected in Ser (76.3%) and Gly (34.6%) from the cell hydrolysates. This indicates that exogenous Ser was efficiently taken up from the axenic medium and might be converted into Gly by serine hydroxymethyltransferase (CBU1419). Furthermore, metabolites due to Ser conversion into pyruvate, acetyl-CoA, intermediates of the TCA cycle and their downstream products showed high ^{13}C-enrichments (palmitate: 24.0% > stearate: 21.8% > DAP: 16.3% > Ala: 13.8% > Asp: 9.0% > Glu: 7.5% > fumarate: 5.2% > succinate: 4.4% > malate: 3.8%) (**Figure 2A**, Tables S3 and S5). On the basis of the fractional isotopolog abundances, a more detailed analysis of the metabolic pathways affording the observed patterns (for numerical values, see Table S3) was now done.

Ser and Gly

Ser from the hydrolysate was mainly found as the ^{13}C$_3$-isotopolog (i.e., carrying three ^{13}C-labels; M+3 in **Figure 2A**, Table S5). However, Ser also showed minor amounts of M+2 (i.e., the ^{13}C$_2$-isotopolog) as an indication of metabolic turnover (i.e., degradation to e.g., M+2 Gly and resynthesis of Ser finally leading to M+2 Ser). This is confirmed by the detected isotopolog profile of Gly characterized by the M+2 species.

Ala

High enrichment values in Ala (13.8%) with predominantly M+3 label reflect the formation of its precursor pyruvate from fully labeled M+3 Ser via serine dehydratase (CBU0194). Minor fractions of M+2 and M+1 in Ala also indicate the biosynthesis of this amino acid from M+2 or M+1 labeled pyruvate. This could be explained by pyruvate formation from M+1 and M+2 malate through the action of the malate dehydrogenase (oxaloacetate decarboxylating, CBU0823). Alternatively, or in addition, reactions via the phosphoenolpyruvate carboxykinase (CBU2092) could result in M+2 or M+1

90
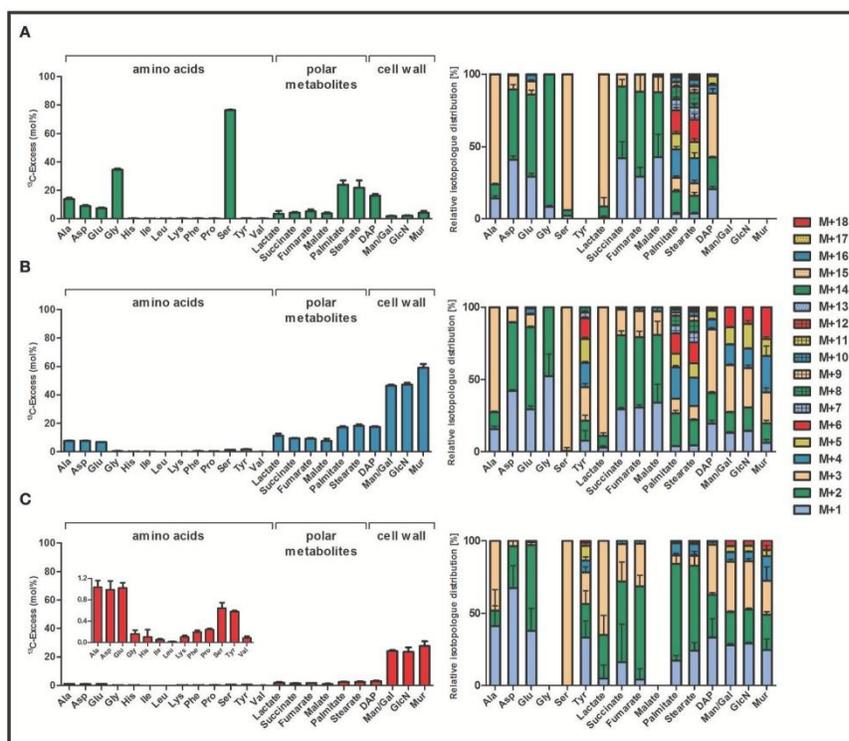
FIGURE 2 | ^{13}C-Excess (mol%) and the fractional isotopolog distributions (%) in key metabolites of *Coxiella burnetii* RSA 439 NMII grown in an axenic ACCM-2 medium supplied with a ^{13}C-labeled tracers. The bacteria were supplemented either with **(A)** 5 mM [U-^{13}C$_3$]serine, **(B)** 5 mM [U-^{13}C$_6$]glucose or **(C)** 5 mM [U-^{13}C$_3$]glycerol. The bacteria were harvested after 7 days of growth. ^{13}C-Excess (mol%) and relative fractions of isotopologs (%) into protein-derived amino acids, methanol-soluble polar metabolites and cell wall components (DAP, Man/Gal, GlcN and Mur) were determined by GC/MS. Error bars indicate standard deviations from the means of six values (2 × biological replicates, 3 × technical GC/MS). For numerical values, see Tables S3 and S5. DAP, diaminopimelate; Man, mannose; Gal, galactose; GlcN, glucosamine; Mur, muramic acid.

label in phosphoenolpyruvate and subsequently in pyruvate due to reactions via pyruvate kinase (CBU1781).

Succinate, Fumarate, Malate, Asp, Glu

Asp (9.0%) directly derived from oxaloacetate and Glu (7.5%) synthesized from α-ketoglutarate were highly ^{13}C-enriched. High levels of M+2 fractions, especially in Glu, are in line with a TCA cycle operating in the oxidative direction, starting from ^{13}C$_2$-acetyl-CoA. Assuming *Si*-specificity of the citrate synthase reaction, both labels from acetyl-CoA are retained in position 4 and 5 of α-ketoglutarate and its product Glu. On the basis of the sequence in the *C. burnetii* genome, the citrate synthase (CBU1410) is indeed expected to be *Si*-specific. Further reaction of [4,5-^{13}C$_2$]α-ketoglutarate via the TCA cycle then results in the detected [1,2-^{13}C$_2$]succinate, [1,2-^{13}C$_2$]fumarate, and [1,2-^{13}C$_2$]malate. [1,2-^{13}C$_2$]oxaloacetate is reflected by the

observed [1,2-^{13}C$_2$]Asp isotopolog. It should be noted that the intrinsic symmetry of succinate randomizes the M+2 label between positions 1,2 and 3,4 finally also leading to [3,4-^{13}C$_2$]isotopologs in malate, oxaloacetate and Asp. The detected minor amounts of M+1 label could then easily be explained by multiple cycling in the TCA. Notably, significant amounts of M+3 isotopologs were also detected in Glu and Asp probably due to ^{13}C-carbon flux from fully labeled pyruvate into M+3 malate via the malate dehydrogenase enzyme (malic enzyme, CBU0823).

Fatty Acids

Palmitate (24.0%) and stearate (21.8%) were highly enriched, again indicating a high carbon flux from the labeled Ser tracer into [^{13}C$_2$]acetyl-CoA. Indeed, the isotopolog profiles of both fatty acids mainly showed M+2 or a multiple of M+2 due to the

3. RESULTS

combination of fully labeled acetyl-CoA building blocks in fatty acid biosynthesis.

DAP

The biosynthesis of the cell wall component DAP, which is also an intermediate for lysine biosynthesis, depends on pyruvate and Asp as precursors. In contrast to Lys, where no ^{13}C-enrichment was detectable, DAP showed high ^{13}C-enrichment (16.3%). This indicates highly active enzymes to form DAP for cell wall formation, but not for Lys biosynthesis. This is remarkable since only one additional step catalyzed by diaminopimelate decarboxylase would be required to form Lys from DAP. Isotopolog distribution in DAP from the experiment with [U-^{13}C$_3$]serine mainly showed M+3 label, which is easily explained by the usage of M+3 labeled pyruvate (see above). Furthermore, some M+2 and M+1 fractions in DAP were also detected, probably due to M+2 and M+1 labeled Asp as a building unit (see above). Isotopologs carrying more than three ^{13}C-atoms may be due to statistical combinations of labeled pyruvate and Asp.

Lactate

Interestingly, also lactate showed some minor ^{13}C-enrichment in the experiment with labeled serine (**Figure 2A**). However, enzymes responsible for lactate biosynthesis from pyruvate seem not to be present in *C. burnetii* based on the genome sequence (Seshadri et al., 2003; Walter et al., 2014). Hypothetically, lactate could be produced from methylglyoxal due to detoxification reactions in this pathogen (Figure S2, for more details, see also below).

Utilization of Glucose

Uptake and incorporation of exogenous glucose were investigated by growth experiments in ACCM-2 supplemented with 5 mM [U-^{13}C$_6$]glucose. Workup and isotope analysis of metabolites was done as described above for the labeling experiments with ^{13}C-Ser. High ^{13}C-excess values (40–50%) could be detected in cell wall sugars indicating that the exogenous glucose tracer was efficiently taken up and metabolized (**Figure 2B**). On this basis, it is obvious that the pathogen can use glucose as a main carbon substrate under the experimental conditions. More specifically, significant ^{13}C-enrichments from [U-^{13}C$_6$]glucose were detected in muramic acid (Mur: 59.1%) > glucosamine (GlcN: 47.2%) > mannose/galactose (Man/Gal: 46.3%) > diaminopimelate (DAP: 17.5%) as well as in fatty acids (stearate: 18.3% > palmitate: 17.3%) and metabolites related to pyruvate biosynthesis and reactions in the TCA cycle (succinate: 9.3% > fumarate: 9.2% > Asp: 7.8% > Ala: 7.7% > malate: 7.5% > Glu: 6.8%). Additionally, low but significant ^{13}C-excess values were detected in Ser (1.4%) and Gly (0.5%), which clearly shows some *de novo* biosynthesis of Ser directly from a fully labeled C$_3$-precursor (pyruvate or 3-phosphoglycerate). Labeled Ser is then directly converted into Gly. This is also reflected by the appearance of almost exclusive M+3 label in Ser and M+2 label in Gly. Low, but significant enrichments could be found in Tyr (1.7%), an amino acid derived from the shikimate pathway. No *de novo* biosynthesis could again be found for His, Ile, Leu, Lys, Phe, Pro and Val (**Figure 2B**, Tables S3 and S6).

Compared to the labeling experiment with [U-^{13}C$_3$]serine, Ala showed lower ^{13}C-enrichments in the experiment with [U-^{13}C$_6$]glucose. However, similar overall ^{13}C-enrichment values appeared in Asp and Glu as well as in fatty acids and DAP in both labeling experiments. This indicates that *C. burnetii* uses glucose as a carbon and energy source at similar rates as Ser. However, glucose is used more efficiently in the formation of amino sugars for cell wall biosynthesis directly or via glycolytic cycling, and serves as a precursor for the *de novo* synthesis of Ser, Gly and Tyr. On the contrary, Ser is almost exclusively metabolized in the TCA cycle for energy generation (**Figures 2A,B**). Like in the labeling experiments with ^{13}C-Ser, also lactate sowed significant ^{13}C-excess values (11.3%). The labeled lactate was again characterized by the M+3 isotopolog although enzymes for the direct biosynthesis via pyruvate are not annotated in *C. burnetii*. However, it can be assumed that this labeling appears due to detoxification reactions via methylglyoxal, which can be formed non-enzymatically from intermediates of glycolytic and gluconeogenetic reactions (Riddle and Lorenz, 1973; Omsland and Heinzen, 2011) (Figure S2). Furthermore, *C. burnetii* features a methylglyoxal synthase (CBU0853), which could catalyze the formation of methylglyoxal from dihydroxyacetone phosphate. The appearance of high amounts of methylglyoxal can therefore be related to high levels of glyceraldehyde 3-phosphate and dihydroxyacetone phosphate. Nevertheless, since methylglyoxal is toxic it has to be degraded via the glyoxalase system resulting in labeled lactate (Booth et al., 2003). However, *C. burnetii* lacks one enzyme of this detoxification system (glyoxalase I) (Seshadri et al., 2003; Omsland and Heinzen, 2011). The slow growth of this intracellular pathogen could therefore be due to avoiding the formation of high levels of methylglyoxal.

Sugars

The highly ^{13}C-enriched amino sugars GlcN and Mur, which are directly derived from cell wall biosynthesis as well as Man/Gal predominantly showed M+3 and M+6 label. M+6 isotopologs indicate the direct usage of fully labeled ^{13}C-glucose for cell wall biosynthesis, whereas M+3 suggests that glucose is efficiently used in glycolytic reactions to form fully labeled triose phosphates and related C$_3$-metabolites. The latter ones can recombine with unlabeled C$_3$-metabolites in gluconeogenetic reactions to form M+3 in Man/Gal and M+3 in GlcN and Mur for cell wall biosynthesis. M+2 label in these compounds could be explained by fully labeled acetyl-CoA entering the TCA cycle generating M+2 malate that could result in M+2 pyruvate by reaction of the malate dehydrogenase enzyme (malic enzyme, CBU0823). Gluconeogenetic reactions could then incorporate the M+2 label into the cell wall sugars. M+4 and M+5 isotopologs might result from combination of two labeled C$_3$-precursors in gluconeogenetic reactions (**Figure 2B** and Table S6).

Fatty Acids

Beside cell wall sugars, also fatty acids carried high amounts of ^{13}C-label demonstrating the efficient conversion of [U-^{13}C$_6$]glucose into fully labeled acetyl-CoA which is subsequently used in *de novo* biosynthesis of fatty acids. This is also represented by the isotopolog patterns, since

92

predominantly M+2 or a multiple of M+2 label was detected in palmitate and stearate (**Figure 2B** and Table S6).

Amino Acids and Polar Metabolites

High rates of carbon flux from glucose via pyruvate and acetyl-CoA is also reflected by the ^{13}C-enrichments of Ala (7.7%), succinate (9.4%), fumarate (9.2%), malate (7.6%), Asp (7.8%) and Glu (6.8%) (**Figure 2B**). High amounts of M+2 isotopologs in these metabolites are related to reactions in the TCA cycle. This clearly showed the usage of fully labeled acetyl-CoA, i.e., M+2, as a precursor, which is combined with oxaloacetate to form M+2 citrate and its M+2 downstream products α-ketoglutarate/Glu, succinate, fumarate, malate, and oxaloacetate/Asp, respectively. Furthermore, M+3 label in succinate, fumarate and malate, but also in Glu and Asp demonstrate the direct carbon flux of fully labeled C$_3$-precursors (as seen in M+3 pyruvate/Ala) into reactions of the TCA cycle via the malic enzyme (CBU0823), which can interconvert malate and pyruvate (**Figure 2B**).

DAP

High values of ^{13}C-enrichment in the cell wall component DAP (17.5%) result from high carbon flux of [U-^{13}C$_6$]glucose into its precursors pyruvate and Asp. In accordance, DAP predominantly showed M+3 label, indicating that fully labeled pyruvate is efficiently used for the biosynthesis of this compound. Nevertheless, also high quantities of M+2 and M+1 label were detectable in DAP, originating from M+2 and M+1 label in Asp. Additionally, also M+5 isotopologs of DAP were detectable in significant amounts, which is due to a combination reaction of fully labeled pyruvate and Asp carrying M+2 label. Similar to the experiments with ^{13}C-Ser, no ^{13}C-label was detectable in Lys, again demonstrating that diaminopimelate decarboxylase, which is responsible for the biosynthesis of this amino acid via DAP, is not present or active in *C. burnetii* (**Figure 2B**).

Tyr

Low, but significant ^{13}C-enrichments were detectable in Tyr (1.8%), an aromatic amino acid derived from the shikimate pathway. Shikimate is made by combination of phosphoenolpyruvate, which is built in glycolytic and gluconeogenetic reactions, and erythrose 4-phosphate, which is a key metabolite of the PPP. Subsequently, formation of chorismate occurs by reaction of shikimate with one more molecule of phosphoenolpyruvate (**Figure 3C**). Biosynthesis of tyrosine then occurs either directly from chorismate or via phenylalanine depending on the metabolic potential of the respective organism (**Figure 1**). Since no enrichment was detectable in phenylalanine in the labeling experiments of *C. burnetii* with ^{13}C-glucose (**Figure 2B**), it can be concluded that this pathogen is auxotrophic for phenylalanine, but nevertheless can use the shikimate/chorismate pathway for direct biosynthesis of tyrosine.

The isotopolog profile of Tyr showed a complex mixture of M+1 to M+8 isotopologs (**Figure 3D**). The high amounts of M+3 in Tyr can be explained by the incorporation of M+3 PEP. Since one of the PEP precursors is decarboxylated during the biosynthetic pathway, the high fractions of M+2 labeling are also obvious (**Figure 3**). The high fraction of M+4

in Tyr could reflect erythrose 4-phosphate formation from fully labeled M+6 fructose 6-phosphate via the transketolase reactions. Furthermore, M+3 label in erythrose 4-phosphate can occur due to glycolytic reactions that form fully labeled glyceraldehyde 3-phosphate which is subsequently entering the PPP. Labeled glyceraldehyde 3-phosphate can also be used in gluconeogenetic reactions to form M+3 isotopologs of fructose which is subsequently leading to M+3 or M+1 labeled erythrose 4-phosphate due to further transketolase conversions (**Figure 3A**). Higher labeling (M+5 to M+8) is a result from various combination reactions from differently labeled C$_4$ and C$_3$ precursors in Tyr biosynthesis (**Figure 3**).

Utilization of Glycerol

To investigate whether *C. burnetii* can use further carbon sources besides Ser and glucose, labeling experiments were performed in ACCM-2 supplemented with 5 mM [U-^{13}C$_3$]glycerol. Bacteria were again harvested 7 days post inoculation and ^{13}C-enrichments and isotopolog profiles in key metabolites were determined by GC/MS. High ^{13}C-excess values were predominantly found in the cell wall sugars Mur (27.5%), GlcN (23.5%) as well as in Man/Gal (24.1%). The cell wall component DAP however, acquired ^{13}C-label at 3.1% (**Figure 2C**).

Some ^{13}C-enrichments were also detected in fatty acids (stearate: 2.6%; palmitate: 2.6%). Additionally, minor labeling was found in Ala, Asp, Glu, Ser and Tyr (1.0–0.6%) as well as in intermediates of the TCA cycle (1.6–1.0%). Furthermore, lactate (1.9%) showed low but significant enrichment. No carbon flux occurred into Gly, His, Ile, Leu, Lys, Phe, Pro and Val (**Figure 2C**, Tables S3 and S7).

Sugars

Since hexoses and amino sugars derived from the cell wall showed by far the highest ^{13}C-incorporation (twenty-fold more ^{13}C-enrichment than in amino acids related to the TCA cycle), glycerol is predominantly used by *C. burnetii* for gluconeogenetic reactions obviously to provide precursors for cell wall biosynthesis. This is also represented by the isotopolog profiles of the sugars under study, all of which mainly showed M+3 indicating the direct usage of fully labeled ^{13}C$_3$-precursors. Furthermore, the formation of M+6 isotopologs in these sugars could only occur if two fully labeled ^{13}C$_3$-precursors are combined, again representing the high carbon flux from [U-^{13}C$_3$]glycerol into gluconeogenetic reactions and cell wall biosynthesis (**Figure 2C**).

Fatty Acids and TCA Cycle-Derived Intermediates and Products

Fatty acids like palmitate and stearate as well as amino acids related to the TCA cycle showed minor ^{13}C-enrichments. On this basis, it can be assumed that some labeled glycerol was also directed toward the biosynthesis of acetyl-CoA, which is subsequently used in biosynthetic formation of fatty acids or in the TCA cycle for energy generation, respectively. This is also represented by the isotopolog profiles of these metabolites, mainly displaying the M+2 molecules. Fatty acids additionally showed low amounts of M+4 isotopologs due to combination of

3. RESULTS

FIGURE 3 | Transfer of ^{13}C-label into tyrosine and its precursors. Transfer of ^{13}C-label from [U-^{13}C$_6$]glucose **(A)** or [U-^{13}C$_3$]glycerol **(B)** into erythrose 4-phosphate (left) and PEP (right) due to distinct metabolic reactions in *C. burnetii*. This includes reactions of the pentose phosphate pathway (transketolase and transaldolase) as well as glycolytic and gluconeogenetic reactions. The respective isotopologs with the highest occurrence are highlighted (gray background). **(C)** Scheme of the biosynthesis of tyrosine in *C. burnetii*. The nine carbon atoms of tyrosine are derived from one molecule of erythrose 4-phosphate (four carbon atoms marked in blue) and two PEP molecules (marked in green and bright orange). Due to a final decarboxylation reaction, one carbon atom of the first PEP molecule (green) becomes lost. **(D)** Detected isotopolog composition of Tyr in the labeling experiment with [U-^{13}C$_6$]glucose or [U-^{13}C$_3$]glycerol, respectively. M+X, M represents the mass of the unlabeled metabolite plus X labeled ^{13}C-atoms. PEP, phosphoenolpyruvate.

two fully labeled acetyl-CoA precursors. However, no isotopologs carrying more than four ^{13}C-atoms were detectable in contrast to the experiments with ^{13}C-Ser and ^{13}C-glucose, again illustrating the lower carbon flux from glycerol toward the TCA cycle. Similar to the previously discussed labeling experiments, M+3 label occurred in intermediates of the TCA cycle due to reactions of the malic enzyme, which can transfer M+3 label from pyruvate into malate and subsequently into oxaloacetate (**Figure 2C**).

Ser and Tyr

Low, but significant enrichment in Ser with exclusive M+3 label again shows *de novo* biosynthesis of this amino acids via fully labeled C$_3$-precursors in *C. burnetii*. Interestingly, glycerol, like glucose, was also used in the shikimate pathway for some *de novo* biosynthesis of Tyr (**Figures 2C,3D**). The

predominant M+3 label could be explained by the usage of M+3 phosphoenolpyruvate and/or M+3 erythrose 4-phosphate in the biosynthetic pathway as described above for the glucose experiment (**Figures 3B,C**).

DAP

Compared to the ^{13}C-enrichments in further amino acids, relatively high amounts of ^{13}C were found in the cell wall component DAP (3.1%). Thereby, M+1, M+2, and M+3 were the highest fractions in this metabolite. This was different to the labeling experiments with Ser and glucose, where also M+4 and M+5 isotopologs were observed. The high amounts of M+3 isotopologs are directly derived from fully labeled pyruvate whereas M+2 and M+1 label is explained from Asp due to M+2 and M+1 labeling in oxaloacetate. Since no M+4 and M+5

94

isotopologs were detected, it can be assumed that no combination reaction with labeled pyruvate and labeled Asp occurred in this experiment. Again, no enrichment was detectable in Lys due to the missing diaminopimelate decarboxylase in *C. burnetii*. (**Figure 2C**).

Differential Substrate Usage of *C. burnetii*

To compare the relative contributions of serine, glucose and glycerol as carbon nutrients for *C. burnetii*, we have used concentrations of 5 mM for each of the labeled compounds as supplements to the medium. However, it can be expected that minor amounts of these compounds in unlabeled form are present in ACMM-2. Therefore, we have estimated these concentrations on the basis of the published data (Sales et al., 1995; Omsland et al., 2011; Sandoz et al., 2016a). Glycerol does not seem to be present in ACMM-2 and the concentrations of unlabeled serine and glucose are reported as 1.68 mM and 1.39 mM, respectively. Taking into account the amounts of unlabeled serine and glucose, the incorporation rates for serine and glucose can be estimated as ^{13}C-excess (determined in the experiment with [U-^{13}C$_3$]serine) × 1.34 or ^{13}C-excess (determined in the experiment with [U-^{13}C$_6$]glucose) × 1.27 (Table S4, Figure S3).

To illustrate the differential carbon flux from the three labeled precursors [U-^{13}C$_3$]serine, [U-^{13}C$_6$]glucose and [U-^{13}C$_3$]glycerol, we selected four metabolic markers that are characteristic for specific carbon fluxes toward distinct metabolic pathways. Specifically, Ala was chosen as a marker metabolite for pyruvate biosynthesis and carbon flux toward e.g., the TCA cycle. Asp reflects a marker metabolite for the TCA cycle since it is directly derived from oxaloacetate, DAP is a marker metabolite for cell wall biosynthesis and finally GlcN represents a central cell wall component which is built from sugars including their formation via gluconeogenetic reactions. The %-incorporation values into these marker metabolites are compared in **Figure 4A**.

When grown with 5 mM ^{13}C-Ser as a tracer, only marker metabolites related to ^{13}C-carbon flux directed toward the TCA cycle display high ^{13}C-incoroporation, whereas only very low ^{13}C-incorporation was detectable in GlcN. In contrast, predominantly the amino sugar GlcN derived from gluconeogenetic reactions and cell wall biosynthesis reveal high enrichment values in the experiment with 5 mM ^{13}C-glycerol, whereas Ala and Asp showed lower ^{13}C-excess values. Nevertheless, also the cell wall component DAP showed higher incorporation values compared to other metabolites derived from the TCA cycle in the experiment with [U-^{13}C$_3$]glycerol. The labeling experiments with 5 mM ^{13}C-glucose revealed high enrichment values in both groups (TCA cycle related markers and cell wall components) (**Figure 4A**). It turns out that serine and glucose are used as carbon nutrients at similar rates for feeding the glycolytic pathway providing pyruvate (for example, as a precursor for Ala and DAP) and acetyl-CoA (as a precursor for fatty acids and as a substrate for the TCA cycle). A major fraction of glucose is directly shuffled into hexose precursors for cell wall biosynthesis, as evident from the high incorporation rate into glucosamine. Glycerol, however, is rarely utilized as a carbon substrate for feeding glycolysis or the TCA, but is
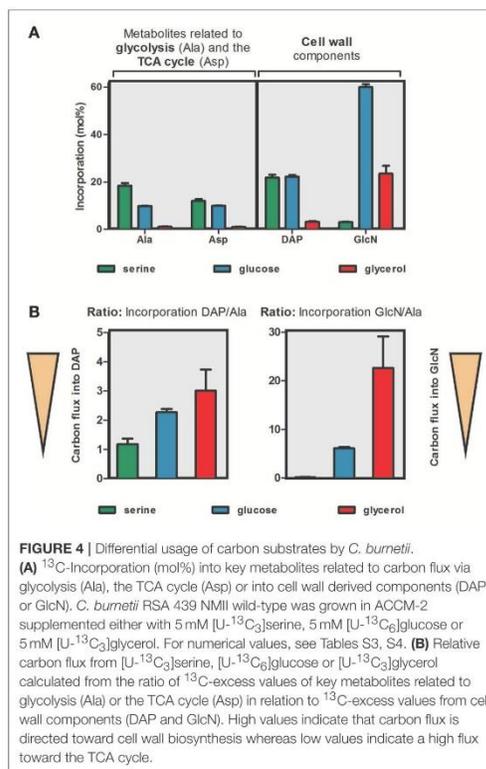

FIGURE 4 | Differential usage of carbon substrates by *C. burnetii*. **(A)** ^{13}C-Incorporation (mol%) into key metabolites related to carbon flux via glycolysis (Ala), the TCA cycle (Asp) or into cell wall derived components (DAP or GlcN). *C. burnetii* RSA 439 NMII wild-type was grown in ACMM-2 supplemented either with 5 mM [U-^{13}C$_3$]serine, 5 mM [U-^{13}C$_6$]glucose or 5 mM [U-^{13}C$_3$]glycerol. For numerical values, see Tables S3, S4. **(B)** Relative carbon flux from [U-^{13}C$_3$]serine, [U-^{13}C$_6$]glucose or [U-^{13}C$_3$]glycerol calculated from the ratio of ^{13}C-excess values of key metabolites related to glycolysis (Ala) or the TCA cycle (Asp) in relation to ^{13}C-excess values from cell wall components (DAP and GlcN). High values indicate that carbon flux is directed toward cell wall biosynthesis whereas low values indicate a high flux toward the TCA cycle.

mainly used as a glucogenic source to fill up the pool of hexose phosphates required in cell wall biosynthesis, e.g., glucosamine (i.e., when glucose is not present at high concentrations in the environment). Interestingly, serine cannot serve as an efficient glucogenic substrate even at low glucose concentrations in the medium, as gleaned from the low incorporation of ^{13}C-serine into glucosamine (**Figure 4A**).

To better display the relative carbon fluxes from a given substrate toward pyruvate biosynthesis, the TCA cycle and cell wall components, we now calculated the ratios of the ^{13}C-excess values in DAP and GlcN over the ^{13}C-excess values of Ala (Tables S8 and S9). High values indicate that ^{13}C-carbon flux is directed toward cell wall biosynthesis e.g., of GlcN or DAP. Low values reflect high ^{13}C-carbon fluxes into the TCA cycle e.g., for energy generation.

In the experiment with [U-^{13}C$_3$]serine as a precursor, the lowest values for both of these ratios were obtained, indicating the preferential usage of serine in the TCA cycle for energy generation by *C. burnetii*. Especially, the ratio "^{13}C-excess GlcN/Ala" was very low, again reflecting the missing carbon flux from Ser into gluconeogenetic reactions and biosynthesis of

GlcN. Minor carbon flux from Ser into DAP via the TCA cycle is also evident. In contrast, highest values for both ratios (^{13}C-excess DAP/Ala and ^{13}C-excess GlcN/Ala) were obtained when [U-^{13}C$_3$]glycerol was used as precursor. Therefore, this precursor seems to be especially fed into gluconeogenetic reactions for biosynthesis of cell wall sugars. However, glycerol is also shuffled into the TCA cycle albeit at lower rates, again predominantly serving the biosynthesis of the cell wall component DAP. Ratios were also high when [U-^{13}C$_6$]glucose was used as a precursor but did not reach the levels in the experiment with labeled glycerol. However, also glucose seems to be shuffled prevalently into cell wall biosynthesis directly or via glycolytic turnover (i.e., degradation by glycolysis and gluconeogenesis from C$_3$-substrates). Moreover, the ratio "^{13}C-excess DAP/Ala" was higher in this labeling experiment compared to that with ^{13}C-Ser as a precursor. This indicates that glucose is also preferred for DAP biosynthesis although carbon flux into the TCA cycle seems to be similar in the experiments with glucose and Ser (**Figure 4B**).

In summary, these results show that carbohydrates and predominantly glycerol are preferred substrates of *C. burnetii* for the formation of cell wall components either directly using exogenous sugars or via gluconeogenetic reactions and via the TCA cycle to synthesize DAP. In contrast, serine serves as a substrate which is predominantly shuffled into the TCA cycle for energy generation and does not serve gluconeogenetic reactions efficiently. These findings support the model of a bipartite metabolic network which is discussed below.

DISCUSSION

In contrast to the genomes of other strictly intracellular bacteria, such as *Chlamydia trachomatis* or *Rickettsia*, the genome of *C. burnetii* reflects a high degree of metabolic capacities in a highly interconnected metabolic network with the potential usage of a single carbon substrate. On the other hand, its capacity to grow extracellularly in minimal media is restricted and indicates multiple substrate usages as described before for several intracellular bacteria (Grubmüller et al., 2014; Häuslein et al., 2015; Mehlitz et al., 2016). Here, we indeed show usage of exogenous serine, glucose and glycerol by *C. burnetii* during axenic growth with these substrates feeding specific sections of a partite metabolic network.

Incorporation rates and isotopolog profiles of amino acids, fatty acids, sugars and further metabolic intermediates demonstrate that glucose is efficiently taken up and utilized by *C. burnetii*, however, glucose alone does not support axenic growth of this pathogen in ACCM-2 (Figure S1) or in a minimal defined medium (ACCM-D) (Sandoz et al., 2016a). Furthermore, a classical hexokinase has not been identified in the genome of *C. burnetii*. The virtual absence of this essential enzymatic reaction for glucose catabolism could be by-passed by enzyme I of the bacterial phosphoenolpyruvate: sugar phosphotransferase system (PTS, CBU1550) and the histidine phosphocarrier protein (HPr, CBU0743) which are both present in *C. burnetii*

(Seshadri et al., 2003). In line with our findings, differential gene expression studies also suggest that glucose is among the major substrates under *in vivo* conditions (Kuley et al., 2015). Our data confirm that *C. burnetii* can use glucose directly for the biosynthesis of cell wall compounds, but also to generate energy via glycolysis and the TCA cycle. This metabolic strategy is different to that of its close relative *L. pneumophila*, which mainly uses amino acids as energy source, as a possible strategy to limit the metabolic stress on the host cell, since disturbed glucose levels in eukaryotic cells are directly linked to apoptosis (Zhao et al., 2008). Considering that growth of *C. burnetii* is slower than that of *L. pneumophila*, a continuous low-rate usage of glucose by intracellular *C. burnetii* could therefore be possible without a further disturbance of host cell regulatory effects.

The labeling data show, for the first time, the effective uptake and usage of glycerol by *C. burnetii*. This provides direct evidence that, besides amino acids and glucose, further carbon sources not present in the currently used axenic media can comprise nutritional factors in the growth of this pathogen. Despite the identification of genes encoding enzymes involved in the catabolism of glycerol in the genome of *C. burnetii*, no glycerol transporter has been identified until now (Seshadri et al., 2003). Nevertheless, incorporation of this nutrient could also occur via passive diffusion through the bacterial membrane (Romijn et al., 1972; McElhaney et al., 1973). Our data now show that glycerol is preferably used in gluconeogenetic reactions, thereby predominantly serving the biosynthesis of peptidoglycan building units, like GlcN and Mur. A minor fraction of the glycerol supply is used for pyruvate formation as a precursor in DAP biosynthesis which is also required for the peptidoglycan layer of *C. burnetii*. Interestingly, the amount of peptidoglycan in the SCV of this pathogen is about 2.7-fold higher than the amount in the LCV (Amano et al., 1984). This could indicate that glycerol becomes a more important substrate at later stages during the developmental cycle of *C. burnetii*, e.g., when the formation of the SCV is initialized. Like *L. pneumophila*, also *C. burnetii* uses Ser for energy generation in the TCA cycle (Eylert et al., 2010; Häuslein et al., 2015; Gillmaier et al., 2016). In contrast to *L. pneumophila*, however, almost no carbon flux occurred from Ser into gluconeogenetic reactions, indicating that the metabolism of Ser is more restricted to energy generation in *C. burnetii* than in *L. pneumophila*.

Altogether, *C. burnetii* features a bipartite-type metabolic network which is similar but not identical to that reported recently for its close relative *L. pneumophila* (Schunder et al., 2014; Häuslein et al., 2015) (**Figure 5**). Section 1 of the partite model comprises glycolytic and gluconeogenetic reactions, cell wall biosynthesis derived from hexoses, the ED pathway (in the case of *L. pneumophila*), the PPP and the shikimate pathway (in the case of *C. burnetii*). On the other hand, section 2 includes the TCA cycle, fatty acid and amino acid biosynthesis using acetyl-CoA or TCA cycle derived intermediates as precursors. On this basis, section 2 of the model represents more the energy generating part, since high amounts of ATP, NADH/H$^+$ and FADH$_2$ are derived from the TCA cycle and the electron transfer chain. In section

96

FIGURE 5 | The bipartite metabolic model of *C. burnetii* **(A)** and *L. pneumophila* **(B)**. The network is divided into two modules. Module 1 comprises glycolytic and gluconeogenetic reactions, the ED pathway, the shikimate/chorismate pathway as well as the biosynthesis of cell wall components. Module 2 includes the TCA cycle, fatty acid and PHB biosynthesis as well as the biosynthesis of the central cell wall component DAP. Color and size of arrows indicate direction and intensity of carbon flux from serine (green), glucose (blue) and glycerol (red). Serine serves as a main carbon and energy source which is predominantly metabolized in the TCA cycle for energy generation in both pathogens (Module 2). Nevertheless, in *C. burnetii* serine is not metabolized in as high rates as in *L. pneumophila*. Furthermore, carbon flux from this amino acid occurs exclusively into the second part of metabolism (TCA cycle) in *C. burnetii*, whereas carbon flux from serine also occurs into the upper part of metabolism in *L. pneumophila*. Glucose catabolism differs in both pathogenic bacteria. While *C. burnetii* degrades glucose in glycolytic reactions, *L. pneumophila* uses predominantly the Entner-Doudoroff pathway. Thereby, *C. burnetii* uses glucose very efficiently in both parts of metabolism, also for tyrosine biosynthesis via the shikimate pathway. In contrast, usage of glucose by *L. pneumophila* is much lower and more restricted toward the upper part of metabolism. Glycerol is metabolized at very low rates by *L. pneumophila* and thereby used exclusively in gluconeogenetic reactions and the PPP. In contrast, it effectively serves as carbon source for both modules in *C. burnetii*, and also for tyrosine biosynthesis in the shikimate pathway. Furthermore, glycerol is preferably used for cell wall biosynthesis by *C. burnetii*. α-KGA, α-ketoglutarate; DAP, diaminopimelate; Pyr, pyruvate; OAA, oxaloacetate; Acyl-CoA, acetyl-CoA; Man, mannose; Gal, galactose; 3-HB, 3-hydroxybutyrate; PHB, poly-hydroxybutyrate; PEP, phosphoenolpyruvate; GAP, glyceraldehyde 3-phosphate; DHAP, dihydroxyacetone phosphate; TK, transketolase; TA, transaldolase; G3P, glycerol 3-phosphate; PPP, pentose phosphate pathway; TCA, TCA cycle.

1, however, high amounts of NADPH/H$^+$ are produced via the PPP, and this section predominantly serves anabolic purposes and more represents the energy consuming part of metabolism.

In *C. burnetii* and *L. pneumophila*, glycerol and glucose are preferably shuffled into section 1 of the metabolic network predominantly serving anabolic processes, especially cell wall biosynthesis. Serine on the other hand is used in section 2 of the network with the TCA cycle for energy generation (Eylert et al., 2010; Häuslein et al., 2015; Gillmaier et al., 2016) (**Figure 5**).

Notably and despite the fact that *C. burnetii* and *L. pneumophila* are close relatives, there are also considerable differences in their metabolic concepts, since glucose and glycerol are more important nutrients for *C. burnetii* than for *L. pneumophila*. Specifically, in *C. burnetii*, glucose can also be shuffled efficiently into section 2 of the metabolism while in *L. pneumophila* this section is quite restricted for the usage of serine as carbon supply (Keen and Hoffman, 1984).

In *L. pneumophila*, all enzymes for glycolytic reactions as well as for the ED pathway are reflected in their genomes (Cazalet et al., 2004; Chien et al., 2004), whereas in *C. burnetii* genes encoding the ED pathway are partly missing (Seshadri et al., 2003). However, in a striking difference, glucose catabolism occurs via the ED pathway in *L. pneumophila* and via glycolysis in *C. burnetii* (McDonald and Mallavia, 1971; Eylert et al., 2010) (**Figure 5**).

The directed carbon flux from the carbon substrates under study furthermore suggests a growth phase dependent utilization of these nutrients under intracellular conditions. Since Ser is predominantly shuffled into the TCA cycle via pyruvate and acetyl-CoA for e.g., energy generation via NADH and respiration, these metabolic processes are predominantly induced during early replication in the CCV, when *C. burnetii* appears in its LCV (Coleman et al., 2007). In contrast, glucose and glycerol could preferably be used at later growth phases than serine, probably when the cells start to develop into the SCV, since these precursors predominantly serve the biosynthesis

3. RESULTS

of peptidoglycan, which is present in higher amounts in this morphological form (Amano et al., 1984).

Interestingly, enzymes for the biosynthesis of the energy storage compound poly-3-hydroxybutyrate (PHB) are not present in *C. burnetii* (Seshadri et al., 2003), whereas its biosynthesis plays a central role in the metabolism and life cycle of *L. pneumophila* (Keen and Hoffman, 1984; Gillmaier et al., 2016). Furthermore, degradation of PHB by *L. pneumophila* seems to be an important factor for long term survival of this intracellular pathogen in the environment (Li et al., 2015). For biosynthesis of this storage compound, which is predominantly produced during the late growth phase, *L. pneumophila* preferably uses serine and glucose to provide acetyl-CoA as the building units for 3-hydroxybutyrate and its polymer (Eisenreich and Heuner, 2016; Gillmaier et al., 2016). The reason for the apparent inability of *C. burnetii* to build PHB is unknown, but could be linked to the acidified conditions in the CCV. Nevertheless, this raises questions about the long-term survival strategies of *C. burnetii* (Seshadri et al., 2003).

A further difference in the metabolic potential of these two intracellular pathogens is the active shikimate pathway in *C. burnetii*. Our data clearly show that *C. burnetii* is able to synthesize Tyr *de novo* via this metabolic pathway and is thus not auxotroph for Tyr as it was concluded from recent growth experiments in the minimal defined medium ACCM-D (Sandoz et al., 2016a). In contrast, *L. pneumophila* seems to be auxotroph for the biosynthesis of aromatic amino acids (Eylert et al., 2010; Häuslein et al., 2015; Gillmaier et al., 2016) at least under *in vitro* conditions, although almost all enzymes of this biosynthetic route appear to be present based on the genome sequence (Chien et al., 2004). However, the metabolic role or importance of the shikimate pathway in *C. burnetii* or *L. pneumophila* has not been studied extensively until now. On one hand, *in vitro* grown *L. pneumophila* does not need to use this pathway for the *de novo* biosynthesis of aromatic amino acids and rather imports these amino acids from the medium. On the other hand, recent studies demonstrated that mutants of *L. pneumophila* concerning two enzymes of the shikimate pathway, *aroB* and *aroE,* were defective in infection and replication inside of human macrophages (Jones et al., 2015).

Since the shikimate pathway is not present in mammalian, this biosynthetic pathway is a potential target for drug development agains pathogenic bacteria (Consigli and Paretsky, 1962). Especially the enolpyruvylshikimate 3-phosphate synthase (EPSP synthase) that catalyzes the biosynthesis of 5-enolpyruvylshikimate 3-phosphate from shikimate 3-phosphate and PEP, which is subsequently converted to chorismate in the downstream reactions of this metabolic pathway, could be a promising target for new antibiotics against *C. burnetii* and further pathogens (Ferreras et al., 2005; Lemaître et al., 2014; Light et al., 2016). In general, the EPSP synthases are divided into two classes dependent on their sensitivity toward the herbicide glyphosate. Thereby, class I EPSP synthases, which are present in plants and some Gram positive bacteria, are highly sensitive toward this herbicide, whereas class II EPSP synthases retain

their catalytic activity in the presence of glyphosate (Franklin et al., 2015; Light et al., 2016). These class II EPSP synthases, which have been found in some glyphosate-tolerant bacteria, also differ in their genome sequence compared to the class I enzymes (Duke and Powles, 2008; Pollegioni et al., 2011). However, class II EPSP synthases, like the synthase of *C. burnetii* (CBU0526) are not as well studied as the well-known class I EPSP synthases (Duke and Powles, 2008; Pollegioni et al., 2011).

Nevertheless, besides the EPSP synthases also other enzymes of this biosynthetic pathway represent potential drug targets in various pathogens including *Mycobacterium tuberculosis* and *Helicobacter pylori* and are in the focus of current research (Parish and Stoker, 2002; Ducati et al., 2007; Vianna and De Azevedo, 2012; Blanco et al., 2013). Notably, mutations in the gene encoding the type-II EPSP synthase (CBU0526) and the shikimate dehydrogenase of *C. burnetii* (CBU0010) also showed significant intracellular growth defects (Martinez et al., 2014, and unpublished results), strongly suggesting that the shikimate route is indeed essential for intracellular *C. burnetii*.

In summary, *C. burnetii* features a bipartite metabolic network resembling the topology of its closely relative *L. pneumophila* with amino acids as major nutrients. However, in comparison to *L. pneumophila*, *C. burnetii* shows higher rates in the usages of glucose and glycerol, especially for cell wall biosynthesis and for the synthesis of tyrosine. These differences could reflect the lower replication rates of *C. burnetii* in comparison to *L. pneumophila*, thereby imprinting a lower burden to adapt to the limited nutrient supply under intracellular conditions. However, the general concept of multi-substrate usage in a bipartite metabolic network is also valid for *C. burnetii* and could benefit the robustness and survival of the intracellular pathogen.

AUTHOR CONTRIBUTIONS

WE, IH, FrC, and MB designed the study and wrote the manuscript. IH, FrC, SR, and FaC performed the experimental work.

ACKNOWLEDGMENTS

SUPPLEMENTARY MATERIAL

The Supplementary Material for this article can be found online at: http://journal.frontiersin.org/article/10.3389/fcimb.2017.00285/full#supplementary-material

98

REFERENCES

Amano, K., Williams, J., McCaul, T., and Peacock, M. (1984). Biochemical and immunological properties of *Coxiella burnetii* cell wall and peptidoglycan-protein complex fractions. *J. Bacteriol.* 160, 982–988.

Andersson, S. G., and Kurland, C. G. (1998). Reductive evolution of resident genomes. *Trends Microbiol.* 6, 263–268. doi: 10.1016/S0966-842X(98)01312-2

Arricau-Bouvery, N., and Rodolakis, A. (2005). Is Q fever an emerging or re-emerging zoonosis? *Vet. Res.* 36, 327–349. doi: 10.1051/vetres:2005010

Babudieri, B. (1959). Q fever: a zoonosis. *Adv. Vet. Sci.* 5:422.

Beare, P. A., Gilk, S. D., Larson, C. L., Hill, J., Stead, C. M., Omsland, A., et al. (2011). Dot/Icm type IVB secretion system requirements for *Coxiella burnetii* growth in human macrophages. *MBio* 2, e00175–e00111. doi: 10.1128/mBio.00175-11

Blanco, B., Prado, V. N., Lence, E., Otero, J. M., Garcia-Doval, C., Van Raaij, M. J., et al. (2013). *Mycobacterium tuberculosis* shikimate kinase inhibitors: design and simulation studies of the catalytic turnover. *J. Am. Chem. Soc.* 135, 12366–12376. doi: 10.1021/ja405853p

Booth, I., Ferguson, G., Miller, S., Li, C., Gunasekera, B., and Kinghorn, S. (2003). Bacterial production of methylglyoxal: a survival strategy or death by misadventure? *Biochem. Soc. Trans.* 31, 1406–1408. doi: 10.1042/bst0311406

Burstein, D., Amaro, F., Zusman, T., Lifshitz, Z., Cohen, O., Gilbert, J. A., et al. (2016). Uncovering the *Legionella* genus effector repertoire-strength in diversity and numbers. *Nat. Genet.* 48:167. doi: 10.1038/ng.3481

Carey, K. L., Newton, H. J., Lührmann, A., and Roy, C. R. (2011). The *Coxiella burnetii* Dot/Icm system delivers a unique repertoire of type IV effectors into host cells and is required for intracellular replication. *PLoS Pathog.* 7:e1002056. doi: 10.1371/journal.ppat.1002056

Cazalet, C., Rusniok, C., Bruggemann, H., Zidane, N., Magnier, A., Ma, L., et al. (2004). Evidence in the *Legionella pneumophila* genome for exploitation of host cell functions and high genome plasticity. *Nat. Genet.* 36, 1165–1173. doi: 10.1038/ng1447

Chen, C., Banga, S., Mertens, K., Weber, M. M., Gorbaslieva, I., Tan, Y., et al. (2010). Large-scale identification and translocation of type IV secretion substrates by *Coxiella burnetii*. *Proc. Natl. Acad. Sci. U.S.A.* 107, 21755–21760. doi: 10.1073/pnas.1010485107

Chien, M., Morozova, I., Shi, S., Sheng, H., Chen, J., Gomez, S. M., et al. (2004). The genomic sequence of the accidental pathogen *Legionella pneumophila*. *Science* 305, 1966–1968. doi: 10.1126/science.1099776

Coleman, S. A., Fischer, E. R., Cockrell, D. C., Voth, D. E., Howe, D., Mead, D. J., et al. (2007). Proteome and antigen profiling of *Coxiella burnetii* developmental forms. *Infect. Immun.* 75, 290–298. doi: 10.1128/IAI.00883-06

Coleman, S. A., Fischer, E. R., Howe, D., Mead, D. J., and Heinzen, R. A. (2004). Temporal analysis of *Coxiella burnetii* morphological differentiation. *J. Bacteriol.* 186, 7344–7352. doi: 10.1128/JB.186.21.7344-7352.2004

Consigli, R. A., and Paretsky, D. (1962). Oxidation of glucose 6-phosphate and isocitrate by *Coxiella burnetii*. *J. Bacteriol.* 83, 206–207.

Ducati, R., Basso, L., and Santos, D. (2007). Mycobacterial shikimate pathway enzymes as targets for drug design. *Curr. Drug Targets* 8, 423–435. doi: 10.2174/138945007780059004

Duke, S. O., and Powles, S. B. (2008). Glyphosate: a once-in-a-century herbicide. *Pest. Manag. Sci.* 64, 319–325. doi: 10.1002/ps.1518

Eisenreich, W., and Heuner, K. (2016). The life stage-specific pathometabolism of *Legionella pneumophila*. *FEBS Lett.* 590, 3868–3886. doi: 10.1002/1873-3468.12326

Eylert, E., Herrmann, V., Jules, M., Gillmaier, N., Lautner, M., Buchrieser, C., et al. (2010). Isotopologue profiling of *Legionella pneumophila*: role of serine and glucose as carbon substrates. *J. Biol. Chem.* 285, 22232–22243. doi: 10.1074/jbc.M110.128678

Eylert, E., Schar, J., Mertins, S., Stoll, R., Bacher, A., Goebel, W., et al. (2008). Carbon metabolism of *Listeria monocytogenes* growing inside macrophages. *Mol. Microbiol.* 69, 1008–1017. doi: 10.1111/j.1365-2958.2008.06337.x

Ferreras, J. A., Ryu, J.-S., Di Lello, F., Tan, D. S., and Quadri, L. E. (2005). Small-molecule inhibition of siderophore biosynthesis in *Mycobacterium tuberculosis* and *Yersinia pestis*. *Nat. Chem. Biol.* 1, 29–32. doi: 10.1038/nchembio706

Fournier, P.-E., Marrie, T. J., and Raoult, D. (1998). Diagnosis of Q fever. *J. Clin. Microbiol.* 36, 1823–1834.

Franklin, M. C., Cheung, J., Rudolph, M. J., Burshteyn, F., Cassidy, M., Gary, E., et al. (2015). Structural genomics for drug design against the pathogen *Coxiella burnetii*. *Proteins* 83, 2124–2136. doi: 10.1002/prot.24841

Gillmaier, N., Schunder, E., Kutzner, E., Tlapak, H., Rydzewski, K., Herrmann, V., et al. (2016). Growth-related metabolism of the carbon storage poly-3-hydroxybutyrate in *Legionella pneumophila*. *J. Biol. Chem.* 291, 6471–6482. doi: 10.1074/jbc.M115.693481

Grubmüller, S., Schauer, K., Goebel, W., Fuchs, T. M., and Eisenreich, W. (2014). Analysis of carbon substrates used by *Listeria monocytogenes* during growth in J774A.1 macrophages suggests a bipartite intracellular metabolism. *Front. Cell. Infect. Microbiol.* 4:156. doi: 10.3389/fcimb.2014.00156

Hackstadt, T., and Williams, J. (1983). pH dependence of the *Coxiella burnetii* glutamate transport system. *J. Bacteriol.* 154, 598–603.

Hackstadt, T., and Williams, J. C. (1981a). Biochemical stratagem for obligate parasitism of eukaryotic cells by *Coxiella burnetii*. *Proc. Natl. Acad. Sci. U.S.A.* 78, 3240–3244. doi: 10.1073/pnas.78.5.3240

Hackstadt, T., and Williams, J. C. (1981b). Stability of the adenosine 5′-triphosphate pool in *Coxiella burnetii*: influence of pH and substrate. *J. Bacteriol.* 148, 419–425.

Häuslein, I., Manske, C., Goebel, W., Eisenreich, W., and Hilbi, H. (2015). Pathway analysis using ^{13}C-glycerol and other carbon tracers reveals a bipartite metabolism of *Legionella pneumophila*. *Mol. Microbiol.* 100, 229–246. doi: 10.1111/mmi.13313

Hofer, U. (2016). Bacterial genomics: *Legionella*'s toolbox of effectors. *Nat. Rev. Microbiol.* 14, 133–133. doi: 10.1038/nrmicro.2016.8

Hubber, A., and Roy, C. R. (2010). Modulation of host cell function by *Legionella pneumophila* type IV effectors. *Annu. Rev. Cell Dev. Biol.* 26, 261–283. doi: 10.1146/annurev-cellbio-100109-104034

Jones, S. C., Price, C. T., Santic, M., and Kwaik, Y. A. (2015). Selective requirement of the shikimate pathway of *Legionella pneumophila* for intravacuolar growth within human macrophages but not within *Acanthamoeba*. *Infect. Immun.* 83, 2487–2495. doi: 10.1128/IAI.00294-15

Keen, M. G., and Hoffman, P. S. (1984). Metabolic pathways and nitrogen metabolism in *Legionella pneumophila*. *Curr. Microbiol.* 11, 81–88. doi: 10.1007/BF01567708

Kern, T., Kutzner, E., Eisenreich, W., and Fuchs, T. M. (2016). Pathogen–nematode interaction: nitrogen supply of *Listeria monocytogenes* during growth in *Caenorhabditis elegans*. *Environ. Microbiol. Rep.* 8, 20–29. doi: 10.1111/1758-2229.12344

Kuley, R., Bossers-Devries, R., Smith, H. E., Smits, M. A., Roest, H. I., and Bossers, A. (2015). Major differential gene regulation in *Coxiella burnetii* between *in vivo* and *in vitro* cultivation models. *BMC Genomics* 16:953. doi: 10.1186/s12864-015-2143-7

Larson, C. L., Martinez, E., Beare, P. A., Jeffrey, B., Heinzen, R. A., and Bonazzi, M. (2016). Right on Q: genetics begin to unravel *Coxiella burnetii* host cell interactions. *Future Microbiol.* 11, 919–939. doi: 10.2217/fmb-2016-0044

Lemaître, C., Bidet, P., Benoist, J.-F., Schlemmer, D., Sobral, E., D'humières, C., et al. (2014). The ssbL gene harbored by the ColV plasmid of an *Escherichia coli* neonatal meningitis strain is an auxiliary virulence factor boosting the production of siderophores through the shikimate pathway. *J. Bacteriol.* 196, 1343–1349. doi: 10.1128/JB.01153-13

Li, L., Mendis, N., Trigui, H., and Faucher, S. P. (2015). Transcriptomic changes of *Legionella pneumophila* in water. *BMC Genomics* 16:1. doi: 10.1186/s12864-015-1869-6

Light, S. H., Krishna, S. N., minasov, G., and Anderson, W. F. (2016). An unusual cation-binding site and distinct domain–domain interactions distinguish class II enolpyruvylshikimate-3-phosphate synthases. *Biochemistry* 55, 1239–1245. doi: 10.1021/acs.biochem.5b00553

Madariaga, M. G., Rezai, K., Trenholme, G. M., and Weinstein, R. A. (2003). Q fever: a biological weapon in your backyard. *Lancet Infect. Dis.* 3, 709–721. doi: 10.1016/S1473-3099(03)00804-1

Martinez, E., Allombert, J., Cantet, F., Lakhani, A., Yandrapalli, N., Neyret, A., et al. (2016). *Coxiella burnetii* effector CvpB modulates phosphoinositide metabolism for optimal vacuole development. *Proc. Natl. Acad. Sci. U.S.A.* 113, E3260–E3269. doi: 10.1073/pnas.1522811113

Martinez, E., Cantet, F., Fava, L., Norville, I., and Bonazzi, M. (2014). Identification of OmpA, a *Coxiella burnetii* protein involved in host cell invasion,

3. RESULTS

by multi-phenotypic high-content screening. *PLoS Pathog.* 10:e1004013. doi: 10.1371/journal.ppat.1004013

Maurin, M., and Raoult, D. F. (1999). Q fever. *Clin. Microbiol. Rev.* 12, 518–553.

McDonald, T. L., and Mallavia, L. (1970). Biochemistry of *Coxiella burnetii*: 6-phosphogluconic acid dehydrogenase. *J. Bacteriol.* 102, 1–5.

McDonald, T. L., and Mallavia, L. (1971). Biochemistry of *Coxiella burnetii*: Embden-Meyerhof pathway. *J. Bacteriol.* 107, 864–869.

McElhaney, R. N., De Gier, J., and Van Der Neut-Kok, E. (1973). The effect of alterations in fatty acid composition and cholesterol content on the nonelectrolyte permeability of *Acholeplasma laidlawii* B cells and derived liposomes. *Biochimica et Biophysica Acta (BBA)-Biomembranes* 298, 500–512. doi: 10.1016/0005-2736(73)90376-3

Mehlitz, A., Eylert, E., Huber, C., Lindner, B., Vollmuth, N., Karunakaran, K., et al. (2016). Metabolic adaptation of *Chlamydia trachomatis* to mammalian host cells. *Mol. Microbiol.* 103, 1004–1019. doi: 10.1111/mmi.13603

Miller, J. D., and Thompson, H. A. (2002). Permeability of *Coxiella burnetii* to ribonucleosides. *Microbiology* 148, 2393–2403. doi: 10.1099/00221287-148-8-2393

Moffatt, J. H., Newton, P., and Newton, H. J. (2015). *Coxiella burnetii*: turning hostility into a home. *Cell. Microbiol.* 17, 621–631. doi: 10.1111/cmi.12432

Newton, H. J., McDonough, J. A., and Roy, C. R. (2013). Effector protein translocation by the *Coxiella burnetii* Dot/Icm type IV secretion system requires endocytic maturation of the pathogen-occupied vacuole. *PLoS ONE* 8:e54566. doi: 10.1371/journal.pone.0054566

Omsland, A., Beare, P. A., Hill, J., Cockrell, D. C., Howe, D., Hansen, B., et al. (2011). Isolation from animal tissue and genetic transformation of *Coxiella burnetii* are facilitated by an improved axenic growth medium. *Appl. Environ. Microbiol.* 77, 3720–3725. doi: 10.1128/AEM.02826-10

Omsland, A., Cockrell, D. C., Howe, D., Fischer, E. R., Virtaneva, K., Sturdevant, D. E., et al. (2009). Host cell-free growth of the Q fever bacterium *Coxiella burnetii*. *Proc. Natl. Acad. Sci. U.S.A.* 106, 4430–4434. doi: 10.1073/pnas.0812074106

Omsland, A., and Heinzen, R. A. (2011). Life on the outside: the rescue of *Coxiella burnetii* from its host cell. *Annu. Rev. Microbiol.* 65, 111–128. doi: 10.1146/annurev-micro-090110-102927

Paretsky, D., Consigli, R. A., and Downs, C. M. (1962). Studies on the physiology of rickettsiae III. Glucose phosphorylation and hexokinase activity in *Coxiella burnetii*. *J. Bacteriol.* 83, 538–543.

Parish, T., and Stoker, N. G. (2002). The common aromatic amino acid biosynthesis pathway is essential in *Mycobacterium tuberculosis*. *Microbiology* 148, 3069–3077. doi: 10.1099/00221287-148-10-3069

Pollegioni, L., Schonbrunn, E., and Siehl, D. (2011). Molecular basis of glyphosate resistance–different approaches through protein engineering. *FEBS J.* 278, 2753–2766. doi: 10.1111/j.1742-4658.2011.08214.x

Riddle, V., and Lorenz, F. (1973). Nonenzymic formation of toxic levels of methylglyoxal from glycerol and dihydroxyacetone in Ringer's phosphate suspensions of avian spermatozoa. *Biochem. Biophys. Res. Commun.* 50, 27–34. doi: 10.1016/0006-291X(73)91058-9

Romijn, J., Van Golde, L., McElhaney, R., and Van Deenen, L. (1972). Some studies on the fatty acid composition of total lipids and phosphatidylglycerol from *Acholeplasma laidlawii* B and their relation to the premeability of intact cells of this organism. *Biochimica et Biophysica Acta (BBA)-Lipids Lipid Metab.* 280, 22–32. doi: 10.1016/0005-2760(72)90209-3

Sales, M., De Freitas, O., Zucoloto, S., Okano, N., Padovan, G., Dos Santos, J., et al. (1995). Casein, hydrolyzed casein, and amino acids that simulate casein produce the same extent of mucosal adaptation to massive bowel resection in adult rats. *Am. J. Clin. Nutr.* 62, 87–92.

Sandoz, K. M., Beare, P. A., Cockrell, D. C., and Heinzen, R. A. (2016a). Complementation of arginine auxotrophy for genetic transformation of *Coxiella burnetii* by use of a defined axenic medium. *Appl. Environ. Microbiol.* 82, 3042–3051. doi: 10.1128/AEM.00261-16

Sandoz, K. M., Popham, D. L., Beare, P. A., Sturdevant, D. E., Hansen, B., Nair, V., et al. (2016b). Transcriptional profiling of *Coxiella burnetii* reveals extensive cell wall remodeling in the small cell variant developmental form. *PLoS ONE* 11:e0149957. doi: 10.1371/journal.pone.0149957

Schnappinger, D., Ehrt, S., Voskuil, M. I., Liu, Y., Mangan, J. A., Monahan, I. M., et al. (2003). Transcriptional adaptation of *Mycobacterium tuberculosis* within macrophages: insights into the phagosomal environment. *J. Exp. Med.* 198, 693–704. doi: 10.1084/jem.20030846

Schunder, E., Gillmaier, N., Kutzner, E., Eisenreich, W., Herrmann, V., Lautner, M., et al. (2014). Amino acid uptake and metabolism of *Legionella pneumophila* hosted by *Acanthamoeba castellanii*. *J. Biol. Chem.* 289, 21040–21054. doi: 10.1074/jbc.M114.570085

Segal, G. (2013). "The *Legionella pneumophila* two-component regulatory systems that participate in the regulation of Icm/Dot effectors," in *Molecular Mechanisms in Legionella Pathogenesis*, ed H. Hilbi (Munich: Max-von-Pettenkofer Institute), 35–52.

Seshadri, R., Paulsen, I. T., Eisen, J. A., Read, T. D., Nelson, K. E., Nelson, W. C., et al. (2003). Complete genome sequence of the Q-fever pathogen *Coxiella burnetii*. *Proc. Natl. Acad. Sci. U.S.A.* 100, 5455–5460. doi: 10.1073/pnas.0931379100

Tesh, M. J., and Miller, R. D. (1981). Amino acid requirements for *Legionella pneumophila* growth. *J. Clin. Microbiol.* 13, 865–869.

Tesh, M. J., Morse, S. A., and Miller, R. D. (1983). Intermediary metabolism in *Legionella pneumophila*: utilization of amino acids and other compounds as energy sources. *J. Bacteriol.* 154, 1104–1109.

Van Schaik, E. J., Chen, C., Mertens, K., Weber, M. M., and Samuel, J. E. (2013). Molecular pathogenesis of the obligate intracellular bacterium *Coxiella burnetii*. *Nat. Rev. Microbiol.* 11, 561–573. doi: 10.1038/nrmicro3049

Vianna, C. P., and De Azevedo, W. F. (2012). Identification of new potential *Mycobacterium tuberculosis* shikimate kinase inhibitors through molecular docking simulations. *J. Mol. Model.* 18, 755–764. doi: 10.1007/s00894-011-1113-5

Walter, M. C., Ohrman, C., Myrtennas, K., Sjodin, A., Bystrom, M., Larsson, P., et al. (2014). Genome sequence of *Coxiella burnetii* strain Namibia. *Stand. Genomic Sci.* 9:22. doi: 10.1186/1944-3277-9-22

Weber, M. M., Chen, C., Rowin, K., Mertens, K., Galvan, G., Zhi, H., et al. (2013). Identification of *Coxiella* type IV secretion substrates required for intracellular replication and *Coxiella*-containing vacuole formation. *J. Bacteriol.* 195, 3914–3924. doi: 10.1128/JB.00071-13

Zhao, Y., Wieman, H. L., Jacobs, S. R., and Rathmell, J. C. (2008). Mechanisms and methods in glucose metabolism and cell death. *Meth. Enzymol.* 442, 439–457. doi: 10.1016/S0076-6879(08)01422-5

Zhu, W., Banga, S., Tan, Y., Zheng, C., Stephenson, R., Gately, J., et al. (2011). Comprehensive identification of protein substrates of the Dot/Icm type IV transporter of *Legionella pneumophila*. *PLoS ONE* 6:e17638. doi: 10.1371/journal.pone.0017638

Zomorodipour, A., and Andersson, S. G. (1999). Obligate intracellular parasites: *Rickettsia prowazekii* and *Chlamydia trachomatis*. *FEBS Lett.* 452, 11–15. doi: 10.1016/S0014-5793(99)00563-3

100

_____

4   <u>DISCUSSION</u>

4.1   The bipartite metabolism of *L. pneumophila*

For a long time, the common opinion about the metabolic potential of *L. pneumophila* was, that this intracellular replicating pathogen is only capable of efficiently metabolizing amino acids. Indeed, amino acids and especially serine represent the preferred carbon and energy source (Pine *et al.*, 1979; George *et al.*, 1980; Tesh and Miller, 1981). However, labeling experiments proved the potential of *L. pneumophila* to efficiently use further carbon sources like glucose (Eylert *et al.*, 2010; Gillmaier *et al.*, 2016). Furthermore, the expression of *glpK* and *glpD* has been shown to be upregulated during intracellular replication of *L. pneumophila* in macrophages, indicating the usage of glycerol in the nutrition of this pathogen (Faucher *et al.*, 2011). In this study, detailed analysis of the metabolic potential of *L. pneumophila* JR32 was performed using different *in vitro* and *in vivo* experimental setups. Although glycerol did not support extracellular replication, labeling experiments using [U-^{13}C$_3$]glycerol in the newly developed MDM demonstrated that this substrate is indeed metabolized by this pathogen. Glycerol did furthermore support *in vivo* replication in *A. castellanii* and macrophages when added 4 h post infection and a *L. pneumophila glpD* deletion mutant was outcompeted during co-infection in amoeba with the wild-type. Furthermore, using extensive growth phase dependent *in vitro* and *in vivo* isotopologue profiling experiments with [U-^{13}C$_3$]glycerol, [U-^{13}C$_6$]glucose and [U-^{13}C$_3$]serine it was demonstrated that certain nutrients are serving distinct metabolic pathways in this pathogen. Thereby, the respective carbon fluxes are partitioned in a bipartite metabolic network, which could be a beneficial adaption strategy for the intracellular survival of *L. pneumophila*. This bipartite metabolism is divided into two modules. Module 1 comprises gluconeogenetic reactions, the PPP as well as reactions of the ED pathway. Although the PPP is incomplete in *L. pneumophila* since the oxidative branch (6-phophogluconate-dehydrogenase) as well as the transaldolase are missing, the non-oxidative part is still sufficient for carbohydrate conversion and supply of C5 sugars, which are essential precursors for histidine, purine and pyrimidine biosynthesis (Cazalet *et al.*, 2004; Chien *et al.*, 2004). Besides that, module 1 provides the precursors for cell wall biosynthesis as well as NADPH/H$^+$. In total this module represents the energy consuming anabolic part of *L. pneumophila* metabolism. On the other hand, module 2 represents the energy generating part since it comprises the lower part of glycolysis as well as reactions of the TCA cycle which

generate high amounts of ATP, NADH/H$^+$ and FADH$_2$. In this bipartite metabolism carbon flow from glycerol and glucose is predominantly directed towards gluconeogenetic reactions and the PPP (module 1) while serine is used for energy generation in module 2 (see section 3.1). Carbon flux is furthermore dependent on the developmental stage, since serine is extensively used during replication while glucose and glycerol are preferred substrates at later growth phases.

The concept of a modular metabolism has also been identified in further intracellular replicating pathogens like *Listeria monocytogenes* or *Mycobacterium tuberculosis*. Thus, this metabolic concept in which carbon flux derived from different carbon sources is predetermined, seems to be a general concept and could be beneficial in intracellular replication. However, there appears to be differences in the modulated carbon fluxes dependent on the respective replication niche of the pathogen. In contrast to *L. pneumophila*, glycerol is efficiently used for energy generation in *L. monocytogenes,* a pathogen which replicates in the cytosolic compartment (Schneebeli and Egli, 2013). In contrast to *Legionella*, *L. monocytogenes* is able to grow on glucose and glycerol as sole carbon source, whereas labeling experiments showed incorporation of amino acids but only usage for protein biosynthesis and not in catabolic reactions, as it is the case for *L. pneumophila* (Eylert *et al.*, 2010; Schneebeli and Egli, 2013; Grubmüller *et al.*, 2014). However, similar to the bipartite metabolism observed in *L. pneumophila*, carbohydrates like Glu-6-P are shuffled into the PPP (module1) (Grubmüller *et al.*, 2014). The modulated metabolism of *M. tuberculosis* also shows high carbon fluxes from glucose into module 1 (PPP and early steps of the glycolytic pathway). Like *L. monocytogenes, M. tuberculosis* also incorporates amino acids from the host but only uses them directly for protein biosynthesis. In contrast, acetate represents the main carbon source for energy generation in module 2 (TCA cycle). Dependent on the co-substrate, carbon flux from glycerol occurs towards module 1 (in presence of glucose) or module 2 (in presence of acetate) (de Carvalho *et al.*, 2010; Beste *et al.*, 2013)

In *L. pneumophila*, glycerol seems to play only a minor role in the nutrition of this pathogen, since lowest ^{13}C-enrichment values were obtained in the experiments with ^{13}C-glycerol and only at later growth phases. However, it seems to be important at later developmental stages, when the bacteria develop into its transmissive form. This is triggered by nutrient starvation,

_____

in particular limited amino acids concentration, inside the host. In its virulent transmissive form, this pathogen is flagellated and probably capable of lysing the LCV and host cell membranes, which could result in an increased excess to glycerol as an alternative carbon source at later growth phases. Furthermore, *in vivo* labeling experiments performed in this study using ^{13}C-glycerol proofed that this substrate reaches the LCV and directly serves Man formation. However, the genome of *L. pneumophila* only reveals a glycerol 3-phosphate transporter (GlpT), indicating that rather glycerol 3-phosphate (G3P) than glycerol is used *in vivo* (Cazalet *et al.*, 2004; Chien *et al.*, 2004). An eukaryotic GlpK (NP_997609) from experiments with RAW 264.7 macrophages has been identified in proteome analysis of purified LCV, indicating that glycerol which could reach the host cytosol by diffusion is phosphorylated and subsequently transported into the LCV (Hoffmann *et al.*, 2014b). The importance of glycerol as an *in vivo* substrate was also shown when a *L. pneumophila* ΔglpD mutant was outcompeted during coinfection with the wild-type in *A. castellanii*. Since, this substrate is almost exclusively used in gluconeogenetic reactions and in the PPP during *in vivo* as well as *in vivo* replication, this also underlines the importance of these biosynthetic routes and effective carbon flux into these pathways during late stages of infection. This study proofs that the gluconeogenetic pathway is active in *L. pneumophila* although a homologue of a fructose 1,6-bisphosphatase has not been found in the *Legionella* spp. and only a phosphofructokinase has been annotated (Chien *et al.*, 2004; Cazalet *et al.*, 2010). Nevertheless, this enzyme could favor gluconeogenetic reactions since fructose 1,6-bisphosphatase activity has been determined as 10-fold higher than phosphofructokinase activity (Keen and Hoffman, 1984). Furthermore, the annotated phosphofructokinase in *L. pneumophila (lpd1913; pfkA)* shows homology to bacterial and eukaryotic ones, which are pyrophosphate dependent and reversible PfkA enzymes. Therefore, this annotated phosphofructokinase could possibly catalyze reactions in both directions.

4.2 CsrA dependent regulation of the bipartite metabolism in *L. pneumophila*

Performing comparative metabolic analysis with the *L. pneumophila* Paris wild-type and the respective CsrA knock down mutant, the regulatory role of CsrA has been investigated in this work. The *csrA* mutant used in this study has been characterized in a previous study. Thereby extensive transcriptome and proteome analysis in combination with RNA-Co-

immunoprecipitation experiments were performed, followed by deep sequencing of the wild-type and its *csrA* mutant (Sahr *et al.*, 2017). Most importantly, this mutant is characterized by a transmissive phenotype, which appears already during exponential growth. Additionally, the CsrA knock down affected numerous enzymes involved in serine metabolism, the preferred carbon and energy source of *L. pneumophila* during replication (George *et al.*, 1980; Tesh *et al.*, 1983). Particularly, the putative serine transporter (*lpp2269*) and the serine dehydratase (*lpp0854*) as well as numerous enzymes involved in pyruvate metabolism and in the TCA cycle were downregulated on transcriptome and/or proteome level during E phase dependent on the CsrA knock down (Sahr *et al.*, 2017) (**Figure 5-5**). This indicated a reduced metabolism of serine in the *csrA* mutant which was confirmed in oxygen consumption experiments performed in this work. Determination of OCR revealed a downregulated bacterial respiration when serine was added to the *L. pneumophila csrA* mutant. CsrA is therefore crucial for the wild-type, since it clearly enhances serine uptake and metabolism and therefore energy supply during replication of this pathogen. The regulation of serine metabolism by CsrA furthermore affects the bipartite metabolism in *L. pneumophila*. In both bacterial strains, carbon flux from serine predominantly occurred towards the TCA cycle for energy generation during exponential growth (**Figure 3-4**). However, carbon flux from serine was even more restricted to module 2 of metabolism in the *csrA* mutant while simultaneously carbon flux into module 2 was reduced (**Figure 4-1**). However, since it was observed that bacterial respiration is in general reduced in this mutant (**Figure 3-1**), serine is more likely used to form metabolic intermediates instead of energy production. To sum this up, serine metabolism is downregulated dependent on the CsrA knock down, whereas carbon flux is even more restricted to the TCA cycle in the *csrA* mutant (**Figure 4-1**).

In contrast to the experiments with ^{13}C-serine, comparative isotopologue analysis using [U-^{13}C$_6$]glucose with the *L. pneumophila* wild-type and its *csrA* mutant showed a reduced carbon flux into the energy generating part of metabolism. On the other hand, usage of glucose in gluconeogenetic reactions and in the PPP was not affected in absence of CsrA (**Figure 3-4**). Effects of the CsrA knock down were investigated on a transcriptome and proteome level in combination with RNA-Co-immunoprecipitation and revealed numerous affected genes in the ED pathway, glycolysis and in glucose incorporation in the *csrA* mutant (Sahr *et al.*, 2017) (**Figure 5-6**). These data revealed that in presence of CsrA the putative glucose transporter

_____

(Lpp0488), which was identified as direct target of CsrA, is downregulated during exponential growth on protein level. Simultaneously, enzymes related to glucose metabolism were positively affected in presence of CsrA. In detail, all genes of the ED pathway (*lpp0483, lpp0484, lpp0485,* and *lpp0487*) where downregulated on transcriptome level in the *csrA* mutant, whereas *lpp0483, lpp0484* and *lpp0485* could additionally be identified as direct targets of CsrA. Also all enzymes of the second part of glycolysis (*lpp0535, lpp2838, lpp0153, lpp0152, lpp2020,* and *lpp0151*) have shown to be directly targeted by this post-transcriptional regulator, but only *lpp2838* was additionally reduced on transcriptome level. Same was true for one enzyme of the PPP (*lpp0108*) during E phase in the *csrA* mutant (Sahr *et al.*, 2017) (**Figure 5-6**). The fact that glucose is more preferred as a substrate at later growth phases in *L. pneumophila* wild-type (see section 3.1) might be related to the negative effect of CsrA on glucose incorporation, since high concentrations of CsrA are present in the bacteria during replication. On the other hand, CsrA levels are reduced at transmissive stage due to binding of this global regulator to small non-coding sRNAs Rsm X, Y, Z, which are built as a result of low nutrient conditions. This also leads to a reduced carbon flux directed towards module 2, since the positive effects of CsrA on biosynthetic pathways responsible for glucose catabolism (ED pathway, glycolysis, PPP) are reduced. However, at the same time also the reductive effect of CsrA on glucose uptake is reduced at PE phase.

Interestingly, the operon *lpp0151-lpp0154* comprises three genes of the second part of the glycolytic cascade (glyceraldehyde 3-phoshate, phosphoglycerate kinase, pyruvate kinase) and additionally the transketolase enzyme of the PPP (**Figure 5-6**). Furthermore, this operon has been identified as a direct target of CsrA, which induces the transcription level of the three glycolytic enzymes by simultaneously not affecting transcription levels of the transketolase enzyme (Sahr *et al.*, 2017). CsrA therefore enhances the carbon flux from glucose into module 1 in *L. pneumophila* wild-type during replication but it also represses the uptake of glucose at the same time. In contrast, the amount of pyruvate derived from glucose degradation *via* GAP is reduced in the *csrA* mutant. However, GAP derived from glucose is still shuffled into reactions of the PPP in same amounts as in the wild-type. Therefore, this operon seems to be a key target of CsrA in the regulation of metabolic fluxes in the bipartite metabolism of *L. pneumophila*. This is also in agreement with the isotopologue analysis of *L. pneumophila* wild-type and its *csrA* mutant. Unchanged or slightly induced ^{13}C-enrichment values in His (PPP)

or sugars (gluconeogenesis) in contrast to reduced ^{13}C-lable in pyruvate (Ala) or TCA cycle related metabolites (Glu) in absence of CsrA supports the idea that glucose uptake is induced in the *csrA* mutant but the amount of GAP build from glucose degradation is more efficiently shuffled into reactions of the PPP by the transketolase (direct usage of GAP) which is not affected by CsrA. Carbon flux into the TCA cycle is reduced due to the missing inductive effect of CsrA on pyruvate biosynthesis from GAP (Sahr *et al.*, 2017). Since this does surely also affect reactions in the opposite gluconeogenetic direction (biosynthesis of glyceraldehyde 3-phophate from pyruvate), carbon flux from serine into the upper part of metabolism is reduced, which was demonstrated by the labeling experiments with [U-^{13}C$_3$]serine. This again emphasizes the crucial role of the CsrA regulation of the operon *lpp0151-lpp0154* in the growth phase dependent adjustment of carbon fluxes from different substrates.

The CsrA knock down in *L. pneumophila* dramatically affected the metabolism of glycerol. Comparative labeling experiments with the wild-type and the *csrA* mutant using [U-^{13}C$_3$]glycerol revealed dramatically induced ^{13}C-incorporation levels in marker metabolites leading to ^{13}C-excess values in the *csrA* mutant which were more than twice as high as in the wild-type. This clearly shows that in absence of CsrA glycerol metabolism is dramatically upregulated. A growth phase dependent metabolism of glycerol was already observed in labeling experiments with the *L. pneumophila* wild-type (see section 3.1). Labeling experiments with the *csrA* mutant now elucidate the crucial role of CsrA in glycerol metabolism dependent on the respective developmental stage. This is furthermore supported by comparative proteome analysis of the *L. pneumophila* wild-type and the *csrA* mutant during E phase, since the amount of the GlpK enzyme (Lpp1369) has shown to be significantly upregulated dependent on the CsrA knock down (**Figure 5-6**) (Sahr *et al.*, 2017). This emerges the role of CsrA as a repressor of glycerol metabolism during the replicative phase in the *L. pneumophila* wild-type. Since the amount of CsrA is reduced in the bacteria at later stages, this effect decreases. This agrees with the low ^{13}C-incorporation rates derived from [U-^{13}C$_3$]glycerol during replication and the increased carbon flux at transmissive stage in the wild-type. Since the *csrA* mutant already shows a transmissive phenotype during exponential growth due to lower amounts of CsrA, the amount of GlpK is probably already upregulated at early developmental stages leading to a dramatically increased carbon flux derived from glycerol. Furthermore, ^{13}C flux into the TCA cycle slightly increased in the *csrA* mutant due to the

_____

dramatically upregulated incorporation and metabolism of [U-^{13}C$_3$]glycerol. However, simultaneously the carbon flux from this substrate was even more restricted to module 1 (PPP, ED pathway, gluconeogenesis) in absence of CsrA (**Figure 3-4**). This effect might be related to the reduced biosynthesis of pyruvate from GAP in absence of CsrA, due to the missing induction of the three glycolytic enzymes in the operon *lpp0151-lpp0154*. At the same time, carbon flux into gluconeogenetic reactions and into the PPP (directly *via* GAP) is not affected (**Figure 5-6**).
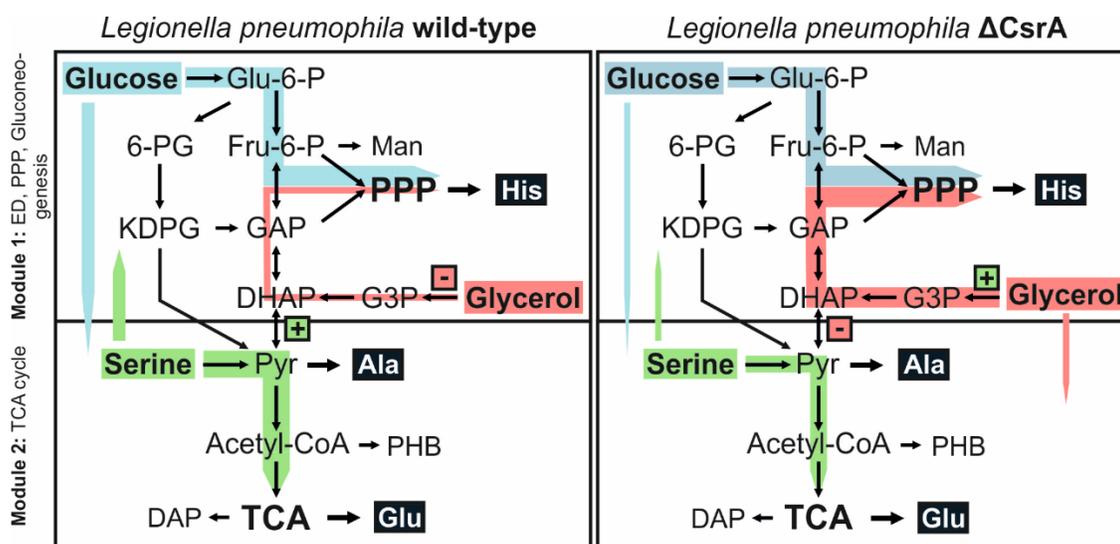
Figure 4-1: Regulation of core metabolic fluxes by CsrA in the bipartite metabolism in *L. pneumophila* Paris. The bipartite metabolism comprises two modules. Module 1 includes reactions of the ED pathway, glycolytic and gluconeogenetic reactions as well as the PPP. Module comprises the TCA cycle. Main carbon fluxes are indicated in coloured arrows (blue: glucose; red: glycerol; green: serine). The left side illustrates carbon fluxes in the *L. pneumophila* wild-type whereas the right side represents the main carbon fluxes in the *csrA* mutant. In both strains, serine is used in the second module (TCA cycle) for energy generation, although carbon flux is partly reduced in the *csrA* mutant. In addition, serine usage in module 1 is also lowered dependent on CsrA. In contrast to serine metabolism, carbon flux from glucose is predominantly directed towards module 1 and only partly towards energy generation. The carbon flux from glucose into module 2 was reduced in the *csrA* mutant, whereas no differences could be observed in the carbon flux directed towards module 1. Glycerol metabolism was very low in the *L. pneumophila* wild type and almost exclusively restricted to module 1. In contrast, carbon flux from glycerol was dramatically increased in the *csrA* strain and did also partly occur towards module 2, although the main carbon flux was still directed towards the first module of metabolism. Up- or downregulated enzymes dependent on CsrA are indicated in framed plus [+] or minus [-] sings. CsrA induces glycolytic enzymes (lpp0151, lpp0152, lpp0153) by simultaneously downregulating enzymes related to glycerol metabolism (lpp1369) in th*e L. pneumophila* wild-type. Abbreviations: Glu-6-P, glucose 6-phosphate; Fru-6-P, fructose 6-phosphate; 6-PG, 6-phosphogluconate; KDPG, 2-keto-3-desoxy-phosphogluconate; GAP, Glyceraldehyde 3-phosphate; DHAP, Dihydroxyacetone phosphate; G3P, Glycerol 3-phosphate; Pyr, pyruvate; PPP, pentose phosphate pathway; PHB, polyhydroxybutyrate; DAP, diaminopimelate; Man, mannose; ED pathway, Entner-Doudoroff pathway; TCA, tricarboxylic acid cycle.

In summary, these data highlight the crucial role of CsrA in the life stage specific metabolism of *L. pneumophila* besides its well-known function as a central regulator of the developmental switch in the biphasic life cycle of this intracellular pathogen. During replication, CsrA induces the uptake and metabolism of serine, the main carbon and energy source of *L. pneumophila* (George *et al.*, 1980; Tesh and Miller, 1981), thereby ensuring a sufficient nutrient supply into the TCA cycle for effective energy generation and therefore intracellular replication. At later developmental stages, if favored nutrients are getting limited, CsrA induces the uptake and metabolism of alternative carbon sources like glucose but especially glycerol. At the same time carbon flux from these substrates into the TCA cycle is reduced by CsrA, whereas their usage in anabolic processes is enhanced. This key regulatory role of CsrA in the bipartite metabolism of *L. pneumophila* is thereby predominantly related to its regulation of the operon *lpp0151-lpp0154*, which comprises three glycolytic enzymes at the interface of module 1 and module 2 (**Figure 4-1**).

Such a regulatory role of the CsrA-system on metabolic processes in a growth phase dependent manner has also been reported for *E. coli*. Early studies revealed that in this pathogen, biosynthesis of glycogen is inhibited during exponential growth (Romeo *et al.*, 1993; Yang *et al.*, 1996). Further investigations in this bacterium identified CsrA as a global director of carbon flux derived from glucose since it activates carbon flow into glycolytic reactions by simultaneously repressing the gluconeogenetic pathway (Sabnis *et al.*, 1995; Romeo, 1998). Recent experiments with numerous CsrA related mutant strains using *E. coli* Nissle 1917 clearly identified CsrA as the only crucial regulator in carbon nutrition in this pathogen. This study also confirmed previous results, since a Δ*csrA51* mutant strain comprising reduced amounts of this regulator showed a downregulation in carbon flux from glucose directed towards glycolytic reactions and oxidative metabolism (Revelles *et al.*, 2013). This agrees with the previously reported inductive effect of CsrA on glycolysis in *E. coli* (Sabnis *et al.*, 1995; Romeo, 1998). However, this Δ*csrA51* mutant also showed significant growth defects while growing on further carbon sources like *e.g.* acetate, emphasizing the central role of this post-transcriptional regulator in nutrient utilization. Moreover, acetate was shown to additionally inhibit the growth of an *E. coil csrA* mutant in rich media (Wei *et al.*, 2000; Revelles *et al.*, 2013). However, although no enzyme of the ED pathway has been identified yet as a direct target of CsrA in *E. coli*, the respective *csrA* mutant showed significant growth defects on

_____

compounds which are utilized by this pathway (Murray and Conway, 2005; Revelles *et al.*, 2013). The influence of this post-transcriptional regulator on the ED pathway is furthermore emphasized by the observation that this route is predominantly used in the Δ*csrA51* mutant for gluconate catabolism (Revelles *et al.*, 2013). Taken together, CsrA is identified as the global regulator in carbon metabolism in *E. coli* although direct targets of CsrA related to biosynthetic processes are widely unknown in this pathogen, except of glycolytic and gluconeogenetic targets as well as some identified targets in the TCA cycle and glycolate shunt (Wei *et al.*, 2000; Edwards *et al.*, 2011; Revelles *et al.*, 2013; Morin *et al.*, 2016).

Besides *E. coli*, the influence of CsrA on core metabolic processes has been investigated in further pathogenic bacteria like *Campylobacter jejuni* or *Pseudomonas aeruginosa*. Experiments with *C. jejuni* wild-type and a *csrA* mutant using comparative proteome analysis revealed, besides induced expressions of virulence related proteins, also differential expression levels of numerous enzymes, which are involved to core metabolic processes e.g. amino acid metabolism of TCA cycle related enzymes (Fields *et al.*, 2016). Transcriptome studies in *P. aeruginosa* identified an enzyme involved in the methylglyoxal detoxification process as a direct target of CsrA/RsmA in this pathogen. Furthermore, using a sequence-based prediction approach several direct targets of this global regulator have been identified in *P. aeruginosa*, including an enzyme of the gluconeogenetic cascade (Kulkarni *et al.*, 2014).

In *Yersinia pseudotuberculosis*, an ancestor of *Yersinia pestis*, ^{13}C-fluxome experiments with the wild-type and various mutants concerning specific virulence factors including CsrA were recently performed. When this pathogen was grown on glucose as sole carbon source high conversion rates of this substrate into pyruvate have been detected for the wild-type. This rate was even higher in the respective *csrA* mutant (13% increase), which showed a reduction of 56% in growth and substrate uptake. Simultaneously, the amount of all other detected by-products was reduced. Interestingly, the TCA cycle was upregulated in absence of CsrA by 10 % in *Y. pseudotuberculosis* whereas the PPP was downregulated in the *csrA* mutant. This indicates a repressive effect of CsrA on carbon flux into the TCA cycle but an inductive effect on reactions in the PPP at the same time (Bücker *et al.*, 2014). This metabolic concept seems to be contrarious to the regulatory concept of CsrA present in *L. pneumophila* (**Figure 4-1**). However, these different regulatory concepts controlled by CsrA emphasizes its global role in

the metabolic adaption of different bacteria to enable efficient nutrient supply in their respective environmental niches and growth phase. In case of intracellular pathogens, this also involves the adaption on the host metabolism. Since this post-transcriptional regulator also controls virulence traits in bacteria, there could also be a direct link to the pathogenicity dependent on metabolic processes in the respective organism. In total, the very specific "pathometabolism" of the respective bacteria is probably partly a result of adaptive evolutionary processes of the CsrA-regulatory system dependent on the different environments (Eisenreich *et al.*, 2015; Vakulskas *et al.*, 2015; Van Assche *et al.*, 2015).

4.3 Growth phase dependent carbon flux derived from fatty acid degradation in *L. pneumophila*

In this study the effective degradation and carbon flux into core metabolic processes derived from a fatty acid was show for the first time in *L. pneumophila*, identifying this substrate as a nutrient of this intracellular pathogen. Labeling experiments using [1,2,3,4-^{13}C$_4$]palmitic acid revealed that this long-chain fatty acid predominantly serves the biosynthesis of PHB (see section 3.2.3). This carbon and energy storage compound is crucial for the long-term survival of this pathogen and is predominantly built at later developmental stages (James *et al.*, 1999; Garduno *et al.*, 2002; Al-Bana *et al.*, 2014). The fact that ß-oxidation and formation of PHB is metabolically linked was already investigated in further bacteria like *Pseudomonas putida* (Huijberts *et al.*, 1994) and was assumed to be present in *L. pneumophila* recently (Eisenreich and Heuner, 2016). Furthermore, this pathogen also features numerous phospholipases, which have been partly characterized as virulence factors. Since they are predominantly expressed at later growth phases, metabolisation of fatty acids could be linked to later developmental stages of *L. pneumophila* (Flieger *et al.*, 2000; Flieger *et al.*, 2004; Schunder *et al.*, 2010). A link between the development of virulence trains and fatty acid degradation is furthermore emphasized by the fact that short-chain fatty acids are triggering the switch from replication to the transmissive virulent stage (Edwards *et al.*, 2009). Additionally, lipolytic activities have also been detected for *L. pneumophila* cell-associated enzymes, indicating that host-membrane-lysis could be a key virulence factor of this intracellular pathogen (Bender *et al.*, 2009). The high phospholipolytic potential is furthermore linked to Legionnaires disease development in the patient (Kuhle and Flieger, 2013). Thereby, the major lipolytic activity of *L. pneumophila* is related to the cell-associated hemolytic phospholipase A (PlaB), which

_____

preferably hydrolyzes long-chain fatty acids with more than twelve carbon atoms (Bender *et al.*, 2009). In summary, this could indicate that this pathogen lyses the host cell membranes at transmissive virulent stage and could subsequently use the released cell-wall derived substrates (fatty acids and glycerol) as nutrients and for PHB biosynthesis. A coordination of nutrient usage for PHB biosynthesis dependent on the developmental stage has been reported recently based on labeling experiments (Gillmaier *et al.*, 2016) and supports the idea of and increased carbon supply from fatty acids into PHB biosynthesis at later growth phases.

This hypothesis was investigated using oxygen consumption experiments as well as labeling experiments with the *csrA* mutant in comparison to the *L. pneumophila* wild-type. Thereby, the OCR of the wild-type indicated the usage of palmitic acid as well as of butanoate already in the aerobic respiration during exponential growth. Since contrarious results were obtained during the experiments with the CsrA knock down mutant, a positive effect of this regulator on the uptake and metabolism of fatty acids was implicated. However, proteome and transcriptome data as well as comparative labeling experiments with [1,2,3,4-^{13}C$_4$]palmitic acid revealed a more complex role of CsrA in the metabolism of fatty acids especially concerning the preferred usage for the biosynthesis of PHB dependent on the developmental stage of this pathogen (Brüggemann *et al.*, 2006; Sahr *et al.*, 2017). It was shown that enzymes responsible for the formation of this carbon and energy storage compound are upregulated during post-exponential growth of *L. pneumophila* (Hindre *et al.*, 2008; Hayashi *et al.*, 2010). A crucial role of CsrA in the regulation of these enzymes was demonstrated recently using proteome and transcriptome analysis. Particularly, this post-transcriptional regulator negatively affected the acetoacetyl-CoA reductase genes *lpp0620, lpp0621* and *lpp2322* on transcriptome (except of *lpp0620*) and proteome level whereas *lpp0620* and *lpp2322* and a polyhydroxyalkanoate synthase (*lpp2038*) could additionally be identified as direct targets of CsrA in *L. pneumophila* (Brüggemann *et al.*, 2006; Sahr *et al.*, 2017) (**Figure 5-7**). This indicates that CsrA is crucial for the growth phase dependent formation of PHB, since it inhibits its biosynthesis during replication whereas the respective enzymes seem to be upregulated in absence of CsrA.
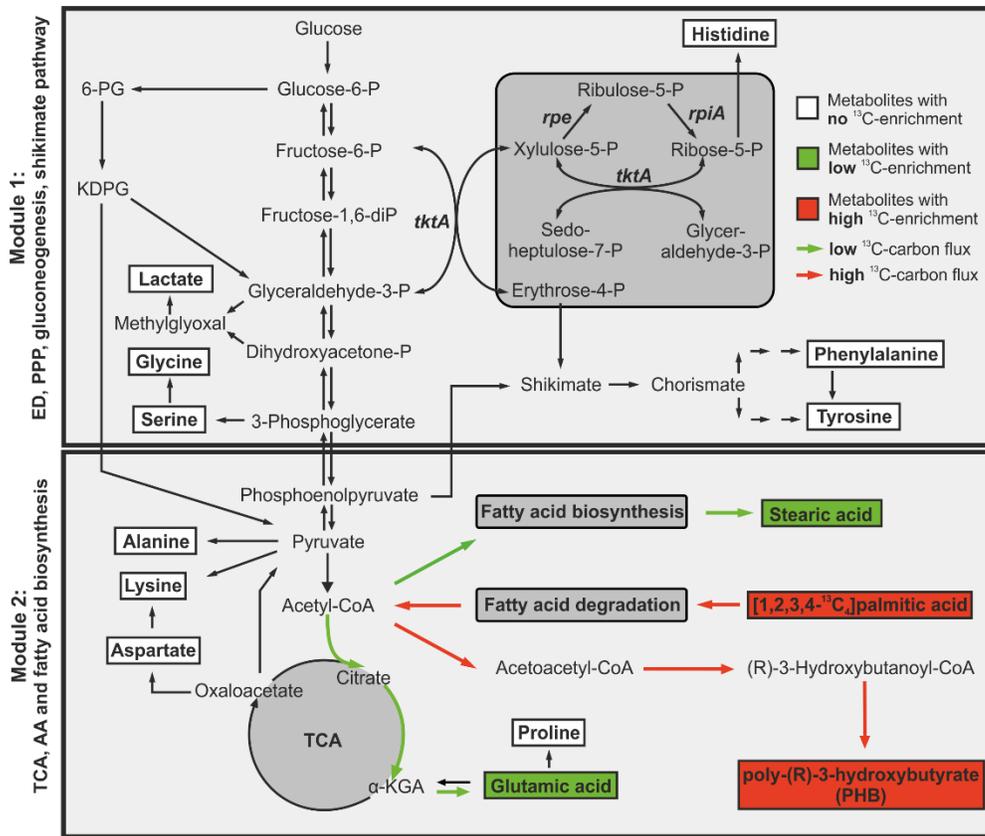
Figure 4-2: Carbon fluxes derived from palmitic acid degradation in *L. pneumophila*. Acetyl-CoA derived from palmitic acid degradation is almost exclusively shuffled into module 2 in both strains. Thereby, this substrate predominantly serves for PHB biosynthesis (red arrows and framed metabolites). In the *csrA* mutant a minor carbon flux into the TCA cycle was also detectable (green arrows and framed metabolites).

Using a Co-immunoprecipitation approach, it was furthermore demonstrated that most of the respective enzymes involved in PHB biosynthesis are indeed directly targeted by CsrA. This also applies for a long-chain fatty acid transporter (*lpp1773*), emphasizing the link between PHB formation and fatty acid metabolism (Sahr *et al.*, 2017). A coordinative role of CsrA in the growth phase dependent usage of acetyl-CoA derived from fatty acid degradation was also demonstrated in the labeling experiments using [1,2,3,4-^{13}C$_4$]palmitic acid which revealed increased ^{13}C-label in PHB in the experiments with the *csrA* mutant (**Figure 4-2**).

In summary, these data show for the first time the effective usage of palmitic acid by *L. pneumophila*. Thereby, carbon flux from this substrate predominantly served PHB biosynthesis. The crucial coordinative role of CsrA in the growth phase dependent PHB formation and fatty acid degradation was elucidated using a CsrA knock down mutant. Thereby, this post-transcriptional regulator represses the biosynthesis of PHB during

_____

replication. At later developmental stages carbon flux from fatty acid degradation into PHB biosynthesis is induced, since the amount of CsrA is reduced due to the binding on sRNA Rsm X, Y, Z. This leads to an increased incorporation of fatty acids by a simultaneously upregulated PHB production.

4.4 The bipartite metabolic topology in *C. burnetii*

Performing *in vitro* labeling experiments with the *C. burnetii* RSA 439 NMII strain in a recently developed axenic growth medium using [U-^{13}C$_3$]serine, [U-^{13}C$_6$]glucose and [U-^{13}C$_3$]glycerol as tracers, a bipartite metabolic network could be identified in this intracellular pathogen, resembling the topology of its close relative *L. pneumophila* (Omsland *et al.*, 2009; Omsland *et al.*, 2011). Nevertheless, the metabolic concepts also showed some differences. In both pathogens, serine served as main carbon and energy source, which is efficiently shuffled into the TCA cycle (module 2 of metabolism). However, while serine represents the main substrate in the nutrition of *L. pneumophila*, it is not metabolized in as high rates by *C. burnetii*. In addition, carbon derived from serine degradation was almost exclusively used in reactions of the TCA cycle in *C. burnetii,* while *L. pneumophila* additionally uses serine to feed the first module of metabolism (gluconeogenetic reactions, ED pathway, glycolysis, PPP) besides the high carbon flux from serine into module 2 (TCA cycle). Glucose on the other hand, is mainly shuffled into the first module in both pathogens. However, the metabolic concept of this first module differs since *L. pneumophila* uses reactions of the ED pathway for glucose degradation while *C. burnetii* uses the glycolytic pathway (McDonald and Mallavia, 1971; Seshadri *et al.*, 2003; Eylert *et al.*, 2010). Furthermore, glucose is metabolized in higher rates by *C. burnetii* and is additionally shuffled into reactions of the TCA cycle, whereas carbon flux from glucose is more restricted towards the upper part of metabolism in *L. pneumophila*. Interestingly, *C. burnetii* shows higher metabolic potential since it is also capable of using this compound for tyrosine biosynthesis *via* reactions of the shikimate/chorismate pathway. The usage of glycerol is very low in case of *L. pneumophila* and only occurs at later developmental stages of this pathogen. Thereby, carbon flux is restricted to gluconeogenetic reactions and the PPP. In contrast, glycerol is efficiently metabolized by *C. burnetii* but also used in the upper part of metabolism as a precursor for cell wall biosynthesis in gluconeogenetic reaction as well as *via* PEP serving the biosynthesis of DAP. In addition, carbon flux from this substrate also occurred into the shikimate/chorismate pathway for the biosynthesis of tyrosine in *C. burnetii*. In

summary, carbohydrates like glucose and glycerol are more important for the nutritional concept of *C. burnetii* than for *L. pneumophila*. In case of glucose this could be related to the slower growth of *C. burnetii,* which could in consequence limit the metabolic stress on the host cell, since glucose concentrations are directly linked to apoptosis (Zhao *et al.*, 2008). Since amino acids are present in high amounts in the host, they are used as major carbon and energy supply in both intracellular pathogens. In total, the general concept of multi-substrate usage in a bipartite metabolic network, which was identified for *L. pneumophila*, seems to be also valid for *C. burnetii*. This emphasizes the idea that this concept might be beneficial for the robustness and survival of intracellular pathogens in general.

4.5 Outlook

The observation that intracellular pathogens feature a bipartite metabolic topology, where serine is used for energy generation but glucose and glycerol preferably for gluconeogenesis and the PPP, might be a procedure of these pathogens to use carbon supply from the host by simultaneously avoiding host cell damage and the activation of defense mechanisms. This knowledge helps to better understand the complex interaction processes of these two antagonists. The extended knowledge about the metabolic network in the intracellular pathogens *L. pneumophila* and *C. burnetii* could furthermore help to identify novel drug targets. In case of *L. pneumophila* the ED pathway attracted some attention since this pathway is not present in mammalian cells but important for intracellular replication of this pathogen (Harada *et al.*, 2010). Also, the *glpD* deletion mutant showed significant intracellular growth defects, emphasizing the role of glycerol as a substrate and highlight the respective catabolic pathway as potential target. In case of *C. burnetii*, it was demonstrated that the shikimate/chorismate pathway is active and used for tyrosine biosynthesis. Since this biosynthetic route is also not present in mammalian cells it represents a further potential drug target for this pathogen. This idea is supported by the observation that respective mutants of *C. burnetii* concerning enzymes of this biosynthetic pathway (the type-II EPSP synthase CBU0526 or the shikimate dehydrogenase CBU0010) show a significant phenotype (Martinez *et al.*, 2014) (and unpublished data). Interestingly *L. pneumophila* deletion mutants concerning the two enzymes (AroB and AroE) of the shikimate pathway also showed defects in infection of human macrophages and intracellular replication demonstrating the dependence of this pathogen on this biosynthetic pathway, although it did not show *de novo* biosynthesis of

_____

aromatic amino acids in this study (Jones *et al.*, 2015). Similar results were also observed with further pathogens like *Mycobacterium tuberculosis* and *Helicobacter pylori* (Parish and Stoker, 2002; Ducati *et al.*, 2007; Vianna and de Azevedo, 2012; Blanco *et al.*, 2013). This emphasizes the role of metabolic pathway in general as potential drug targets, which should be focused on in future researched to develop new antibiotics. To achieve this goal, global knowledge of the bacterial metabolism and particularly concerning the interplay and adaption to the host is crucial and requires further studies including *in vivo* labeling experiments to its fully understanding.

5   <u>SUPPLEMENTARY MATERIAL</u>

5.1   Supplementary Material: Pathway analysis using ^{13}C-glycerol and other carbon tracers reveals a bipartite metabolism of *Legionella pneumophila*

Häuslein, I.[#], Manske, C.[#], Goebel, W., Eisenreich W.[†], and Hilbi, H.[†] (**2015**). *Molecular microbiology* 100**,** 229-246.

Supporting Information

Pathway analysis using ^{13}C-glycerol and other carbon tracers

reveals a bipartite metabolism of *Legionella pneumophila*

Ina Häuslein[1#,] Christian Manske[2#], Werner Goebel[2], Wolfgang Eisenreich[1]* and Hubert Hilbi[2,3]*

[1] *Lehrstuhl für Biochemie, Technische Universität München, Munich, Germany*

[2] *Max von Pettenkofer Institut, Ludwig-Maximilians Universität, Munich, Germany*

[3] *Institute of Medical Microbiology, University of Zürich, Switzerland*

[#] These authors contributed equally to the work.

Running title: Bipartite metabolism of *L. pneumophila*

Key words: amoeba, *Legionella*, isotopologue profiling, macrophage, metabolism, nutrition, pathogen vacuole, type IV secretion

*Address correspondence to Wolfgang Eisenreich, Lichtenbergstrasse 4, 85747 Garching, Germany, Tel +49-89-289-13336, Fax +49-89-289-13363, e-mail wolfgang.eisenreich@ch.tum.de; or Hubert Hilbi, Gloriastrasse 30, 8006 Zürich, Switzerland, Tel +41-44-634-2650, Fax +41-44-634-4906, e-mail hilbi@imm.uzh.ch

Figure S1
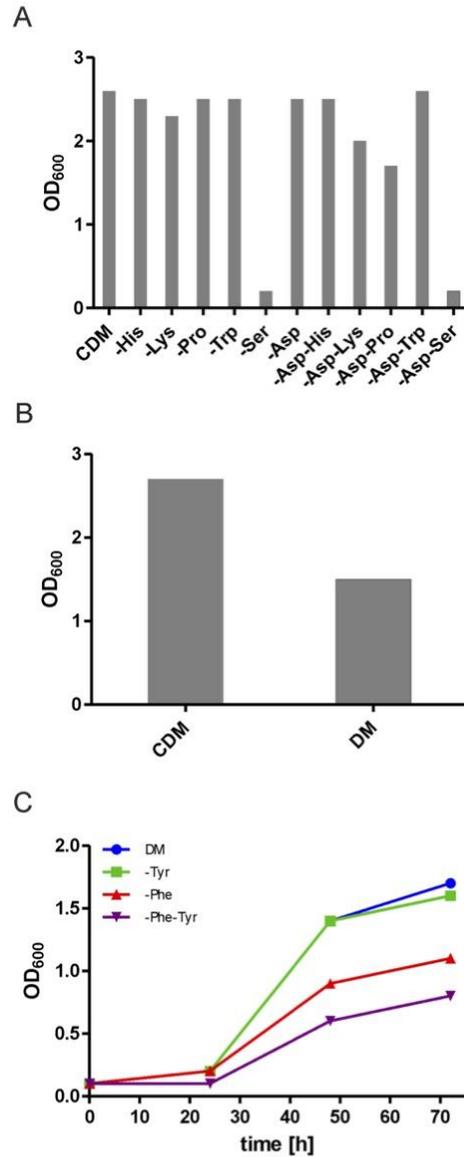
Figure S1. Development of a new chemically defined *Legionella* growth medium. *L. pneumophila* was grown in CDM or CDM depleted of single amino acids or pairs of amino acids with a starting OD_{600} of 0.1. (**A**) After 48 h, optical density was measured. (**B**) After 72 h, growth was compared in CDM and DM (defined medium) lacking His, Lys, Asp, Trp and Glu. (**C**) Growth curve comparison of *L. pneumophila* growing in DM or in DM lacking Tyr, Phe or Tyr and Phe.

Figure S2
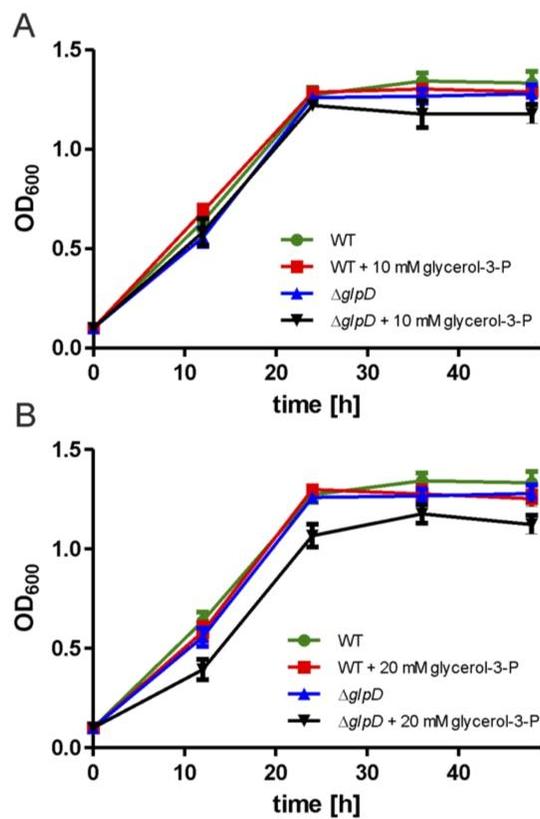
Figure S2. Extracellular growth *of L. pneumophila* with glycerol-3-phosphate. Extracellular growth of *L. pneumophila* wild-type and mutant Δ*glpD* in MDM with and without (**A**) 10 mM or (**B**) 20 mM glycerol-3-phosphate. Optical density at 600 nm was determined at the time points indicated. Mean and SD of triplicates are shown.

Figure S3
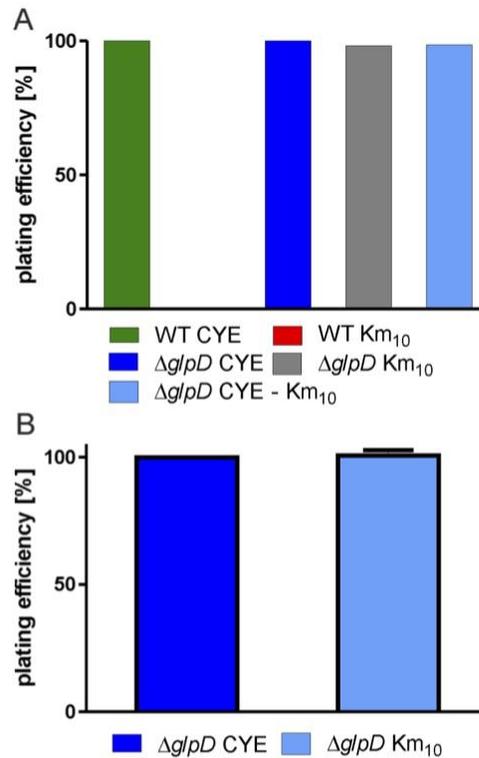
Figure S3. Plating efficiency of *L. pneumophila* Δ*glpD*. (**A**) *L. pneumophila* wild-type (WT) or mutant Δ*glpD* were grown in AYE overnight and then plated on CYE plates or CYE plates containing 10 µg/ml kanamycin (Km$_{10}$). In addition, colonies of Δ*glpD* grown on CYE were transferred to CYE/Km$_{10}$ plates. The plating efficiency [%] was determined for all strains and conditions. (**B**) *A. castellanii* was infected with *L. pneumophila* Δ*glpD* (MOI = 0.01) and incubated for 3 days. Cells were lysed with 0.8 % saponin and aliquots were plated on CYE plates and CYE/Km$_{10}$ plates to determine the plating efficiency of Δ*glpD* after amoeba passage. Data are representative of three independent experiments.

Figure S4
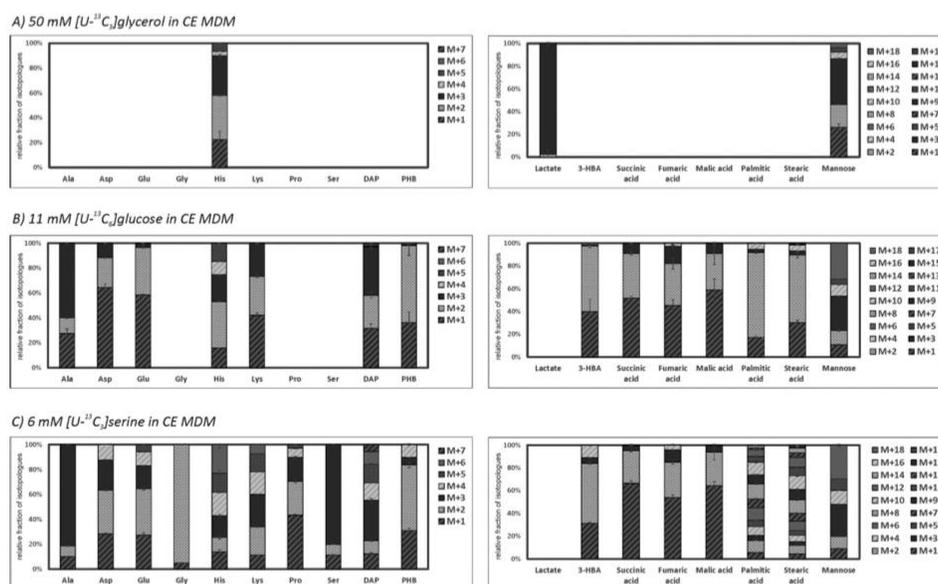
Figure S4. Comparison of ^{13}C-profiles of metabolites from time series. Comparison of isotopologue patterns of protein-derived amino acids, DAP, PHB, methanol-soluble metabolites and mannose of wild-type *L. pneumophila* grown in CE MDM with either (**A**) 50 mM [U-^{13}C$_3$]glycerol, (**B**) 11 mM [U-^{13}C$_6$]glucose or (**C**) 6 mM [U-^{13}C$_3$]serine as precursor. Shown are only patterns of metabolites that had significant enrichment of ^{13}C-label after 48 h of growth (^{13}C-enrichment > 1%). Columns indicate the relative fraction (in %) of the ^{13}C-isotopologues (M+1 to M+18) from three technical replicates. For numerical values, see Table S4.

Figure S5
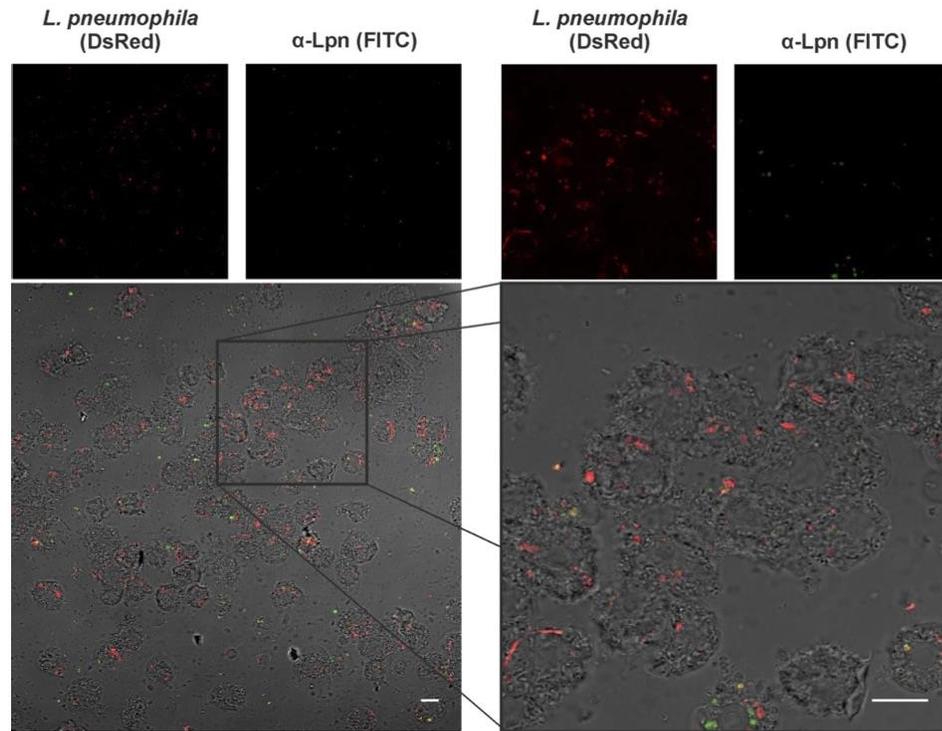
Figure S5. Infection efficiency for intracellular isotopologue profiling. Confluent *A. castellanii* amoeba (in a 75 cm^2 cell culture flask) were infected (MOI 50) with *L. pneumophila* wild-type harboring plasmid pSW001 (constitutive DsRed). Cells were incubated for 1 h, washed once with Ac buffer and detached from the surface using a cell scraper. Harvested cells were spun onto poly-lysine coated cover slips and fixed with 4% PFA. The samples were stained using a FITC-conjugated anti-*L. pneumophila* antibody [α-Lpn (FITC)] and mounted on microscopy slides. Shown are overview (left) and zoom (right) of infected cells. Scale bars, 10 μm. Images are representative of three independent experiments.

Figure S6
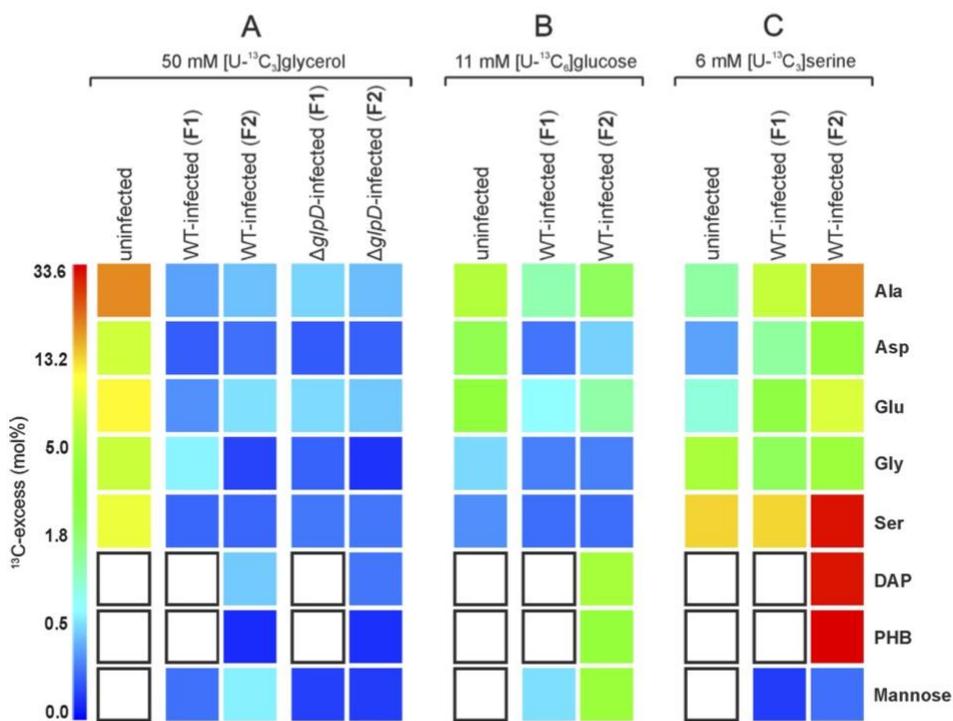
Figure S6. Analysis of amino acids, DAP and PHB of *L. pneumophila* grown in *A. castellanii*. *A. castellanii* amoeba were infected (MOI 50) with either wild-type *L. pneumophila* or the Δ*glpD* mutant strain and washed 1 h p.i. to remove extracellular bacteria. 5 h post infection (**A**) 50 mM [U-$^{13}C_3$]glycerol, (**B**) 11 mM [U-$^{13}C_6$]glucose or (**C**) 6 mM [U-$^{13}C_3$]serine were added, and 15 h p.i. the cells were lysed. Eukaryotic cell debris and bacteria were separated, resulting in fractions F1 (F1), containing eukaryotic cell debris and fraction F2 (F2), containing *L. pneumophila*. ^{13}C-excess of Ala, Asp, Glu, Gly, Ser, DAP, PHB and mannose in F1 and F2 of wild-type- or Δ*glpD*-infected amoeba, fed with (**A**) [U-$^{13}C_3$]glycerol, (**B**) [U-$^{13}C_6$]glucose or (**C**) [U-$^{13}C_3$]serine was analysed. Color map correlates to mean and SD of two independent experiments. For numerical values, see Table S5.

Figure S7
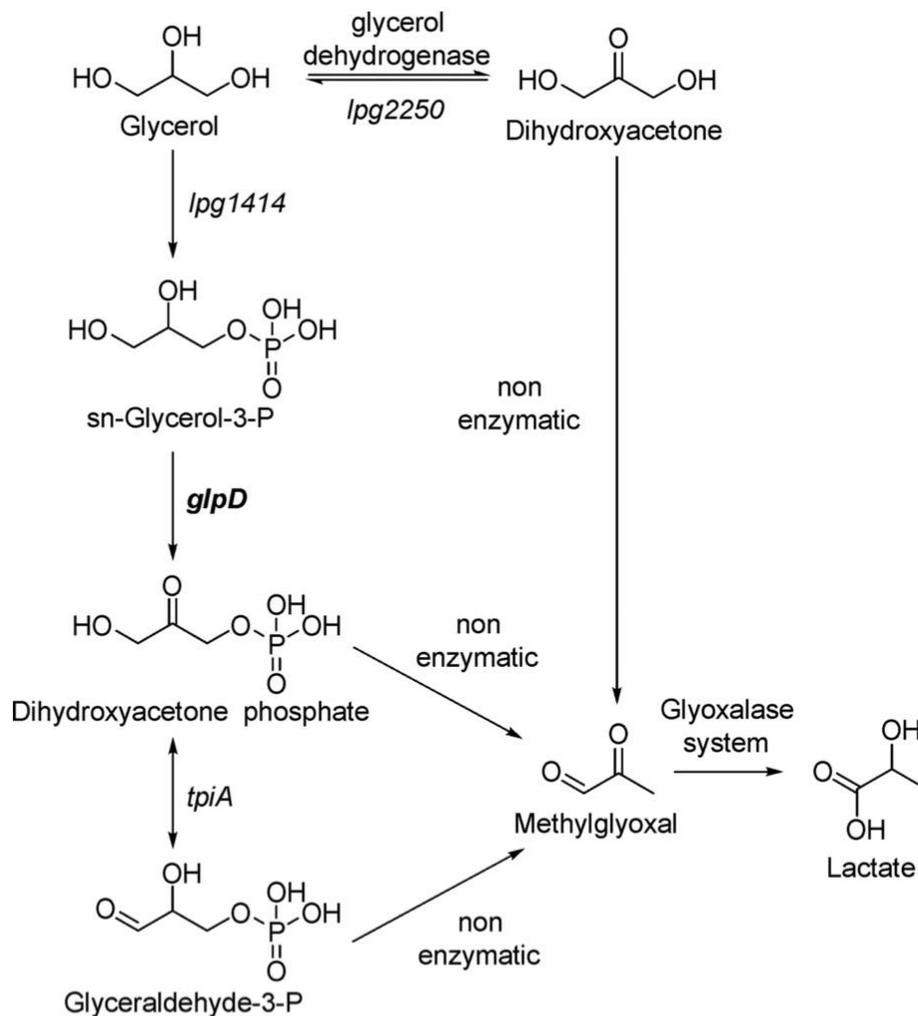
Figure S7. Proposed metabolism of methylglyoxal by *L. pneumophila*. Methylglyoxal is a toxic byproduct of several metabolic pathways and can be derived non-enzymatically from dihydroxyacetone, dihydroxyacetonephosphate or glycerinaldehyde-3-phosphate. In a detoxification reaction, methylglyoxal is then degraded to lactate within the glyoxalase system. In the *L. pneumophila* Δ*glpD* mutant strain, methylglyoxal can be derived from dihydroxyacetone directly made from glycerol. This reaction is catalyzed by a glycerol dehydrogenase (supposedly *lpg2250*; annotated as alcohol dehydrogenase with 27% identity to *E. coli* GldA).

Table S1. Strains, plasmids and primers used in this study.

Strain, plasmid, primer	Relevant properties, sequence [a]	Reference
E. coli		
TOP10		Invitrogen
L. pneumophila		
JR32	*L. pneumophila* Philadelphia-1 serogroup 1	(1)
CM01 (Δ*glpD*)	JR32 *glpD*::Km	This study
GS3011 (Δ*icmT*)	JR32 *icmT*3011::Km	(2)
Plasmids		
pCM018	pLAW344, *glpD*::Km	This study
pCM021	pCR33-M45-*glpD*	This study
pCR33	pMMMB207C-RBS, M45-(Gly)$_5$, Δ*mobA*, Cm	(3)
pLAW344	*oriT* (RK2), *oriR* (ColE1), *sacB*, Cm, Ap	(4)
pNT-28	pMMB207C, *gfp* (constitutive)	(5)
pUC4K	*oriR* (pBR322), Ap, MCS::Km	Amersham
Primers		
glpD-BamHI-fo-Kompl	GGAGAT<u>GGATCC</u>ATGGATCAGGTTTTTGATG	
glpD-SalI-re-Kompl	TTGATG<u>GTCGAC</u>TTAGTGAAATACGAGCTC	
glpD-LB-XbaI-fo	TATGCTT<u>CTAGA</u>AAAACTGGTTTATCACCTGTATTGAG	
glpD-LB-SalI-re	GAACTA<u>GTCGAC</u>GCTATTGACCAGGGAACAAG	
glpD-RB-SalI-fo	CAGCAT<u>GTCGAC</u>TTGTTGCGCCAATTCTTTTA	
glpD-RB-XbaI-re	CAAAAA<u>TCTAGA</u>GAATCAGGTGGGTTGGTGTC	
Kan2-fo	ACCTACAACAAAGCTCTCATCAACC	
Kan-re	GCAATGTAACATCAGAGATTTTGAG	

[a] Restriction sites underlined.

References

1. Sadosky, A. B., Wiater, L. A., and Shuman, H. A. (1993) Identification of *Legionella pneumophila* genes required for growth within and killing of human macrophages. *Infect Immun* **61**, 5361-5373.

2. Segal, G., and Shuman, H. A. (1998) Intracellular multiplication and human macrophage killing by *Legionella pneumophila* are inhibited by conjugal components of IncQ plasmid RSF1010. *Mol Microbiol* **30**, 197-208.

3. Weber, S. S., Ragaz, C., Reus, K., Nyfeler, Y., and Hilbi, H. (2006) *Legionella pneumophila* exploits PI(4)*P* to anchor secreted effector proteins to the replicative vacuole. *PLoS Pathog* **2**, e46.

4. Wiater, L. A., Sadosky, A. B., and Shuman, H. A. (1994) Mutagenesis of *Legionella pneumophila* using Tn*903*dIIl*lacZ*: identification of a growth-phase-regulated pigmentation gene. *Mol Microbiol* **11**, 641-653.

5. Tiaden, A., Spirig, T., Weber, S. S., Brüggemann, H., Bosshard, R., Buchrieser, C., and Hilbi, H. (2007) The *Legionella pneumophila* response regulator LqsR promotes host cell interactions as an element of the virulence regulatory network controlled by RpoS and LetA. *Cell Microbiol* **9**, 2903-2920

Table S2. Composition of CDM, MDM and CE MDM.

Compound	CDM [mg/l]	MDM [mg/l]	CE MDM [mg/l]
ACES	10000	10000	10000
Arginine	350	350	350
Cysteine	400	400	400
Isoleucine	470	470	470
Leucine	640	640	640
Methionine	200	200	200
Threonine	330	330	330
Valine	480	480	480
Serine (6 mM)	650	650	650
Proline	115	115	115
Phenylalanine	350	350	350
Aspartate	510	0	0
Glutamate	600	0	0
Histidine	150	0	0
Lysine	650	0	0
Tryptophan	100	0	0
Tyrosine	400	0	0
Glycerol (50 mM)	0	0	4605 (3654 μL)
Glucose (11 mM)	0	0	1982
NH_4Cl	315	315	315
NaCl	50	50	50
$CaCl_2 \times 2\ H_2O$	25	25	25
KH_2PO_4	1180	1180	1180
$MgSO_4 \times 7\ H_2O$	70	70	70
Fe-pyrophosphate hydrate ($Fe_4O_{21}P_6$)	250	250	250

Table S3A. Retention time and mass fragments of derivatized metabolites used for isotopologue calculations.

Metabolite	RT [a] [min]	[M-15]$^+$	[M-57]$^+$	[M-85]$^+$
Ala	6.7		m/z 260	
Gly	7.0		m/z 246	
Val	8.5		m/z 288	
Leu	9.1			m/z 274
Ile	9.5			m/z 274
Pro	10.1			m/z 258
Ser	13.2		m/z 390	
Phe	14.5		m/z 336	
Asp	15.4		m/z 418	
Glu	16.8		m/z 432	
Lys	18.1		m/z 431	
His	20.4		m/z 432	
Tyr	21.0		m/z 466	
DAP	6.3		m/z 589	
PHB	9.1	m/z 233		
Lactate	17.8		m/z 261	
3-Hydroxybutyric acid	21.6		m/z 275	
Succinic acid	27.5		m/z 289	
Fumaric acid	28.7		m/z 287	
Malic acid	39.1		m/z 419	
Palmitic acid	44.0		m/z 313	
Stearic acid	49.4		m/z 341	
Citric acid	53.3		m/z 591	
Mannose	8.7	m/z 287		

[a] RT, retention time.

Table S3B. ^{13}C-Excess (mol%) from [U-^{13}C$_3$]glycerol at 48 h. ^{13}C-Excess (mol%) of amino acids, DAP, PHB, polar metabolites and mannose from experiments with *L. pneumophila* wild-type and Δ*glpD* grown in MDM supplemented with 50 mM [U-^{13}C$_3$]glycerol for 48 h. Mean and SD from three independent experiments are shown.

50 mM [U-^{13}C$_3$]glycerol	*L. pneumophila* WT	*L. pneumophila* Δ*glpD*
Ala	0.34% ± 0.04%	0.23% ± 0.21%
Asp	0.36% ± 0.05%	0.12% ± 0.02%
Glu	0.55% ± 0.03%	0.20% ± 0.04%
Gly	0.11% ± 0.04%	0.08% ± 0.02%
His	3.01% ± 0.05%	0.06% ± 0.03%
Ile	0.09% ± 0.01%	0.07% ± 0.02%
Leu	0.01% ± 0.00%	0.01% ± 0.00%
Lys	0.39% ± 0.02%	0.12% ± 0.01%
Phe	0.07% ± 0.01%	0.06% ± 0.01%
Pro	0.18% ± 0.01%	0.09% ± 0.01%
Ser	0.10% ± 0.01%	0.12% ± 0.03%
Tyr	0.10% ± 0.02%	0.08% ± 0.02%
Val	0.12% ± 0.01%	0.13% ± 0.04%
DAP	0.74% ± 0.09%	0.17% ± 0.08%
PHB	0.12% ± 0.06%	0.00% ± 0.00%
Lactate	0.97% ± 0.20%	0.71% ± 0.29%
3-Hydroxybutyric acid	0.61% ± 0.05%	0.22% ± 0.06%
Succinic acid	0.24% ± 0.03%	0.09% ± 0.02%
Fumaric acid	0.32% ± 0.03%	0.15% ± 0.07%
Malic acid	0.70% ± 0.16%	0.29% ± 0.05%
Palmitic acid	0.15% ± 0.01%	0.07% ± 0.02%
Stearic acid	0.60% ± 0.05%	0.44% ± 0.06%
Citric acid	0.21% ± 0.03%	0.17% ± 0.01%
Mannose	5.75% ± 0.65%	0.12% ± 0.08%

Table S3C. Relative fractions of isotopologues (mol%) from [U-^{13}C$_3$]glycerol at 48 h. Relative fractions of isotopologues (mol%) of histidine, lactate and mannose from *L. pneumophila* wild-type and Δ*glpD* grown in MDM supplemented with 50 mM [U-^{13}C$_3$]glycerol for 48 h. M+x represents the mass of the unlabelled metabolite plus x labelled ^{13}C-atoms. Mean and SD from three independent experiments are shown.

	L. pneumophila WT + 50 mM [U-^{13}C$_3$]glycerol		
	His	**Lactate**	**Mannose**
M+1	1.85% ± 0.23%	0.00% ± 0.00%	2.13% ± 0.12%
M+2	3.41% ± 0.06%	0.03% ± 0.03%	1.95% ± 0.26%
M+3	2.12% ± 0.07%	0.95% ± 0.19%	5.40% ± 0.58%
M+4	0.39% ± 0.03%		0.72% ± 0.12%
M+5	0.86% ± 0.06%		0.66% ± 0.17%
M+6	0.00% ± 0.00%		1.02% ± 0.18%
	L. pneumophila Δ*glpD* + 50 mM [U-^{13}C$_3$]glycerol		
		Lactate	
M+1		0.00% ± 0.00%	
M+2		0.02% ± 0.03%	
M+3		0.70% ± 0.29%	

Table S4A. Kinetics of ^{13}C-excess (mol%) from [U-^{13}C$_3$]glycerol. ^{13}C-excess (mol%) of amino acids, DAP, PHB, polar metabolites and mannose from time series experiments with *L. pneumophila* wild-type grown in CE MDM supplemented with 50 mM [U-^{13}C$_3$]glycerol.

50 mM [U-^{13}C$_3$]glycerol	12 h	24 h	36 h	48 h
Ala	0.36% ± 0.13%	0.37% ± 0.06%	0.54% ± 0.06%	0.61% ± 0.08%
Asp	0.37% ± 0.04%	0.28% ± 0.07%	0.48% ± 0.01%	0.49% ± 0.03%
Glu	0.68% ± 0.05%	0.55% ± 0.04%	0.74% ± 0.01%	0.77% ± 0.02%
Gly	0.44% ± 0.16%	0.41% ± 0.21%	0.32% ± 0.18%	0.38% ± 0.15%
His	0.33% ± 0.11%	0.66% ± 0.03%	2.70% ± 0.02%	3.00% ± 0.05%
Ile	0.19% ± 0.02%	0.20% ± 0.04%	0.16% ± 0.01%	0.19% ± 0.03%
Leu	0.11% ± 0.02%	0.05% ± 0.02%	0.10% ± 0.05%	0.03% ± 0.03%
Lys	0.12% ± 0.03%	0.13% ± 0.03%	0.36% ± 0.02%	0.46% ± 0.01%
Phe	0.17% ± 0.02%	0.20% ± 0.08%	0.18% ± 0.04%	0.15% ± 0.06%
Pro	0.09% ± 0.04%	0.15% ± 0.02%	0.31% ± 0.03%	0.31% ± 0.02%
Ser	0.10% ± 0.07%	0.17% ± 0.05%	0.13% ± 0.06%	0.14% ± 0.06%
Tyr	0.12% ± 0.03%	0.19% ± 0.02%	0.10% ± 0.04%	0.24% ± 0.07%
Val	0.05% ± 0.02%	0.05% ± 0.05%	0.03% ± 0.01%	0.03% ± 0.03%
DAP	0.27% ± 0.03%	0.25% ± 0.07%	0.72% ± 0.15%	0.80% ± 0.05%
PHB	0.42% ± 0.03%	0.27% ± 0.19%	0.29% ± 0.12%	0.52% ± 0.17%
Lactate				1.44% ± 0.05%
3-Hydroxybutyric acid				0.41% ± 0.06%
Succinic acid				0.22% ± 0.01%
Fumaric acid				0.29% ± 0.03%
Malic acid				0.55% ± 0.14%
Palmitic acid				0.19% ± 0.02%
Stearic acid				0.30% ± 0.01%
Citric acid				0.08% ± 0.01%
Mannose				4.51% ± 0.12%

Table S4B. Kinetics of ^{13}C-excess (mol%) from [U-^{13}C$_6$]glucose. ^{13}C-Excess (mol%) of amino acids, DAP, PHB, polar metabolites and mannose from time series experiments with *L. pneumophila* wild-type grown in CE MDM supplemented with 11 mM [U-^{13}C$_6$]glucose.

11 mM [U-^{13}C$_6$]glucose	12 h	24 h	36 h	48 h
Ala	1.44% ± 0.03%	2.25% ± 0.02%	3.57% ± 0.10%	4.26% ± 0.07%
Asp	0.88% ± 0.02%	1.32% ± 0.07%	2.31% ± 0.03%	2.61% ± 0.04%
Glu	0.94% ± 0.03%	1.30% ± 0.02%	2.08% ± 0.03%	2.36% ± 0.01%
Gly	0.39% ± 0.05%	0.40% ± 0.03%	0.39% ± 0.06%	0.50% ± 0.04%
His	9.16% ± 0.08%	15.15% ± 0.04%	18.74% ± 0.05%	20.72% ± 0.01%
Ile	0.21% ± 0.02%	0.20% ± 0.01%	0.22% ± 0.01%	0.25% ± 0.01%
Leu	0.00% ± 0.00%	0.37% ± 0.33%	0.15% ± 0.02%	0.34% ± 0.36%
Lys	0.71% ± 0.00%	1.46% ± 0.04%	2.47% ± 0.05%	2.73% ± 0.04%
Phe	0.13% ± 0.02%	0.15% ± 0.03%	0.17% ± 0.03%	0.13% ± 0.03%
Pro	0.24% ± 0.04%	0.32% ± 0.02%	1.17% ± 0.05%	1.43% ± 0.04%
Ser	0.23% ± 0.10%	0.28% ± 0.03%	0.22% ± 0.06%	0.44% ± 0.01%
Tyr	0.04% ± 0.01%	0.07% ± 0.02%	0.03% ± 0.01%	0.06% ± 0.01%
Val	0.04% ± 0.04%	0.07% ± 0.01%	0.04% ± 0.02%	0.08% ± 0.01%
DAP	1.24% ± 0.14%	1.85% ± 0.13%	3.18% ± 0.08%	3.64% ± 0.08%
PHB	0.92% ± 0.11%	1.17% ± 0.14%	1.53% ± 0.17%	1.64% ± 0.20%
Lactate				0.29% ± 0.03%
3-Hydroxybutyric acid				1.45% ± 0.08%
Succinic acid				1.46% ± 0.03%
Fumaric acid				1.50% ± 0.14%
Malic acid				2.16% ± 0.28%
Palmitic acid				1.38% ± 0.03%
Stearic acid				1.52% ± 0.03%
Citric acid				0.19% ± 0.05%
Mannose				31.88% ± 0.08%

Table S4C. Kinetics of ^{13}C-excess (mol%) from [U-^{13}C$_3$]serine. ^{13}C-Excess (mol%) of amino acids, DAP, PHB, polar metabolites and mannose from time series experiments with *L. pneumophila* wild-type grown in CE MDM supplemented with 6 mM [U-^{13}C$_3$]serine.

6 mM [U-^{13}C$_3$]serine	12 h	24 h	36 h	48 h
Ala	56.77% ± 0.37%	74.60% ± 0.62%	66.83% ± 0.26%	64.03% ± 0.28%
Asp	23.90% ± 0.17%	34.34% ± 0.19%	28.94% ± 0.14%	28.20% ± 0.15%
Glu	21.57% ± 0.02%	29.00% ± 0.38%	21.99% ± 0.10%	20.38% ± 0.05%
Gly	20.53% ± 0.14%	28.58% ± 0.27%	22.94% ± 0.18%	22.72% ± 0.05%
His	35.79% ± 1.13%	62.05% ± 3.23%	56.35% ± 2.55%	55.88% ± 3.32%
Ile	0.09% ± 0.01%	0.09% ± 0.00%	0.04% ± 0.01%	0.06% ± 0.02%
Leu	0.00% ± 0.00%	0.01% ± 0.01%	0.00% ± 0.00%	0.00% ± 0.00%
Lys	25.24% ± 0.12%	50.22% ± 0.22%	43.86% ± 0.21%	42.45% ± 0.21%
Phe	0.17% ± 0.06%	0.13% ± 0.02%	0.14% ± 0.02%	0.12% ± 0.01%
Pro	0.05% ± 0.04%	0.01% ± 0.02%	4.70% ± 0.14%	4.45% ± 0.06%
Ser	71.13% ± 0.17%	91.61% ± 0.17%	64.59% ± 0.20%	60.83% ± 0.30%
Tyr	0.25% ± 0.05%	0.12% ± 0.08%	0.11% ± 0.04%	0.12% ± 0.04%
Val	0.16% ± 0.05%	0.16% ± 0.08%	0.09% ± 0.02%	0.07% ± 0.02%
DAP	46.62% ± 0.17%	55.02% ± 0.12%	41.05% ± 0.21%	38.31% ± 0.24%
PHB	29.97% ± 0.51%	39.16% ± 0.56%	16.75% ± 0.21%	15.70% ± 0.67%
Lactate				0.31% ± 0.11%
3-Hydroxybutyric acid				12.45% ± 0.31%
Succinic acid				3.53% ± 0.09%
Fumaric acid				5.63% ± 0.27%
Malic acid				4.34% ± 0.19%
Palmitic acid				32.64% ± 1.73%
Stearic acid				34.26% ± 1.93%
Citric acid				0.15% ± 0.01%
Mannose				40.40% ± 0.59%

Table S4D. Relative fractions of isotopologues (mol%) of amino acids, DAP and PHB from *L. pneumophila* wild-type grown in CE MDM supplemented with either **(i)** 50 mM [U-^{13}C$_3$]glycerol, **(ii)** 11 mM [U-^{13}C$_6$]glucose or **(iii)** 6 mM [U-^{13}C$_3$]serine of 48 h time points from time series experiments. M+x represents the mass of the unlabelled metabolite plus x labelled ^{13}C-atoms. Mean and SD from three independent experiments are shown.

i) 50 mM [U-^{13}C$_3$]glycerol

	Ala	Asp	Glu	Gly	His	Lys	Pro	Ser	DAP	PHB
M+1	1.52% ± 0.19%	4.58% ± 0.19%	4.72% ± 0.05%		1.71% ± 0.52%					
M+2	0.69% ± 0.02%	1.71% ± 0.03%	3.09% ± 0.04%		2.72% ± 0.03%					
M+3	3.29% ± 0.02%	0.81% ± 0.02%	0.24% ± 0.01%		2.41% ± 0.10%					
M+4		0.00% ± 0.00%	0.00% ± 0.01%		0.28% ± 0.01%					
M+5			0.03% ± 0.00%		0.50% ± 0.01%					
M+6					0.00% ± 0.00%					
M+7										

ii) 11 mM [U-^{13}C$_6$]glucose

	Ala	Asp	Glu	Gly	His	Lys	Pro	Ser	DAP	PHB
M+1					7.26% ± 0.06%	3.74% ± 0.18%			3.73% ± 0.42%	1.43% ± 0.34%
M+2					17.14% ± 0.08%	2.77% ± 0.08%			3.12% ± 0.23%	2.43% ± 0.31%
M+3					9.91% ± 0.04%	2.37% ± 0.04%			4.60% ± 0.16%	0.03% ± 0.03%
M+4					4.87% ± 0.06%	0.00% ± 0.00%			0.07% ± 0.12%	0.04% ± 0.02%
M+5					6.71% ± 0.06%	0.00% ± 0.00%			0.17% ± 0.05%	
M+6					0.00% ± 0.00%	0.00% ± 0.00%			0.09% ± 0.02%	
M+7									0.01% ± 0.01%	

iii) 6 mM [U-^{13}C$_3$]serine

	Ala	Asp	Glu	Gly	His	Lys	Pro	Ser	DAP	PHB
M+1	7.21% ± 0.11%	14.46% ± 0.39%	12.10% ± 0.84%	1.16% ± 0.03%	12.71% ± 1.56%	9.01% ± 0,13%	4.83% ± 0.08%	7.78% ± 0.27%	9.24% ± 0.64%	9.97% ± 0.56%
M+2	5.94% ± 0.11%	17.90% ± 0.21%	16.40% ± 0.45%	22.14% ± 0.07%	10.57% ± 1.30%	17.65% ± 0.23%	3.05% ± 0.16%	5.78% ± 0.08%	7.83% ± 0.65%	16.90% ± 0.64%
M+3	57.66% ± 0.32%	12.51% ± 0.15%	8.23% ± 0.10%		15.86% ± 1.01%	20.63% ± 0.16%	2.15% ± 0.10%	54.38% ± 0.26%	24.13% ± 0.94%	1.95% ± 0.02%
M+4		6.24% ± 0.03%	4.93% ± 0.12%		16.91% ± 0.30%	14.24% ± 0.15%	0.81% ± 0.07%		10.28% ± 0.19%	3.29% ± 0.26%
M+5			2.52% ± 0.06%		14.03% ± 2.34%	11.44% ± 0.12%	0.31% ± 0.04%		11.05% ± 0.41%	
M+6					20.88% ± 2.55%	5.73% ± 0.06%			7.72% ± 0.65%	
M+7									4.03% ± 0.54%	

Table S4E. Relative fractions of isotopologues (mol%) of polar metabolites and mannose from *L. pneumophila* wild-type grown in CE MDM supplemented with either (**i**) 50 mM [U-^{13}C$_3$]glycerol, (**ii**) 11 mM [U-^{13}C$_6$]glucose or (**iii**) 6 mM [U-^{13}C$_3$]serine of 48 h time points from time series experiments. M+x represents the mass of the unlabelled metabolite plus x labelled ^{13}C-atoms. Mean and SD from three independent experiments are shown.

i) 50 mM [U-^{13}C$_3$]glycerol

	Lactate	3-HBA	Succinic acid	Fumaric acid	Malic acid	Palmitic acid	Stearic acid	Mannose
M+1	0.00% ± 0.00%							2.81% ± 0.34%
M+2	0.03% ± 0.06%							2.15% ± 0.02%
M+3	1.42% ± 0.02%							4.36% ± 0.08%
M+4								0.62% ± 0.04%
M+5								0.42% ± 0.05%
M+6								0.38% ± 0.02%

ii) 11 mM [U-^{13}C$_6$]glucose

	Lactate	3-HBA	Succinic acid	Fumaric acid	Malic acid	Palmitic acid	Stearic acid	Mannose
M+1		1.41% ± 0.39%	1.93% ± 0.07%	1.55% ± 0.17%	4.30% ± 0.56%	1.94% ± 0.15%	4.29% ± 0.30%	5.44% ± 0.29%
M+2		2.04% ± 0.06%	1.46% ± 0.04%	1.25% ± 0.16%	1.84% ± 0.55%	8.40% ± 0.09%	8.50% ± 0.38%	6.24% ± 0.21%
M+3		0.04% ± 0.04%	0.33% ± 0.01%	0.52% ± 0.05%	0.49% ± 0.10%	0.30% ± 0.06%	0.49% ± 0.03%	15.18% ± 0.23%
M+4		0.04% ± 0.01%	0.00% ± 0.01%	0.09% ± 0.06%	0.02% ± 0.04%	0.58% ± 0.03%	0.75% ± 0.04%	5.19% ± 0.19%
M+5						0.03% ± 0.00%	0.06% ± 0.01%	2.39% ± 0.12
M+6						0.01% ± 0.00%	0.09% ± 0.00%	15.84% ± 0.25%
M+7						0.00% ± 0.00%	0.01% ± 0.00%	
M+8						0.00% ± 0.00%	0.02% ± 0.00%	
M+9						0.00% ± 0.00%	0.00% ± 0.00%	
M+10						0.00% ± 0.00%	0.00% ± 0.00%	
M+11						0.00% ± 0.00%	0.00% ± 0.00%	
M+12						0.00% ± 0.00%	0.02% ± 0.01%	
M+13						0.00% ± 0.00%	0.01% ± 0.00%	
M+14						0.00% ± 0.00%	0.00% ± 0.00%	
M+15						0.00% ± 0.00%	0.01% ± 0.00%	
M+16						0.00% ± 0.00%	0.01% ± 0.00%	

| | M+17 | 0.00% ± 0.00% |
| | M+18 | 0.00% ± 0.00% |

iii) 6 mM [U-^{13}C$_3$]serine

	Lactate	3-HBA	Succinic acid	Fumaric acid	Malic acid	Palmitic acid	Stearic acid	Mannose
M+1		7.98% ± 0.22%	6.77% ± 0.23%	7.35% ± 0.30%	7.89% ± 0.39%	4.35% ± 0.06%	3.43% ± 0.14%	5.59% ± 0.29%
M+2		13.42% ± 0.33%	2.92% ± 0.10%	4.22% ± 0.24%	3.60% ± 0.84%	7.96% ± 0.15%	5.73% ± 5.18%	6.59% ± 0.10%
M+3		1.27% ± 0.06%	0.46% ± 0.04%	1.47% ± 0.04%	0.70% ± 0.33%	3.31% ± 0.18%	2.59% ± 0.07%	17.50% ± 0.18%
M+4		2.80% ± 0.13%	0.04% ± 0.02%	0.57% ± 0.06%	0.05% ± 0.09%	5.90% ± 0.15%	4.15% ± 0.20%	7.47% ± 0.12%
M+5						4.19% ± 0.11%	3.20% ± 0.11%	6.27% ± 0.19%
M+6						8.32% ± 0.37%	6.33% ± 0.28%	18.31% ± 0.65%
M+7						5.91% ± 0.31%	5.33% ± 0.26%	
M+8						10.03% ± 0.47%	9.14% ± 0.53%	
M+9						6.05% ± 0.28%	6.80% ± 0.42%	
M+10						8.42% ± 0.52%	9.42% ± 0.50%	
M+11						3.79% ± 0.31%	5.65% ± 0.30%	
M+12						4.49% ± 0.32%	6.64% ± 0.40%	
M+13						1.36% ± 0.11%	3.09% ± 0.23%	
M+14						1.33% ± 0.13%	3.08% ± 0.27%	
M+15						0.19% ± 0.02%	0.98% ± 0.09%	
M+16						0.16% ± 0.02%	0.84% ± 0.07%	
M+17							0.15% ± 0.02%	
M+18							0.10% ± 0.01%	

Table S4F. Ratio of ^{13}C-excess in histidine to ^{13}C-excess in alanine calculated from time series experiments with *L. pneumophila* wild-type grown in CE MDM with either 50 mM [U-^{13}C$_3$]glycerol, 11 mM [U-^{13}C$_6$]glucose or 6 mM [U-^{13}C$_3$]serine as precursor. Shown is the ratio of means from samples taken after 12 h, 24 h, 36 h or 48 h. SD was calculated from the highest possible (**+**) and the lowest possible (**-**) value.

Ratio: ^{13}C-Excess [mol%] His/^{13}C-Excess [mol%] Ala											
	12 h	+	-	24 h	+	-	36 h	+	-	48 h	+	-
50 mM [U-^{13}C$_3$]glycerol	0.94	1.05	0.48	1.79	0.49	0.34	4.99	0.71	0.56	4.92	0.89	0.67
11 mM [U-^{13}C$_6$]glucose	6.34	0.21	0.20	6.74	0.07	0.07	5.25	0.17	0.16	4.87	0.08	0.08
6 mM [U-^{13}C$_3$]serine	0.63	0.02	0.02	0.83	0.05	0.05	0.84	0.04	0.04	0.87	0.06	0.06

Table S5A. ^{13}C-Excess (mol%) of alanine, aspartate, glutamate, glycine, serine, DAP, PHB and mannose from experiments with uninfected *A. castellanii* and amoeba infected with *L. pneumophila* wild-type or Δ*glpD*. Infections were supplemented with either (**i**) 50 mM [U-[13]C$_3$]glycerol, (**ii**) 11 mM [U-[13]C$_6$]glucose or (**iii**) 6 mM [U-[13]C$_3$]serine 5 h post infection. Cells were lysed and fractionated 15 h post infection, resulting in fraction 1 (F1), containing eukaryotic cell debris and fraction 2 (F2), containing *L. pneumophila* bacteria.

	i) 50 mM [U-[13]C$_3$]glycerol				
	uninfected	WT-infected (F1)	WT-infected (F2)	Δ*glpD*-infected (F1)	Δ*glpD*-infected (F2)
Ala	17.83% ± 0.28%	0.37% ± 0.19%	0.48% ± 0.14%	0.55% ± 0.22%	0.46% ± 0.11%
Asp	7.51% ± 0.37%	0.18% ± 0.13%	0.22% ± 0.08%	0.17% ± 0.09%	0.19% ± 0.05%
Glu	10.65% ± 0.06%	0.32% ± 0.10%	0.61% ± 0.26%	0.58% ± 0.24%	0.51% ± 0.18%
Gly	7.22% ± 0.18%	0.68% ± 0.89%	0.12% ± 0.10%	0.19% ± 0.14%	0.08% ± 0.10%
Ser	9.26% ± 0.18%	0.20% ± 0.11%	0.20% ± 0.05%	0.25% ± 0.03%	0.24% ± 0.02%
DAP			0.52% ± 0.04%		0.24% ± 0.03%
PHB			0.06% ± 0.03%		0.07% ± 0.10%
Mannose		0.23% ± 0.19%	0.67% ± 0.07%	0.11% ± 0.04%	0.10% ± 0.04%

	ii) 11 mM [U-[13]C$_6$]glucose				
	uninfected	WT-infected (F1)	WT-infected (F2)		
Ala	5.98% ± 0.12%	1.22% ± 0.16%	2.06% ± 0.44%		
Asp	2.33% ± 0.04%	0.24% ± 0.00%	0.54% ± 0.17%		
Glu	3.09% ± 0.07%	0.74% ± 0.16%	1.28% ± 0.39%		
Gly	0.57% ± 0.22%	0.27% ± 0.17%	0.27% ± 0.07%		
Ser	0.31% ± 0.06%	0.22% ± 0.01%	0.22% ± 0.02%		
DAP			5.18% ± 1.30%		
PHB			3.91% ± 1.11%		
Mannose		0.60% ± 0.27%	4.47% ± 0.40%		

	iii) 6 mM [U-[13]C$_3$]serine				
	uninfected	WT-infected (F1)	WT-infected (F2)		
Ala	1.32% ± 0.07%	6.85% ± 1.07%	17.90% ± 0.44%		
Asp	0.37% ± 0.09%	1.36% ± 0.50%	3.82% ± 0.05%		
Glu	0.93% ± 0.10%	2.66% ± 1.35%	8.18% ± 0.05%		
Gly	5.43% ± 0.15%	2.11% ± 0.59%	4.64% ± 0.11%		
Ser	12.63% ± 0.08%	12.52% ± 2.21%	31.51% ± 0.16%		
DAP			31.35% ± 0.23%		
PHB			33.64% ± 1.00%		
Mannose		0.10% ± 0.04%	0.22% ± 0.08%		

Table S5B. Relative fraction of isotopologues in alanine, aspartate, glutamate, glycine, serine, DAP und PHB (mol%) of *in vivo* infection and separation experiments. *A. castellanii* amoeba were either fed with (**i**) 50 mM [U-^{13}C$_3$]glycerol, (**ii**) 11 mM [U-^{13}C$_6$]glucose or (**iii**) 6 mM [U-^{13}C$_3$]serine. M+x represents the mass of the unlabelled metabolite plus x labelled ^{13}C-atoms. Mean and SD from two independent experiments are shown.

i) 50 mM [U-^{13}C$_3$]glycerol

A. castellanii uninfected

	Ala	Asp	Glu	Gly	Ser
M+1	3.20% ± 0.39%	3.08% ± 0.08%	4.57% ± 0.33%	2.06% ± 0.19%	11.77% ± 1.35%
M+2	2.76% ± 0.10%	3.61% ± 0.23%	7.78% ± 0.11%	6.19% ± 0.08%	4.31% ± 0.53%
M+3	14.92% ± 0.20%	4.20% ± 0.31%	4.69% ± 0.12%		2.46% ± 0.41%
M+4		1.79% ± 0.06%	2.86% ± 0.06%		
M+5			1.52% ± 0.00%		

WT-infectetd F1

	Ala	Asp	Glu	Gly	Ser
M+1	0.13% ± 0.18%	0.30% ± 0.17%	0.59% ± 0.39%	1.20% ± 1.61%	0.00% ± 0.00%
M+2	0.01% ± 0.02%	0.00% ± 0.00%	0.28% ± 0.22%	0.08% ± 0.09%	0.00% ± 0.00%
M+3	0.32% ± 0.12%	0.14% ± 0.11%	0.05% ± 0.05%		0.20% ± 0.11%
M+4		0.00% ± 0.00%	0.04% ± 0.06%		
M+5			0.03% ± 0.03%		

WT-infectetd F2

	Ala	Asp	Glu	Gly	Ser	DAP	PHB
M+1	0.25% ± 0.24%	0.75% ± 0.28%	1.82% ± 0.87%	0.12% ± 0.14%	0.00% ± 0.00%	0.40% ± 0.52%	0.01% ± 0.02%
M+2	0.03% ± 0.04%	0.00% ± 0.00%	0.60% ± 0.22%	0.06% ± 0.03%	0.00% ± 0.00%	0.74% ± 0.09%	0.10% ± 0.02%
M+3	0.38% ± 0.03%	0.05% ± 0.02%	0.00% ± 0.00%		0.20% ± 0.05%	0.55% ± 0.06%	0.01% ± 0.01%
M+4		0.00% ± 0.00%	0.00% ± 0.00%			0.01% ± 0.02%	0.01% ± 0.01%
M+5			0.00% ± 0.00%			0.00% ± 0.00%	
M+6						0.00% ± 0.00%	
M+7						0.00% ± 0.00%	

ΔglpD-infectetd F1

	Ala	Asp	Glu	Gly	Ser
M+1	0.21% ± 0.11%	0.65% ± 0.34%	1.15% ± 0.47%	0.23% ± 0.13%	0.05% ± 0.07%
M+2	0.07% ± 0.07%	0.00% ± 0.00%	0.85% ± 0.36%	0.07% ± 0.07%	0.00% ± 0.00%
M+3	0.43% ± 0.13%	0.01% ± 0.01%	0.00% ± 0.00%		0.23% ± 0.05%
M+4		0.00% ± 0.00%	0.00% ± 0.00%		
M+5			0.01% ± 0.00%		

ΔglpD-infectetd F2

	Ala	Asp	Glu	Gly	Ser	DAP	PHB
M+1	0.13% ± 0.02%	0.73% ± 0.22%	1.11% ± 0.42%	0.10% ± 0.14%	0.00% ± 0.00%	0.26% ± 0.01%	0.20% ± 0.26%
M+2	0.07% ± 0.06%	0.00% ± 0.00%	0.70% ± 0.23%	0.03% ± 0.03%	0.00% ± 0.00%	0.42% ± 0.11%	0.04% ± 0.06%
M+3	0.37% ± 0.07%	0.00% ± 0.01%	0.00% ± 0.01%		0.24% ± 0.02%	0.17% ± 0.14%	0.00% ± 0.00%
M+4		0.00% ± 0.00%	0.00% ± 0.00%			0.01% ± 0.00%	0.00% ± 0.00%
M+5			0.00% ± 0.00%			0.00% ± 0.01%	
M+6						0.00% ± 0.00%	
M+7						0.00% ± 0.00%	

ii) 11 mM [U-^{13}C$_6$]glucose

A. castellanii uninfected

	Ala	Asp	Glu	Gly	Ser
M+1	2.60% ± 0.29%	3.47% ± 0.20%	3.88% ± 0.61%	0.77% ± 0.28%	0.10% ± 0.17%
M+2	1.45% ± 0.09%	1.72% ± 0.20%	3.66% ± 0.11%	0.18% ± 0.10%	0.00% ± 0.00%
M+3	4.15% ± 0.08%	0.74% ± 0.09%	0.92% ± 0.11%		0.28% ± 0.08%
M+4		0.04% ± 0.02%	0.29% ± 0.03%		
M+5			0.07% ± 0.01%		

WT-infectetd F1

	Ala	Asp	Glu	Gly	Ser
M+1	0.62% ± 0.73%	0.59% ± 0.25%	1.00% ± 0.57%	0.36% ± 0.34%	0.00% ± 0.00%
M+2	0.07% ± 0.05%	0.00% ± 0.00%	0.96% ± 0.69%	0.06% ± 0.03%	0.00% ± 0.00%
M+3	0.97% ± 0.44%	0.11% ± 0.08%	0.15% ± 0.11%		0.21% ± 0.00%
M+4		0.00% ± 0.01%	0.01% ± 0.01%		
M+5			0.05% ± 0.02%		

WT-infectetd F2

	Ala	Asp	Glu	Gly	Ser	DAP	PHB
M+1	0.60% ± 0.56%	1.21% ± 0.35%	2.19% ± 0.30%	0.35% ± 0.17%	0.00% ± 0.00%	2.79% ± 1.91%	1.90% ± 0.15%
M+2	0.26% ± 0.15%	0.24% ± 0.14%	1.75% ±0.99%	0.09% ± 0.01%	0.00% ± 0.00%	2.81% ± 0.08%	5.9% ± 2.57%
M+3	1.68% ± 0.72%	0.16% ± 0.12%	0.16% ± 0.12%		0.22% ± 0.03%	7.18% ± 2.61%	0.17% ± 0.22%
M+4		0.00% ± 0.00%	0.01% ± 0.01%			0.41% ± 0.52%	0.26% ± 0.16%
M+5			0.04% ± 0.02%			0.52% ± 0.07%	
M+6						0.26% ± 0.14%	
M+7						0.03% ± 0.01%	

iii) 6 mM [U-^{13}C$_3$]serine

A. castellanii uninfected

	Ala	Asp	Glu	Gly	Ser
M+1	1.71% ± 0.33%	1.15% ± 0.40%	2.75% ± 0.15%	1.82% ± 0.02%	3.63% ± 0.73%
M+2	0.42% ± 0.06%	0.07% ± 0.10%	0.93% ± 0.21%	4.52% ± 0.14%	2.71% ± 0.13%
M+3	0.47% ± 0.01%	0.06% ± 0.04%	0.01% ± 0.01%		9.61% ± 0.24%
M+4		0.00% ± 0.00%	0.00% ± 0.00%		
M+5			0.01% ± 0.00%		

WT-infectetd F1

	Ala	Asp	Glu	Gly	Ser
M+1	0.32% ± 0.35%	1.20% ± 0.33%	1.49% ± 0.92%	0.50% ± 0.03%	0.80% ± 0.94%
M+2	0.43% ± 0.08%	0.66% ± 0.45%	2.61% ± 1.60%	1.86% ± 0.82%	0.42% ± 0.41%
M+3	6.46% ± 1.35%	0.71% ± 0.35%	0.84% ± 0.69%		11.97% ± 2.53%
M+4		0.20% ± 0.14%	0.59% ± 0.52%		
M+5			0.34% ± 0.26%		

WT-infectetd F2

	Ala	Asp	Glu	Gly	Ser	DAP	PHB
M+1	0.80% ± 0.28%	2.39% ± 0.03%	3.32% ± 0.18%	0.68% ± 0.10%	1.32% ± 0.87%	3.02% ± 0.26%	4.20% ± 0.28%
M+2	1.06% ± 0.00%	2.44% ± 0.10%	7.58% ± 0.37%	4.30% ± 0.11%	1.20% ± 0.17%	4.54% ± 0.19%	32.68% ± 0.63%
M+3	16.93% ± 0.71%	1.83% ± 0.07%	2.96% ± 0.08%		30.28% ± 0.63%	26.13% ± 0.73%	3.19% ± 0.33%
M+4		0.63% ± 0.03%	2.03% ± 0.09%			6.78% ± 0.52%	13.86% ± 0.79%
M+5			1.09% ± 0.02%			9.26% ± 0.10%	
M+6						6.51% ± 0.29%	
M+7						2.35% ± 0.01%	

_____

5.2 Supplementary Material: *Legionella pneumophila* CsrA regulates a metabolic switch from amino acid to glycerolipid metabolism

Häuslein, I., Sahr, T., Escoll, P., Klausner, N., Eisenreich, W., and Buchrieser, C., (**2017**). **Submitted**
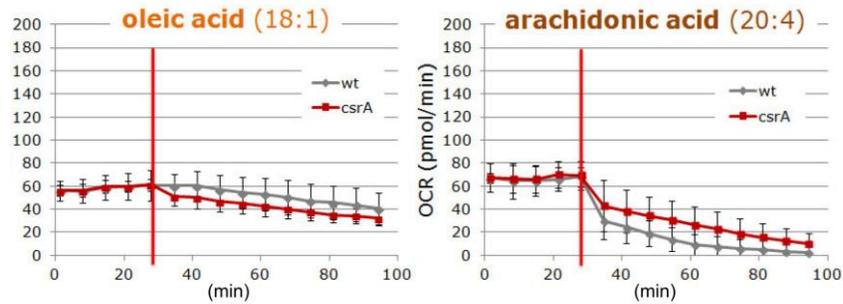
Figure 5-1: Oxygen consumption experiments with oleic acid and arachidonic acid. Bacterial respiration, expressed as OCR, was quantified using an XFe96 Extracellular Flux Analyzer according to the manufacturer instructions (Seahorse Bioscience). Basal OCR was measured prior to the injection to assure uniform cellular seeding (see section 2.2.2.3). OCR of *L. pneumophila* wild-type compared to its *csrA* mutant were measured in presents of oleic acid and arachidonic acid. Both substrates were used in a concentration of 0.1 mM. (Adapted from Tobias Sahr, Institut Pasteur in Paris)
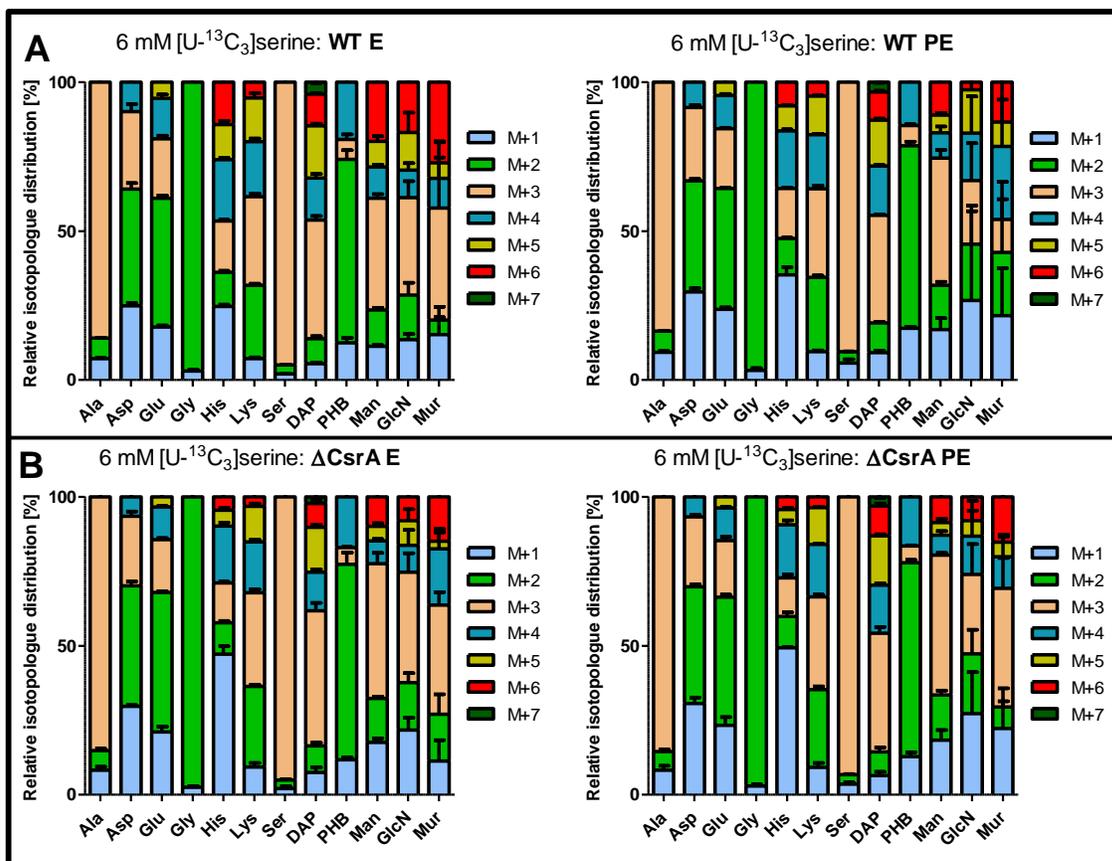
Figure 5-2: [13]C Isotopologue patterns from experiments with *L. pneumophila* using [U-[13]C$_3$]serine as precursor. Shown are relative isotopologue distributions (mol%) in ^{13}C enriched metabolites (^{13}C-excess > 0.5 mol%) of *L. pneumophila* wild-type (**A**) and the *csrA* mutant (**B**). Bacterial stains were cultures in CE MDM in presents of **6 mM [U-[13]C$_3$]serine**. Harvest of cell occurred at E phase (OD$_{600}$ = 0.35) as well as in PE phase (OD$_{600}$ = 0.80). Isotopologue distributions where calculated by isotopologue profiling and display means and SDs of six values (3 technical replicates x 2 biological replicates). Shown are relative fractions (%) of isotopologues (M+1 to M+7). For numerical values, see **Table 5-5**.
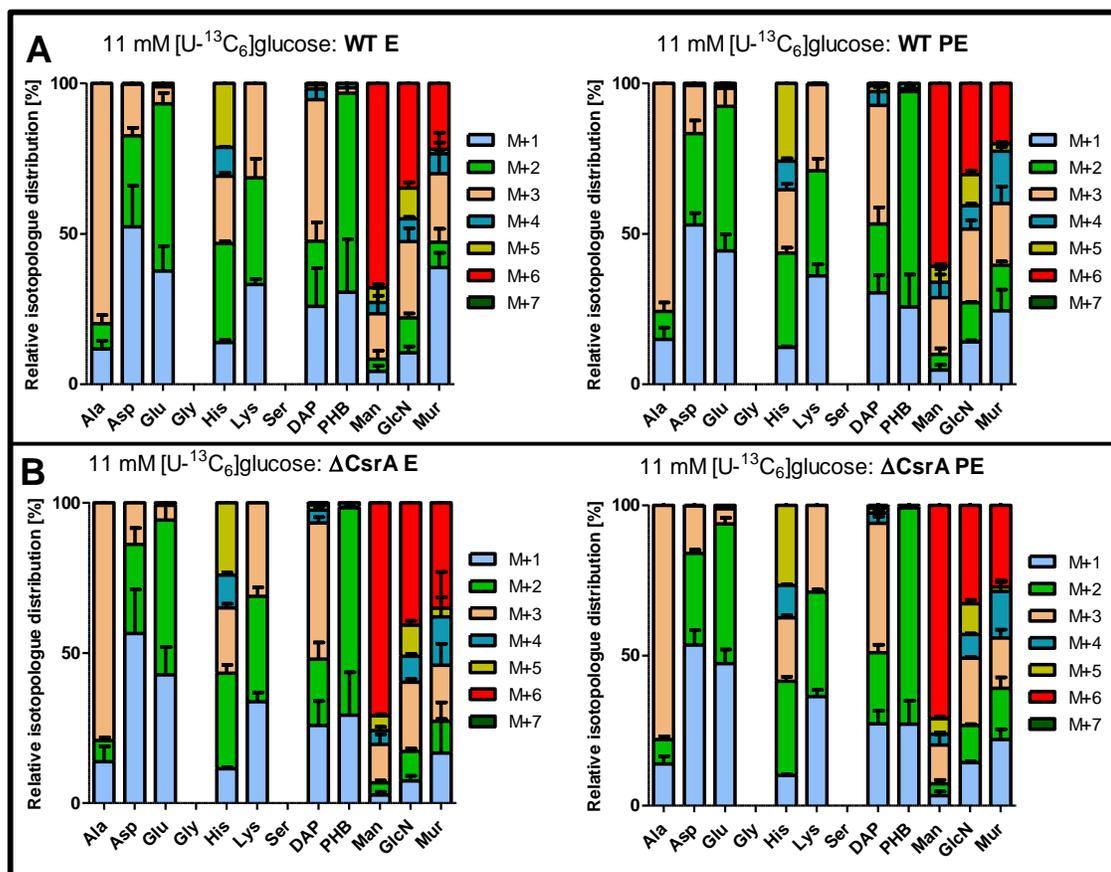
Figure 5-3: ^{13}C Isotopologue patterns from experiments with *L. pneumophila* using [U-^{13}C$_6$]glucose as precursor. Shown are relative isotopologue distributions (mol%) in ^{13}C enriched metabolites (^{13}C-excess > 0.5 mol%) of *L. pneumophila* wild-type (**A**) and the *csrA* mutant (**B**). Bacterial stains were cultures in CE MDM in presents of **11 mM [U-^{13}C$_6$]glucose**. Harvest of cell occurred at E phase (OD$_{600}$ = 0.35) as well as in PE phase (OD$_{600}$ = 0.80). Isotopologue distributions where calculated by isotopologue profiling and display means and SDs of six values (3 technical replicates x 2 biological replicates). Shown are relative fractions (%) of isotopologues (M+1 to M+7). For numerical values, see **Table 5-6**.
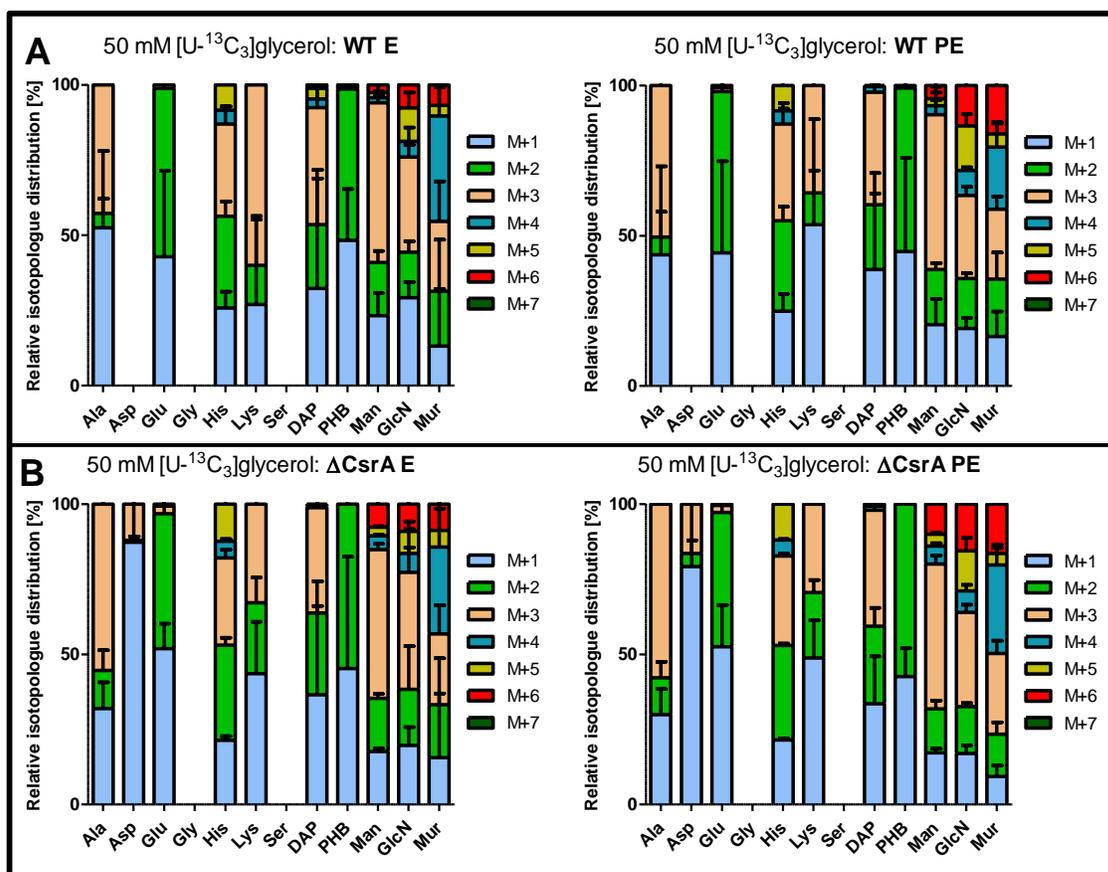
Figure 5-4: [13]C Isotopologue patterns from experiments with *L. pneumophila* using [U-[13]C$_3$]glycerol as precursor. Shown are relative isotopologue distributions (mol%) in ^{13}C enriched metabolites (^{13}C-excess > 0.5 mol%) of *L. pneumophila* wild-type (**A**) and the *csrA* mutant (**B**). Bacterial stains were cultures in CE MDM in presents of **50 mM [U-[13]C$_3$]glycerol**. Harvest of cell occurred at E phase (OD$_{600}$ = 0.35) as well as in PE phase (OD$_{600}$ = 0.80). Isotopologue distributions where calculated by isotopologue profiling and display means and SDs of six values (3 technical replicates x 2 biological replicates). Shown are relative fractions (%) of isotopologues (M+1 to M+7). For numerical values, see **Table 5-7.**
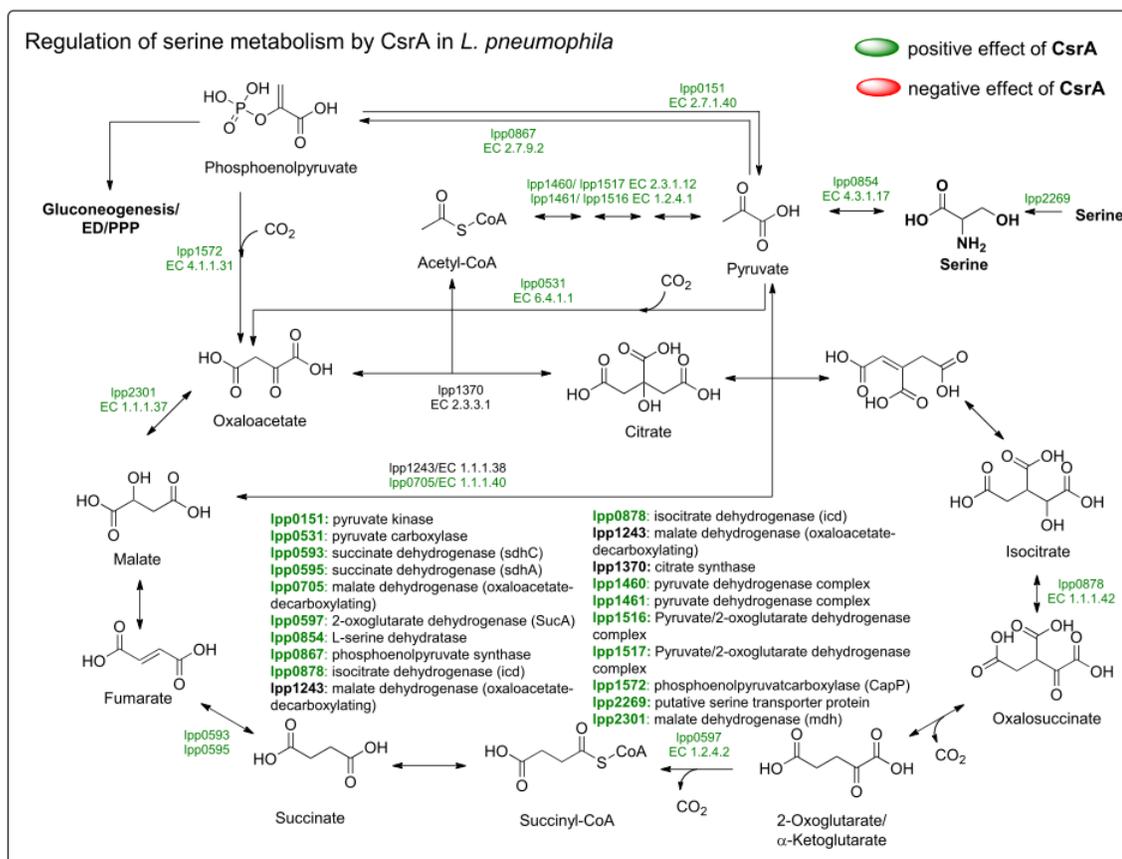
Figure 5-5: CsrA related regulation of serine metabolism in *L. pneumophila* based on extensive transcriptome and proteome analysis in combination with RNA-Co-immunoprecipitation experiments followed by deep sequencing of the wild-type and its *csrA* mutant (Sahr *et al.*, 2017). In total 516 RNAs have been identified to be affected by CsrA. Based on these data, this figure illustrates positive effects in green and enzymes which are negatively affected are indicated in red (Sahr *et al.*, 2017). In short, CsrA seems to positively affect enzymes of the TCA cycle as well as serine incorporation during E phase in *L. pneumophila*.
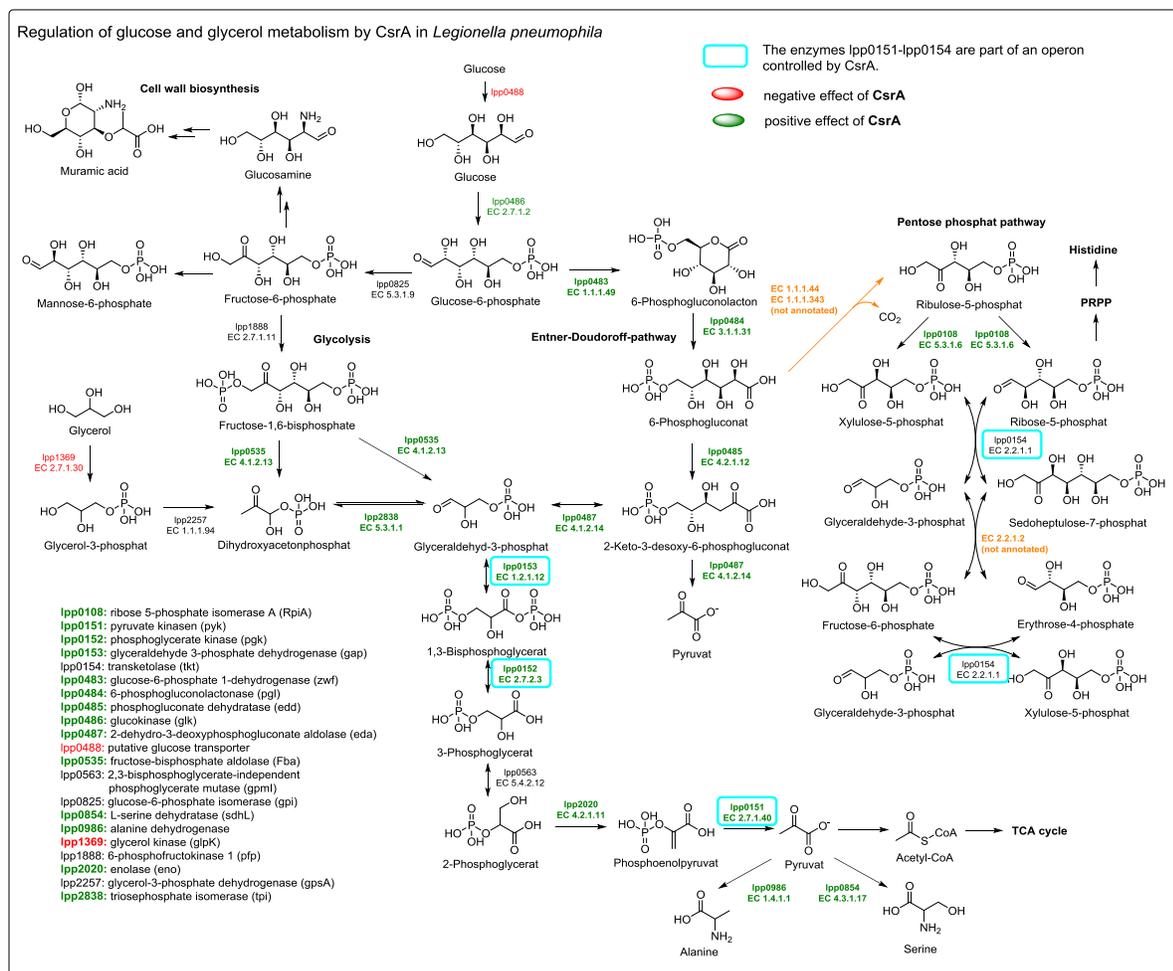
Figure 5-6: CsrA related regulation of glucose and glycerol metabolism in *L. pneumophila* based on extensive transcriptome and proteome analysis in combination with RNA-Co-immunoprecipitation experiments followed by deep sequencing of the wild-type and its *csrA* mutant (Sahr *et al.*, 2017). In total 516 RNAs have been identified to be affected by CsrA. Based on these data, this figure illustrates positive effects in green and enzymes which are negatively affected are indicated in red (Sahr *et al.*, 2017). In short, CsrA seems to positively effect enzymes of the ED pathway, glycolytic and gluconeogenetic reactions during E growth phase. On the other hand, CsrA negatively affect the uptake of glucose as well as glycerol metabolism.
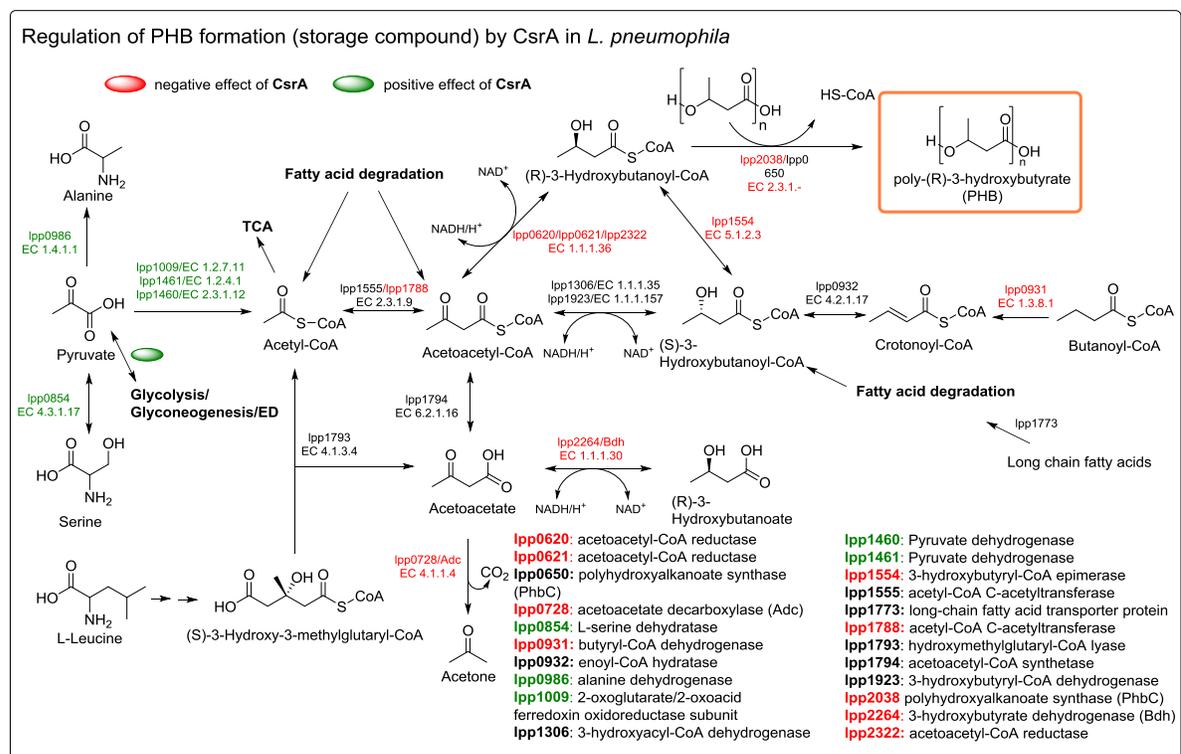
Figure 5-7: CsrA related regulation of PHB metabolism in *L. pneumophila* based on extensive transcriptome and proteome analysis in combination with RNA-Co-immunoprecipitation experiments followed by deep sequencing of the wild-type and its *csrA* mutant (Sahr *et al.*, 2017). In total 516 RNAs have been identified to be affected by CsrA. Based on these data, this figure illustrates positive effects in green and enzymes which are negatively affected are indicated in red (Sahr *et al.*, 2017). In short, CsrA seems to negatively affect PHB biosynthesis during E growth phase.

5. SUPPLEMENTARY MATERIAL

Table 5-1: ^{13}C-Excess (mol%) of protein-derived amino acids, DAP, PHB, Man, GlcN and Mur from experiments with *L. pneumophila* wild-type and its *csrA* mutant in presents of **6 mM [U-[13]C$_3$]serine**. Labeling experiments were performed in CE MDM. Harvest of bacterial cells occurred at E phase (OD_{600} = 0.35) and PE phase (OD_{600} = 0.80). Data are means and SDs of six values (3 technical replicates x 2 biological replicates).

[U-[13]C$_3$]serine	WT E	WT PE	ΔCsrA E	ΔCsrA PE
Ala	59.14% ± 2.60%	63.22% ± 0.79%	56.73% ± 0.62%	62.63% ± 1.20%
Asp	23.17% ± 1.98%	25.87% ± 0.51%	19.03% ± 0.84%	22.13% ± 0.07%
Glu	20.19% ± 1.03%	24.77% ± 0.15%	16.91% ± 0.19%	21.66% ± 0.85%
Gly	18.02% ± 0.70%	16.73% ± 1.33%	14.50% ± 0.15%	14.18% ± 1.51%
Ile	0.04% ± 0.01%	0.06% ± 0.02%	0.05% ± 0.02%	0.06% ± 0.01%
Leu	0.01% ± 0.00%	0.01% ± 0.01%	0.01% ± 0.01%	0.01% ± 0.01%
Lys	37.06% ± 2.48%	40.66% ± 0.80%	33.18% ± 1.07%	37.50% ± 0.48%
Phe	0.13% ± 0.07%	0.12% ± 0.06%	0.12% ± 0.06%	0.13% ± 0.07%
Pro	0.23% ± 0.04%	0.35% ± 0.03%	0.25% ± 0.04%	0.28% ± 0.05%
Ser	82.59% ± 0.61%	82.69% ± 0.24%	87.13% ± 8.61%	84.91% ± 3.21%
Tyr	0.07% ± 0.03%	0.09% ± 0.02%	0.11% ± 0.05%	0.07% ± 0.06%
Val	0.04% ± 0.03%	0.03% ± 0.02%	0.01% ± 0.01%	0.04% ± 0.02%
DAP	38.48% ± 1.44%	43.51% ± 0.40%	33.20% ± 1.84%	43.41% ± 0.78%
PHB	26.98% ± 2.98%	28.84% ± 0.94%	26.56% ± 1.70%	29.73% ± 0.87%
His	37.87% ± 2.99%	36.48% ± 0.65%	25.91% ± 0.72%	28.40% ± 2.46%
Man	24.95% ± 2.49%	19.56% ± 1.63%	13.13% ± 0.65%	12.99% ± 0.75%
GlcN	24.14% ± 2.19%	20.48% ± 4.99%	13.99% ± 3.22%	17.08% ± 3.99%
Mur	32.62% ± 6.07%	31.96% ± 6.56%	24.03% ± 2.07%	27.54% ± 4.41%

Table 5-2: ^{13}C-Excess (mol%) of protein-derived amino acids, DAP, PHB, Man, GlcN and Mur from experiments with *L. pneumophila* wild-type and its *csrA* mutant in presents of **11 mM [U-^{13}C$_6$]glucose.** Labeling experiments were performed in CE MDM. Harvest of bacterial cells occurred at E phase (OD$_{600}$ = 0.35) and PE phase (OD$_{600}$ = 0.80). Data are means and SDs of six values (3 technical replicates x 2 biological replicates).

[U-^{13}C$_6$]glucose	WT E	WT PE	ΔCsrA E	ΔCsrA PE
Ala	3.95% ± 0.23%	6.30% ± 0.94%	4.15% ± 0.23%	4.80% ± 0.10%
Asp	1.57% ± 0.20%	3.13% ± 0.42%	1.53% ± 0.26%	2.09% ± 0.07%
Glu	1.50% ± 0.04%	2.77% ± 0.46%	1.41% ± 0.61%	1.86% ± 0.07%
Gly	0.10% ± 0.09%	0.11% ± 0.04%	0.07% ± 0.05%	0.12% ± 0.09%
Ile	0.06% ± 0.04%	0.05% ± 0.02%	0.06% ± 0.01%	0.06% ± 0.03%
Leu	0.02% ± 0.02%	0.01% ± 0.01%	0.01% ± 0.01%	0.01% ± 0.00%
Lys	2.31% ± 0.17%	3.98% ± 0.46%	2.55% ± 0.18%	3.19% ± 0.04%
Phe	0.09% ± 0.04%	0.12% ± 0.01%	0.09% ± 0.04%	0.08% ± 0.02%
Pro	0.22% ± 0.03%	0.24% ± 0.04%	0.22% ± 0.04%	0.24% ± 0.04%
Ser	0.22% ± 0.08%	0.36% ± 0.20%	0.19% ± 0.06%	0.16% ± 0.03%
Tyr	0.10% ± 0.03%	0.08% ± 0.02%	0.06% ± 0.02%	0.10% ± 0.05%
Val	0.04% ± 0.03%	0.02% ± 0.02%	0.02% ± 0.01%	0.05% ± 0.03%
DAP	3.21% ± 058%	5.19% ± 1.33%	3.42% ± 0.27%	3.76% ± 0.12%
PHB	1.76% ± 0.67%	3.17% ± 1.35%	1.72% ± 0.32%	1.99% ± 0.28%
His	19.93% ± 0.67%	26.97% ± 2.05%	23.62% ± 2.53%	28.59% ± 0.14%
Man	46.94% ± 9.19%	61.03% ± 9.50%	61.08% ± 2.38%	60.70% ± 13.10%
GlcN	31.62% ± 4.59%	36.68% ± 4.53%	38.91% ± 2.25%	34.47% ± 1.58%
Mur	16.58% ± 2.20%	28.51% ± 1.34%	21.57% ± 11.48%	25.05% ± 2.77%

Table 5-3: ^{13}C-Excess (mol%) of protein-derived amino acids, DAP, PHB, Man, GlcN and Mur from experiments with *L. pneumophila* wild-type and its *csrA* mutant in presents of **50 mM [U-^{13}C$_3$]glycerol**. Labeling experiments were performed in CE MDM. Harvest of bacterial cells occurred at E phase (OD$_{600}$ = 0.35) and PE phase (OD$_{600}$ = 0.80). Data are means and SDs of six values (3 technical replicates x 2 biological replicates).

[U-^{13}C$_3$]glycerol	WT E	WT PE	ΔCsrA E	ΔCsrA PE
Ala	0.51% ± 0.11%	0.83% ± 0.27%	1.11% ± 0.05%	1.42% ± 0.16%
Asp	0.24% ± 0.07%	0.33% ± 0.23%	0.49% ± 0.05%	0.63% ± 0.09%
Glu	0.27% ± 0.05%	0.48% ± 0.19%	0.48% ± 0.03%	0.77% ± 0.12%
Gly	0.08% ± 0.07%	0.03% ± 0.06%	0.08% ± 0.04%	0.08% ± 0.08%
Ile	0.08% ± 0.04%	0.07% ± 0.05%	0.09% ± 0.04%	0.07% ± 0.05%
Leu	0.06% ± 0.06%	0.06% ± 0.06%	0.06% ± 0.05%	0.04% ± 0.04%
Lys	0.33% ± 0.06%	0.57% ± 0.18%	0.71% ± 0.04%	0.94% ± 0.13%
Phe	0.16% ± 0.11%	0.16% ± 0.09%	0.15% ± 0.08%	0.16% ± 0.08%
Pro	0.31% ± 0.05%	0.26% ± 0.07%	0.26% ± 0.07%	0.27% ± 0.14%
Ser	0.14% ± 0.04%	0.12% ± 0.06%	0.16% ± 0.06%	0.13% ± 0.04%
Tyr	0.12% ± 0.05%	0.11% ± 0.06%	0.11% ± 0.03%	0.13% ± 0.03%
Val	0.04% ± 0.03%	0.04% ± 0.06%	0.04% ± 0.04%	0.05% ± 0.03%
DAP	0.55% ± 0.11%	1.08% ± 0.11%	0.98% ± 0.08%	1.56% ± 0.14%
PHB	0.57% ± 0.23%	0.49% ± 0.17%	0.49% ± 0.19%	0.68% ± 0.19%
His	5.45% ± 0.90%	6.40% ± 1.08%	13.79% ± 1.35%	13.99% ± 0.03%
Man	4.22% ± 0.98%	6.27% ± 1.24%	12.70% ± 0.56%	16.00% ± 0.79%
GlcN	6.56% ± 1.42%	18.35% ± 2.44%	13.44% ± 2.03%	23.35% ± 5.19%
Mur	8.61% ± 1.58%	20.39% ± 5.24%	19.65% ± 5.43%	28.21% ± 5.14%

Table 5-4: ^{13}C-Excess (mol%) of protein-derived amino acids, DAP, PHB, LACT and STE from experiments with *L. pneumophila* wild-type and its *csrA* mutant in present of **0.8 mM [1,2,3,4-^{13}C$_4$]palmitic acid**. Labeling experiments were performed in CE MDM. Harvest of bacterial cells occurred at E phase (OD$_{600}$ = 0.35) and PE phase (17d). Data are means and SDs of six values (3 technical replicates x 2 biological replicates).

0.8 mM [1.2.3.4-^{13}C$_4$]palmitic acid	WT E	WT PE	ΔCsrA E	ΔCsrA PE
Ala	0.14% ± 0.07%	0.12% ± 0.05%	0.19% ± 0.05%	0.14% ± 0.03%
Asp	0.27% ± 0.05%	0.17% ± 0.06%	0.44% ± 0.09%	0.23% ± 0.04%
Glu	0.50% ± 0.03%	0.52% ± 0.06%	0.78% ± 0.08%	0.54% ± 0.07%
Gly	0.06% ± 0.06%	0.10% ± 0.06%	0.07% ± 0.04%	0.07% ± 0.07%
His	0.13% ± 0.03%	0.15% ± 0.09%	0.16% ± 0.09%	0.24% ± 0.14%
Ile	0.12% ± 0.04%	0.07% ± 0.03%	0.14% ± 0.05%	0.07% ± 0.02%
Leu	0.07% ± 0.03%	0.01% ± 0.01%	0.12% ± 0.07%	0.02% ± 0.01%
Lys	0.22% ± 0.07%	0.18% ± 0.09%	0.22% ± 0.07%	0.23% ± 0.05%
Phe	0.18% ± 0.02%	0.13% ± 0.04%	0.19% ± 0.04%	0.22% ± 0.02%
Pro	0.00% ± 0.00%	0.03% ± 0.04%	0.00% ± 0.00%	0.06% ± 0.05%
Ser	0.17% ± 0.04%	0.14% ± 0.05%	0.17% ± 0.26%	0.20% ± 0.04%
Tyr	0.14% ± 0.06%	0.15% ± 0.07%	0.18% ± 0.05%	0.15% ± 0.09%
Val	0.04% ± 0.03%	0.06% ± 0.03%	0.09% ± 0.08%	0.08% ± 0.06%
DAP	0.18% ± 0.06%	0.11% ± 0.10%	0.56% ± 0.23%	0.31% ± 0.35%
PHB	2.79% ± 1.52%	3.36% ± 0.91%	4.93% ± 0.35%	6.32% ± 0.76%
LACT	0.16% ± 0.06%	0.28% ± 0.29%	0.16% ± 0.19%	0.30% ± 0.18%
STE	0.19% ± 0.02%	0.35% ± 0.23%	0.41% ± 0.12%	0.45% ± 0.05%

Table 5-5: Relative fractions of isotopologues (mol%) of protein-derived amino acids, DAP, PHB, Man, GlcN and Mur from experiments with *L. pneumophila* wild-type and its *csrA* mutant in presents of **6 mM [U-^{13}C$_3$]serine**. Labeling experiments were performed in CE MDM using. M+X represents the mass of the unlabeled metabolite plus X labeled ^{13}C-atoms. Data are means and SDs of six values (3 technical replicates x 2 biological replicates).

[U-^{13}C$_3$]serine: WT E						
	M+1	**M+2**	**M+3**	**M+4**	**M+5**	**M+6**	**M+7**
Ala	4.55% ± 0.16%	4.40% ± 0.06%	54.68% ± 2.63%				
Asp	10.46% ± 0.39%	16.43% ± 0.86%	10.92% ± 1.08%	4.15% ± 0.68%			
Glu	7.29% ± 0.22%	17.77% ± 0.39%	8.17% ± 0.43%	5.59% ± 0.52%	2.24% ± 0.25%		
Gly	0.57% ± 0.06%	17.73% ± 0.71%					
His	17.23% ± 0.45%	8.03% ± 0.32%	11.93% ± 0.27%	14.38% ± 0.40%	8.23% ± 0.86%	9.91% ± 2.16%	
Lys	4.92% ± 0.32%	16.87% ± 0.37%	20.33% ± 0.75%	12.62% ± 0.79%	10.06% ± 1.06%	3.66% ± 0.63%	
Ser	1.75% ± 0.05%	2.59% ± 0.07%	80.28% ± 0.59%				
DAP	3.95% ± 0.26%	5.91% ± 0.65%	28.43% ± 0.99%	10.07% ± 0.99%	12.46% ± 0.50%	7.60% ± 0.26%	2.87% ± 0.22%
PHB	5.82% ± 0.78%	28.53% ± 1.42%	3.11% ± 0.78%	8.92% ± 1.58%			
Man	4.81% ± 0.18%	5.22% ± 0.30%	15.90% ± 0.56%	4.48% ± 0.29%	3.67% ± 0.68%	8.41% ± 2.00%	
GlcN	5.71% ± 0.81%	6.34% ± 1.75%	13.78% ± 2.33%	3.91% ± 0.99%	5.34% ± 2.84%	7.13% ± 1.77%	
Mur	8.12% ± 3.16%	2.66% ± 2.33%	20.05% ± 11.78%	5.35% ± 3.71%	2.76% ± 3.86%	14.48% ± 4.97%	

[U-^{13}C$_3$]serine: WT PE						
	M+1	**M+2**	**M+3**	**M+4**	**M+5**	**M+6**	**M+7**
Ala	6.47% ± 0.28%	4.87% ± 0.11%	57.82% ± 0.77%				
Asp	14.48% ± 0.58%	18.18% ± 0.30%	11.99% ± 0.45%	4.17% ± 0.12%			
Glu	12.66% ± 0.36%	21.62% ± 0.14%	10.72% ± 0.18%	5.96% ± 0.27%	2.38% ± 0.10%		
Gly	0.56% ± 0.12%	16.44% ± 1.28%					
His	27.92% ± 1.97%	9.63% ± 0.24%	13.27% ± 0.20%	15.25% ± 0.43%	6.64% ± 0.19%	6.28% ± 0.17%	
Lys	7.40% ± 0.34%	19.42% ± 0.48%	23.05% ± 0.87%	14.11% ± 0.26%	10.08% ± 0.13%	3.63% ± 0.09%	
Ser	4.99% ±1.12%	3.26% ± 0.19%	78.85% ± 0.28%				
DAP	7.77% ± 0.53%	8.38% ± 0.34%	30.52% ± 0.32%	14.03% ± 0.27%	12.98% ± 0.51%	8.05% ± 0.26%	2.74% ± 0.16%
PHB	9.18% ± 0.28%	32.33% ± 0.73%	3.62% ± 0.22%	7.66% ± 0.52%			
Man	6.53% ± 1.46%	5.71% ± 0.47%	16.44% ± 1.06%	3.29% ± 0.81%	2.27% ± 0.26%	4.26% ± 0.92%	
GlcN	11.71% ± 13.14%	8.29% ± 5.64%	9.36% ± 5.47%	6.96% ± 5.43%	6.36% ± 5.82%	1.15% ± 1.00%	
Mur	13.11% ± 9.66%	12.85% ± 10.80%	6.68% ± 7.67%	14.87% ± 9.49%	4.94% ± 8.46%	8.12% ± 7.87%	

[U-^{13}C$_3$]serine: ΔCsrA E						
	M+1	**M+2**	**M+3**	**M+4**	**M+5**	**M+6**	**M+7**
Ala	5.08% ± 0.71%	4.04% ± 0.35%	52.34% ± 1.05%				
Asp	10.94% ± 0.18%	14.94% ± 0.51%	8.59% ± 0.58%	2.38% ± 0.22%			
Glu	7.80% ± 0.65%	17.31% ± 0.16%	6.55% ± 0.20%	4.05% ± 0.12%	1.25% ± 0.11%		
Gly	0.37% ± 0.06%	14.31% ± 0.14%					
His	30.77% ± 1.77%	6.84% ± 0.44%	8.79% ± 0.24%	12.46% ± 0.77%	3.48% ± 0.52%	2.90% ± 0.20%	
Lys	6.12% ± 0.82%	17.66% ± 0.38%	20.55% ± 0.72%	11.18% ± 0.46%	7.77% ± 0.56%	2.07% ± 0.21%	
Ser	1.81% ± 0.73%	2.67% ± 0.21%	84.74% ± 8.71%				
DAP	4.95% ± 1.11%	5.92% ± 0.63%	29.88% ± 1.80%	8.60% ± 0.60%	9.92% ± 0.59%	5.27% ± 0.37%	1.47% ± 0.31%
PHB	5.49% ± 0.34%	30.61% ± 1.81%	2.62% ± 0.11%	7.92% ± 0.88%			
Man	4.67% ± 0.37%	3.92% ± 0.15%	11.99% ± 0.93%	2.00% ± 0.19%	1.32% ± 0.27%	2.61% ± 0.32%	
GlcN	6.30% ± 1.20%	4.59% ± 0.92%	10.72% ± 1.85%	2.63% ± 1.51%	2.39% ± 1.11%	2.30% ± 1.01%	
Mur	4.98% ± 3.04%	6.82% ± 2.94%	16.00% ± 1.93%	8.24% ± 2.93%	1.14% ± 1.27%	6.49% ± 1.65%	

[U-^{13}C$_3$]serine: ΔCsrA PE						
	M+1	**M+2**	**M+3**	**M+4**	**M+5**	**M+6**	**M+7**
Ala	5.58% ± 1.02%	4.25% ± 0.55%	57.93% ± 0.53%				
Asp	13.18% ± 0.86%	16.81% ± 0.39%	10.09% ± 0.31%	2.87% ± 0.18%			
Glu	11.04% ± 1.29%	20.35% ± 0.43%	9.01% ± 0.61%	5.19% ± 0.10%	1.75% ± 0.06%		
Gly	0.43% ± 0.07%	13.97% ± 1.49%					
His	36.30% ± 0.18%	7.73% ± 1.06%	9.55% ± 0.85%	13.13% ± 1.05%	3.70% ± 0.48%	3.16% ± 0.59%	
Lys	6.68% ± 1.10%	19.05% ± 0.82%	22.72% ± 0.53%	12.86% ± 0.23%	8.95% ± 0.26%	2.65% ± 0.08%	
Ser	3.11% ± 0.53%	2.82% ± 0.25%	81.99% ± 2.88%				
DAP	5.27% ± 1.06%	6.54% ± 1.21%	32.62% ± 1.71%	13.19% ± 0.62%	13.63% ± 0.38%	8.22% ± 0.69%	2.49% ± 0.29%
PHB	6.76% ± 0.77%	34.25% ± 0.49%	2.96% ± 0.13%	8.69% ± 0.78%			
Man	4.94% ± 0.92%	4.10% ± 0.39%	12.65% ± 0.20%	1.79% ± 0.38%	1.16% ± 0.35%	2.32% ± 0.33%	
GlcN	10.25% ± 5.20%	7.52% ± 3.06%	10.03% ± 3.83%	4.84% ± 4.41%	1.94% ± 1.29%	3.00% ± 2.65%	
Mur	11.72% ± 4.79%	3.76% ± 3.33%	21.00% ± 5.35%	5.54% ± 3.91%	2.57% ± 0.99%	8.00% ± 4.85%	

Table 5-6: Relative fractions of isotopologues (mol%) of protein-derived amino acids, DAP, PHB, Man, GlcN and Mur from experiments with *L. pneumophila* wild-type and its *csrA* mutant in presents of **11 mM [U-^{13}C$_6$]glucose**. Labeling experiments were performed in CE MDM. M+X represents the mass of the unlabeled metabolite plus X labeled ^{13}C-atoms. Data are means and SDs of six values (3 technical replicates x 2 biological replicates).

	M+1	M+2	M+3	M+4	M+5	M+6	M+7
[U-^{13}C$_6$]glucose: WT E							
Ala	0.52% ± 0.12%	0.37% ± 0.13%	3.53% ± 0.20%				
Asp	1.98% ± 0.52%	1.15% ± 0.10%	0.65% ± 0.06%	0.01% ± 0.01%			
Glu	1.65% ± 0.36%	2.43% ± 0.16%	0.25% ± 0.03%	0.02% ± 0.02%	0.03% ± 0.01%		
Gly							
His	5.72% ± 0.31%	13.44% ± 0.32%	9.15% ± 0.52%	3.93% ± 0.08%	8.75% ± 1.00%	0.00% ± 0.00%	
Lys	2.31% ± 0.13%	2.48% ± 0.44%	2.19% ± 0.14%	0.00% ± 0.00%	0.00% ± 0.00%	0.00% ± 0.00%	
Ser							
DAP	2.47% ± 1.22%	2.08% ± 0.59%	4.49% ± 0.74%	0.34% ± 0.15%	0.13% ± 0.08%	0.04% ± 0.04%	0.01% ± 0.03%
PHB	1.23% ± 0.71%	2.67% ± 0.98%	0.07% ± 0.16%	0.06% ± 0.05%			
Man	2.42% ± 1.05%	2.25% ± 1.61%	8.41% ± 4.86%	2.12% ± 1.19%	2.73% ± 0.62%	37.89% ± 13.91%	
GlcN	4.98% ± 0.96%	5.49% ± 0.72%	12.01% ± 2.13%	3.60% ± 0.32%	4.85% ± 0.91%	16.51% ± 2.74%	
Mur	13.34% ± 1.67%	2.90% ± 1.53%	7.81% ± 2.76%	2.28% ± 2.40%	0.50% ± 0.78%	7.55% ± 1.40%	
[U-^{13}C$_6$]glucose: WT PE							
Ala	1.08% ± 0.29%	0.67% ± 0.22%	5.50% ± 0.82%				
Asp	4.02% ± 0.30%	2.30% ± 0.33%	1.21% ± 0.21%	0.06% ± 0.04%			
Glu	3.71% ± 0.45%	4.01% ± 0.64%	0.50% ± 0.17%	0.08% ± 0.05%	0.06% ± 0.02%		
Gly							
His	6.48% ± 0.20%	16.58% ± 1.00%	11.21% ± 1.07%	5.06% ± 0.47%	13.67% ± 1.03%	0.00% ± 0.00%	
Lys	4.45% ± 0.46%	4.30% ± 0.51%	3.54% ± 0.37%	0.02% ± 0.03%	0.03% ± 0.04%	0.00% ± 0.00%	
Ser							
DAP	4.84% ± 0.95%	3.65% ± 0.89%	6.28% ± 1.64%	0.73% ± 0.26%	0.31% ± 0.16%	0.13% ± 0.07%	0.01% ± 0.01%
PHB	1.82% ± 0.76%	5.06% ± 2.09%	0.07% ± 0.09%	0.13% ± 0.07%			
Man	3.58% ± 1.39%	3.96% ± 1.51%	14.26% ± 7.23%	3.92% ± 1.86%	4.01% ± 0.53%	46.03% ± 16.40%	
GlcN	8.17% ± 0.35%	7.56% ± 0.18%	14.27% ± 1.72%	4.53% ± 0.38%	6.02% ± 0.77%	17.63% ± 3.24%	
Mur	13.11% ± 3.76%	8.07% ± 0.73%	11.08% ± 2.99%	9.29% ± 0.83%	1.31% ± 0.39%	10.81% ± 0.46%	
[U-^{13}C$_6$]glucose: ΔCsrA E							
Ala	0.65% ± 0.24%	0.33% ± 0.05%	3.71% ± 0.19%				
Asp	2.19% ± 0.57%	1.15% ± 0.21%	0.54% ± 0.09%	0.00% ± 0.01%			
Glu	1.83% ± 0.40%	2.21% ± 0.22%	0.21% ± 0.07%	0.01% ± 0.01%	0.03% ± 0.00%		
Gly							
His	5.35% ± 0.26%	14.78% ± 1.30%	10.12% ± 0.65%	5.08% ± 0.39%	11.22% ± 1.81%	0.00% ± 0.00%	
Lys	2.61% ± 0.24%	2.72% ± 0.23%	2.41% ± 0.22%	0.00% ± 0.00%	0.00% ± 0.00%	0.00% ± 0.00%	
Ser							
DAP	2.63% ± 0.83%	2.25% ± 0.56%	4.60% ± 0.20	0.44% ± 0.12%%	0.17% ± 0.08%	0.07% ± 0.05%	0.01% ± 0.01%
PHB	1.16% ± 0.57%	2.74% ± 0.43%	0.01% ± 0.01%	0.06% ± 0.02%			
Man	1.98% ± 0.67%	2.78% ± 0.59%	9.07% ± 2.37%	3.26% ± 0.94%	3.46% ± 0.37%	50.23% ± 0.55%	
GlcN	4.10% ± 0.90%	5.32% ± 0.56%	12.59% ± 0.61%	4.76% ± 0.36%	5.65% ± 0.82%%	22.28% ± 1.23%	
Mur	5.64% ± 3.82%	3.56% ± 2.14%	6.29% ± 2.42%	5.46% ± 5.03%	0.98% ± 1.22%	11.85% ± 8.81%	
[U-^{13}C$_6$]glucose: ΔCsrA PE							
Ala	0.76% ± 0.14%	0.44% ± 0.06%	4.26% ± 0.06%				
Asp	2.75% ± 0.25%	1.57% ± 0.06%	0.81% ± 0.07%	0.01% ± 0.02%			
Glu	2.72% ± 0.27%	2.68% ± 0.12%	0.29% ± 0.03%	0.03% ± 0.02%	0.04% ± 0.00%		
Gly							
His	5.58% ± 0.21%	17.18% ± 0.76%	11.56% ± 0.49%	5.92% ± 0.22%	14.65% ± 0.53%	0.00% ± 0.00%	
Lys	3.62% ± 0.21%	3.45% ± 0.09%	2.88% ± 0.11%	0.00% ± 0.00%	0.00% ± 0.00%	0.00% ± 0.00%	
Ser							
DAP	3.09% ± 0.51%	2.69% ± 0.31%	4.90% ± 0.25%	0.39% ± 0.10%	0.18% ± 0.13%	0.09% ± 0.04%	0.02% ± 0.03%
PHB	1.24% ± 0.36%	3.30% ± 0.43%	0.01% ± 0.01%	0.03% ± 0.04%			
Man	2.35% ± 1.01%	2.78% ± 0.94%	9.13% ± 2.49%	2.55% ± 0.43%	3.63% ± 0.41%	50.09% ± 16.03%	
GlcN	7.68% ± 0.23%	6.65% ± 0.24%	11.99% ± 0.25%	4.28% ± 0.14%	5.44% ± 0.71%	17.59% ± 1.22%	
Mur	9.78% ± 1.52%	7.55% ± 1.61%	7.45% ± 1.19%	6.80% ± 1.65%	0.68% ± 0.78%	12.08% ± 2.48%	

Table 5-7: Relative fractions of isotopologues (mol%) of protein-derived amino acids, DAP, PHB, Man, GlcN and Mur from experiments with *L. pneumophila* wild-type and its *csrA* mutant in presents of **50 mM [U-^{13}C$_3$]glycerol**. Labeling experiments were performed in CE MDM. M+X represents the mass of the unlabeled metabolite plus X labeled ^{13}C-atoms. Data are means and SDs of six values (3 technical replicates x 2 biological replicates*)*.

[U-^{13}C$_3$]glycerol: WT E						
	M+1	**M+2**	**M+3**	**M+4**	**M+5**	**M+6**	**M+7**
Ala	0,43% ± 0,21%	0,04% ± 0,04%	0,35% ± 0,03%				
Asp							
Glu	0,36% ± 0,24%	0,47% ± 0,08%	0,01% ± 0,03%	0,00% ± 0,00%	0,00% ± 0,01%		
Gly							
His	3,53% ± 0,75%	4,17% ± 0,67%	4,20% ± 0,80%	0,62% ± 0,17%	1,16% ± 0,09%	0,00% ± 0,00%	
Lys	0,23% ± 0,25%	0,11% ± 0,13%	0,51% ± 0,04%	0,00% ± 0,00%	0,00% ± 0,00%	0,00% ± 0,00%	
Ser							
DAP	0,55% ± 0,62%	0,36% ± 0,31%	0,66% ± 0,22%	0,05% ± 0,06%	0,06% ± 0,12%	0,01% ± 0,02%	0,01% ± 0,02%
PHB	0,71% ± 0,25%	0,74% ± 0,48%	0,01% ± 0,03%	0,01% ± 0,02%			
Man	2,37% ± 0,76%	1,79% ± 0,40%	5,41% ± 1,38%	0,16% ± 0,08%	0,18% ± 0,04%	0,26% ± 0,08%	
GlcN	4,15% ± 0,74%	2,15% ± 0,52%	4,49% ± 0,59%	0,74% ± 0,65%	1,58% ± 0,73%	1,09% ± 0,71%	
Mur	2,15% ± 3,07%	2,95% ± 2,79%	3,77% ± 2,17%	5,70% ± 2,05%	0,59% ± 0,97%	1,10% ± 0,88%	

[U-^{13}C$_3$]glycerol: WT PE						
	M+1	**M+2**	**M+3**	**M+4**	**M+5**	**M+6**	**M+7**
Ala	0,52% ± 0,35%	0,07% ± 0,10%	0,60% ± 0,12%				
Asp							
Glu	0,67% ± 0,46%	0,81% ± 0,28%	0,02% ± 0,02%	0,00% ± 0,00%	0,01% ± 0,01%		
Gly							
His	3,98% ± 0,92%	4,80% ± 0,75%	5,14% ± 1,09%	0,69% ± 0,12%	1,34% ± 0,14%	0,00% ± 0,00%	
Lys	1,01% ± 0,66%	0,20% ± 0,14%	0,67% ± 0,09%	0,00% ± 0,00%	0,00% ± 0,00%	0,00% ± 0,00%	
Ser							
DAP	1,44% ± 0,94%	0,80% ± 0,39%	1,39% ± 0,20%	0,07% ± 0,07%	0,00% ± 0,00%	0,00% ± 0,01%	0,01% ± 0,01%
PHB	0,56% ± 0,39%	0,68% ± 0,16%	0,01% ± 0,01%	0,00% ± 0,00%			
Man	2,95% ± 1,22%	2,63% ± 0,31%	7,41% ± 1,33%	0,42% ± 0,28%	0,35% ± 0,28%	0,62% ± 0,37%	
GlcN	6,54% ± 1,18%	5,67% ± 0,59%	9,44% ± 0,98%	2,84% ± 0,32%	5,04% ± 1,35%	4,56% ± 0,96%	
Mur	6,22% ± 3,13%	7,14% ± 3,36%	8,77% ± 1,61%	7,78% ± 3,13%	1,62% ± 1,32%	6,05% ± 2,55%	

[U-^{13}C$_3$]glycerol: ΔCsrA E						
	M+1	**M+2**	**M+3**	**M+4**	**M+5**	**M+6**	**M+7**
Ala	0,48% ± 0,13%	0,19% ± 0,10%	0,83% ± 0,10%				
Asp	1,37% ± 0,35%	0,01% ± 0,02%	0,19% ± 0,06%	0,00% ± 0,00%			
Glu	0,82% ± 0,13%	0,71% ± 0,11%	0,04% ± 0,05%	0,00% ± 0,00%	0,01% ± 0,01%		
Gly							
His	6,90% ± 0,47%	10,25% ± 0,81%	9,39% ± 0,88%	1,80% ± 0,23%	4,00% ± 0,52%	0,00% ± 0,00%	
Lys	0,98% ± 0,39%	0,53% ± 0,19%	0,74% ± 0,09%	0,00% ± 0,00%	0,00% ± 0,00%	0,00% ± 0,00%	
Ser							
DAP	1,24% ± 1,00%	0,92% ± 0,36%	1,19% ± 0,30%	0,01% ± 0,02%	0,02% ± 0,04%	0,00% ± 0,00%	0,01% ± 0,03%
PHB	0,57% ± 0,47%	0,69% ± 0,16%	0,00% ± 0,00%	0,00% ± 0,00%			
Man	4,81% ± 0,26%	4,79% ± 0,41%	13,47% ± 0,52%	1,23% ± 0,12%	0,79% ± 0,08%	2,09% ± 0,21%	
GlcN	5,48% ± 1,68%	5,18% ± 3,98%	10,79% ± 2,32%	1,73% ± 2,28%	2,07% ± 0,91%	2,52% ± 0,96%	
Mur	5,80% ± 7,94%	6,53% ± 5,75%	8,78% ± 3,50%	10,70% ± 5,92%	2,09% ± 2,67%	3,24% ± 3,76%	

[U-^{13}C$_3$]glycerol: ΔCsrA PE						
	M+1	**M+2**	**M+3**	**M+4**	**M+5**	**M+6**	**M+7**
Ala	0,56% ± 0,16%	0,23% ± 0,10%	1,08% ± 0,08%				
Asp	1,45% ± 0,45%	0,08% ± 0,08%	0,30% ± 0,04%	0,00% ± 0,00%			
Glu	1,33% ± 0,35%	1,13% ± 0,14%	0,06% ± 0,05%	0,00% ± 0,00%	0,01% ± 0,00%		
Gly							
His	7,10% ± 0,16%	10,38% ± 0,21%	9,81% ± 0,29%	1,76% ± 0,11%	3,93% ± 0,14%	0,00% ± 0,00%	
Lys	1,53% ± 0,39%	0,68% ± 0,13%	0,92% ± 0,11%	0,00% ± 0,00%	0,00% ± 0,00%	0,00% ± 0,00%	
Ser							
DAP	1,74% ± 0,82%	1,34% ± 0,31%	2,00% ± 0,21%	0,07% ± 0,07%	0,03% ± 0,03%	0,00% ± 0,00%	0,00% ± 0,01%
PHB	0,73% ± 0,16%	0,98% ± 0,33%	0,00% ± 0,00%	0,00% ± 0,00%			
Man	5,61% ± 0,47%	4,77% ± 0,90%	15,72% ± 0,93%	1,93% ± 0,31%	1,30% ± 0,18%	3,24% ± 0,47%	
GlcN	7,22% ± 1,15%	6,62% ± 0,50%	13,27% ± 1,09%	3,01% ± 0,89%	5,68% ± 1,85%	6,57% ± 3,11%	
Mur	4,49% ± 1,73%	6,72% ± 1,92%	12,87% ± 2,07%	14,12% ± 2,70%	1,85% ± 1,44%	7,83% ± 5,26%	

Table 5-8: Relative fractions of isotopologues (mol%) of PHB and glutamic acid from *L. pneumophila* WT and its *csrA* mutant from labeling experiments with **0.8 mM [1,2,3,4-^{13}C$_4$]palmitic acid**. Labeling experiments were performed in CE MDM. M+X represents the mass of the unlabeled metabolite plus X labeled ^{13}C-atoms. Data are means and SDs of six values (3 technical replicates x 2 biological replicates).

	PHB			
	WT E	**WT PE**	**ΔCsrA E**	**ΔCsrA PE**
M+1	1.93% ± 2.01%	1.21% ± 1.12%	1.67% ± 2.03%	1.02% ± 0.59%
M+2	3.32% ± 2.09%	4.60% ± 1.11%	7.65% ± 1.14%	10.49% ± 1.26%
M+3	0.17% ± 0.37%	0.51% ± 0.66%	0.09% ± 0.18%	0.15% ± 0.22%
M+4	0.52% ± 0.51%	0.38% ± 0.38%	0.62% ± 0.57%	0.71% ± 0.33%
	Glutamic acid			
	WT E	**WT PE**	**ΔCsrA E**	**ΔCsrA PE**
M+1	0.33% ± 0.18%	0.30% ± 0.17%	0.83% ± 0.30%	0.41% ± 0.21%
M+2	0.89% ± 0.12%	1.05% ± 0.20%	1.22% ± 0.22%	0.99% ± 0.19%
M+3	0.11% ± 0.03%	0.01% ± 0.03%	0.14% ± 0.02%	0.03% ± 0.03%
M+4	0.00% ± 0.00%	0.01% ± 0.02%	0.02% ± 0.02%	0.01% ± 0.02%
M+6	0.01% ± 0.01%	0.02% ± 0.01%	0.03% ± 0.01%	0.03% ± 0.01%

Table 5-9: Ratio of ^{13}C-excess in **histidine** to **alanine** calculated for E phase and PE phase for experiments with L. *pneumophila* wild-type and its *csrA* mutant. Labeling experiments were performed in CE MDM using either 6 mM [U-^{13}C$_3$]serine, 11 mM [U-^{13}C$_6$]glucose or 50 mM [U-^{13}C$_3$]glycerol. SDs was calculated from the highest possible (+) and the lowest possible (-) value.

Ratio: ^{13}C-Excess (mol%) **His**/^{13}C-Excess (mol %) **Ala**												
	WT E	**+**	**-**	**WT PE**	**+**	**-**	**ΔCsrA E**	**+**	**-**	**ΔCsrA PE**	**+**	**-**
6 mM [U-^{13}C$_3$]serine	0.64	0.08	0.08	0.58	0.02	0.02	0.46	0.02	0.02	0.45	0.05	0.05
11 mM [U-^{13}C$_6$]glucose	5.04	0.49	0.44	4.28	1.13	0.84	5.69	0.97	0.87	5.95	0.16	0.15
50 mM [U-^{13}C$_3$]glycerol	10.67	5.11	3.32	7.76	5.74	2.90	12.39	1.92	1.74	9.88	1.28	1.02

Table 5-10: Ratio of ^{13}C-excess in **histidine** to **glutamine** calculated for E phase and PE phase for experiments with L. *pneumophila* wild-type and its *csrA* mutant. Labeling experiments were performed in CE MDM using either 6 mM [U-^{13}C$_3$]serine, 11 mM [U-^{13}C$_6$]glucose or 50 mM [U-^{13}C$_3$]glycerol. SDs was calculated from the highest possible (+) and the lowest possible (-) value.

Ratio: ^{13}C-Excess (mol%) **His**/^{13}C-Excess (mol %) **Glu**												
	WT E	**+**	**-**	**WT PE**	**+**	**-**	**ΔCsrA E**	**+**	**-**	**ΔCsrA PE**	**+**	**-**
6 mM [U-^{13}C$_3$]serine	1.88	0.26	0.23	1.47	0.04	0.03	1.53	0.06	0.06	1.31	0.17	0.16
11 mM [U-^{13}C$_6$]glucose	13.33	0.85	0.80	9.75	2.81	2.01	16.70	4.21	3.34	15.41	0.70	0.65
50 mM [U-^{13}C$_3$]glycerol	19.98	7.96	5.69	13.38	12.90	5.46	28.86	5.06	4.44	18.25	3.32	2.44

5.3 Supplementary Material: Multiple substrate usage of *Coxiella burnetii* to feed a bipartite metabolic network

Häuslein, I., Cantet, F., Reschke, S., Chen, F., Bonazzi, M., and Eisenreich, W. (**2017**). *Frontiers in Cellular and Infection Microbiology* 7.

Multiple substrate usage of *Coxiella burnetii* to feed a bipartite metabolic network

Ina Häuslein [1], Franck Cantet[2], Sarah Reschke[1], Fan Chen[1], Matteo Bonazzi[2*], and Wolfgang Eisenreich[1*]

* Correspondence:
Wolfgang Eisenreich
wolfgang.eisenreich@ch.tum.de
Matteo Bonazzi
Matteo.bonazzi@cpbs.cnrs.fr

Supplementary Figures and Tables
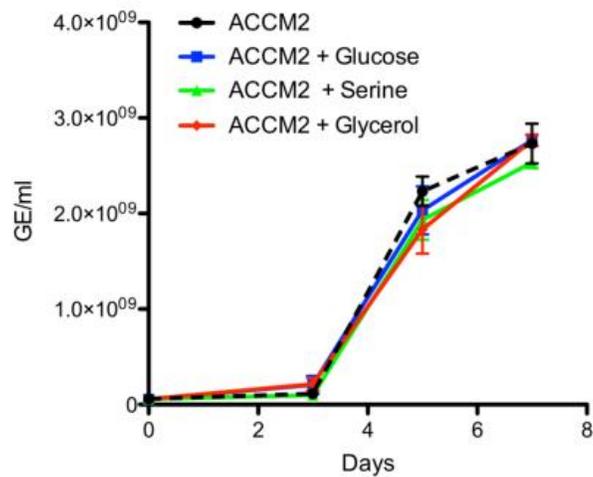
Supplementary Figure 1: Growth curves of *C. burnetii* in ACCM-2 in the presence of additional 5 mM glucose, serine or glycerol. To analyze the effect of additional amounts of serine, glucose or glycerol on the *in vitro* growth of *C. burnetii*, Acidified Citrate Cysteine Medium 2 (ACCM-2, **Table S1**) was supplemented with each substrate at 5 mM and inoculated with *Coxiella burnetii* RSA 493 NMII at $2x10^7$ GE/mL. Bacteria were cultured in a humidified atmosphere of 5% CO_2 and 2.5% O_2 at 37°C and replication was assessed at 0, 3, 5, 7 days post-inoculation using the PicoGreen assay as previously described (Martinez et al., 2014). Values are means ± SD of three independent experiments.

_____
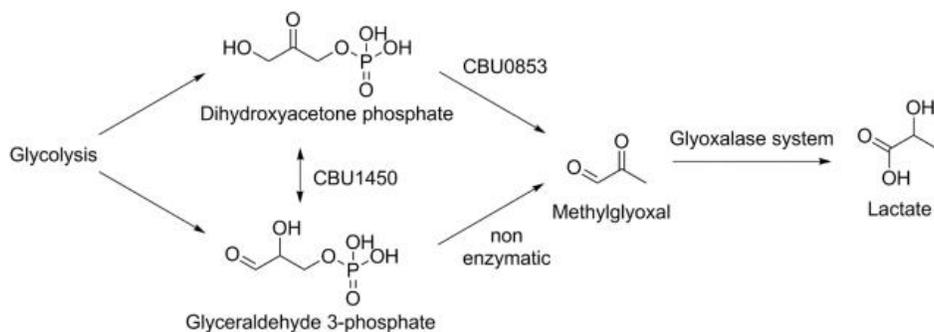
Supplementary Figure S2: Proposed metabolism of methylglyoxal/lactate by *C. burnetii* (Wattam et al., 2013; Kanehisa et al., 2017). Lactate is probably built *via* methylglyoxal in *C. burnetii*, since enzymes for the direct synthesis from pyruvate have not been annotated yet in this pathogen. Methylglyoxal is a known byproduct of metabolic processes and can be generally built non enzymatically from intermediates of glycolysis (dihydroxyacetone phosphate and glyceraldehyde 3-phosphate). Furthermore, *C. burnetii* features a methylglyoxal synthase (CBU0853), which could catalyze the formation of methylglyoxal from dihydroxyacetone phosphate. Since methylglyoxal is toxic, it is typically degraded in a detoxification process *via* the glyoxalase system. However, one enzyme (glyoxalase I) seems to be missing, whereas the second enzyme (glyoxalase II, CBU0314) is annotated in *C. burnetii*.
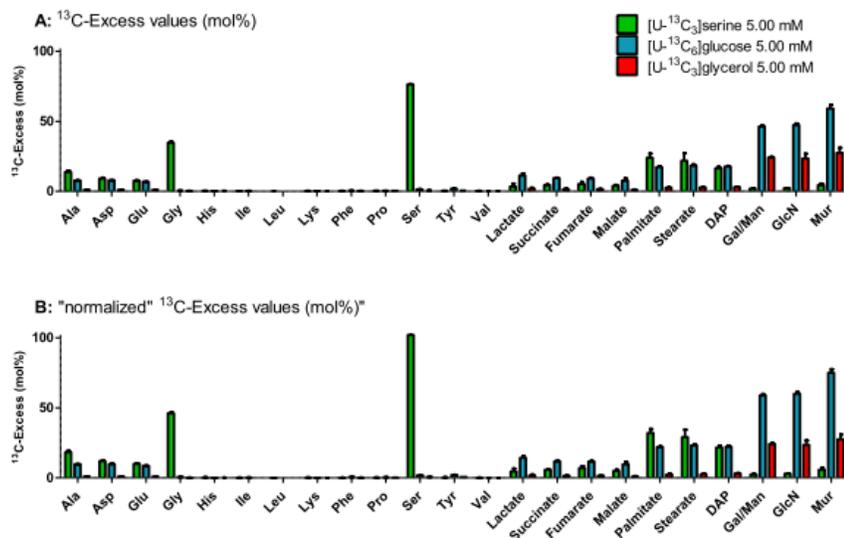
Supplementary Figure S3: Comparison of ¹³C-excess values (mol%) from labeling experiments to "normalized" values (mol%). (A) ¹³C-Excess values (mol%) of protein-derived amino acids, methanol-soluble polar metabolites, DAP, Gal/Man, GlcN and Mur from experiments with *Coxiella burnetii* RSA 493 NMII wild-type grown in ACCM-2 supplemented with 5 mM [U-¹³C₃]serine, 5 mM [U-¹³C₆]glucose or 5 mM [U-¹³C₃]glycerol. (B) To estimate the carbon fluxes into these key metabolites under the experimental conditions, the ¹³C-excess values (mol%) from the experiments were multiplied ("normalized") with the respective factors (¹³C-serine: 1.336; ¹³C-glucose: 1.270) to calculate the values (mol%) that would be reached if only labeled free serine or glucose would be present in the ACCM-2 medium. ACCM-2 comprises 1.68 mM free serine and 1.39 mM free glucose (Sales et al., 1995; Omsland et al., 2011; Sandoz et al., 2016). Since no glycerol is present in this medium, this calculation is not needed for the experiment with ¹³C-glycerol. *Abbreviations*: DAP, diaminopimelic acid; Man, mannose; Gal, galactose; GlcN, glucosamine; Mur, muramic acid.

_____

Table S1: Composition of Acidified Citrate Cysteine Medium 2 (ACCM-2). All components are dissolved in 1000 mL ddH$_2$0. The pH is adjusted to 4.75 and the solution is sterilized by filtration.

Component	[mg/L]	[mol/L]
Citric acid	2568.00	0.0134000
Sodium citrate	4740.00	0.0161000
Potassium phosphate	500.00	0.0036700
Magnesium chloride	200.00	0.0009800
Calcium chloride	13.20	0.0000197
Iron sulfate	2.78	0.0000100
Sodium chloride	7280.00	0.1254000
L-cysteine	263.40	0.0015000
Bacto Neopeptone	100.00	n/a
Casamino acids	2500.00	n/a
Methyl-B-Cyclodextrin	1000.00	
RPMI w/glutamax	125.00	n/a
Deionized H$_2$O	865.00	n/a

Table S2: Retention times in the GC-MS runs and mass fragments of TBDMS-derivatives of amino acids and methanol soluble polar metabolites and TMS-derivatives of cell wall derived hexoses (Man/Gal, GlcN and Mur) used for isotopologue calculations.

Metabolite	RT [min]	$[M-15]^+$	$[M-57]^+$	$[M-85]^+$	$[M-176]^+$
Ala	6.7		m/z 260		
Gly	7.0		m/z 246		
Val	8.5		m/z 288		
Leu	9.1			m/z 274	
Ile	9.5			m/z 274	
Pro	10.1		m/z 286		
Ser	13.2		m/z 390		
Phe	14.5		m/z 336		
Asp	15.4		m/z 418		
Glu	16.8		m/z 432		
Lys	18.1		m/z 431		
His	20.4		m/z 440		
Tyr	21.0		m/z 466		
DAP	23.4		m/z 589		
Lactate	17.8		m/z 261		
Succinate	27.5		m/z 289		
Fumarate	28.7		m/z 287		
Malate	39.1		m/z 419		
Palmitate	44.0		m/z 313		
Stearate	49.4		m/z 341		
Man/Gal	8.7	m/z 287			
GlcN	32.6	m/z 452			
Mur	36.7				m/z 434

Table S3: ^{13}C-Excess (mol%) of protein-derived amino acids, methanol-soluble polar metabolites, diaminopimelate (DAP), mannose/galactose (Man/Gal), glucosamine (GlcN) and muramic acid (Mur) from experiments with *Coxiella burnetii* RSA 493 NMII wild-type grown in ACCM-2 supplemented with 5 mM [U-[13]C$_3$]serine, 5 mM [U-[13]C$_6$]glucose or 5 mM [U-[13]C$_3$]glycerol. Cells were harvested after 7 days of growth at 37°C. Data are means and standard deviations of six values (3 technical replicates x 2 biological replicates).

[13]C-Excess (mol%)	[U-[13]C$_3$]serine	[U-[13]C$_6$]glucose	[U-[13]C$_3$]glycerol
Ala	13.78% ± 1.02%	7.73% ± 0.11%	1.04% ± 0.12%
Asp	8.99% ± 0.70%	7.79% ± 0.17%	0.99% ± 0.16%
Glu	7.47% ± 0.48%	6.83% ± 0.08%	1.02% ± 0.10%
Gly	34.59% ± 0.86%	0.48% ± 0.10%	0.16% ± 0.07%
His	0.23% ± 0.19%	0.11% ± 0.05%	0.10% ± 0.14%
Ile	0.12% ± 0.08%	0.19% ± 0.05%	0.05% ± 0.02%
Leu	0.09% ± 0.09%	0.03% ± 0.02%	0.01% ± 0.01%
Lys	0.18% ± 0.11%	0.11% ± 0.03%	0.10% ± 0.03%
Phe	0.16% ± 0.10%	0.48% ± 0.11%	0.19% ± 0.04%
Pro	0.25% ± 0.06%	0.37% ± 0.05%	0.24% ± 0.02%
Ser	76.35% ± 0.31%	1.37% ± 0.08%	0.64% ± 0.11%
Tyr	0.26% ± 0.14%	1.75% ± 0.09%	0.58% ± 0.02%
Val	0.15% ± 0.15%	0.08% ± 0.03%	0.08% ± 0.04%
Lactate	3.41% ± 2.11%	11.27% ± 1.44%	1.87% ± 0.63%
Succinate	4.37% ± 0.46%	9.35% ± 0.44%	1.50% ± 0.30%
Fumarate	5.25% ± 1.51%	9.16% ± 0.64%	1.61% ± 0.02%
Malate	3.79% ± 0.74%	7.62% ± 1.64%	1.01% ± 0.63%
Palmitate	23.98% ± 2.95%	17.31% ± 0.62%	2.58% ± 0.23%
Stearate	21.77% ± 5.28%	18.27% ± 1.01%	2.60% ± 0.41%%
DAP	16.32% ± 1.18%	17.51% ± 0.60%	3.13% ± 0.30%
Man/Gal	1.84% ± 0.34%	46.34% ± 0.92%	24.14% ± 0.59%
GlcN	2.25% ± 0.14%	47.22% ± 1.26%	23.47% ± 3.27%
Mur	4.37% ± 1.15%	59.09% ± 2.56%	27.53% ± 3.45%

Table S4: **Normalized ^{13}C-incorporation (mol%) of protein-derived amino acids, methanol-soluble polar metabolites, diaminopimelate (DAP), mannose/galactose (Man/Gal), glucosamine (GlcN) and muramic acid (Mur) from experiments with *Coxiella burnetii* RSA 493 NMII wild-type grown in ACCM-2 supplemented with 5 mM [U-^{13}C$_3$]serine, 5 mM [U-^{13}C$_6$]glucose or 5 mM [U-^{13}C$_3$]glycerol.** To evaluate the incorporation (%) into these key metabolites under the experimental conditions, the ^{13}C-excess values (mol%) from the experiments were multiplied with the respective factor (^{13}C-serine: 1.336; ^{13}C-glucose: 1.270) to calculate the ^{13}C-excess values (mol%) that would be reached if only labeled free serine or glucose would be present in the axenic media. ACCM-2 comprises 1.68 mM free serine and 1.39 mM free glucose. Since no glycerol is present in this media, this calculation is not needed for the experiment with ^{13}C-glycerol.

^{13}C-Excess (mol%)	[U-^{13}C$_3$]serine	[U-^{13}C$_6$]glucose	[U-^{13}C$_3$]glycerol
Ala	18.41% ± 1.02%	9.82% ± 0.11%	1.04% ± 0.12%
Asp	12.01% ± 0.70%	9.89% ± 0.17%	0.99% ± 0.16%
Glu	9.98% ± 0.48%	8.68% ± 0.08%	1.02% ± 0.10%
Gly	46.22% ± 0.86%	0.60% ± 0.10%	0.16% ± 0.07%
His	0.30% ± 0.19%	0.14% ± 0.05%	0.10% ± 0.14%
Ile	0.16% ± 0.08%	0.24% ± 0.05%	0.05% ± 0.02%
Leu	0.12% ± 0.09%	0.04% ± 0.02%	0.01% ± 0.01%
Lys	0.24% ± 0.11%	0.14% ± 0.03%	0.10% ± 0.03%
Phe	0.21% ± 0.10%	0.61% ± 0.11%	0.19% ± 0.04%
Pro	0.34% ± 0.06%	0.47% ± 0.05%	0.24% ± 0.02%
Ser	102.00% ± 0.31%	1.74% ± 0.08%	0.64% ± 0.11%
Tyr	0.35% ± 0.14%	2.22% ± 0.09%	0.58% ± 0.02%
Val	0.20% ± 0.15%	0.10% ± 0.03%	0.08% ± 0.04%
Lactate	4.55% ± 2.11%	14.32% ± 1.44%	1.87% ± 0.63%
Succinate	5.84% ± 0.46%	11.87% ± 0.44%	1.50% ± 0.30%
Fumarate	7.02% ± 1.51%	11.64% ± 0.64%	1.61% ± 0.02%
Malate	5.06% ± 0.74%	9.68% ± 1.64%	1.01% ± 0.63%
Palmitate	32.03% ± 2.95%	21.99% ± 0.62%	2.58% ± 0.23%
Stearate	29.09% ± 5.28%	23.20% ± 1.01%	2.60% ± 0.41%%
DAP	21.80% ± 1.18%	22.24% ± 0.06%	3.13% ± 0.30%
Man/Gal	2.46% ± 0.34%	58.86% ± 0.92%	24.14% ± 0.59%
GlcN	3.00% ± 0.14%	59.97% ± 1.26%	23.47% ± 3.27%
Mur	5.84% ± 1.15%	75.05% ± 2.56%	27.53% ± 3.45%

Table S5: Relative fractions of isotopologues (mol%) in protein-derived amino acids, methanol-soluble polar metabolites, diaminopimelate (DAP), mannose/galactose (Man/Gal), glucosamine (GlcN) and muramic acid (Mur) from experiments with _Coxiella burnetii_ RSA 493 NMII wild-type grown in ACCM-2 supplemented with 5 mM [U-^{13}C$_3$]serine. M+X represents the mass of the unlabeled metabolite plus X labeled ^{13}C-atoms. Shown are mean and standard deviations of six values (3 technical replicates x 2 biological replicates

5 mM [U-^{13}C$_3$]serine										
	Ala	Asp	Glu	Gly	Ser	Tyr	Lactate	Succinate	Fumarate	Malate
M+1	2.26% ± 0.28%	8.64% ± 0.51%	5.71% ± 0.44%	3.05% ± 0.33%	1.73% ± 0.14%		0.02% ± 0.05%	4.40% ± 1.19%	3.36% ± 0.71%	3.78% ± 1.38%
M+2	1.50% ± 0.13%	10.21% ± 0.74%	11.11% ± 0.61%	33.07% ± 0.70%	3.12% ± 0.09%		0.28% ± 0.22%	5.20% ± 0.50%	6.71% ± 2.15%	3.95% ± 1.05%
M+3	12.03% ± 0.90%	2.09% ± 0.23%	1.81% ± 0.18%		73.69% ± 0.42%		3.21% ± 1.97%	0.87% ± 0.22%	1.36% ± 0.37%	0.97% ± 0.31%
M+4		0.16% ± 0.06%	0.87% ± 0.18%					0.02% ± 0.02%	0.03% ± 0.07%	0.14% ± 0.10%
M+5			0.10% ± 0.01%							
M+6										
M+7										
M+8										
M+9										

	Palmitate	Stearate	DAP	Man/Gal	GlcN	Mur
M+1	2.74% ± 0.71%	2.63% ± 0.58%	9.09% ± 0.71%			
M+2	11.73% ± 0.94%	8.87% ± 1.62%	9.64% ± 0.30%			
M+3	7.28% ± 0.88%	6.20% ± 1.48%	19.51% ± 1.44%			
M+4	14.95% ± 1.58%	12.51% ± 2.77%	2.59% ± 0.53%			
M+5	8.29% ± 1.06%	7.87% ± 1.95%	2.69% ± 0.31%			
M+6	12.24% ± 1.56%	11.23% ± 2.75%	0.51% ± 0.04%			
M+7	5.75% ± 0.75%	6.20% ± 1.56%	0.06% ± 0.03%			
M+8	6.66% ± 0.90%	7.06% ± 1.76%				
M+9	2.57% ± 0.38%	3.36% ± 0.87%				
M+10	2.51% ± 0.36%	3.16% ± 0.82%				
M+11	0.74% ± 0.10%	1.24% ± 0.34%				
M+12	0.60% ± 0.08%	1.00% ± 0.27%				
M+13	0.12% ± 0.02%	0.32% ± 0.09%				
M+14	0.07% ± 0.02%	0.21% ± 0.06%				
M+15	0.02% ± 0.01%	0.05% ± 0.02%				
M+16	0.07% ± 0.08%	0.04% ± 0.01%				
M+17		0.01% ± 0.01%				
M+18		0.01% ± 0.02%				

Table S6: Relative fractions of isotopologues (mol%) of protein-derived amino acids, methanol-soluble polar metabolites, diaminopimelate (DAP), mannose/galactose (Man/Gal), glucosamine (GlcN) and muramic acid (Mur) from experiments with *Coxiella burnetii* RSA 493 NMII wild-type grown in ACCM-2 supplemented with 5 mM [U-^{13}C$_6$]glucose. M+X represents the mass of the unlabeled metabolite plus X labeled ^{13}C-atoms. Shown are mean and standard deviations of six values (3 technical replicates x 2 biological replicates.

	Ala	Asp	Glu	Gly	Ser	Tyr	Lactate	Succinate	Fumarate	Malate
M+1	1.42% ± 0.19%	7.74% ± 0.17%	5.28% ± 0.42%	0.34% ± 0.10%	0.01% ± 0.03%	0.31% ± 0.27%	0.36% ± 0.16%	5.77% ± 0.19%	5.85% ± 0.32%	5.51% ± 2.05%
M+2	1.06% ± 0.07%	8.74% ± 0.11%	10.19% ± 0.14%	0.31% ± 0.06%	0.00% ± 0.00%	0.54% ± 0.15%	0.97% ± 0.23%	9.95% ± 0.62%	9.22% ± 0.77%	7.63% ± 1.50%
M+3	6.55% ± 0.04%	1.86% ± 0.04%	1.62% ± 0.12%		1.36% ± 0.08%	0.91% ± 0.10%	10.51% ± 1.27%	3.53% ± 0.13%	3.49% ± 0.29%	2.66% ± 0.48%
M+4		0.09% ± 0.10%	0.77% ± 0.03%			0.67% ± 0.04%		0.28% ± 0.04%	0.47% ± 0.04%	0.44% ± 0.11%
M+5			0.12% ± 0.02%			0.65% ± 0.05%				
M+6						0.56% ± 0.04%				
M+7						0.17% ± 0.05%				
M+8						0.14% ± 0.04%				
M+9						0.00% ± 0.00%				

	Palmitate	Stearate	DAP	Man/Gal	GlcN	Mur
M+1	2.47% ± 0.19%	2.96% ± 0.09%	9.04% ± 1.01%	10.75% ± 0.65%	12.16% ± 0.41%	5.71% ± 2.14%
M+2	13.92% ± 1.24%	11.79% ± 0.45%	9.62% ± 0.48%	11.70% ± 0.37%	13.52% ± 0.21%	12.29% ± 1.81%
M+3	6.18% ± 0.21%	6.37% ± 0.13%	20.27% ± 0.57%	26.77% ± 0.61%	22.79% ± 1.82%	19.37% ± 2.83%
M+4	13.42% ± 0.73%	13.01% ± 0.25%	3.12% ± 0.43%	11.71% ± 0.36%	11.40% ± 0.47%	23.03% ± 6.27%
M+5	5.74% ± 0.13%	6.67% ± 0.22%	2.95% ± 0.33%	9.66% ± 0.52%	14.31% ± 2.02%	10.78% ± 1.32%
M+6	8.67% ± 0.24%	9.66% ± 0.28%	0.87% ± 0.22%	11.41% ± 0.49%	9.77% ± 0.66%	20.03% ± 1.57%
M+7	3.42% ± 0.37%	4.61% ± 033%	0.15% ± 0.08%			
M+8	4.03% ± 0.41%	5.23% ± 0.40%				
M+9	1.43% ± 0.26%	2.26% ± 0.30%				
M+10	1.41% ± 0.23%	2.15% ± 0.30%				
M+11	0.43% ± 0.12%	0.83% ± 0.18%				
M+12	0.35% ± 0.11%%	0.69% ± 0.17%				
M+13	0.08% ± 0.03%	0.23% ± 0.07%				
M+14	0.04% ± 0.02%	0.16% ± 0.05%				
M+15	0.00% ± 0.01%	0.05% ± 0.01%				
M+16	0.00% ± 0.00%	0.03% ± 0.01%				
M+17		0.01% ± 0.00%				
M+18		0.00% ± 0.00%				

Table S7: Relative fractions of isotopologues (mol%) of protein-derived amino acids, methanol-soluble polar metabolites, diaminopimelate (DAP), mannose/galactose (Man/Gal), glucosamine (GlcN) and muramic acid (Mur) from experiments with *Coxiella burnetii* RSA 493 NMII wild-type grown in ACCM-2 supplemented with 5 mM [U-^{13}C$_3$]glycerol. M+X represents the mass of the unlabeled metabolite plus X labeled ^{13}C-atoms. Shown are mean and standard deviations of six values (3 technical replicates x 2 biological replicates.

5 mM [U-^{13}C$_3$]glycerol									
	Ala	Asp	Glu	Gly	Ser	Tyr	Lactate	Succinate	Fumarate	Malate
M+1	0.62% ± 0.38%	1.95% ± 0.45%	1.15% ± 0.47%		0.00% ± 0.00%	0.69% ± 0.24%	0.11% ± 0.19%	0.45% ± 0.74%	0.12% ± 0.20%	
M+2	0.16% ± 0.05%	0.84% ± 0.13%	1.80% ± 0.18%		0.00% ± 0.00%	0.48% ± 0.19%	0.64% ± 0.29%	1.57% ± 0.38%	1.81% ± 0.21%	
M+3	0.73% ± 0.04%	0.11% ± 0.04%	0.06% ± 0.05%		0.64% ± 0.11%	0.46% ± 0.08%	1.40% ± 0.43%	0.73% ± 0.32%	0.83% ± 0.05%	
M+4		0.00% ± 0.00%	0.00% ± 0.00%			0.17% ± 0.05%		0.06% ± 0.08%	0.05% ± 0.07%	
M+5			0.03% ± 0.03%			0.21% ± 0.04%				
M+6						0.05% ± 0.03%				
M+7						0.00% ± 0.00%				
M+8						0.01% ± 0.02%				
M+9						0.01% ± 0.01%				

	Palmitate	Stearate	DAP	Man/Gal	GlcN	Mur
M+1	3.34% ± 0.68%	5.45% ± 1.26%	3.50% ± 1.35%	16.25% ± 0.64%	15.92% ± 0.33%	15.02% ± 4.69%
M+2	13.08% ± 1.41%	13.28% ± 2.22%	3.10% ± 0.16%	13.48% ± 0.48%	12.77% ± 0.51%	14.89% ± 1.26%
M+3	1.13% ± 0.07%	1.55% ± 0.25%	3.66% ± 0.36%	20.37% ± 1.15%	18.28% ± 0.93%	14.34% ± 5.79%
M+4	1.63% ± 0.10%	1.84% ± 0.25%	0.20% ± 0.11%	3.90% ± 0.30%	3.53% ± 0.35%	10.42% ± 2.32%
M+5	0.17% ± 0.01%	0.24% ± 0.03%	0.06% ± 0.06%	2.42% ± 0.25%	2.28% ± 0.21%	2.55% ± 1.96%
M+6	0.13% ± 0.01%	0.20% ± 0.02%	0.01% ± 0.02%	2.13% ± 0.31%	1.82% ± 0.25%	3.83% ± 1.49%
M+7	0.01% ± 0.01%	0.02% ± 0.00%	0.00% ± 0.00%			
M+8	0.00% ± 0.00%	0.02% ± 0.00%				
M+9	0.00% ± 0.00%	0.00% ± 0.00%				
M+10	0.00% ± 0.00%	0.00% ± 0.00%				
M+11	0.00% ± 0.00%	0.00% ± 0.00%				
M+12	0.00% ± 0.00%	0.00% ± 0.00%				
M+13	0.00% ± 0.00%	0.00% ± 0.00%				
M+14	0.00% ± 0.00%	0.00% ± 0.00%				
M+15	0.00% ± 0.00%	0.00% ± 0.00%				
M+16	0.00% ± 0.01%	0.00% ± 0.00%				
M+17		0.00% ± 0.00%				
M+18		0.00% ± 0.00%				

Table S8: Ratio of ^{13}C-excess in diaminopimelate (DAP) to ^{13}C-excess in Ala calculated from experiments with *Coxiella burnetii* RSA 493 NMII wild-type grown in ACCM-2 supplemented with 5 mM [U-^{13}C$_3$]serine, 5 mM [U-^{13}C$_6$]glucose or 5 mM [U-^{13}C$_3$]glycerol. Cells were harvested after 7 days of growth at 37°C. Standard deviation was calculated from the highest possible (+) and the lowest possible (-) value.

Ratio: ^{13}C-excess (mol%) DAP/^{13}C-excess (mol %) Ala								
5 mM [U-^{13}C$_3$]serine	+	-	5 mM [U-^{13}C$_6$]glucose	+	-	5 mM [U-^{13}C$_3$]glycerol	+	-
1.18	0.19	0.16	2.27	0.11	0.11	3.01	0.72	0.57

Table S9: Ratio of ^{13}C-excess in glucosamine (GlcN) to ^{13}C-excess in Ala calculated from experiments with *Coxiella burnetii* RSA 493 NMII wild-type grown in ACCM-2 supplemented with 5 mM [U-^{13}C$_3$]serine, 5 mM [U-^{13}C$_6$]glucose or 5 mM [U-^{13}C$_3$]glycerol. Cells were harvested after 7 days of growth at 37°C. Standard deviation was calculated from the highest possible (+) and the lowest possible (-) value.

Ratio: ^{13}C-excess (mol%) GlcN/^{13}C-excess (mol %) Ala								
5 mM [U-^{13}C$_3$]serine	+	-	5 mM [U-^{13}C$_6$]glucose	+	-	5 mM [U-^{13}C$_3$]glycerol	+	-
0.16	0.02	0.02	6.11	0.25	0.25	22.61	6.51	5.16

Kanehisa, M., Furumichi, M., Tanabe, M., Sato, Y., and Morishima, K. (2017). KEGG: new perspectives on genomes, pathways, diseases and drugs. *Nucleic Acids Research* 45, D353-D361.

Omsland, A., Beare, P.A., Hill, J., Cockrell, D.C., Howe, D., Hansen, B., Samuel, J.E., and Heinzen, R.A. (2011). Isolation from animal tissue and genetic transformation of *Coxiella burnetii* are facilitated by an improved axenic growth medium. *Applied and Environmental Microbiology* 77, 3720-3725.

Sales, M., De Freitas, O., Zucoloto, S., Okano, N., Padovan, G., Dos Santos, J., and Greene, L. (1995). Casein, hydrolyzed casein, and amino acids that simulate casein produce the same extent of mucosal adaptation to massive bowel resection in adult rats. *The American Journal of Clinical Nutrition* 62, 87-92.

Sandoz, K.M., Beare, P.A., Cockrell, D.C., and Heinzen, R.A. (2016). Complementation of arginine auxotrophy for genetic transformation of *Coxiella burnetii* by use of a defined axenic medium. *Applied and Environmental Microbiology* 82, 3042-3051.

Wattam, A.R., Abraham, D., Dalay, O., Disz, T.L., Driscoll, T., Gabbard, J.L., Gillespie, J.J., Gough, R., Hix, D., and Kenyon, R. (2013). PATRIC, the bacterial bioinformatics database and analysis resource. *Nucleic Acids Research*, gkt1099.
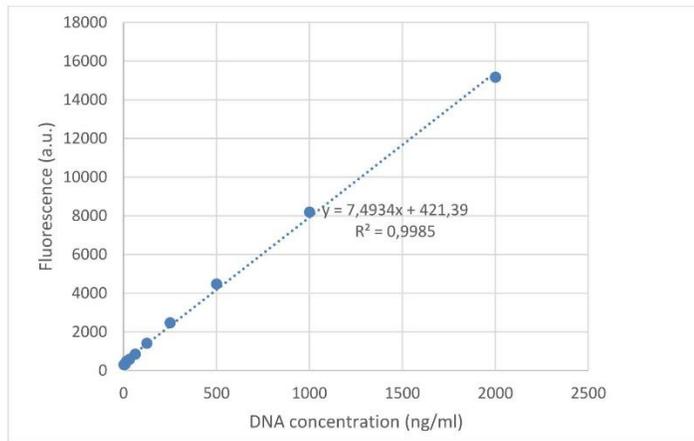
Fluorescence	ng/ml
15169	2000
8195	1000
4477	500
2472	250
1415	125
850	62.5
582	31.25
481	15.6
332	7.8
316	3.9
305	1.95

LIST OF ABBREVIATIONS

%	percent
°C	degrees Celsius
µL	microliter
µm	micrometer
3-HBA	3-hydroxybutyrate
6-PG	6-phosphogluconate
ABC transporter	ATP-binding cassette transporter
ACCM-2	Acidified Citrate Cysteine Medium 2
ACES	N-(2-acetamido)-2-aminoethanesulfonic acid
ADP	adenosine diphosphate
Ala	alanine
Arg	arginine
Asn	asparagine
Asp	aspartate
ATP	adenosine triphosphate
BCYE	buffered charcoal yeast extract
CCV	*Coxiella*-containing vacuole
CE MDM	carbon-enriched minimal defined medium
CsrA	carbon storage regulator A
Cys	cysteine
DAP	diaminopimelic acid
DHAP	dihydroxyacetone phosphate
DNA	deoxyribonucleic acid
E phase	exponential growth phase
ED pathway	Entner-Doudoroff pathway
EI	enzyme I
EII	enzyme II
EPF	exponential phase form
FADH$_2$	flavin adenine dinucleotide
Fru-6-P	fructose 6-phosphate
g	gram
G3P	glycerol 3-phosphate
Gal	galactose
GAP	glyceraldehyde 3-phosphate
GC/MS	gas chromatography/mass spectrometry

GDP	guanosine diphosphate
GlcN	glucosamine
Gln	glutamine
glpD	glycerol 3-phosphate dehydrogenase
glpK	glycerol kinase
Glu	glutamate
Glu-6-P	glucose 6-phosphate
Gly	glycine
h	hour
His	histidine
HPr	heat-stable or histidinephosphorylatable protein
icm/dot	intracellular multiplication/defective organelle trafficking
IHF	integration host factor
Ile	isoleucine
KDPG	2-keto-3-deoxy-6-phosphogluconate
kPa	kilo Pascal
L	liter
LACT	lactate
LCV	*Legionella*-containing vacuole
Leu	leucine
Lys	lysine
M	molar
Man	mannose
MDM	minimal defined medium
Met	methionine
MFS	Major facilitator superfamily
mg	milligram
MIF	mature infectious form
min	minutes
mL	milliliter
mm	millimeter
mM	millimolar
mRNA	messenger RNA
Mur	muramic acid
NAD(P)H	nicotinamide adenine dinucleotide (phosphate)
ng	nanogram
OD$_{600}$	optical density at 600 nanometer

PBS	phosphate-buffered saline
PDL	Poly-D-lysine
PE phase	Post-exponential growth phase
PEP	phosphoenolpyruvate
pH	Potential of hydrogen
PHB	polyhydroxybutyrate
Phe	phenylalanine
ppGpp	guanosine-3',5'-bispyrophosphate
PPP	pentose phosphate pathway
Pro	proline
PTS	phosphoenolpyruvate: carbohydrate phosphotransferase system
RNA	ribonucleic acid
rpe	ribulose-phosphate 3-epimerase
RPF	replicative phase form
rpiA	ribulose 5-phophate isomerase
rpm	rounds per minute
RT	retention time
s	seconds
SCV	Small-cell variant
SD	standard deviation
Ser	serine
SPF	stationary phase form
STE	stearic acid
T4BSS	type IVB secretion system
T4SS	type IV secretion system
TBDMS	tert-butyl-dimethylsilyl
TCA	tricarboxylic acid
Thr	threonine
tktA	transketolase
TMS	trimethylsilyl
tRNA	transfer RNA
Trp	tryptophan
Tyr	tyrosine
Val	valine
α-KGA	α-ketoglutarate

LIST OF FIGURES

174

LIST OF TABLES

REFERENCES

Abu Kwaik, Y. (2015). Nutrition-based evolution of intracellular pathogens. *Environmental Microbiology Reports* 7**,** 2-3.

Abu Kwaik, Y., and Bumann, D. (2013). Microbial quest for food *in vivo*: 'nutritional virulence' as an emerging paradigm. *Cellular Microbiology* 15**,** 882-890.

Abu Kwaik, Y., and Bumann, D. (2015). Host delivery of favorite meals for intracellular pathogens. *PLoS Pathogens* 11**,** e1004866.

Achouak, W., Heulin, T., and Pagès, J.-M. (2001). Multiple facets of bacterial porins. *FEMS Microbiology Letters* 199**,** 1-7.

Acimovic, Y., and Coe, I.R. (2002). Molecular evolution of the equilibrative nucleoside transporter family: identification of novel family members in prokaryotes and eukaryotes. *Molecular Biology and Evolution* 19**,** 2199-2210.

Al-Khodor, S., Kalachikov, S., Morozova, I., Price, C.T., and Kwaik, Y.A. (2009). The PmrA/PmrB two-component system of *Legionella pneumophila* is a global regulator required for intracellular replication within macrophages and protozoa. *Infection and Immunity* 77**,** 374-386.

Al-Bana, B.H., Haddad, M.T., and Garduño, R.A. (2014). Stationary phase and mature infectious forms of *Legionella pneumophila* produce distinct viable but non-culturable cells. *Environmental Microbiology* 16**,** 382-395.

Alkhuder, K., Meibom, K.L., Dubail, I., Dupuis, M., and Charbit, A. (2009). Glutathione provides a source of cysteine essential for intracellular multiplication of *Francisella tularensis*. *PLoS Pathogens* 5**,** e1000284.

Amann, R., Springer, N., Schönhuber, W., Ludwig, W., Schmid, E.N., Müller, K., and Michel, R. (1997). Obligate intracellular bacterial parasites of acanthamoebae related to *Chlamydia* spp. *Applied and environmental microbiology* 63**,** 115-121.

Anderson, A.J., and Dawes, E.A. (1990). Occurrence, metabolism, metabolic role, and industrial uses of bacterial polyhydroxyalkanoates. *Microbiological Reviews* 54**,** 450-472.

Anderson, A.J., Haywood, G.W., and Dawes, E.A. (1990). Biosynthesis and composition of bacterial poly(hydroxyalkanoates). *International Journal of Biological Macromolecules* 12**,** 102-105.

Andersson, S.G., and Kurland, C.G. (1998). Reductive evolution of resident genomes. *Trends in Microbiology* 6**,** 263-268.

Angelakis, E., and Raoult, D. (2010). Q fever. *Veterinary microbiology* 140**,** 297-309.

Arricau-Bouvery, N., and Rodolakis, A. (2005). Is Q fever an emerging or re-emerging zoonosis? *Veterinary Research* 36**,** 327-349.

Babudieri, B. (1959). Q fever: a zoonosis. *Advances in Veterinary Science* 5**,** 422.

Baca, O., Klassen, D., and Aragon, A. (1992). Entry of *Coxiella burnetii* into host cells. *Acta Virologica* 37**,** 143-155.

Bachman, M.A., and Swanson, M.S. (2001). RpoS co-operates with other factors to induce *Legionella pneumophila* virulence in the stationary phase. *Molecular Microbiology* 40**,** 1201-1214.

Baldwin, S.A., Beal, P.R., Yao, S.Y., King, A.E., Cass, C.E., and Young, J.D. (2004). The equilibrative nucleoside transporter family, SLC29. *Pflügers Archiv* 447**,** 735-743.

Barabote, R.D., and Saier, M.H. (2005). Comparative genomic analyses of the bacterial phosphotransferase system. *Microbiology and Molecular Biology Reviews* 69**,** 608-634.

Beare, P.A., Gilk, S.D., Larson, C.L., Hill, J., Stead, C.M., Omsland, A., Cockrell, D.C., Howe, D., Voth, D.E., and Heinzen, R.A. (2011). Dot/Icm type IVB secretion system requirements for *Coxiella burnetii* growth in human macrophages. *MBio* 2**,** e00175-00111.

Beare, P.A., Unsworth, N., Andoh, M., Voth, D.E., Omsland, A., Gilk, S.D., Williams, K.P., Sobral, B.W., Kupko, J.J., 3rd, Porcella, S.F., Samuel, J.E., and Heinzen, R.A. (2009). Comparative genomics reveal extensive transposon-mediated genomic plasticity and diversity among potential effector proteins within the genus *Coxiella*. *Infection and Immunity* 77**,** 642-656.

Bechah, Y., Verneau, J., Amara, A.B., Barry, A.O., Lépolard, C., Achard, V., Panicot-Dubois, L., Textoris, J., Capo, C., and Ghigo, E. (2014). Persistence of *Coxiella burnetii*, the agent of Q fever, in murine adipose tissue. *PloS One* 9**,** e97503.

Bender, J., Rydzewski, K., Broich, M., Schunder, E., Heuner, K., and Flieger, A. (2009). Phospholipase PlaB of *Legionella pneumophila* represents a novel lipase family: protein residues essential for lipolytic activity, substrate specificity, and hemolysis. *Journal of Biological Chemistry* 284**,** 27185-27194.

Beste, D.J., Nöh, K., Niedenführ, S., Mendum, T.A., Hawkins, N.D., Ward, J.L., Beale, M.H., Wiechert, W., and Mcfadden, J. (2013). ^{13}C-flux spectral analysis of host-pathogen metabolism reveals a mixed diet for intracellular *Mycobacterium tuberculosis*. *Chemistry and Biology* 20**,** 1012-1021.

Blanco, B., Prado, V.N., Lence, E., Otero, J.M., Garcia-Doval, C., Van Raaij, M.J., Llamas-Saiz, A.L., Lamb, H., Hawkins, A.R., and GonzáLez-Bello, C.N. (2013). *Mycobacterium tuberculosis* shikimate kinase inhibitors: design and simulation studies of the catalytic turnover. *Journal of the American Chemical Society* 135**,** 12366-12376.

Boshuizen, H.C., Neppelenbroek, S.E., Van Vliet, H., Schellekens, J.F., Den Boer, J.W., Peeters, M.F., and Conyn-Van Spaendonck, M.A. (2001). Subclinical *Legionella* infection in workers near the source of a large outbreak of Legionnaires` disease. *Journal of Infectious Diseases* 184**,** 515-518.

Brenner, D.J., Steigerwalt, A.G., and Mcdade, J.E. (1979). Classification of the Legionnaires' disease bacterium: *Legionella pneumophila*, genus novum, species nova, of the family Legionellaceae, familia nova. *Annals of Internal Medicine* 90**,** 656-658.

Brüggemann, H., Hagman, A., Jules, M., Sismeiro, O., Dillies, M.A., Gouyette, C., Kunst, F., Steinert, M., Heuner, K., Coppee, J.Y., and Buchrieser, C. (2006). Virulence strategies for infecting phagocytes deduced from the *in vivo* transcriptional program of *Legionella pneumophila*. *Cellular Microbiology* 8**,** 1228-1240.

Brzuszkiewicz, E., Schulz, T., Rydzewski, K., Daniel, R., Gillmaier, N., Dittmann, C., Holland, G., Schunder, E., Lautner, M., and Eisenreich, W. (2013). *Legionella oakridgensis* ATCC 33761 genome sequence and phenotypic characterization reveals its replication capacity in amoebae. *International Journal of Medical Microbiology* 303**,** 514-528.

Bücker, R., Heroven, A.K., Becker, J., Dersch, P., and Wittmann, C. (2014). The pyruvate-tricarboxylic acid cycle node. *Journal of Biological Chemistry* 289**,** 30114-30132.

Burnet, F.M., and Freeman, M. (1937). Experimental studies on the virus of "Q" fever. *Medical Journal of Australia* 2**,** 299-305.

Burstein, D., Amaro, F., Zusman, T., Lifshitz, Z., Cohen, O., Gilbert, J.A., Pupko, T., Shuman, H.A., and Segal, G. (2016). Uncovering the *Legionella* genus effector repertoire-strength in diversity and numbers. *Nature Genetics* 48**,** 167.

Byrne, B., and Swanson, M.S. (1998). Expression of *Legionella pneumophila* virulence traits in response to growth conditions. *Infection and Immunity* 66**,** 3029-3034.

Calverley, M., Erickson, S., Read, A.J., and Harmsen, A.G. (2012). Resident alveolar macrophages are susceptible to and permissive of *Coxiella burnetii* infection. *PloS One* 7**,** e51941.

Carey, K.L., Newton, H.J., Lührmann, A., and Roy, C.R. (2011). The *Coxiella burnetii* Dot/Icm system delivers a unique repertoire of type IV effectors into host cells and is required for intracellular replication. *PLoS Pathogens* 7**,** e1002056.

REFERENCES

Casadevall, A. (2008). Evolution of intracellular pathogens. *Annual Review of Microbiology* 62**,** 19-33.

Casadevall, A., and Pirofski, L.-A. (1999). Host-pathogen interactions: redefining the basic concepts of virulence and pathogenicity. *Infection and Immunity* 67**,** 3703-3713.

Cazalet, C., Gomez-Valero, L., Rusniok, C., Lomma, M., Dervins-Ravault, D., Newton, H.J., Sansom, F.M., Jarraud, S., Zidane, N., Ma, L., Bouchier, C., Etienne, J., Hartland, E.L., and Buchrieser, C. (2010). Analysis of the *Legionella longbeachae* genome and transcriptome uncovers unique strategies to cause Legionnaires' disease. *PLoS Genetics* 6**,** e1000851.

Cazalet, C., Rusniok, C., Bruggemann, H., Zidane, N., Magnier, A., Ma, L., Tichit, M., Jarraud, S., Bouchier, C., Vandenesch, F., Kunst, F., Etienne, J., Glaser, P., and Buchrieser, C. (2004). Evidence in the *Legionella pneumophila* genome for exploitation of host cell functions and high genome plasticity. *Nature Genetics* 36**,** 1165-1173.

Chen, C., Banga, S., Mertens, K., Weber, M.M., Gorbaslieva, I., Tan, Y., Luo, Z.-Q., and Samuel, J.E. (2010). Large-scale identification and translocation of type IV secretion substrates by *Coxiella burnetii*. *Proceedings of the National Academy of Sciences* 107**,** 21755-21760.

Chien, M., Morozova, I., Shi, S., Sheng, H., Chen, J., Gomez, S.M., Asamani, G., Hill, K., Nuara, J., Feder, M., Rineer, J., Greenberg, J.J., Steshenko, V., Park, S.H., Zhao, B., Teplitskaya, E., Edwards, J.R., Pampou, S., Georghiou, A., Chou, I.C., Iannuccilli, W., Ulz, M.E., Kim, D.H., Geringer-Sameth, A., Goldsberry, C., Morozov, P., Fischer, S.G., Segal, G., Qu, X., Rzhetsky, A., Zhang, P., Cayanis, E., De Jong, P.J., Ju, J., Kalachikov, S., Shuman, H.A., and Russo, J.J. (2004). The genomic sequence of the accidental pathogen *Legionella pneumophila*. *Science* 305**,** 1966-1968.

Choy, A., and Roy, C.R. (2013). Autophagy and bacterial infection: an evolving arms race. *Trends in Microbiology* 21**,** 451-456.

Cianciotto, N.P. (2007). Iron acquisition by *Legionella pneumophila*. *Biometals* 20**,** 323-331.

Cogliati, S., Costa, J.G., Ayala, F.R., Donato, V., and Grau, R. (2016). Bacterial spores and its relatives as agents of mass destruction. *Journal of Bioterrorism and Biodefense* 7**,** 1-12.

Coleman, S.A., Fischer, E.R., Cockrell, D.C., Voth, D.E., Howe, D., Mead, D.J., Samuel, J.E., and Heinzen, R.A. (2007). Proteome and antigen profiling of *Coxiella burnetii* developmental forms. *Infection and Immunity* 75**,** 290-298.

Coleman, S.A., Fischer, E.R., Howe, D., Mead, D.J., and Heinzen, R.A. (2004). Temporal analysis of *Coxiella burnetii* morphological differentiation. *Journal of Bacteriology* 186**,** 7344-7352.

Consigli, R.A., and Paretsky, D. (1962). Oxidation of glucose 6-phosphate and isocitrate by *Coxiella burnetii*. *Journal of Bacteriology* 83**,** 206-207.

Correia, A.M., Ferreira, J.S., Borges, V., Nunes, A., Gomes, B., Capucho, R., Gonçalves, J., Antunes, D.M., Almeida, S., and Mendes, A. (2016). Probable person-to-person transmission of Legionnaires' disease. *New England Journal of Medicine* 374**,** 497-498.

D'auria, G., Jimenez-Hernandez, N., Peris-Bondia, F., Moya, A., and Latorre, A. (2010). *Legionella pneumophila* pangenome reveals strain-specific virulence factors. *BMC Genomics* 11**,** 181.

Dalebroux, Z.D., Edwards, R.L., and Swanson, M.S. (2009). SpoT governs *Legionella pneumophila* differentiation in host macrophages. *Molecular Microbiology* 71**,** 640-658.

Dalebroux, Z.D., Yagi, B.F., Sahr, T., Buchrieser, C., and Swanson, M.S. (2010). Distinct roles of ppGpp and DksA in *Legionella pneumophila* differentiation. *Molecular Microbiology* 76**,** 200-219.

Davis, G.E., Cox, H.R., Parker, R., and Dyer, R. (1938). A filter-passing infectious agent isolated from ticks. *Public Health Reports* 53**,** 2259-2311.

De Carvalho, L.P.S., Fischer, S.M., Marrero, J., Nathan, C., Ehrt, S., and Rhee, K.Y. (2010). Metabolomics of *Mycobacterium tuberculosis* reveals compartmentalized co-catabolism of carbon substrates. *Chemistry and Biology* 17**,** 1122-1131.

Dean, M., and Allikmets, R. (1995). Evolution of ATP-binding cassette transporter genes. *Current Opinion in Genetics & Development* 5**,** 779-785.

Debroy, S., Dao, J., Söderberg, M., Rossier, O., and Cianciotto, N.P. (2006). *Legionella pneumophila* type II secretome reveals unique exoproteins and a chitinase that promotes bacterial persistence in the lung. *Proceedings of the National Academy of Sciences* 103**,** 19146-19151.

Declerck, P. (2010). Biofilms: the environmental playground of *Legionella pneumophila*. *Environmental Microbiology* 12**,** 557-566.

Derrick, E.H. (1937). "Q" Fever, a new fever entity: clinical features, diagnosis and laboratory investigation. *Medical Journal of Australia* 2**,** 281-299.

Deutscher, J., Aké, F.M.D., Derkaoui, M., Zébré, A.C., Cao, T.N., Bouraoui, H., Kentache, T., Mokhtari, A., Milohanic, E., and Joyet, P. (2014). The bacterial phosphoenolpyruvate: carbohydrate phosphotransferase system: regulation by protein phosphorylation and phosphorylation-dependent protein-protein interactions. *Microbiology and Molecular Biology Reviews* 78**,** 231-256.

Deutscher, J., Francke, C., and Postma, P.W. (2006). How phosphotransferase system-related protein phosphorylation regulates carbohydrate metabolism in bacteria. *Microbiology and Molecular Biology Reviews* 70**,** 939-1031.

Deutscher, J., Galinier, A., and Martin-Verstraete, I. (2002). "Carbohydrate uptake and metabolism," in *Bacillus subtilis and its closest relatives: from genes to cells*. ASM Press, Washington, DC, 129-150.

Drozanski, W. (1956). Fatal bacterial infection in soil amoebae. *Acta Microbiologica Polonica* 5**,** 315-317.

Ducati, R., Basso, L., and Santos, D. (2007). Mycobacterial shikimate pathway enzymes as targets for drug design. *Current Drug Targets* 8**,** 423-435.

Durham-Colleran, M.W., Verhoeven, A.B., and Van Hoek, M.L. (2010). *Francisella novicida* forms *in vitro* biofilms mediated by an orphan response regulator. *Microbial Ecology* 59**,** 457-465.

Duron, O., Noël, V., Mccoy, K.D., Bonazzi, M., Sidi-Boumedine, K., Morel, O., Vavre, F., Zenner, L., Jourdain, E., and Durand, P. (2015). The recent evolution of a maternally-inherited endosymbiont of ticks led to the emergence of the Q fever pathogen, *Coxiella burnetii*. *PLoS Pathogens* 11**,** e1004892.

Edwards, A.N., Patterson-Fortin, L.M., Vakulskas, C.A., Mercante, J.W., Potrykus, K., Vinella, D., Camacho, M.I., Fields, J.A., Thompson, S.A., and Georgellis, D. (2011). Circuitry linking the Csr and stringent response global regulatory systems. *Molecular Microbiology* 80**,** 1561-1580.

Edwards, P.R., and Ewing, W.H. (1972). *Identification of enterobacteriaceae.*

Edwards, R.L., Dalebroux, Z.D., and Swanson, M.S. (2009). *Legionella pneumophila* couples fatty acid flux to microbial differentiation and virulence. *Molecular Microbiology* 71**,** 1190-1204.

Eisenreich, W., Heesemann, J., Rudel, T., and Goebel, W. (2015). Metabolic adaptations of intracellullar bacterial pathogens and their mammalian host cells during infection ("pathometabolism"). *Microbiology Spectrum* 3.

Eisenreich, W., and Heuner, K. (2016). The life stage-specific pathometabolism of *Legionella pneumophila*. *FEBS Letters* 590**,** 3868-3886.

Ensminger, A.W., and Isberg, R.R. (2009). *Legionella pneumophila* Dot/Icm translocated substrates: a sum of parts. *Current Opinion in Microbiology* 12**,** 67-73.

Ensminger, A.W., Yassin, Y., Miron, A., and Isberg, R.R. (2012). Experimental evolution of *Legionella pneumophila* in mouse macrophages leads to strains with altered determinants of environmental survival. *PLoS Pathogens* 8**,** e1002731.

Essenberg, R.C., Seshadri, R., Nelson, K., and Paulsen, I. (2002). Sugar metabolism by *Brucellae*. *Veterinary Microbiology* 90**,** 249-261.

REFERENCES

Eylert, E., Herrmann, V., Jules, M., Gillmaier, N., Lautner, M., Buchrieser, C., Eisenreich, W., and Heuner, K. (2010). Isotopologue profiling of *Legionella pneumophila*: role of serine and glucose as carbon substrates. *The Journal of Biological Chemisty* 285**,** 22232-22243.

Eylert, E., Schar, J., Mertins, S., Stoll, R., Bacher, A., Goebel, W., and Eisenreich, W. (2008). Carbon metabolism of *Listeria monocytogenes* growing inside macrophages. *Molecular Microbiology* 69**,** 1008-1017.

Fath, M.J., and Kolter, R. (1993). ABC transporters: bacterial exporters. *Microbiological Reviews* 57**,** 995-1017.

Faucher, S.P., Mueller, C.A., and Shuman, H.A. (2011). *Legionella pneumophil*a transcriptome during intracellular multiplication in human macrophages. *Frontiers in Microbiology* 2**,** 60.

Faulkner, G., and Garduno, R.A. (2002). Ultrastructural analysis of differentiation in *Legionella pneumophila*. *Journal of Bacteriology* 184**,** 7025-7041.

Feeley, J.C., Gibson, R.J., Gorman, G.W., Langford, N.C., Rasheed, J.K., Mackel, D.C., and Baine, W.B. (1979). Charcoal-yeast extract agar: primary isolation medium for *Legionella pneumophila*. *Journal of Clinical Microbiology* 10**,** 437-441.

Feldman, M., Zusman, T., Hagag, S., and Segal, G. (2005). Coevolution between nonhomologous but functionally similar proteins and their conserved partners in the *Legionella* pathogenesis system. *Proceedings of the National Academy of Sciences* 102**,** 12206-12211.

Fields, B.S. (1996). The molecular ecology of *legionellae*. *Trends in Microbiology* 4**,** 286-290.

Fields, B.S., Benson, R.F., and Besser, R.E. (2002). *Legionella* and Legionnaires' disease: 25 years of investigation. *Clinical Microbiology Reviews* 15**,** 506-526.

Fields, J.A., Li, J., Gulbronson, C.J., Hendrixson, D.R., and Thompson, S.A. (2016). *Campylobacter jejuni* CsrA regulates metabolic and virulence associated proteins and is necessary for mouse colonization. *PloS One* 11**,** e0156932.

Flieger, A., Gong, S., Faigle, M., Deeg, M., Bartmann, P., and Neumeister, B. (2000). Novel phospholipase A activity secreted by *Legionella* species. *Journal of Bacteriology* 182**,** 1321-1327.

Flieger, A., Rydzewski, K., Banerji, S., Broich, M., and Heuner, K. (2004). Cloning and characterization of the gene encoding the major cell-associated phospholipase A of *Legionella pneumophila*, plaB, exhibiting hemolytic activity. *Infection and Immunity* 72**,** 2648-2658.

Fonseca, M.V., Sauer, J.-D., Crepin, S., Byrne, B., and Swanson, M.S. (2014). The phtC-phtD locus equips *Legionella pneumophila* for thymidine salvage and replication in macrophages. *Infection and Immunity* 82**,** 720-730.

Fournier, P.-E., Marrie, T.J., and Raoult, D. (1998). Diagnosis of Q fever. *Journal of Clinical Microbiology* 36**,** 1823-1834.

Franke, J., and Kessin, R. (1977). A defined minimal medium for axenic strains of *Dictyostelium discoideum*. *Proceedings of the National Academy of Sciences* 74**,** 2157.

Fraser-Liggett, C.M. (2005). Insights on biology and evolution from microbial genome sequencing. *Genome Research* 15**,** 1603-1610.

Fraser, D.W., Tsai, T.R., Orenstein, W., Parkin, W.E., Beecham, H.J., Sharrar, R.G., Harris, J., Mallison, G.F., Martin, S.M., and Mcdade, J.E. (1977). Legionnaires' disease: description of an epidemic of pneumonia. *New England Journal of Medicine* 297**,** 1189-1197.

Gal-Mor, O., and Segal, G. (2003). The *Legionella pneumophila* GacA homolog (LetA) is involved in the regulation of icm virulence genes and is required for intracellular multiplication in *Acanthamoeba castellanii*. *Microbial Pathogenesis* 34**,** 187-194.

Garduno, R.A., Garduno, E., Hiltz, M., and Hoffman, P.S. (2002). Intracellular growth of *Legionella pneumophila* gives rise to a differentiated form dissimilar to stationary-phase forms. *Infection and Immunity* 70**,** 6273-6283.

_____

George, J.R., Pine, L., Reeves, M.W., and Harrell, W.K. (1980). Amino acid requirements of *Legionella pneumophila*. *Journal of Clinical Microbiology* 11**,** 286-291.

Gil, R., Latorre, A., and Moya, A. (2004). Bacterial endosymbionts of insects: insights from comparative genomics. *Environmental Microbiology* 6**,** 1109-1122.

Gillmaier, N., Schunder, E., Kutzner, E., Tlapak, H., Rydzewski, K., Herrmann, V., Stammler, M., Lasch, P., Eisenreich, W., and Heuner, K. (2016). Growth-related metabolism of the carbon storage poly-3-hydroxybutyrate in *Legionella pneumophila*. *The Journal of Biological Chemisty* 291**,** 6471-6482.

Glick, T.H., Gregg, M.B., Berman, B., Mallison, G., Rhodes, W.W., and Kassanoff, I. (1978). Pontiac fever an epidemic of unknown etiology in a health department: I. Clinical and epidemiologic aspects. *American Journal of Epidemiology* 107**,** 149-160.

Goetz, M., Bubert, A., Wang, G., Chico-Calero, I., Vazquez-Boland, J.-A., Beck, M., Slaghuis, J., Szalay, A.A., and Goebel, W. (2001). Microinjection and growth of bacteria in the cytosol of mammalian host cells. *Proceedings of the National Academy of Sciences* 98**,** 12221-12226.

Graham, J.G., Macdonald, L.J., Hussain, S.K., Sharma, U.M., Kurten, R.C., and Voth, D.E. (2013). Virulent *Coxiella burnetii* pathotypes productively infect primary human alveolar macrophages. *Cellular Microbiology* 15**,** 1012-1025.

Graham, J.G., Winchell, C.G., Kurten, R.C., and Voth, D.E. (2016). Development of an *ex vivo* tissue platform to study the human lung response to *Coxiella burnetii*. *Infection and Immunity* 84**,** 1438-1445.

Gray, J.H., Owen, R.P., and Giacomini, K.M. (2004). The concentrative nucleoside transporter family, SLC28. *Pflügers Archiv* 447**,** 728-734.

Grubmüller, S., Schauer, K., Goebel, W., Fuchs, T.M., and Eisenreich, W. (2014). Analysis of carbon substrates used by *Listeria monocytogenes* during growth in J774A.1 macrophages suggests a bipartite intracellular metabolism. *Frontiers in Cellular and Infection Microbiology* 4**,** 1-14.

Hackstadt, T., and Williams, J. (1981a). Incorporation of macromolecular precursors by *Coxiella burnetii* in an axenic medium. *Rickettsiae and rickettsial diseases. Academic Press, Inc., New York***,** 431-440.

Hackstadt, T., and Williams, J.C. (1981b). Biochemical stratagem for obligate parasitism of eukaryotic cells by *Coxiella burnetii*. *Proceedings of the National Academy of Siences* 78**,** 3240-3244.

Hales, L.M., and Shuman, H.A. (1999). *Legionella pneumophila* contains a type II general secretion pathway required for growth in amoebae as well as for secretion of the Msp protease. *Infection and Immunity* 67**,** 3662-3666.

Hammer, B.K., and Swanson, M.S. (1999). Co-ordination of *Legionella pneumophila* virulence with entry into stationary phase by ppGpp. *Molecular Microbiology* 33**,** 721-731.

Hammer, B.K., Tateda, E.S., and Swanson, M.S. (2002). A two-component regulator induces the transmission phenotype of stationary-phase *Legionella pneumophila*. *Molecular Microbiology* 44**,** 107-118.

Haneburger, I., and Hilbi, H. (2013). "Phosphoinositide lipids and the *Legionella pathogen* vacuole," in *Molecular Mechanisms in Legionella Pathogenesis*. Springer, 155-173.

Harada, E., Iida, K., Shiota, S., Nakayama, H., and Yoshida, S. (2010). Glucose metabolism in *Legionella pneumophila*: dependence on the Entner-Doudoroff pathway and connection with intracellular bacterial growth. *Journal of Bacteriology* 192**,** 2892-2899.

Hayashi, T., Nakamichi, M., Naitou, H., Ohashi, N., Imai, Y., and Miyake, M. (2010). Proteomic analysis of growth phase-dependent expression of *Legionella pneumophila* proteins which involves regulation of bacterial virulence traits. *PLoS One* 5**,** e11718.

Herrmann, V., Eidner, A., Rydzewski, K., Blädel, I., Jules, M., Buchrieser, C., Eisenreich, W., and Heuner, K. (2011). GamA is a eukaryotic-like glucoamylase responsible for glycogen- and starch-

REFERENCES

degrading activity of *Legionella pneumophila*. *International Journal of Medical Microbiology* 301**,** 133-139.

Higgins, C.F. (1992). ABC transporters: from microorganisms to man. *Annual Review of Cell Biology* 8**,** 67-113.

Hilbi, H., Hoffmann, C., and Harrison, C.F. (2011). *Legionella* spp. outdoors: colonization, communication and persistence. *Environmental Microbiology Reports* 3**,** 286-296.

Hindre, T., Brüggemann, H., Buchrieser, C., and Hechard, Y. (2008). Transcriptional profiling of *Legionella pneumophila* biofilm cells and the influence of iron on biofilm formation. *Microbiology* 154**,** 30-41.

Hofer, U. (2016). Bacterial genomics: *Legionella*'s toolbox of effectors. *Nature Reviews Microbiology* 14**,** 133-133.

Hoffmann, C., Finsel, I., Otto, A., Pfaffinger, G., Rothmeier, E., Hecker, M., Becher, D., and Hilbi, H. (2014a). Functional analysis of novel Rab GTPases identified in the proteome of purified *Legionella*-containing vacuoles from macrophages. *Cellular Microbiology* 16**,** 1034-1052.

Hoffmann, C., Harrison, C.F., and Hilbi, H. (2014b). The natural alternative: protozoa as cellular models for *Legionella* infection. *Cellular Microbiology* 16**,** 15-26.

Hood, M.I., and Skaar, E.P. (2012). Nutritional immunity: transition metals at the pathogen–host interface. *Nature Reviews Microbiology* 10**,** 525-537.

Hookey, J., Saunders, N., Fry, N., Birtles, R., and Harrison, T. (1996). Phylogeny of *Legionellaceae* based on small-subunit ribosomal DNA sequences and proposal of *Legionella lytica* comb. nov. for *Legionella*-like amoebal pathogens. *International Journal of Systematic and Evolutionary Microbiology* 46**,** 526-531.

Horenkamp, F.A., Mukherjee, S., Alix, E., Schauder, C.M., Hubber, A.M., Roy, C.R., and Reinisch, K.M. (2014). *Legionella pneumophila* subversion of host vesicular transport by SidC effector proteins. *Traffic* 15**,** 488-499.

Horwitz, M.A. (1984). Phagocytosis of the Legionnaires' disease bacterium (*Legionella pneumophila*) occurs by a novel mechanism: engulfment within a pseudopod coil. *Cell* 36**,** 27-33.

Horwitz, M.A., and Maxfield, F.R. (1984). *Legionella pneumophila* inhibits acidification. *The Journal of Cell Biology* 99**,** 1936-1943.

Hovel-Miner, G., Pampou, S., Faucher, S.P., Clarke, M., Morozova, I., Morozov, P., Russo, J.J., Shuman, H.A., and Kalachikov, S. (2009). σS controls multiple pathways associated with intracellular multiplication of *Legionella pneumophila*. *Journal of Bacteriology* 191**,** 2461-2473.

Howe, D., and Heinzen, R.A. (2006). *Coxiella burnetii* inhabits a cholesterol-rich vacuole and influences cellular cholesterol metabolism. *Cellular Microbiology* 8**,** 496-507.

Howe, D., Melnicáková, J., Barák, I., and Heinzen, R.A. (2003). Maturation of the *Coxiella burnetii* parasitophorous vacuole requires bacterial protein synthesis but not replication. *Cellular Microbiology* 5**,** 469-480.

Howe, D., Shannon, J.G., Winfree, S., Dorward, D.W., and Heinzen, R.A. (2010). *Coxiella burnetii* phase I and II variants replicate with similar kinetics in degradative phagolysosome-like compartments of human macrophages. *Infection and Immunity* 78**,** 3465-3474.

Hubber, A., and Roy, C.R. (2010). Modulation of host cell function by *Legionella pneumophila* type IV effectors. *Annual Review of Cell and Developmental Biology* 26**,** 261-283.

Huijberts, G.N., De Rijk, T.C., De Waard, P., and Eggink, G. (1994). [13]C nuclear magnetic resonance studies of *Pseudomonas putida* fatty acid metabolic routes involved in poly(3-hydroxyalkanoate) synthesis. *Journal of Bacteriology* 176**,** 1661-1666.

Ingalls, C.S., and Brent, M.M. (1983). Defined minimal growth medium for *Acanthamoeba polyphaga*. *The Journal of Protozoology* 30**,** 606-608.

_____

Isaac, D.T., and Isberg, R. (2014). Master manipulators: an update on *Legionella pneumophila* Icm/Dot translocated substrates and their host targets. *Future Microbiology* 9**,** 343-359.

Isberg, R.R., O'connor, T.J., and Heidtman, M. (2009). The *Legionella pneumophila* replication vacuole: making a cosy niche inside host cells. *Nature Reviews Microbiology* 7**,** 13-24.

James, B.W., Mauchline, W.S., Dennis, P.J., Keevil, C.W., and Wait, R. (1999). Poly-3-hydroxybutyrate in *Legionella pneumophila*, an energy source for survival in low-nutrient environments. *Applied and Environmental Microbiology* 65**,** 822-827.

Jones, S.C., Price, C.T., Santic, M., and Kwaik, Y.A. (2015). Selective requirement of the shikimate pathway of *Legionella pneumophila* for intravacuolar growth within human macrophages but not within *Acanthamoeba*. *Infection and Immunity* 83**,** 2487-2495.

Kadouri, D., Jurkevitch, E., Okon, Y., and Castro-Sowinski, S. (2005). Ecological and agricultural significance of bacterial polyhydroxyalkanoates. *Critical Reviews in Microbiology* 31**,** 55-67.

Karupiah, G., Hunt, N., King, N., and Chaudhri, G. (1999). NADPH oxidase, Nramp1 and nitric oxide synthase 2 in the host antimicrobial response. *Reviews in Immunogenetics* 2**,** 387-415.

Katz, S.M., and Hammel, J.M. (1987). The effect of drying, heat, and pH on the survival of *Legionella pneumophila*. *Annals of Clinical and Laboratory Science* 17**,** 150-156.

Keen, M.G., and Hoffman, P.S. (1984). Metabolic pathways and nitrogen metabolism in *Legionella pneumophila*. *Current Microbiology* 11**,** 81-88.

Kentner, D., Martano, G., Callon, M., Chiquet, P., Brodmann, M., Burton, O., Wahlander, A., Nanni, P., Delmotte, N., Grossmann, J., Limenitakis, J., Schlapbach, R., Kiefer, P., Vorholt, J.A., Hiller, S., and Bumann, D. (2014). *Shigella* reroutes host cell central metabolism to obtain high-flux nutrient supply for vigorous intracellular growth. *Proceedings of the National Academy of Sciences* 111**,** 9929-9934.

Khajanchi, B.K., Odeh, E., Gao, L., Jacobs, M.B., Philipp, M.T., Lin, T., and Norris, S.J. (2016). Phosphoenolpyruvate phosphotransferase system components modulate gene transcription and virulence of *Borrelia burgdorferi*. *Infection and Immunity* 84**,** 754-764.

Khavkin, T., and Tabibzadeh, S.S. (1988). Histologic, immunofluorescence, and electron microscopic study of infectious process in mouse lung after intranasal challenge with *Coxiella burnetii*. *Infection and Immunity* 56**,** 1792-1799.

Koebnik, R., Locher, K.P., and Van Gelder, P. (2000). Structure and function of bacterial outer membrane proteins: barrels in a nutshell. *Molecular Microbiology* 37**,** 239-253.

Kotrba, P., Inui, M., and Yukawa, H. (2001). Bacterial phosphotransferase system (PTS) in carbohydrate uptake and control of carbon metabolism. *Journal of Bioscience and Bioengineering* 92**,** 502-517.

Kuhle, K., and Flieger, A. (2013). *Legionella* phospholipases implicated in virulence. *Current Topics in Microbiology and Immunology* 376**,** 175-209.

Kuley, R., Bossers-Devries, R., Smith, H.E., Smits, M.A., Roest, H.I., and Bossers, A. (2015). Major differential gene regulation in *Coxiella burnetii* between *in vivo* and *in vitro* cultivation models. *BMC Genomics* 16**,** 953.

Kulkarni, P.R., Jia, T., Kuehne, S.A., Kerkering, T.M., Morris, E.R., Searle, M.S., Heeb, S., Rao, J., and Kulkarni, R.V. (2014). A sequence-based approach for prediction of CsrA/RsmA targets in bacteria with experimental validation in *Pseudomonas aeruginosa*. *Nucleic Acids Research* 42**,** 6811-6825.

Kundig, W., Ghosh, S., and Roseman, S. (1964). Phosphate bound to histidine in a protein as an intermediate in a novel phospho-transferase system. *Proceedings of the National Academy of Sciences* 52**,** 1067-1074.

REFERENCES

Larson, C.L., Martinez, E., Beare, P.A., Jeffrey, B., Heinzen, R.A., and Bonazzi, M. (2016). Right on Q: genetics begin to unravel *Coxiella burnetii* host cell interactions. *Future Microbiology* 11**,** 919-939.

Law, C.J., Maloney, P.C., and Wang, D.-N. (2008). Ins and outs of major facilitator superfamily antiporters. *Annual Review Microbiology* 62**,** 289-305.

Lemoigne, M. (1926). Produits de deshydration et de polymerisation de l´acide beta-oxybutyric. *Bulletin De La Societe De Chimie Biologique* 8**,** 770-782.

Liles, M.R., Edelstein, P.H., and Cianciotto, N.P. (1999). The prepilin peptidase is required for protein secretion by and the virulence of the intracellular pathogen *Legionella pneumophila*. *Molecular Microbiology* 31**,** 959-970.

Linka, N., Hurka, H., Lang, B.F., Burger, G., Winkler, H.H., Stamme, C., Urbany, C., Seil, I., Kusch, J., and Neuhaus, H.E. (2003). Phylogenetic relationships of non-mitochondrial nucleotide transport proteins in bacteria and eukaryotes. *Gene* 306**,** 27-35.

Lomma, M., Dervins-Ravault, D., Rolando, M., Nora, T., Newton, H., Sansom, F., Sahr, T., Gomez-Valero, L., Jules, M., and Hartland, E. (2010). The *Legionella pneumophila* F-box protein Lpp2082 (AnkB) modulates ubiquitination of the host protein parvin B and promotes intracellular replication. *Cellular Microbiology* 12**,** 1272-1291.

Madariaga, M.G., Rezai, K., Trenholme, G.M., and Weinstein, R.A. (2003). Q fever: a biological weapon in your backyard. *The Lancet Infectious Diseases* 3**,** 709-721.

Manske, C., and Hilbi, H. (2014). Metabolism of the vacuolar pathogen *Legionella* and implications for virulence. *Frontiers in Cellular and Infection Microbiology* 4**,** 125.

Marger, M.D., and Saier, M.H. (1993). A major superfamily of transmembrane facilitators that catalyse uniport, symport and antiport. *Trends in Biochemical Sciences* 18**,** 13-20.

Margulis, L. (1971). The origin of plant and animal cells: the serial symbiosis view of the origin of higher cells suggests that the customary division of living things into two kingdoms should be reconsidered. *American Scientist* 59**,** 230-235.

Margulis, L. (1973). *Symbiosis and evolution.*

Marrie, T.J., and Raoult, D. (1997). Q fever—a review and issues for the next century. *International Journal of Antimicrobial Agents* 8**,** 145-161.

Martinez, E., Cantet, F., Fava, L., Norville, I., and Bonazzi, M. (2014). Identification of OmpA, a *Coxiella burnetii* protein involved in host cell invasion, by multi-phenotypic high-content screening. *PLoS Pathogens* 10**,** e1004013.

Maurelli, A.T., Fernandez, R.E., Bloch, C.A., Rode, C.K., and Fasano, A. (1998). "Black holes" and bacterial pathogenicity: a large genomic deletion that enhances the virulence of *Shigella* spp. and enteroinvasive *Escherichia coli*. *Proceedings of the National Academy of Sciences* 95**,** 3943-3948.

Maurin, M., and Raoult, D.F. (1999). Q fever. *Clinical Microbiology Reviews* 12**,** 518-553.

Mccutcheon, J.P. (2010). The bacterial essence of tiny symbiont genomes. *Current Opinion in Microbiology* 13**,** 73-78.

Mccutcheon, J.P., and Moran, N.A. (2012). Extreme genome reduction in symbiotic bacteria. *Nature Reviews Microbiology* 10**,** 13-26.

Mcdade, J.E., Brenner, D.J., and Bozeman, F.M. (1979). Legionnaires' disease bacterium isolated in 1947. *Annals of Internal Medicine* 90**,** 659-661.

Mcdade, J.E., Shepard, C.C., Fraser, D.W., Tsai, T.R., Redus, M.A., and Dowdle, W.R. (1977). Legionnaires' disease: isolation of a bacterium and demonstration of its role in other respiratory disease. *New England Journal of Medicine* 297**,** 1197-1203.

Mcdonald, T.L., and Mallavia, L. (1970). Biochemistry of *Coxiella burnetii*: 6-phosphogluconic acid dehydrogenase. *Journal of Bacteriology* 102**,** 1-5.

_____

Mcdonald, T.L., and Mallavia, L. (1971). Biochemistry of *Coxiella burnetii*: Embden-Meyerhof pathway. *Journal of Bacteriology* 107**,** 864-869.

Mercante, J., Suzuki, K., Cheng, X., Babitzke, P., and Romeo, T. (2006). Comprehensive alanine-scanning mutagenesis of *Escherichia coli* CsrA defines two subdomains of critical functional importance. *Journal of Biological Chemistry* 281**,** 31832-31842.

Mitchell, P. (1967). Translocations through natural membranes. *Advances in Enzymology and Related Areas of Molecular Biology* 29**,** 33-87.

Molina-Arcas, M., Casado, F.J., and Pastor-Anglada, M. (2009). Nucleoside transporter proteins. *Current Vascular Pharmacology* 7**,** 426-434.

Molofsky, A.B., and Swanson, M.S. (2003). *Legionella pneumophila* CsrA is a pivotal repressor of transmission traits and activator of replication. *Molecular Microbiology* 50**,** 445-461.

Molofsky, A.B., and Swanson, M.S. (2004). Differentiate to thrive: lessons from the *Legionella pneumophila* life cycle. *Molecular Microbiology* 53**,** 29-40.

Moran, N.A. (2002). Microbial minimalism: genome reduction in bacterial pathogens. *Cell* 108**,** 583-586.

Moran, N.A., Mccutcheon, J.P., and Nakabachi, A. (2008). Genomics and evolution of heritable bacterial symbionts. *Annual Review of Genetics* 42**,** 165-190.

Morash, M.G., Brassinga, A.K.C., Warthan, M., Gourabathini, P., Garduno, R.A., Goodman, S.D., and Hoffman, P.S. (2009). Reciprocal expression of integration host factor and HU in the developmental cycle and infectivity of *Legionella pneumophila*. *Applied and Environmental Microbiology* 75**,** 1826-1837.

Morin, M., Ropers, D., Letisse, F., Laguerre, S., Portais, J.C., Cocaign-Bousquet, M., and Enjalbert, B. (2016). The post-transcriptional regulatory system CSR controls the balance of metabolic pools in upper glycolysis of *Escherichia coli*. *Molecular Microbiology*.

Murray, E.L., and Conway, T. (2005). Multiple regulators control expression of the Entner-Doudoroff aldolase (Eda) of *Escherichia coli*. *Journal of Bacteriology* 187**,** 991-1000.

Newton, H.J., Ang, D.K., Van Driel, I.R., and Hartland, E.L. (2010). Molecular pathogenesis of infections caused by *Legionella pneumophila*. *Clinical Microbiology Reviews* 23**,** 274-298.

Newton, H.J., Mcdonough, J.A., and Roy, C.R. (2013). Effector protein translocation by the *Coxiella burnetii* Dot/Icm type IV secretion system requires endocytic maturation of the pathogen-occupied vacuole. *PLoS One* 8**,** e54566.

Nguyen, T.M.N., Ilef, D., Jarraud, S., Rouil, L., Campese, C., Che, D., Haeghebaert, S., Ganiayre, F., Marcel, F., and Etienne, J. (2006). A community-wide outbreak of Legionnaires disease linked to industrial cooling towers—how far can contaminated aerosols spread? *Journal of Infectious Diseases* 193**,** 102-111.

Nikaido, H. (1996). Outer membrane. *Escherichia coli and Salmonella***,** 29-47.

Niu, H., Xiong, Q., Yamamoto, A., Hayashi-Nishino, M., and Rikihisa, Y. (2012). Autophagosomes induced by a bacterial Beclin 1 binding protein facilitate obligatory intracellular infection. *Proceedings of the National Academy of Sciences* 109**,** 20800-20807.

O'riordan, M., and Portnoy, D.A. (2002). The host cytosol: front-line or home front? *Trends in Microbiology* 10**,** 361-364.

O'connor, T.J., Adepoju, Y., Boyd, D., and Isberg, R.R. (2011). Minimization of the *Legionella pneumophila* genome reveals chromosomal regions involved in host range expansion. *Proceedings of the National Academy of Sciences* 108**,** 14733-14740.

Omsland, A., Beare, P.A., Hill, J., Cockrell, D.C., Howe, D., Hansen, B., Samuel, J.E., and Heinzen, R.A. (2011). Isolation from animal tissue and genetic transformation of *Coxiella burnetii* are facilitated by an improved axenic growth medium. *Applied and Environmental Microbiology* 77**,** 3720-3725.

Omsland, A., Cockrell, D.C., Howe, D., Fischer, E.R., Virtaneva, K., Sturdevant, D.E., Porcella, S.F., and Heinzen, R.A. (2009). Host cell-free growth of the Q fever bacterium *Coxiella burnetii*. *Proceedings of the National Academy of Siences* 106**,** 4430-4434.

Omsland, A., Hackstadt, T., and Heinzen, R.A. (2013). Bringing culture to the uncultured: *Coxiella burnetii* and lessons for obligate intracellular bacterial pathogens. *PLoS Pathogens* 9**,** e1003540.

Orth, J.D., Conrad, T.M., Na, J., Lerman, J.A., Nam, H., Feist, A.M., and Palsson, B.Ø. (2011). A comprehensive genome-scale reconstruction of *Escherichia coli* metabolism—2011. *Molecular Systems Biology* 7**,** 535.

Pallen, M.J., and Wren, B.W. (2007). Bacterial pathogenomics. *Nature* 449**,** 835-842.

Pao, S.S., Paulsen, I.T., and Saier, M.H. (1998). Major facilitator superfamily. *Microbiology and Molecular Biology Reviews* 62**,** 1-34.

Paretsky, D., Consigli, R.A., and Downs, C.M. (1962). Studies on the physiology of rickettsiae III. Glucose phosphorylation and hexokinase activity in *Coxiella burnetii*. *Journal of Bacteriology* 83**,** 538-543.

Parish, T., and Stoker, N.G. (2002). The common aromatic amino acid biosynthesis pathway is essential in *Mycobacterium tuberculosis*. *Microbiology* 148**,** 3069-3077.

Paulsen, I.T., Sliwinski, M.K., and Saier, M.H. (1998). Microbial genome analyses: global comparisons of transport capabilities based on phylogenies, bioenergetics and substrate specificities. *Journal of Molecular Biology* 277**,** 573-592.

Payne, S.H., and Loomis, W.F. (2006). Retention and loss of amino acid biosynthetic pathways based on analysis of whole-genome sequences. *Eukaryotic Cell* 5**,** 272-276.

Pearce, M.M., and Cianciotto, N.P. (2009). *Legionella pneumophila* secretes an endoglucanase that belongs to the family-5 of glycosyl hydrolases and is dependent upon type II secretion. *FEMS Microbiology Letters* 300**,** 256-264.

Pearson, T., Hornstra, H.M., Sahl, J.W., Schaack, S., Schupp, J.M., Beckstrom-Sternberg, S.M., O'neill, M.W., Priestley, R.A., Champion, M.D., and Beckstrom-Sternberg, J.S. (2013). When outgroups fail; phylogenomics of rooting the emerging pathogen, *Coxiella burnetii*. *Systematic Biology***,** syt038.

Philip, C.B., Hoogstraal, H., Reiss-Gutfreund, R., and Clifford, C.M. (1966). Evidence of rickettsial disease agents in ticks from Ethiopian cattle. *Bulletin of the World Health Organization* 35**,** 127.

Piao, Z., Sze, C.C., Barysheva, O., Iida, K., and Yoshida, S. (2006). Temperature-regulated formation of mycelial mat-like biofilms by *Legionella pneumophila*. *Applied and Environmental Microbiology* 72**,** 1613-1622.

Pine, L., George, J.R., Reeves, M.W., and Harrell, W.K. (1979). Development of a chemically defined liquid medium for growth of *Legionella pneumophila*. *Journal of Clinical Microbiology* 9**,** 615-626.

Poirier, Y. (2002). Polyhydroxyalknoate synthesis in plants as a tool for biotechnology and basic studies of lipid metabolism. *Progress in Lipid Research* 41**,** 131-155.

Powell, B.S., Inada, T., Nakamura, Y., Michotey, V., Cui, X., Reizer, A., Saier, M.H., and Reizer, J. (1995). Novel proteins of the phosphotransferase system encoded within the rpoN operon of *Escherichia coli* Enzyme IIANtr affects growth on organic nitrogen and the conditional lethality of an erats mutant. *Journal of Biological Chemistry* 270**,** 4822-4839.

Price, C.T., Richards, A.M., Von Dwingelo, J.E., Samara, H.A., and Abu Kwaik, Y. (2014). Amoeba host-*Legionella* synchronization of amino acid auxotrophy and its role in bacterial adaptation and pathogenic evolution. *Environmental Microbiology* 16**,** 350-358.

Raoult, D., Tissot-Dupont, H., Foucault, C., Gouvernet, J., Fournier, P.E., Bernit, E., Stein, A., Nesri, M., Harle, J.R., and Weiller, P.J. (2000). Q fever 1985-1998: clinical and epidemiologic features of 1,383 infections. *Medicine* 79**,** 109-123.

Rasis, M., and Segal, G. (2009). The LetA-RsmYZ-CsrA regulatory cascade, together with RpoS and PmrA, post-transcriptionally regulates stationary phase activation of *Legionella pneumophila* Icm/Dot effectors. *Molecular Microbiology* 72**,** 995-1010.

Reizer, J., Bachem, S., Reizer, A., Arnaud, M., Saier Jr, M.H., and Stülke, J. (1999). Novel phosphotransferase system genes revealed by genome analysis–the complete complement of PTS proteins encoded within the genome of *Bacillus subtilis*. *Microbiology* 145**,** 3419-3429.

Reizer, J., Reizer, A., Merrick, M.J., Plunkett, G., Rose, D.J., and Saier, M.H. (1996). Novel phosphotransferase-encoding genes revealed by analysis of the *Escherichia coli* genome: a chimeric gene encoding an enzyme I homologue that possesses a putative sensory transduction domain. *Gene* 181**,** 103-108.

Renesto, P., Ogata, H., Audic, S., Claverie, J.-M., and Raoult, D. (2005). Some lessons from *Rickettsia* genomics. *FEMS Microbiology Reviews* 29**,** 99-117.

Revelles, O., Millard, P., Nougayrède, J.-P., Dobrindt, U., Oswald, E., Létisse, F., and Portais, J.-C. (2013). The carbon storage regulator (Csr) system exerts a nutrient-specific control over central metabolism in *Escherichia coli* strain Nissle 1917. *PloS One* 8**,** e66386.

Ristroph, J.D., Hedlund, K.W., and Gowda, S. (1981). Chemically defined medium for *Legionella pneumophila* growth. *Journal of Clinical Microbiology* 13**,** 115-119.

Robertson, P., Abdelhady, H., and Garduno, R.A. (2014). The many forms of a pleomorphic bacterial pathogen-the developmental network of *Legionella pneumophila*. *Frontiers in Microbiology* 5**,** 670.

Robillard, G., and Broos, J. (1999). Structure/function studies on the bacterial carbohydrate transporters, enzymes II, of the phosphoenolpyruvate-dependent phosphotransferase system. *Biochimica et Biophysica Acta (BBA)-Reviews on Biomembranes* 1422**,** 73-104.

Rolando, M., and Buchrieser, C. (2012). Post-translational modifications of host proteins by *Legionella pneumophila*: a sophisticated survival strategy. *Future Microbiology* 7**,** 369-381.

Romeo, T. (1998). Global regulation by the small RNA-binding protein CsrA and the non-coding RNA molecule CsrB. *Molecular Microbiology* 29**,** 1321-1330.

Romeo, T., Gong, M., Liu, M.Y., and Brun-Zinkernagel, A.-M. (1993). Identification and molecular characterization of *csrA*, a pleiotropic gene from *Escherichia coli* that affects glycogen biosynthesis, gluconeogenesis, cell size, and surface properties. *Journal of Bacteriology* 175**,** 4744-4755.

Rothmeier, E., Pfaffinger, G., Hoffmann, C., Harrison, C.F., Grabmayr, H., Repnik, U., Hannemann, M., Wölke, S., Bausch, A., and Griffiths, G. (2013). Activation of Ran GTPase by a *Legionella* effector promotes microtubule polymerization, pathogen vacuole motility and infection. *PLoS Pathogens* 9**,** e1003598.

Roux, V., Bergoin, M., Lamaze, N., and Raoult, D. (1997). Reassessment of the taxonomic position of *Rickettsiella grylli*. *International Journal of Systematic and Evolutionary Microbiology* 47**,** 1255-1257.

Rowbotham, T. (1986). Current views on the relationships between *amoebae*, *legionellae* and man. *Israel Journal of Medical Sciences* 22**,** 678-689.

Rowbotham, T.J. (1980). Preliminary report on the pathogenicity of *Legionella pneumophila* for freshwater and soil amoebae. *Journal of Clinical Pathology* 33**,** 1179-1183.

Roy, C.R., and Isberg, R.R. (1997). Topology of *Legionella pneumophila* DotA: an inner membrane protein required for replication in macrophages. *Infection and Immunity* 65**,** 571-578.

REFERENCES

Sabnis, N.A., Yang, H., and Romeo, T. (1995). Pleiotropic regulation of central carbohydrate metabolism in *Escherichia coli via* the gene *csrA*. *Journal of Biological Chemistry* 270**,** 29096-29104.

Sahr, T., Brüggemann, H., Jules, M., Lomma, M., Albert-Weissenberger, C., Cazalet, C., and Buchrieser, C. (2009). Two small ncRNAs jointly govern virulence and transmission in *Legionella pneumophila*. *Molecular Microbiology* 72**,** 741-762.

Sahr, T., Rusniok, C., Dervins-Ravault, D., Sismeiro, O., Coppee, J.-Y., and Buchrieser, C. (2012). Deep sequencing defines the transcriptional map of *L. pneumophila* and identifies growth phase-dependent regulated ncRNAs implicated in virulence. *RNA Biology* 9**,** 503-519.

Sahr, T., Rusniok, C., Impens, F., Oliva, G., Sismeiro, O., Coppée, J.-Y., and Buchrieser, C. (2017). The *Legionella pneumophila* genome evolved to accommodate multiple regulatory mechanisms controlled by the CsrA-system. *PLoS Genetics* 13**,** e1006629.

Saier Jr, M.H. (2015). The bacterial phosphotransferase system: new frontiers 50 years after its discovery. *Journal of Molecular Microbiology and Biotechnology* 25**,** 73-78.

Saier, M.H. (2000a). Families of transmembrane sugar transport proteins. *Molecular Microbiology* 35**,** 699-710.

Saier, M.H. (2000b). A functional-phylogenetic classification system for transmembrane solute transporters. *Microbiology and Molecular Biology Reviews* 64**,** 354-411.

Sánchez, J., Souriau, A., Buendia, A., Arricau-Bouvery, N., Martinez, C., Salinas, J., Rodolakis, A., and Navarro, J. (2006). Experimental *Coxiella burnetii* infection in pregnant goats: a histopathological and immunohistochemical study. *Journal of Comparative Pathology* 135**,** 108-115.

Sandoz, K.M., Beare, P.A., Cockrell, D.C., and Heinzen, R.A. (2016). Complementation of arginine auxotrophy for genetic transformation of *Coxiella burnetii* by use of a defined axenic medium. *Applied and Environmental Microbiology* 82**,** 3042-3051.

Schneebeli, R., and Egli, T. (2013). A defined, glucose-limited mineral medium for the cultivation of *Listeria*. *Applied and Environmental Microbiology***,** AEM. 03538-03512.

Schulze-Luehrmann, J., Eckart, R.A., Ölke, M., Saftig, P., Liebler-Tenorio, E., and Lührmann, A. (2016). LAMP proteins account for the maturation delay during the establishment of the *Coxiella burnetii*-containing vacuole. *Cellular Microbiology* 18**,** 181-194.

Schunder, E., Adam, P., Higa, F., Remer, K.A., Lorenz, U., Bender, J., Schulz, T., Flieger, A., Steinert, M., and Heuner, K. (2010). Phospholipase PlaB is a new virulence factor of *Legionella pneumophila*. *International Journal of Medical Microbiology* 300**,** 313-323.

Seshadri, R., Paulsen, I.T., Eisen, J.A., Read, T.D., Nelson, K.E., Nelson, W.C., Ward, N.L., Tettelin, H., Davidsen, T.M., Beanan, M.J., Deboy, R.T., Daugherty, S.C., Brinkac, L.M., Madupu, R., Dodson, R.J., Khouri, H.M., Lee, K.H., Carty, H.A., Scanlan, D., Heinzen, R.A., Thompson, H.A., Samuel, J.E., Fraser, C.M., and Heidelberg, J.F. (2003). Complete genome sequence of the Q-fever pathogen *Coxiella burnetii*. *Proceedings of the National Academy of Sciences* 100**,** 5455-5460.

Sharbati-Tehrani, S., Stephan, J., Holland, G., Appel, B., Niederweis, M., and Lewin, A. (2005). Porins limit the intracellular persistence of *Mycobacterium smegmatis*. *Microbiology* 151**,** 2403-2410.

Shin, S., and Roy, C.R. (2008). Host cell processes that influence the intracellular survival of *Legionella pneumophila*. *Cellular Microbiology* 10**,** 1209-1220.

Steeb, B., Claudi, B., Burton, N.A., Tienz, P., Schmidt, A., Farhan, H., Mazé, A., and Bumann, D. (2013). Parallel exploitation of diverse host nutrients enhances *Salmonella virulence*. *PLoS Pathogens* 9**,** e1003301.

_____

Stein, A., Louveau, C., Lepidi, H., Ricci, F., Baylac, P., Davoust, B., and Raoult, D. (2005). Q fever pneumonia: virulence of *Coxiella burnetii* pathovars in a murine model of aerosol infection. *Infection and Immunity* 73**,** 2469-2477.

Steinbüchel, A., and Schlegel, H.G. (1991). Physiology and molecular genetics of poly(beta-hydroxy-alkanoic acid) synthesis in *Alcaligenes eutrophus*. *Molecular Microbiology* 5**,** 535-542.

Steinert, M., Hentschel, U., and Hacker, J. (2002). *Legionella pneumophila*: an aquatic microbe goes astray. *FEMS Microbiology Reviews* 26**,** 149-162.

Steinert, M., and Heuner, K. (2005). *Dictyostelium* as host model for pathogenesis. *Cellular Microbiology* 7**,** 307-314.

Steinert, M., Heuner, K., Buchrieser, C., Albert-Weissenberger, C., and Glöckner, G. (2007). *Legionella* pathogenicity: genome structure, regulatory networks and the host cell response. *International Journal of Medical Microbiology* 297**,** 577-587.

Stülke, J., and Hillen, W. (1999). Carbon catabolite repression in bacteria. *Current Opinion in Microbiology* 2**,** 195-201.

Tatlock, H. (1944). A Rickettsia-like organism recovered from guinea pigs. *Experimental Biology and Medicine* 57**,** 95-99.

Tesh, M.J., and Miller, R.D. (1981). Amino acid requirements for *Legionella pneumophila* growth. *Journal of Clinical Microbiology* 13**,** 865-869.

Tesh, M.J., Morse, S.A., and Miller, R.D. (1983). Intermediary metabolism in *Legionella pneumophila*: utilization of amino acids and other compounds as energy sources. *Journal of Bacteriology* 154**,** 1104-1109.

Tiaden, A., Spirig, T., Weber, S.S., Brüggemann, H., Bosshard, R., Buchrieser, C., and Hilbi, H. (2007). The *Legionella pneumophila* response regulator LqsR promotes host cell interactions as an element of the virulence regulatory network controlled by RpoS and LetA. *Cellular Microbiology* 9**,** 2903-2920.

Tujulin, E., Macellaro, A., Lilliehöök, B., and Norlander, L. (1998). Effect of endocytosis inhibitors on *Coxiella burnetii* interaction with host cells. *Acta Virologica* 42**,** 125-131.

Vakulskas, C.A., Potts, A.H., Babitzke, P., Ahmer, B.M., and Romeo, T. (2015). Regulation of bacterial virulence by Csr (Rsm) systems. *Microbiology and Molecular Biology Reviews* 79**,** 193-224.

Valster, R.M., Wullings, B.A., and Van Der Kooij, D. (2010). Detection of protozoan hosts for *Legionella pneumophila* in engineered water systems by using a biofilm batch test. *Applied and Environmental Microbiology* 76**,** 7144-7153.

Van Assche, E., Van Puyvelde, S., Vanderleyden, J., and Steenackers, H.P. (2015). RNA-binding proteins involved in post-transcriptional regulation in bacteria. *Frontiers in Microbiology* 6**,** 141.

Van Schaik, E.J., Chen, C., Mertens, K., Weber, M.M., and Samuel, J.E. (2013). Molecular pathogenesis of the obligate intracellular bacterium *Coxiella burnetii*. *Nature Reviews Microbiology* 11**,** 561-573.

Vianna, C.P., and De Azevedo, W.F. (2012). Identification of new potential *Mycobacterium tuberculosis* shikimate kinase inhibitors through molecular docking simulations. *Journal of Molecular Modeling* 18**,** 755-764.

Voth, D.E., Howe, D., and Heinzen, R.A. (2007). *Coxiella burnetii* inhibits apoptosis in human THP-1 cells and monkey primary alveolar macrophages. *Infection and Immunity* 75**,** 4263-4271.

Walter, M.C., Ohrman, C., Myrtennas, K., Sjodin, A., Bystrom, M., Larsson, P., Macellaro, A., Forsman, M., and Frangoulidis, D. (2014). Genome sequence of *Coxiella burnetii* strain Namibia. *Standards in Genomic Sciences* 9**,** 22.

Wang, Q., Millet, Y.A., Chao, M.C., Sasabe, J., Davis, B.M., and Waldor, M.K. (2015). A genome-wide screen reveals that the *Vibrio cholerae* phosphoenolpyruvate phosphotransferase system modulates virulence gene expression. *Infection and Immunity* 83**,** 3381-3395.

REFERENCES

Warren, W.J., and Miller, R.D. (1979). Growth of Legionnaires disease bacterium (*Legionella pneumophila*) in chemically defined medium. *Journal of Clinical Microbiology* 10**,** 50-55.

Weber, M.M., Chen, C., Rowin, K., Mertens, K., Galvan, G., Zhi, H., Dealing, C.M., Roman, V.A., Banga, S., and Tan, Y. (2013). Identification of *Coxiella burnetii* type IV secretion substrates required for intracellular replication and *Coxiella*-containing vacuole formation. *Journal of Bacteriology* 195**,** 3914-3924.

Weber, S., Wagner, M., and Hilbi, H. (2014). Live-cell imaging of phosphoinositide dynamics and membrane architecture during *Legionella* infection. *MBio* 5**,** e00839-00813.

Wei, B., Shin, S., Laporte, D., Wolfe, A.J., and Romeo, T. (2000). Global regulatory mutations in *csrA* and *rpoS* cause severe central carbon stress in *Escherichia coli* in the presence of acetate. *Journal of Bacteriology* 182**,** 1632-1640.

Weiss, E., Peacock, M.G., and Wiliams, J.C. (1980). Glucose and glutamate metabolism of *Legionella pneumophila*. *Current Microbiology* 4**,** 1-6.

Wieland, H., Ullrich, S., Lang, F., and Neumeister, B. (2005). Intracellular multiplication of *Legionella pneumophila* depends on host cell amino acid transporter SLC1A5. *Molecular Microbiology* 55**,** 1528-1537.

Winchell, C.G., Graham, J.G., Kurten, R.C., and Voth, D.E. (2014). *Coxiella burnetii* type IV secretion-dependent recruitment of macrophage autophagosomes. *Infection and Immunity* 82**,** 2229-2238.

Winkler, H.H., and Neuhaus, H.E. (1999). Non-mitochondrial ATP transport. *Trends in Biochemical Sciences* 24**,** 64-68.

Woese, C., Maniloff, J., and Zablen, L. (1980). Phylogenetic analysis of the mycoplasmas. *Proceedings of the National Academy of Sciences* 77**,** 494-498.

Wolf, Y.I., and Koonin, E.V. (2013). Genome reduction as the dominant mode of evolution. *Bioessays* 35**,** 829-837.

Yang, H., Liu, M.Y., and Romeo, T. (1996). Coordinate genetic regulation of glycogen catabolism and biosynthesis in *Escherichia coli via* the CsrA gene product. *Journal of Bacteriology* 178**,** 1012-1017.

Zhao, Y., Altman, B.J., Coloff, J.L., Herman, C.E., Jacobs, S.R., Wieman, H.L., Wofford, J.A., Dimascio, L.N., Ilkayeva, O., and Kelekar, A. (2007). Glycogen synthase kinase 3α and 3β mediate a glucose-sensitive antiapoptotic signaling pathway to stabilize Mcl-1. *Molecular and Cellular Biology* 27**,** 4328-4339.

Zhao, Y., Wieman, H.L., Jacobs, S.R., and Rathmell, J.C. (2008). Mechanisms and methods in glucose metabolism and cell death. *Methods in Enzymology* 442**,** 439-457.

Zhu, W., Banga, S., Tan, Y., Zheng, C., Stephenson, R., Gately, J., and Luo, Z.-Q. (2011). Comprehensive identification of protein substrates of the Dot/Icm type IV transporter of *Legionella pneumophila*. *PloS One* 6**,** e17638.

Zink, S.D., Pedersen, L., Cianciotto, N.P., and Kwaik, Y.A. (2002). The Dot/Icm type IV secretion system of *Legionella pneumophila* is essential for the induction of apoptosis in human macrophages. *Infection and Immunity* 70**,** 1657-1663.

Zusman, T., Aloni, G., Halperin, E., Kotzer, H., Degtyar, E., Feldman, M., and Segal, G. (2007). The response regulator PmrA is a major regulator of the icm/dot type IV secretion system in *Legionella pneumophila* and *Coxiella burnetii*. *Molecular Microbiology* 63**,** 1508-1523.

Zusman, T., Gal-Mor, O., and Segal, G. (2002). Characterization of a *Legionella pneumophila relA* insertion mutant and roles of RelA and RpoS in virulence gene expression. *Journal of Bacteriology* 184**,** 67-75.

APPROVAL LETTER FROM PUBLISHER

Approval letter from publisher of section 3.1

Approval letter from publisher of section 3.3

FRONTIERS COPYRIGHT STATEMENT

192

Re: Approval Letter for the manuscript (#262956) Frontiers in Cellular and Infection Microbiology

Von: "Frontiers Microbiology Production Office" <microbiology.production.office@frontiersin.org>
An: Ina.Haeuslein@gmx.de
Datum: 19.06.2017 11:19:55

Dear Dr. Häuslein,

Thank you for your email and my apologies for taking so long to respond. Yes, you can deposit the article on the TUM website.

Best regards,
David-Anthony

Production Team
Frontiers Microbiology Production Office
****
microbiology.production.office@frontiersin.org

Connect with Frontiers:
www.frontiersin.org
twitter.com/FrontiersIn
facebook.com/FrontiersIn

'Equal Opportunity Research Publishing'

Find out more about Open Science and Frontiers in this TEDx Brussels talk

Frontiers journals take the lead both in volume of articles published and number of citations in their #OA categories

www.frontiersin.org
twitter.com/FrontiersIn
facebook.com/FrontiersIn

'Equal Opportunity Research Publishing'

Find out more about Open Science and Frontiers in this TEDx Brussels talk

Frontiers journals take the lead both in volume of articles published and number of citations in their #OA categories

From: **"Ina Häuslein"** <Ina.Haeuslein@gmx.de>
Date: Mon, Jun 12, 2017 at 12:58 PM
Subject: Approval Letter
To: microbiology.editorial.office@frontiersin.org

Dear Sir or Madam,

I am the author of the following work:

Ina Häuslein, Franck Cantet, Sarah Reschke, Fan Chen, Matteo Bonazzi and Wolfgang Eisenreich. "Multiple substrate usage of Coxiella burnetii to feed a bipartite-type metabolic network" DOI: 10.3389/fcimb.2017.00285 (Original Research, Front. Cell. Infect. Microbiol.; Submitted on: 24 Feb 2017; Research Topic: Pathometabolism of Intracellular Bacteria).

This work is based on my PhD thesis. I wish to include this work within the electronic version of my thesis, which I am required to deposit in the Technische Universität München´s online repository, media TUM (https://mediatum.ub.tum.de/). MediaTUM is a non-commercial facility which is freely and openly available to all. I would be grateful if you could advise if this will be acceptable.

Sincerely yours,

Ina Häuslein

DANKSAGUNG

_____

ganz besonders Herrn Fan Chen, der mir die letzten drei Jahre mit seinem Witz und seinem chinesischen Scharm versüßt hat ;)

Danke an Herrn Dr. Christian Görner für das intensive Coaching während meiner Masterarbeit und seine Freundschaft. Danke an Frau Dr. Stephanie Bretzke und Herrn Dr. Karl Heinz Rimböck für diverse erheiternde Kaffeepausen und Feste.

Der größte Dank gilt meiner Familie, meinen Freunden, Gisi, meiner Mama für ihre wichtige seelische Unterstützung, Dada und der unvergesslichen Gemeinschaft in der OHL 15. Dickes Danke an meine Schwester Lena, mit der ich schon so viel durchlebt habe und die auch in dieser Zeit immer an meiner Seite war. Danke an meinen Freund Patrik für deine Liebe und Geduld, mich immer wieder zu motivieren, wenn es mal schwierig war. Ich liebe dich, großer Flausch! Auf ein neues Abenteuer!

EIDESSTATTLICHE VERSICHERUNG

Die experimentellen Arbeiten zur vorliegenden Dissertation wurden von mir, Ina Häuslein, selbständig im Zeitraum von Januar 2014 bis Juni 2017 an der Fakultät für Chemie, Lehrstuhl für Biochemie der Technischen Universität München durchgeführt.

Die vorliegende Dissertation mit dem Titel „Nutrition of intracellular bacteria: Investigation of the metabolic networks in Legionella pneumophila and Coxiella burnetii using GC/MS based isotopologue profiling" habe ich selbständig verfasst und mich außer der angegebenen keiner weiteren Hilfsmittel bedient.

_____   _____

        Ort, Datum   Unterschrift

LEBENSLAUF

Persönliche Angaben

Ina Häuslein, M.Sc.
Frauenmantelanger 8
80937 München
Tel: 0176/84397906
Ina.Haeuslein@gmx.de
geboren am 27.02.1986 in München

Abschlüsse

01/2014 – 08/2017   **Promotionsstudentin/wissenschaftliche Mitarbeiterin** in einem interdisziplinären EU Forschungsprojekt (Infect-ERA/EUGENPATH) an der Fakultät für Chemie am Lehrstuhl für Biochemie, **TU München** Unter der Betreuung von **Herrn Prof. Dr. Wolfgang Eisenreich**
Titel der Dissertation: „Nutrition of intracellular replicating bacteria: Investigation of the metabolic networks in *Legionella pneumophila* and *Coxiella burnetii* using GC/MS based isotopologue profiling"

2013   **Master of Science** in Chemie (M.Sc.) an der TU München (1.5)
Hauptfach: Organische Chemie
Nebenfach: Biologische Chemie
Master´s Thesis: *"Mechanistic studies on the diterpene cyclase CotB2 by creating and characterization of new diterpene products"* (1.0)

2010   **Bachelor of Science** in Chemie (B.Sc.) an der TU München
Bachelor´s Thesis: *"Optimization of an indirect-competitive immunoassay to detect Aflatoxin B1 and Ochratoxin A in peanuts at the MCR3"*

2006   **Abitur** am Ruperti-Gymnasium in Mühldorf a. Inn